Revision of the Highly Specialized Ant Genus Discothyrea (Hymenoptera: Formicidae) in the Afrotropics with X-Ray Microtomography and 3D Cybertaxonomy

Authors: Hita-Garcia, Francisco, Lieberman, Ziv, Audisio, Tracy L., Liu, Cong, and Economo, Evan P.

Source: Insect Systematics and Diversity, 3(6) : 1-84

Published By: Entomological Society of America

URL: https://doi.org/10.1093/isd/ixz015

Insect Systematics and Diversity, (2019) 3(6): 5; 1–84
doi: 10.1093/isd/ixz015
Taxonomy

Monograph (50-200 pages)

Revision of the Highly Specialized Ant Genus *Discothyrea* (Hymenoptera: Formicidae) in the Afrotropics with X-Ray Microtomography and 3D Cybertaxonomy

Francisco Hita-Garcia,[1,3,†] Ziv Lieberman,[1,2,†] Tracy L. Audisio,[1] Cong Liu,[1] and Evan P. Economo[1]

[1]Biodiversity and Biocomplexity Unit, Okinawa Institute of Science and Techonology Graduate University, 1919-1 Tancha, Onna-son, Okinawa, Japan [2]University of California, Davis, 1 Shields Avenue, Davis, CA, 95616, and [3]Corresponding author, e-mail: fhitagarcia@gmail.com

[†]F.H.G. and Z.L. contributed equally to this study.

Subject Editors: Brendon Boudinot and István Mikó

Received 14 March, 2019; Editorial decision 3 July, 2019

Abstract

Discothyrea Roger, 1863 is a small genus of proceratiine ants with remarkable morphology and biology. However, due to cryptic lifestyle, *Discothyrea* are poorly represented in museum collections and their taxonomy has been severely neglected. We perform the first comprehensive revision of *Discothyrea* in the Afrotropical region through a combination of traditional and three-dimensional (3D) cybertaxonomy based on microtomography (micro-CT). Species diagnostics and morphological character evaluations are based on examinations of all physical specimens and virtual analyses of 3D surface models generated from micro-CT data. Additionally, we applied virtual dissections for detailed examinations of cephalic structures to establish terminology based on homology for the first time in *Discothyrea*. The complete datasets comprising micro-CT data, 3D surface models and videos, still images of volume renderings, and colored stacked images are available online as cybertype datasets (Hita Garcia et al. 2019, http://doi.org/10.5061/dryad.3qm4183). We define two species complexes (*D. oculata* and *D. traegaordhi* complexes) and revise the taxonomy of all species through detailed illustrated diagnostic character plates, a newly developed identification key, species descriptions, and distribution maps. In total, we recognize 20 species; of which, 15 are described as new. We also propose *D. hewitti* Arnold, 1916 as junior synonym of *D. traegaordhi* Santschi, 1914 and *D. sculptior* Santschi, 1913 as junior synonym of *D. oculata* Emery, 1901. Also, we designate a neotype for *D. traegaordhi* to stabilize its status and identity, and we designate a lectotype for *D. oculata*. The observed diversity and endemism are discussed within the context of Afrotropical biogeography and the oophagous lifestyle.

Key words: 3D model, anatomy, cybertype, micro-CT, morphology

In their ~120 million-year evolutionary history, ants have evolved a remarkably wide variety of lifestyles. While many ant clades are highly generalist in their diets and feeding behavior, a few lineages have become hyper-specialized, and perhaps none more so than *Discothyrea*. Species of this genus, for which natural history data are available, are known to primarily feed on arachnid eggs or juveniles, and are typically cryptic, rare, and difficult to collect. As such, we still do not have a handle on the full scope of diversity of *Discothyrea*.

At present, 35 valid species are recognized (Bolton 2019), with most known species located in the tropical and subtropical regions of Africa, Asia, and Oceania, and only a few from the New World and Madagascar (Janicki et al. 2016, Guénard et al. 2017). However, this count must be considered with caution since a high number of new species await formal description. The overall taxonomic situation of the genus is in a very poor condition. Regional revisions do not exist and most species have been treated through single-species descriptions, typically on a limited geographical scale (e.g., Kubota and Terayama 1999, Zacharias and Rajan 2004, Fisher 2005, Terayama 2009, Xu et al. 2014, Bharti et al. 2015). There are some keys available, such as Morisita et al. (1989) for Japan, Terayama (2009) for Taiwan, Sarnat & Economo (2012) for Fiji, and Bharti et al. (2015) for the Oriental region. Nevertheless, none of these are based on a thorough regional revision, and our understanding of species richness, endemism, and biogeographical affinities will improve significantly with further revisionary studies. The taxonomy of the Afrotropical fauna, in particular, has not been addressed in detail

since the notes of Brown (1958a), in which the regional fauna was briefly reviewed and informally divided into two species complexes. Brown (1958a) recognized seven Afrotropical species, of which he described one as new, and also discussed the taxonomic validity of several species. However, due to a lack of material, he did not propose any major taxonomic changes.

Generally, the paucity of specimens has been the primary impediment to robust generic revisions in most parts of the world. Several attributes contribute to the relative rarity of collections of *Discothyrea*. Where known, colony size is very small: Katayama (2013) observed a maximum of 73 workers in a colony of the Japanese species *D. kamiteta* Kubota & Terayama, 1999, while laboratory colonies of the Afrotropical *D. oculata* Emery, 1901 reared by Dejean and Dejean (1998) produced fewer than 20 workers. Individuals are small and retiring, and workers and queens may feign death when disturbed (Katayama 2013). Nests are typically located in leaf litter, humus, and other concealed microhabitats. Furthermore, most material originates from litter samples, which prevents the assembly of nest series that would yield valuable insights into intraspecific variability and ecological habits.

Beyond the details above, life history information is quite sparse and is almost exclusively limited to the species *D. mixta* Brown, 1958, *D. kamiteta*, and *D. oculata* (Brown 1958b, Dejean and Dejean 1998, Dejean et al. 1999, Katayama 2013). These species are specialized predators of spider eggs, which they remove from oothecae and stockpile in the nest; in the case of *D. mixta* and *D. oculata*, live spiderlings may be taken as well. Furthermore, *D. oculata* was observed in the field to found nests within the oothecae of *Ariadna* spiders, a colony-founding strategy termed claustral lestobiosis (Dejean and Dejean 1998). Nevertheless, to which extent this lifestyle is also found in the remainder of congeners remains unclear.

The nonexistence of comprehensive taxonomic or comparative morphology studies treating *Discothyrea* has caused some confusion concerning terminology and usage of several morphological structures. Perhaps the most significant is located on the anterior frons and clypeus where the sclerites of the anterior frons and the clypeus are highly fused and extend anteromedially beyond the clypeo-labral articulation, forming a shelflike projection (Brown 1958a, Keller 2011). Until the present day, terminology and homology considerations are unclear and deserve a thorough examination. Furthermore, until this study, one point of crucial taxonomic importance in *Discothyrea* has been the antennomere count, which was used by nearly all prior authors as a key or sole character for species delimitation (Arnold 1916, Weber 1949, Kubota and Terayama 1999, Zacharias and Rajan 2004, Sosa-Calvo and Longino 2008, Terayama 2009, Xu et al. 2014, Bharti et al. 2015). However, the flagellomeres of *Discothyrea*, excluding the apical club, are generally highly reduced, compressed, and often fused, a problem first acknowledged by Bruch (1919) and discussed in detail by Brown (1958a). Based on the above-mentioned studies, it remains ambiguous whether the antennomere count should be still used for species diagnostics or whether it would not be preferable to strongly discourage its usage. Overall, the lack of comprehensive revisionary treatments, together with an over-reliance on antennomere count and predominantly subjective differences in the shape of the head and propodeum, have caused an obvious shortage of useful and broadly applicable morphological characters for species-level diagnostics. To propel the taxonomy of *Discothyrea* into the 21st century, it is necessary to establish a widely applicable terminology and morphological characters for species-level delineation within a broad revisionary framework.

Within the last decade, innovations in computational and microscopy technology have added virtual, interactive, and three-dimensional (3D) imagery as an additional line of morphological evidence to systematics and taxonomy, with x-ray microtomography (micro-CT) being the most prominent technique (e.g., Faulwetter et al. 2013, Stoev et al. 2013, Fernández et al. 2014, Akkari et al. 2015, Hita Garcia et al. 2017b). The combination of micro-CT scanning with computer-based reconstructions is a cutting-edge imaging technology that generates high-resolution, virtual, and interactive 3D models of whole specimens or anatomical structures of interest (Friedrich and Beutel 2008, Friedrich et al. 2014). Such models can be effortlessly and virtually manipulated to examine any part of the organism under study, thus enabling highly detailed and comprehensive analyses of external or internal morphology in 3D (Friedrich et al. 2014, van de Kamp et al. 2014, Wipfler et al. 2016). The nondestructive and noninvasive nature of the technology renders it perfectly suitable for its usage in the field of invertebrate taxonomy since it permits the scanning of very rare, and often old, species and/or museum specimens, as well as valuable type material (Faulwetter et al. 2013, Fernández et al. 2014, Simonsen and Kitching 2014, Sartori et al. 2016, Hita Garcia et al. 2017b). Furthermore, the use of openly available cybertype datasets linked to the original, physical type material represents another key advantage for the application of micro-CT for taxonomy (Faulwetter et al. 2013, 2014; Stoev et al. 2013; Akkari et al. 2015; Hita Garcia et al. 2017b).

Although micro-CT was initially only used for the taxonomy of a few selected invertebrate groups (Stoev et al. 2013, Akkari et al. 2015, Carbayo et al. 2016, Landschoff and Lemaitre 2017) and even fewer insects (Simonsen and Kitching 2014, Sartori et al. 2016), it is rapidly evolving into a pioneering tool employed in ant taxonomy (Csösz 2012; Fischer et al. 2016; Sarnat et al. 2016; Agavekar et al. 2017; Hita Garcia et al. 2017a,b; Staab et al. 2018). A detailed and critical assessment of the technology and its applications for ant taxonomy was provided by Hita Garcia et al. (2017b). Nevertheless, all of the above studies used micro-CT data either for single-species descriptions (Stoev et al. 2013, Akkari et al. 2015, Carbayo et al. 2016), or taxonomic treatments with a limited taxonomic scope (Simonsen and Kitching 2014; Fischer et al. 2016; Sartori et al. 2016; Agavekar et al. 2017; Hita Garcia et al. 2017a,b, Staab et al. 2018), and so far, the technology has not been tested as an important line of evidence within a larger taxonomic revision including a substantial number of species, as is often the case in entomology.

In this study, we perform the first comprehensive revision of *Discothyrea* in the Afrotropical region through a combination of traditional morphology and 3D cybertaxonomy. We recognize, refine, and diagnose the two species complexes suggested by Brown (1958a): the *D. oculata* and the *D. traegaordhi* complexes. We also revise the taxonomy of all species of both complexes by providing detailed and highly illustrated diagnostic character plates in combination with a newly developed identification key, species descriptions, and distribution maps. Following Hita Garcia et al. (2017a), taxonomic decisions are based on the examination of all physical specimens, as well as on virtual analyses of 3D models generated from high-resolution micro-CT scanning data from all species. This powerful morphological approach permits the observation and assessment of a wealth of characters, many of which are usually less perceivable under light microscopy alone due to the minute and very hairy nature of most *Discothyrea* species, as well as the scarcity of material and often poor physical condition. We also employed 3D models and virtual dissections of cephalic structures to clarify terminology with respect to homology. Furthermore, as in Staab

et al. (2018), we use 3D models for virtual in-depth examinations of surface morphology ('virtual shaving'). The complete datasets comprising the micro-CT raw data, 3D surface models, 3D rotation videos, and colored stacked digital images have been made available online as cybertype datasets (Hita Garcia et al. 2019, http://doi.org/10.5061/dryad.3qm4183).

Material and Methods

Abbreviations of Depositories

Collection abbreviations primarily follow Evenhuis (2018). The material on which this study is based is located and/or was examined at the following institutions:

AFRC AfriBugs, CC., Pretoria, Gauteng, South Africa
AMGS Albany Museum, Grahamstown, South Africa
BMNH The Natural History Museum, London, U.K.
CASC California Academy of Sciences, San Francisco, U.S.A.
HLMD Hessisches Landesmuseum Darmstadt, Darmstadt, Germany
KSMA King Saud University Museum of Arthropods, Riyadh, Kingdom of Saudi Arabia
MCZC Museum of Comparative Zoology, Harvard University, Cambridge, U.S.A.
MHNG Muséum d'Histoire Naturelle de la Ville de Genève, Geneva, Switzerland
MRAC Musée Royal de l'Afrique Centrale, Tervuren, Belgium
NHMB Naturhistorisches Museum, Basel, Switzerland
NHMW Natural History Museum Vienna, Austria
SAMC Iziko Museums of South Africa, Cape Town, South Africa
ZFMK Zoological Research Museum Alexander Koenig, Bonn, Germany

Measurements and Indices

The following measurements and indices are presented as minimum and maximum values, with measurements expressed in millimeters to two decimal places, and are mostly based on Hita Garcia et al. (2014) with some modifications (Fig. 1):

EL Eye length: maximum length of eye, measured in oblique lateral view (Fig. 1B).
HL Head length: maximum length of the head in full-face view, measured from anteromedial point of the clypeus to posteromedial head margin; emargination at either point detracts from HL (Fig. 1A).
HW Head width: maximum width of the head excluding the eyes; measured just posterad the eyes in full-face view (Fig. 1A). When eyes absent, measured from the widest visible point, usually the latitudinal midline of the head.
SL Scape length: maximum length of antennal scape, measured along the anterior face in anterior view, exclusive of the bulbus and bulbus neck (basal condyle) (Fig. 1A).
PH Pronotum height: maximum height of the pronotum in lateral view. Measured from the lowest point of the pronotum, slightly anterodorsad the procoxal articulation, to the highest point of the pronotum in the same plane of focus (Fig. 1E).
PW Pronotum width: maximum width of the pronotum in dorsal view. Measured from the widest point of the pronotal humeri (Fig. 1C).
DML Dorsal mesosoma length: maximum length of mesosoma measured orthogonally from the measuring line for PW to the posterodorsal margin of propodeum (Fig. 1C).
PrH Propodeum height: maximum height of the propodeum in lateral view. Measured from the ventralmost point of the propodeum, just dorsad the metacoxal articulation, to the highest point of the propodeum in the same plane of focus (Fig. 1E).
WL Weber's length: diagonal mesosoma length in lateral view. Measured from anteriormost point of pronotum, excluding the pronotal neck, to the posteriomost projection of the propodeal lobe (Fig. 1E).
HFL Hind femur length: maximum length of the metafemur, measured along the anterior face in anterior view (Fig. 1G).
PeH Petiole height: maximum height of the petiole in lateral view. Measured from apex of node to the ventralmost point of the sternite, excluding the subpetiolar process (Fig. 1F). The ventralmost point is sclerotized and opaque, clearly differentiable from the translucent ventral process. Occasionally this point is in line with or slightly lower than the origin of the ventral process.
PeL: Petiole length: maximum length of the petiolar node in dorsal view, measured at the latitudinal midline; emargination of the anterior or posterior margin detracts from petiole length (Fig. 1D and F). Excludes the helcium if exposed.
PeW Petiole width: maximum transverse width of the petiolar node measured in dorsal view. The slope of the anterior face of the petiole should not be visible (Fig. 1D).
LT3 Length of abdominal tergite 3: maximum length of the third abdominal tergite, measured horizontally in lateral view from a line tangent to the anterolateral extremity to a line tangent to the posterolateral extremity (Fig. 1F).
LT4 Lenth of abdominal tergite 4: maximum length of the fourth abdominal tergite, measured horizontally in lateral view as in LT3 (Fig. 1F).
OI Ocular index: EL/HL*100
CI Cephalic index: HW/HL*100
SI Scape index: SL/HL*100
LMI Lateral mesosomal index: PH/WL*100
DMI Dorsal mesosomal index: PW/WL*100
DMI2 Dorsal mesosomal index 2: PW/DML*100
ASI Abdominal segment index: LT4/LT3*100
HFI Hind femur index: HFL/WL*100
DPeI Dorsal petiolar index: PeW/PeL*100
LPeI Lateral petiolar index: PeH/PeL*100

Total length (TL), traditionally used to represent gross body size, is omitted since it usually provides inconsistency in measurements due to varying body orientation and the difficulty of arranging specimens with all relevant body parts outstretched. We consider WL and HL to be sufficiently representative of body size. To avoid any confusion, we emphasize that DML is not the actual total length of the mesosoma in dorsal view. Instead, it is a measurement that provides information about the relative length of the mesosoma compared among species. Its main use is to calculate DMI2, which is a relative measure of robustness in dorsal view. The index of gastral reflexion (IGR) and length of abdominal sternite IV (LS4) of Ward (1988) are omitted, since the degree to which the sternite is revealed by tergite IV is both very difficult to see and subject to significant bias from distortion in preservation. Moreover, based on results of Hita Garcia et al. (2014) in *Proceratium* Roger, we have found that ASI is a more informative index of gastral proportions, at least in the Afrotropical *Discothyrea* fauna (Fig. 2).

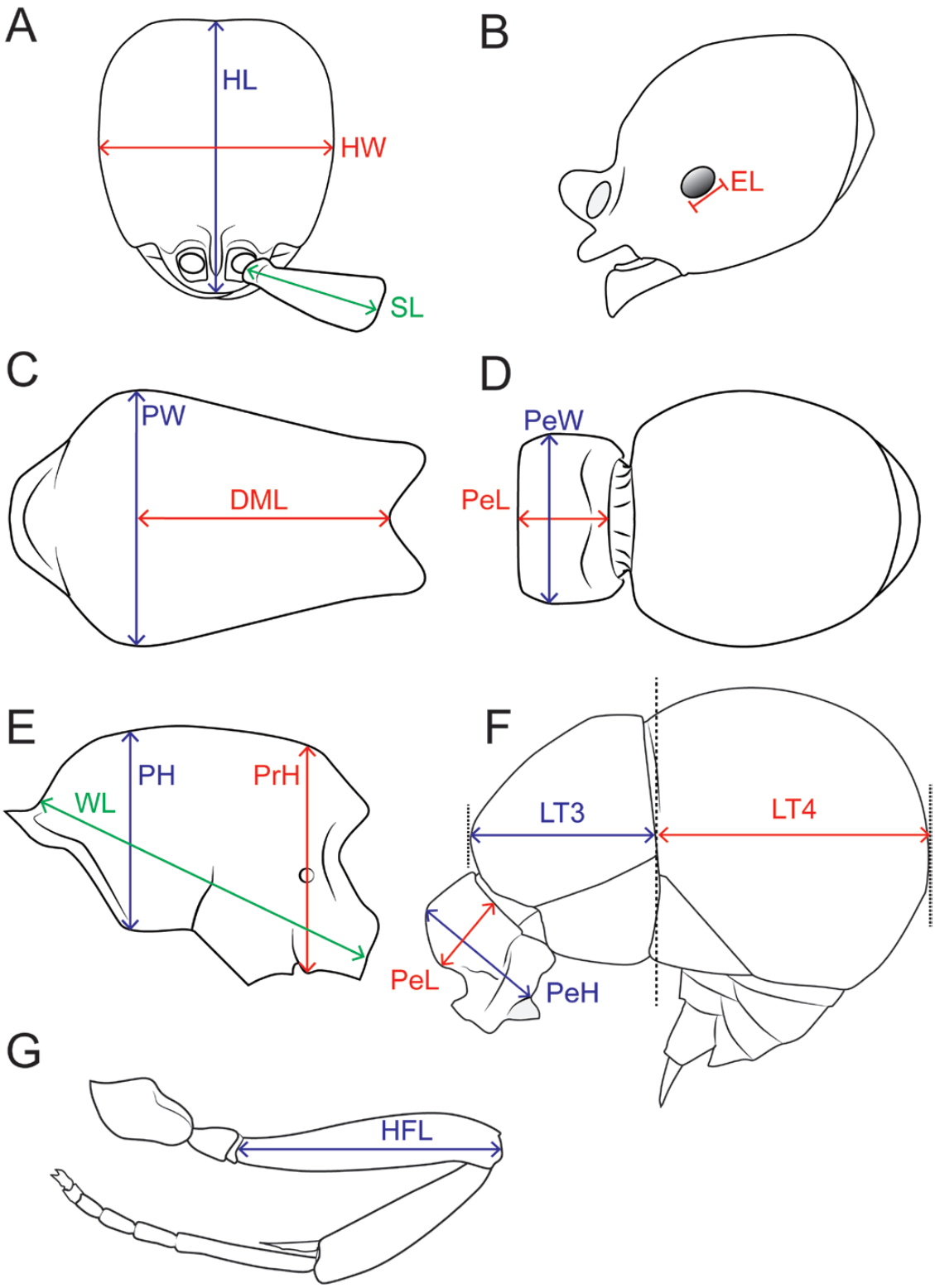

Fig. 1. Schematic line drawings illustrating the measurements used in this study. (A) head in full-face view showing HL, HW, SL; (B) head in profile showing EL; (C) mesosoma in dorsal view showing DML, PW; (D) petiole and gaster showing PeL, PeW; (E) mesosoma in profile showing PH, PrH, WL; (F) petiole and gaster showing LT3, LT4, PeH, PeL; (G) middle leg in anterior view showing HFL.

Terminology

Overall morphological terminology follows Keller (2011), while the terminology describing surface sculpture and setational inclination follow Harris (1979) and Wilson (1955), respectively. Terms for the musculature and skeletal anatomy of the preoral and pharyngeal regions follow Vilhelmsen (1996). The general terms for mandible structures are based on Gotwald (1969).

In *Discothyrea*, the sclerites of the anterior frons and the clypeus are highly fused and extend anteromedially beyond the clypeo-labral articulation, forming a shelflike projection. Despite this fusion, the

Fig. 2. Still images generated from surface display volume renderings of petiole and gaster showing different proportions of abdominal segments III (in orange) and IV (in blue). (A) *D. mixta,* (B) *D. kalypso,* (C) *D. venus.*

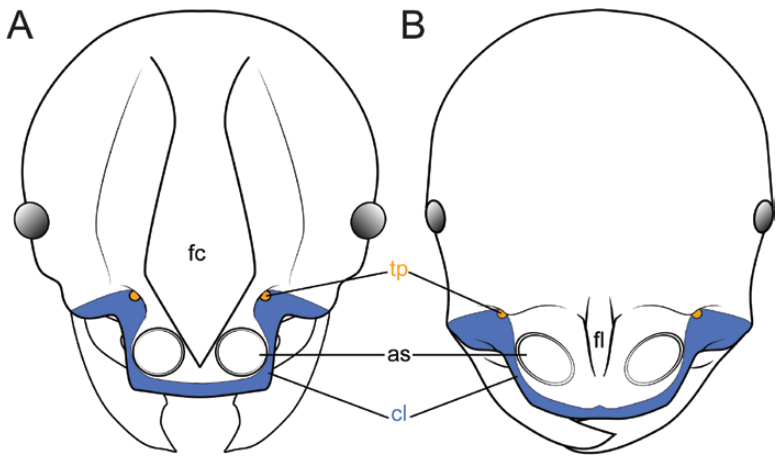

Fig. 3. Schematic line drawings of the head in full-face view showing terminology revealed and used in this study: as = antennal sockets; cl = clypeus (in blue); fl = frontal lamella; fc = frontal carinae; tp = anterior tentorial pits (in orange). (A) *D. mixta,* (B) *D. gaia.*

anteriormost edge of the shelf, as well as the narrow lateral region between the shelf and the anterolateral corners of the gena, containing the anterior tentorial pits, comprise the true clypeus (Fig. 3; see Results and Discussion). Therefore, these areas are referred to simply as the medial and lateral clypeus. Additionally, the frontal carinae are anteromedially fused, and variably modified posteriorly as a broad, elevated plate or as a narrow medial lamella. In the former case the term *frontal carinae* refers to both the lateral extensions of the carinae and the elevated frontal region between them, since the medial delimitation of the carinae is not clear. The latter state is referred to as the *frontal lamella*. We use the term *pedicel* for the second antennomere (first funicular antennomere), as is common throughout most other Hymenoptera. In *Discothyrea*, the flagellomeres are often variably fused, rendering them indistinct externally; the *true antennomere count* is that determined by virtual dissection, while the *apparent antennomere count* represents a range of values obtained from various individuals or through different subjective counting methods (see Discussion). The abbreviations AT and AS indicate *abdominal tergite* and *abdominal sternite*.

Species concept and species delimitation

Despite our preference to include molecular (ideally phylogenomic) data into this study, this was not possible due to logistical and practical reasons. The number of specimens available was very low for several species. Also, the material for these and other species was on loan from natural history museums or private collections that would not permit any destructive DNA extraction. Furthermore, despite the possibilities to nondestructively extract DNA, *Discothyrea* are very small and furry ants, thus not easy to process in such a way without potentially harming pilosity, cuticle or breaking of individual body parts. The number of species that we could have sequenced is less than 20% of the total number, so this taxonomic study had to be done on the basis of morphology alone.

The species delimitations presented here are based on detailed morphological examinations of the worker caste and the identification of discrete character sets for each taxonomic entity proposed as species. Furthermore, we considered habitat, microhabitat, elevation, and distributional data as additional evidence. We follow the Unified Species Concept of De Queiroz (2007) that defines a species as a separately evolving metapopulation lineage. In this framework, criteria laid out in other species concepts, such as the biological species concept and the morphological species concept, are integrated as independent lines of evidence reflecting progress through stages of the speciation process. The discrete gaps observed in morphological, but also ecological and distributional, characteristics of *Discothyrea* species are considered as evidence for long-standing divergence among such separately evolving lineages.

Specimens and imaging

The material for this study was gathered from numerous natural history collections and fellow colleagues in order to maximize coverage of as much of the Afrotropical region as possible (Fig. 4).

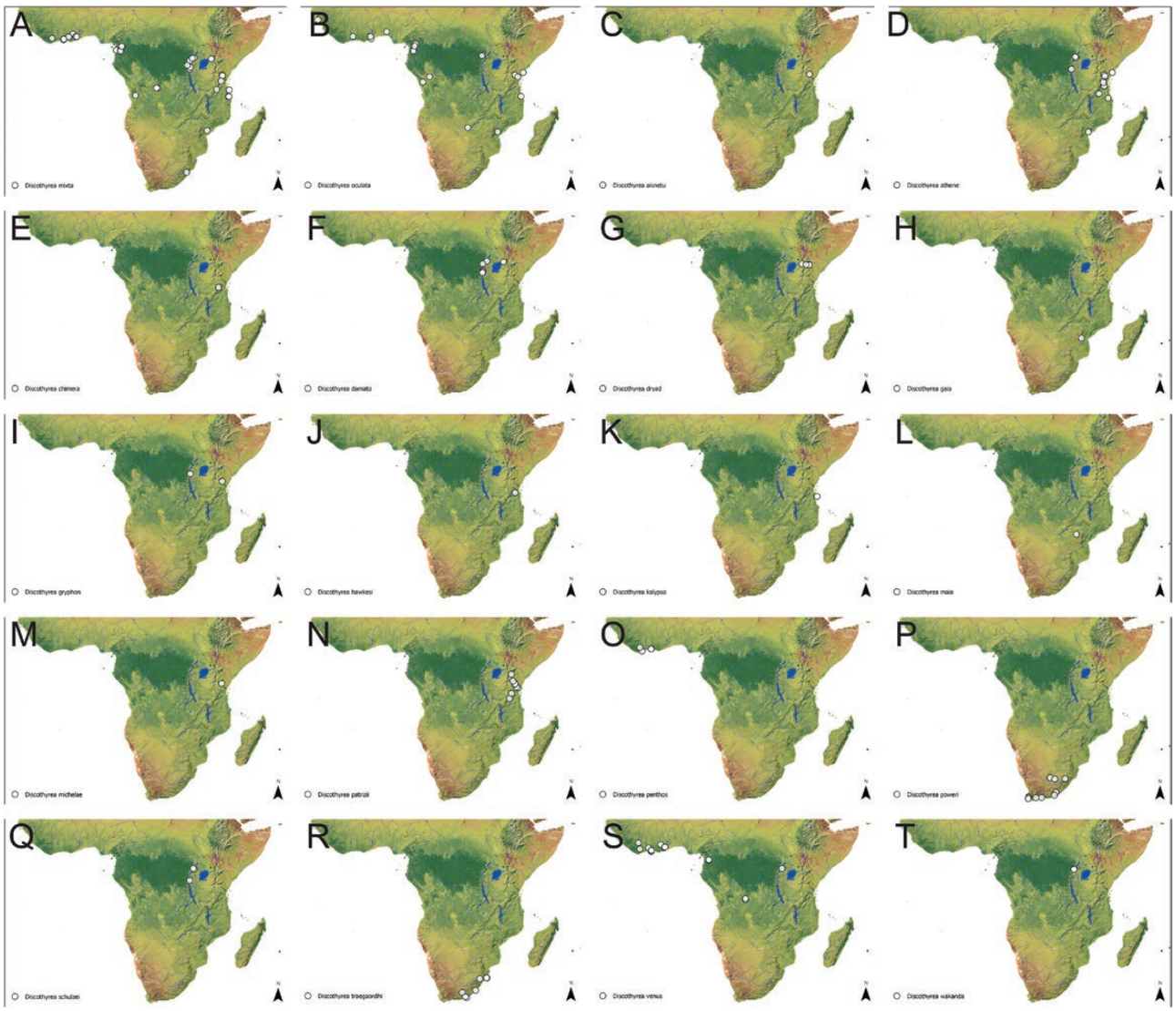

Fig. 4. Maps showing the known distribution ranges of Afrotropical *Discothyrea* species.

All type material, imaged, and measured specimens were assigned unique specimen identifiers (e.g., CASENT#). Dry mounted specimens were examined with a Leica M165C microscope, and measurements were taken with an ocular micrometer at magnifications between 80× and 120×. In order to provide better spatial information of species' distributions, manual georeferencing was performed for all localities from all available collection labels. This was done by doing simple internet browser searches, using internet gazetteers, or by manually searching coordinates in physical maps or atlases. In order to distinguish verbatim GPS coordinates (based on collection labels) from the georeferenced ones we have put the latter data in square brackets. The series of stacked digital color images was created and processed using either a Canon 7D camera in combination with Helicon Focus (version 5.3) or a JVC KY-F75 digital camera and Syncroscopy Auto-Montage software (version 5.0), or a Leica DFC 425 in combination with the Leica Application Suite (version 3.8). The cameras were attached to either a Leica MZ16 or Leica M205C stereomicroscope. All images are available online and can be seen on AntWeb (www.antweb.org) and/or AntWiki (www.antwiki.org). Figure plates were composed with Adobe Illustrator and Photoshop (version CC 2018). Vector illustrations were created with Adobe Illustrator (version CS 5) by tracing specimen photographs.

X-Ray Microtomography

We scanned representatives of all Afrotropical species of *Discothyrea* (Supp Videos S1–S20 [online only]), as well as four species from Asia and Melanesia (Supp Videos S21–S24 [online only]). An overview of specimens used and scanning parameters is provided in Table 1. The specimens were left attached to their paper point, which was clamped to a holding stage. Scan settings were selected in order to yield optimum scan quality and basically follow previous studies (e.g., Fischer et al. 2016; Hita Garcia et al. 2017a,b). In contrast to Hita Garcia et al. (2017a), only full-body scans were done (see discussion for further details). All micro-CT scans were performed using a Zeiss Xradia 510 Versa 3D X-ray microscope operated with the Zeiss Scout-and-Scan Control System software (version 11.1.6411.17883).

Table 1. Data summary giving an overview of the specimens and body parts used for micro-CT scanning (all scans were performed under an optical magnification of 4× and all files are in DICOM format)

Specimen code	Taxon code	Species complex	Type status	Caste	Body part	Voxel size (µm)	Exposure time (s)	Source distance (mm)	Detector distance (mm)	Power (W)	Voltage (kV)
CASENT0235475	*D. aisnetu*	*traegaordhi*	Holotype	w	Whole body	2.8959	3	15.0037	20.0019	3.02	40.25
CASENT0764088	*D. athene*	*traegaordhi*	Holotype	w	Whole body	1.4481	3	15.0037	54.9986	5.02	60.25
CASENT0717827	*D. banna*	*oculata*	Nontype	w	Whole body	2.3976	1	11.0032	20.0034	4.03	50.25
CASENT0235471	*D. chimera*	*traegaordhi*	Holotype	w	Whole body	1.843	3	15.0037	40.0015	4.04	50.24
CASENT0247362	*D. damato*	*traegaordhi*	Holotype	w	Whole body	1.2983	3.5	10.0033	42.001	3.97	50.29
CASENT0717811	*D. diana*	Unknown	Nontype	w	Whole body	1.729	1	11.0066	32.0034	4.98	60.25
CASENT0247374	*D. dryad*	*traegaordhi*	Holotype	w	Whole body	2.1916	3	12.0022	25.0005	3.02	40.25
CASENT0790100	*D. gaia*	*traegaordhi*	Holotype	w	Whole body	2.2526	3	15.0037	29.9976	3.55	45.24
CASENT0790103	*D. gryphon*	*traegaordhi*	Holotype	w	Whole body	2.0272	3	15.0037	35.002	4.04	50.24
CASENT0235470	*D. hawkesi*	*traegaordhi*	Holotype	w	Whole body	1.513	3	15.0037	51.9977	4.53	55.24
CASENT0235468	*D. kalypso*	*traegaordhi*	Holotype	w	Whole body	1.6894	3	15.0037	45.002	4.03	50.24
OKENT0029312	*D. kamiteta*	*oculata*	Nontype	w	Whole body	2.534	1.3	12.0032	20.0015	4	50.24
CASENT0790541	*D. maia*	*traegaordhi*	Holotype	w	Whole body	1.7784	1	10.0037	28.0015	4.98	60.25
CASENT0235469	*D. micheleae*	*traegaordhi*	Holotype	w	Whole body	1.9061	0.8	11.0037	28.0005	5.5	65.23
CASENT0285473	*D. mixta*	*oculata*	Nontype	w	Whole body	2.5339	3	15.0037	25.0005	3.53	45.24
CASENT0790542	*D. mixta*	*oculata*	Nontype	w	Head	0.9132	6	12.5032	80.0016	6.04	70.24
CASENT0195471	*D. oculata*	*oculata*	Nontype	w	Whole body	3.2401	1	12.0033	13.0009	4.03	50.28
CASENT0235472	*D. patrizii*	*traegaordhi*	Nontype	w	Whole body	2.1863	1	11.0037	23.0005	4.54	55.24
CASENT0790105	*D. penthos*	*traegaordhi*	Holotype	w	Whole body	2.2526	3	15.0037	29.9976	3.04	40.24
CASENT0764095	*D. poweri*	*traegaordhi*	Nontype	w	Whole body	2.2526	3	15.0037	29.9976	3.53	45.24
CASENT0790121	*D. schulzei*	*traegaordhi*	Holotype	w	Whole body	1.6161	1.2	11.0022	34.9995	5.54	65.24
CASENT0741903	*D.* SM01	Unknown	Nontype	w	Whole body	1.7291	1	11.0052	32.0005	4.99	60.25
CASENT0790122	*D. traegaordhi*	*traegaordhi*	Neotype	w	Whole body	1.8431	3	15.0037	39.9976	4.03	50.25
CASENT090308	*D.* UG01	*traegaordhi*	Nontype	q	Head	0.6699	15	11.0066	100.0017	3.95	50.25
CASENT0790116	*D. venus*	*traegaordhi*	Holotype	w	Whole body	1.616	1.5	11.0037	35.0015	4.99	60.25
CASENT0790326	*D. wakanda*	*traegaordhi*	Holotype	w	Whole body	2.1863	1	11.0037	23.0005	4.99	60.25

Virtual Reconstruction and Postprocessing of Raw Data

3D reconstructions of the resulting scan projection data were done with the Zeiss Scout-and-Scan Control System Reconstructor (version 11.1.6411.17883) and saved in DICOM file format. Postprocessing of DICOM raw data was performed with Amira software (version 6.3). Virtual examinations of 3D surface models were performed by using either the 'volren' or 'volume rendering' functions. The desired volume renderings were generated by adjusting color space range to a minimum so that the exterior surface of specimens remained visible at the highest available quality. The 3D models were rotated and manipulated to allow a complete virtual examination of the scanned specimens. Images of shaded surface display volume renderings were made with the 'snapshot' function at the highest achievable resolution (usually at around 1900 × 893 pixels). Volumetric surface rendering rotational videos of full body scans were created with the 'camera path' object (5 keyframes, constant velocity for constant rotation speed) and 'movie maker' function (parameters: MPEG format, AntiAlias2, total of 1,200 frames at 60 frames/s, and resolution of 1,920 × 1,080 pixels).

Character recognition and virtual dissections

Following Hita Garcia et al. (2017a), we applied an integrative approach for the study of external morphology by examining the physical material under a light microscope with magnifications up to 120× in combination with virtual examinations of 3D models in Amira. We studied all characters potentially useful for species-level taxonomy of proceratiines based on previous treatments of the group (Brown 1958a; Baroni Urbani and De Andrade 2003; Hita Garcia and Fisher 2014; Hita Garcia et al. 2014, 2015; Staab et al. 2018). Similar to the situation presented by Hita Garcia et al. (Hita Garcia et al. 2017a), several characters were partly hidden or completely obscured by other body parts and were not observable by light microscopy. Due to lack of sufficient material, destructive dissections were not an option, but we were still able to examine all characters by virtually dissecting 3D models of all species. To accomplish this, we sectioned the full-body 3D volumes and examined head, mesosoma, legs, and metasoma independently and used either used general segmentation or "clipping plane" functions to select or deselect body parts. As in Hita Garcia et al. (2017a), all structures of interest were visualized and studied. In order to examine the degree and possible mechanism of flagellar fusion, we virtually dissected the antennae of all Afrotropical and several Asian species of *Discothyrea*, as well as the antennae of selected other species from the same and other subfamilies (Supp Table 25 [online only]).

Data Availability

All specimens used in this study have been databased, and the data are freely accessible on AntWeb (http://www.antweb.org). Each specimen can be traced by a unique specimen identifier attached to its pin. The Cybertype datasets provided in this study consist of the full micro-CT original volumetric datasets (in DICOM format), 3D surface models (in PLY formats), 3D rotation video files (in MP4 format, Supp Videos 1–24 [online only]), all stacked digital color images, and all image plates including all important images of 3D models for each species. All data have been archived and are freely available from the Dryad Digital Repository (Hita Garcia et al. 2019, http://doi.org/10.5061/dryad.3qm4183). In addition to the cybertype data at Dryad, we also provide freely accessible 3D surface models of all treated species on Sketchfab (https://sketchfab.com/arilab/collections/discothyrea).

Results

Discothyrea Roger, 1863

Nomenclature

Discothyrea Roger, 1863. Type-species: *Discothyrea testacea*, by monotypy.

Prodiscothyrea Wheeler, 1916. Type-species: *Prodiscothyrea velutina*, by monotypy.

[Junior synonym of *Discothyrea* by Brown, 1958a]

Pseudosysphincta Arnold, 1916. Type-species: *Pseudosysphincta poweri*, by monotypy. [Junior synonym of *Discothyrea* by Brown, 1958a]

Pseudosphincta Wheeler, 1922. [incorrect subsequent spelling]

Worker Description

Head usually longer than broad, less often approximately as long as broad and subquadrate; posterior head margin transverse to gently rounded; sides of head subparallel, converging anteriorly, or rounded in frontal view; anterolateral corners of gena rounded, squared, or sharply angulate to denticulate; clypeus and frons completely fused, epistomal sulcus absent; clypeus anteriorly produced, overhanging mandible, with anteromedial disc rectangular, convex, sagittate, or weakly emarginate, or anteriomedial disc of clypeus deeply concave, impressed and ventral to anteromedial frontal projection; lateral area of clypeus narrow, concave between antennal sockets and anterolateral corner of gena; frons anteromedially prolonged such that antennal sockets located anterad anterior tentorial pits; frontal carinae anteromedially fused, posteriorly variously modified: as a broad, elevated plate, rhomboid in frontal view, extending from anterior clypeal margin to posterior third of head, forming deep scrobal areas; as a short but broad rhomboid to triangular swelling not reaching midline of head; or as a thin lamella, disciform, lobate, or triangular in profile, sometimes slightly broadened anteromedially, lamella often thinnest basally, sometimes with a distinct translucent fenestra. *Antenna* with 6–11 antennomeres; scape slightly to strongly incrassate apically and typically not surpassing posterior head margin; apical antennomere greatly enlarged, forming a swollen club usually about as long as remaining flagellomeres taken together; subapical flagellomeres highly compressed, one to five flagellomeres proximal to antennal club with both distal and proximal margins deeply invaginated, forming two sclerotic annuli internally per subsegment, first few flagellomeres extremely compressed and externally indistinct, variably overlapping. *Compound eye* variably present, well-developed with multiple ommatidia, globose and protruding from head, eye setose; or eye small and flattened, ommatidia indistinct; or eye reduced to a pigmented spot; or eye entirely absent. *Mandible* with masticatory margin edentate, or with a distinct subapical tooth, denticle, or swelling, and/or with a subbasal angle or denticle, basal angle of mandible rounded, squared, or angulate, sometimes sharply; ectal face of mandible usually with carina confluent with masticatory margin for some of its length, leaving a smooth, depressed mesal region where it diverges from margin that includes subbasal angle or denticle when present; mesal face of mandible asetose, or with prominent row of enlarged setae, setae stout and sometimes apically flattened. *Ventral head surface* with raised, well-defined postocciput, sometimes with an anteromedial carina; with or without raised, rounded tumuli and flattened, unsculptured posterolateral areas. *Palpal formula* variable: 6,4; 5, 4; 4,4; 4,3; 4,3; 1,3 (see Note below); secondary maxillary palpomere tubular, not hammer-shaped; first two proximal maxillary palpomeres highly reduced, partially fused, and transverse in relation to one another, such that the second palpomere articulates perpendicular to the first and third palpomeres in a zigzag arrangement.

Mesosoma variable in shape, gracile to very stocky and robust; usually moderately rounded or posteroventrally sloping in profile but rarely strongly convex, high-rounded; in dorsal view mesosoma subrectangular to strongly narrowed posteriorly; pronotal humeri rounded; promesonotal junction fused, suture entirely absent or very rarely scarcely detectable; pronotomesepisternal junction sutured, unfused; median mesepisternal sulcus absent; posterolateral corners of propodeum unarmed and rounded to strongly angulate or with distinct denticles; declivitous face of propodeum sloping to strongly concave, sometimes finely marginate; propodeal spiracle without bulla, atrial opening round to oval, usually located at or slightly ventrad mid-height of propodeum; propodeal lobes present, short and truncate to lobate or flangelike; metapleural gland present.

Legs usually short, sometimes somewhat elongate; mesotibia variably unarmed, or with an apicoventral seta inserted in a pit, or with a distinct apicoventral spur; mesobasitarsus sometimes very elongate, as long as remaining tarsomeres taken together.

Petiole variable in shape; outline of anterior face nearly round, disciform, rectangular, roughly or distinctly hexagonal, or often clearly pentagonal; dorsal margin of anterior face flat, weakly to strongly rounded, concave, or peaked, sometimes strongly so; anterior face of petiolar node flat, weakly concave, or strongly concave, sometimes most strongly excavate medially such that node almost bilobed; petiolar node often dorsally attenuated and posterodorsally sloping; petiole narrow to very thick anteroposteriorly; in dorsal view petiolar node rectangular to rhomboid, sides parallel to strongly diverging posteriorly; petiolar spiracles opening ventrally, spiracular openings large and round, elliptical, or reniform; anterior disc of petiolar sternite entire, undivided; subpetiolar process variable, from a very small, rounded disc to a strongly projecting, digitate to triangular lobe, when well-developed often with a posteromedial groove at the attachment of the process to the sternite.

Abdominal segment 3 either much longer than abdominal segment 4, subequal in length, or clearly shorter; helcium axial; segment overall roughly campaniform, typically widest just anterad posterior margin; abdominal tergite 3 slightly to strongly prolonged anteriorly past anterior edge of sternite; abdominal sternite 3 concave, sloping, or rounded in profile, with a somewhat distinct to very distinct anterior face, anterior face posteriorly depressed, ventral face with a distinctly elevated anterior border, anterior border flat to deeply concave in ventral view, border variably smooth or with prora, prora narrowly carinulate to strongly raised, either following curvature of border or forming a distinct, rectangular medial plate; abdominal sternite 3 variably evenly increasing in depth posteriorly, with a broad and smooth but differentiated posteromedial lobe, with a broad medial ridge widening to a lobe posteriorly, or with medial ridge narrow and carinate anteriorly; when present, medial carina in profile rounded or squared with distinct anterior face, carina sometimes anteriorly surpassing prora.

Abdominal segment 4 vaulted, roughly to clearly in the shape of a quarter-sphere; abdominal sternite 4 anteriorly either overall sloping to rounded, with a small groove accommodating the posterior margin of abdominal sternite 3, or nearly right-angled, forming a large lip overlapping the posterior margin of abdominal sternite 3.

Sculpture highly variable, but often predominantly punctate-reticulate to foveolate-reticulate or alveolate to areolate; sculpture of abdominal segment 4 typically reduced relative to abdominal segment 3.

Setation variable but unspecialized except for mandibular setae when present.

[Note: all values of palp formula besides 6,4 (Keller 2011) are from Sosa-Calvo and Longino (2008). Keller (2011) noted that this apparent diversity of counts could be due to miscounting and we concur.]

Afrotropical Species Complexes

In this study, we focused on the material from the Afrotropics available to us. As noted above, Brown (1958a) already grouped the then-known species of *Discothyrea* into two complexes. Our examinations clearly confirm the *D. oculata* and *D. traegaordhi* complexes since they are significantly divergent in their respective morphology (Fig. 5). However, on the basis of preliminary analyses of limited material from other regions, we are confident that there at least one or two more complexes found in the Indo-Malayan region and Oceania. We do not define or discuss them in detail due to the scarcity of material available to us and the focus of this study on the Afrotropical region.

Discothyrea oculata Species Complex

Diagnosis

Frontal carinae produced as a broad, elevated plate, rhomboid in frontal view, roof-like in profile; deep scrobal area present, defined medially and anteriorly by the lateral margins of the frontal carinae, extending posteriorly to just anterad the eyes; AT3 much longer than AT4 (ASI 46–60; Fig. 2A; eyes present and well developed, with multiple domed ommatidia, eyes protruding from head (even if weakly so); eyes sometimes large; sculpture very coarse, predominately alveolate to foveate; ventrolateral surface of head with two rounded to subconical tumuli; ventral head surface posteromedially flattened, with reduced to absent sculpture; mesal face of mandible with row of large, broadened setae; petiole broadly disciform to hemispherical in profile, anterior face gently curved, not dorsally anteroposterioly attenuated, subcircular in anterior view; AS3 with anterior concavity bordered anteriorly by prora.

[See Fig. 5A–D for illustrations of diagnostic characters given above.]

Notes

The *oculata*-complex is represented in Africa by two species only: *D. mixta* and *D. oculata*. Despite this low number of species compared with the *D. traegaordhi* complex, both species are very widespread and have the broadest distribution ranges within the genus in this region (Fig. 4A and B). This distinctive complex is the only group present in Madagascar and is well represented in the Oriental and Indomalayan regions, while it is completely absent in the New World. Interestingly, the only species of *Discothyrea* for which detailed natural history data are available (*D. kamiteta, D. mixta, D. oculata*) are species of this complex. It is possible that the distinctive morphology of the complex, particularly the shape of the frontal carinae, deep scrobes and the modified mandibular setae, the deeply alveolate or areolate sculpture, the proportion of abdominal segments 3 and 4, and the anterior development of abdominal sternite 3, is related to oophagy and claustral lestobiotic colony foundation.

Discothyrea traegaordhi Species Complex

Diagnosis

Frontal carinae fused for most of their extent, reduced to a narrow medial lamella, platelike to triangular in profile, apex rounded to acute; linear in frontal view; antennal scrobes absent; AT3 never as long as in *D. oculata* complex (ASI 85–183; Fig. 2C and D); eyes variably developed: either absent, a pigmented spot, or if larger, ommatidia flattened, hence eye not protruding from head; sculpture variable; ventrolateral surface of head without distinct processes; petiole variable, dorsally attenuated anteroposteriorly or broadly cuneate; not disciform or hemispherical in profile, outline usually pentagonal in anterior view, sometimes rectangular or hexagonal or dorsally rounded.

[See Fig. 5E–H for illustrations of diagnostic characters given above.]

Notes

The *traegaordhi* complex is comparatively species-rich with 18 of the 20 known Afrotropical *Discothyrea*. Compared to the two species of the *D. oculata* complex, most species in this complex tend to have rather restricted distribution ranges, with some species apparently endemic to single localities (Fig. 4C–T). The few species that are widespread still have significantly smaller ranges than the two members of the *D. oculata* complex. Based on a preliminary

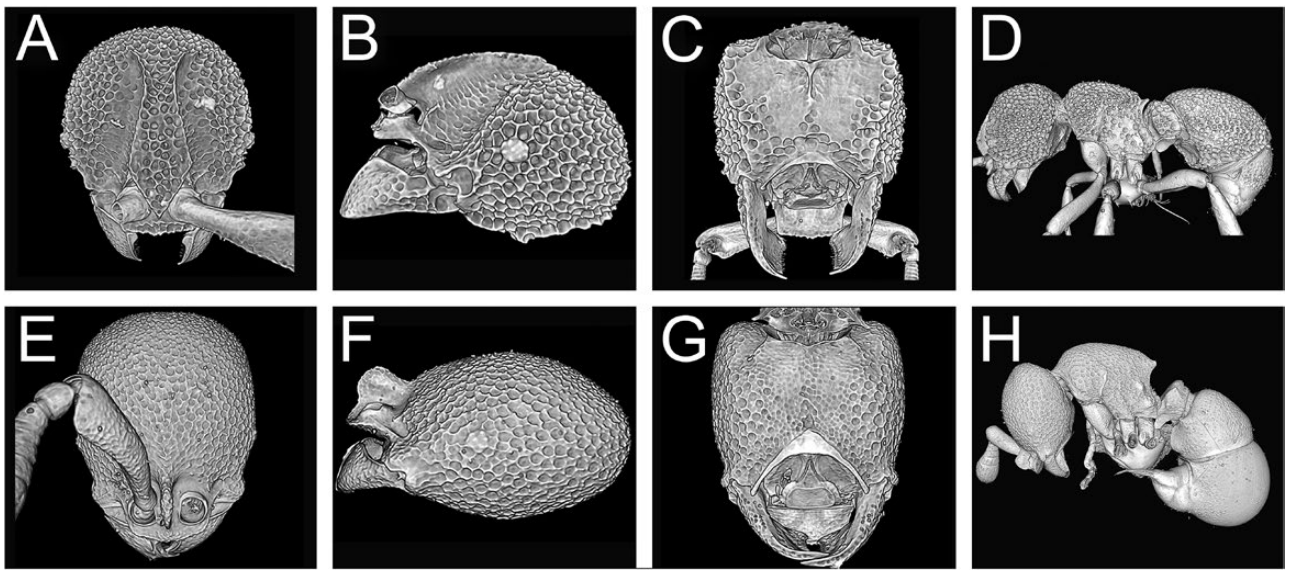

Fig. 5. Still images from surface display volume renderings displaying the general morphology of both species complexes. *Discothyrea oculata* complex, *D. mixta* (CASENT0285473): (A) head in full-face view, (B) head in profile, (C) head in ventral view, (D) body in profile. *Discothyrea traegaordhi* complex, *D. wakanda* (CASENT0790326): (E) head in full-face view, (F) head in profile, (G) head in ventral view, (H) body in profile.

assessment, the majority of species worldwide appear to belong to this complex. If true, then this might be the most widespread complex within the genus, representing all of the New World species, most of the Afrotropical fauna, as well as most species from Australia and Oceania. Its members, however, are apparently absent from the Malagasy, Oriental and Indomalayan regions.

Synoptic List of Afrotropical Species

Discothyrea oculata **Species Complex**
Discothyrea mixta Brown, 1958a
Discothyrea oculata Emery, 1901
= *Discothyrea oculata* var. *sculptior* Santschi, 1913 **syn. n.**

Discothyrea traegaordhi **Species Complex**

Discothyrea aisnetu Hita Garcia & Lieberman **sp. n.**
Discothyrea athene Hita Garcia & Lieberman **sp. n.**
Discothyrea chimera Hita Garcia & Lieberman **sp. n.**
Discothyrea damato Hita Garcia & Lieberman **sp. n.**
Discothyrea dryad Hita Garcia & Lieberman **sp. n.**
Discothyrea gaia Hita Garcia & Lieberman **sp. n.**
Discothyrea gryphon Hita Garcia & Lieberman **sp. n.**
Discothyrea hawkesi Hita Garcia & Lieberman **sp. n.**
Discothyrea kalypso Hita Garcia & Lieberman **sp. n.**
Discothyrea maia Hita Garcia & Lieberman **sp. n.**
Discothyrea michelae Hita Garcia & Lieberman **sp. n.**
Discothyrea patrizii Weber, 1949
Discothyrea penthos Hita Garcia & Lieberman **sp. n.**
Discothyrea poweri (Arnold, 1916)
Discothyrea schulzei Hita Garcia & Lieberman **sp. n.**
Discothyrea traegaordhi Santschi, 1913
= *Discothyrea hewitti* Arnold, 1916 **syn. n.**
Discothyrea venus Hita Garcia & Lieberman **sp. n.**
Discothyrea wakanda Hita Garcia & Lieberman **sp. n.**

Morphological Characters of Taxonomic Importance

Despite the previous considerable lack of useful taxonomic characters for *Discothyrea*, our data show that the Afrotropical fauna is especially rich in morphological characters of high diagnostic value. All body parts investigated have numerous external morphological characters that varied moderately to greatly among species while being highly stable intraspecifically (Figs. 6–14). Overall, we observed a remarkable diversity in the shape of mandibles (Fig. 8; see section about Mandibles below), the cephalic capsule (Fig. 6 and 7), the mesosoma (Figs. 9 and 10), and the metasoma (Fig. 12). Furthermore, some surface areas that are commonly covered by hairs or difficult to examine, such as the anterior clypeus (Fig. 6) or the propodeal declivity (Fig. 11), proved to have some informative variation in character states. The complete removal of pilosity through 'virtual shaving' also showed that there are noticeable differences in surface sculpturing between species, although it must be noted that there is some considerable intraspecific variation in some species. Despite most species possessing a dense pelt of pilosity/pubescence, which appears to be very species-specific, there was some significant variation among several species, especially with the expression of standing pilosity (Fig. 14).

In the following, we present numerous diagnostic image plates displaying this morphological diversity (Figs. 6–12). Each body part was virtually sectioned and dissected from the remainder of the specimen to permit a better examination. These diagnostic plates not only illustrate and aid the identification key provided below, but also serve as a general overview of morphological characters of taxonomic importance and can be used by future taxonomists, parataxonomists, or ecologists to compare whole specimens or body parts in order to quickly gain a better understanding of the species studied.

Mandibles

The main groundplan within *Discothyrea* seems to consist of an edentate triangular mandible with a pronounced blunt carina along its masticatory margin, as can be seen in most African species. Prior to this study, the lack of dentition was considered an autapomorphy of *Discothyrea* (Bolton 2003). However, unexpectedly, we found that two species actually possess teeth/denticles on the apical third of the masticatory margin, namely *D. chimera* (Fig. 8E) and *D. gryphon* (Fig. 8I). While the tooth on the mandible of *D. chimera* is very pronounced and rather large it is definitely smaller and more of a denticle in *D. gryphon*. Furthermore, *D. chimera* also has a small but acute prebasal denticle at the corner between the basal margin and the masticatory margin. This prebasal denticle is also conspicuously visible in *D. damato* (Fig. 8F), *D. dryad* (Fig. 8G), and *D. schulzei* (Fig. 8Q). Several other species, such as *D. athene* (Fig. 8D), *D. hawkesi* (Fig. 8J), and *D. kalypso* (Fig. 8K), have something like a blunt prebasal protuberance on the masticatory margin, located basally close to the corner to the basal margin of the mandible. The masticatory margin appears to be variably shaped from species to species with a more or less pronounced ectal carina that may run the whole length of the margin (in most species) or be interrupted, as in *D. traegaordhi* (Fig. 8R) and *D. wakanda* (Fig. 8T). The latter species also possesses a second, more irregularly shaped carina basally and medially. Another feature not expected before this study is the variety in overall shape and aspect ratio, since some species, such as *D. mixta*, have rather elongated mandibles with a short basal margin and a long masticatory margin, whereas other species, such as *D. maia*, possess a shorter mandible with a long basal margin and a short masticatory margin. There seems to be gradual cline leading from the former to the latter. This higher than expected diversity of mandibular shapes presents the opportunity to apply additional taxonomic characters of high diagnostic value for the species descriptions and the identification key.

Antennomere Count

Our results show that in contrast to the external morphology, the internal structure of *Discothyrea* antennae is consistent and provides a reliable antennomere count. However, as expected, this value often differs from that obtained through surface examination and, in at least *D. mixta* and *D. poweri*, from that given in the original description (Table 2). In the generalized state, each flagellomere has a simple, internal sclerotic ring at its base which connects to a simple internal preapical ring toward the distal end of the prior flagellomere. Externally, adjacent flagellomeres overlap only at the junction of the internal rings, which usually constitute around one-third at most of the subsegment's length and are numerically congruent with the external flagellomere count (Fig. 15). Internally, the sclerotic annuli form a cylindrical channel through which the two branches of the antennal nerves run. The flagellomeres are apparently connected by membranes between the distal and proximal outer walls of adjacent subsegments, by conjunctiva of the internal rings, or by both.

In *Discothyrea*, the flagellomeres take two distinct forms. The proximal flagellomeres are extremely simplified, with a single internal annulus per flagellomere, i.e., the basal and distal rings are not disparate. Two or three of the distal flagellomeres proximal to the club, which itself comprises a single hypertrophied subsegment, have

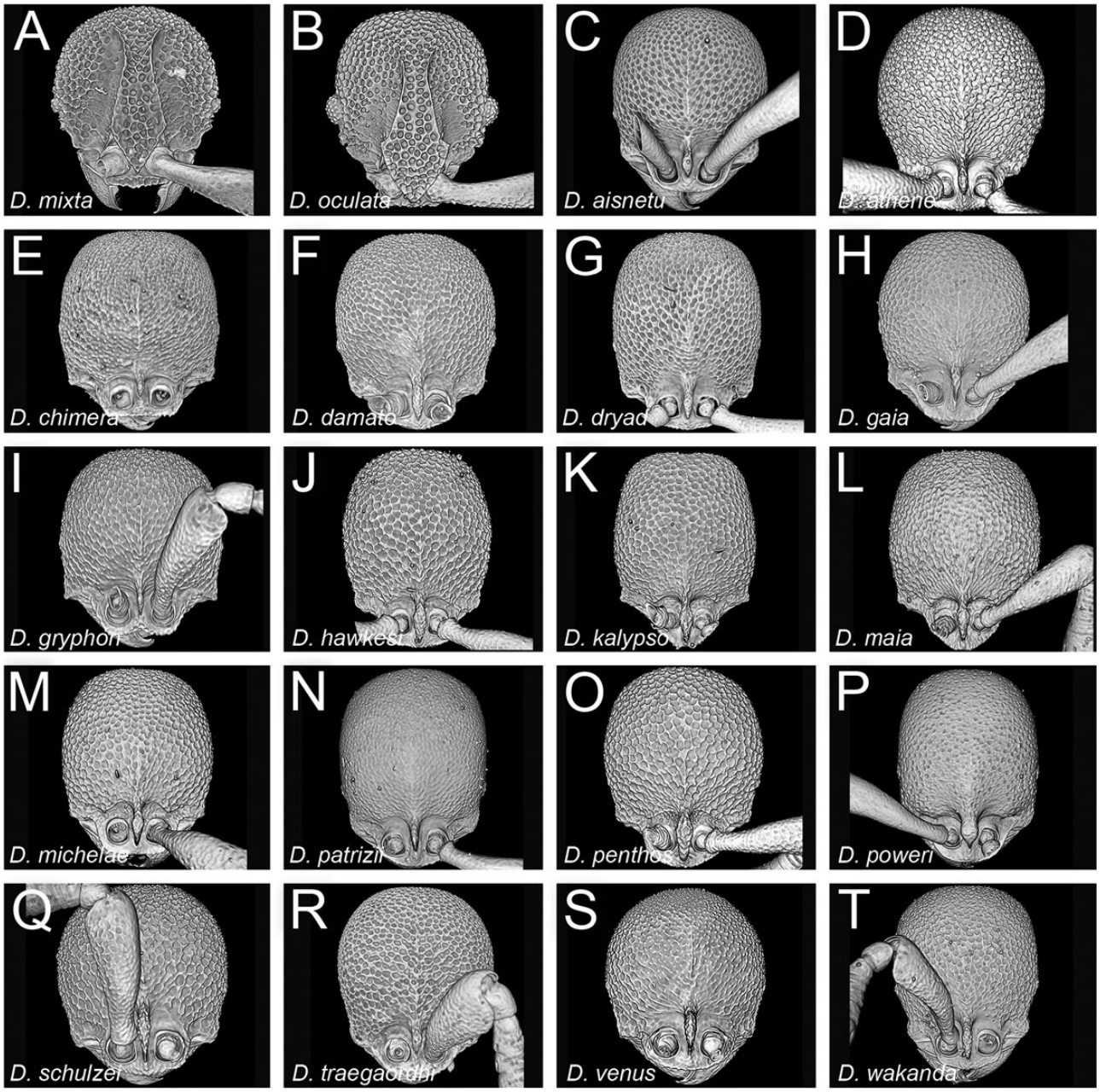

Fig. 6. Diagnostic plate showing still images from surface volume renderings of the head in full-face view (the remainder of the body virtually removed). All Afrotropical species are shown, species names are embedded in each particular image for better comparison and orientation. Specimen codes are given in Table 1.

the internal annuli deeply invaginated, while the entire flagellomere is reduced in length, so that most of the outer wall of a flagellomere rests within a fold of the prior subsegment (Fig. 15D, E, and G–I). The internal channel is therefore highly imbricated, unlike in other ants (Fig. 16). These distal flagellomeres are typically relatively distinct and countable externally. The simple, proximal flagellomeres are tightly fused at their apical and distal margins, and the external plates of these subsegments overlap strongly, such that a single externally apparent subsegment may actually correspond to several internal divisions (Fig. 15H and I). All Afrotropical *Discothyrea*, as well as *D. banna* from and *D. diana* from China, and an undescribed species from Samoa, possess the deeply infolded structure of the distal 2–3 antennomeres and the fusion of the proximal flagellomeres. In *D. gryphon*, which with six antennomeres has the fewest in the Afrotropical fauna, the infolded subsegments plus the club comprise the entire flagellum (Fig. 15I). We therefore hypothesize that reduction in antennomere count in *Discothyrea* takes place through the progressive fusion of subsegments proximal to these modified flagellomeres.

Frontoclypeal Structure

Identifying the homology of elements of the frontoclypeal structure of *Discothyrea* is complicated by its extremely derived morphology. External anatomical landmarks used to differentiate the frons and clypeus in nearly all other ants—namely, the antennal insertions, the anterior tentorial pits, and the epistomal sulcus—are concealed, lost, or highly modified in *Discothyrea*. The frontal region bears the antennae, which are inserted posterad or in line with the anterior tentorial pits in all genera except *Discothyrea* (and the proceratiine *Problomyrmex*), in which the antennae are located far anterad the

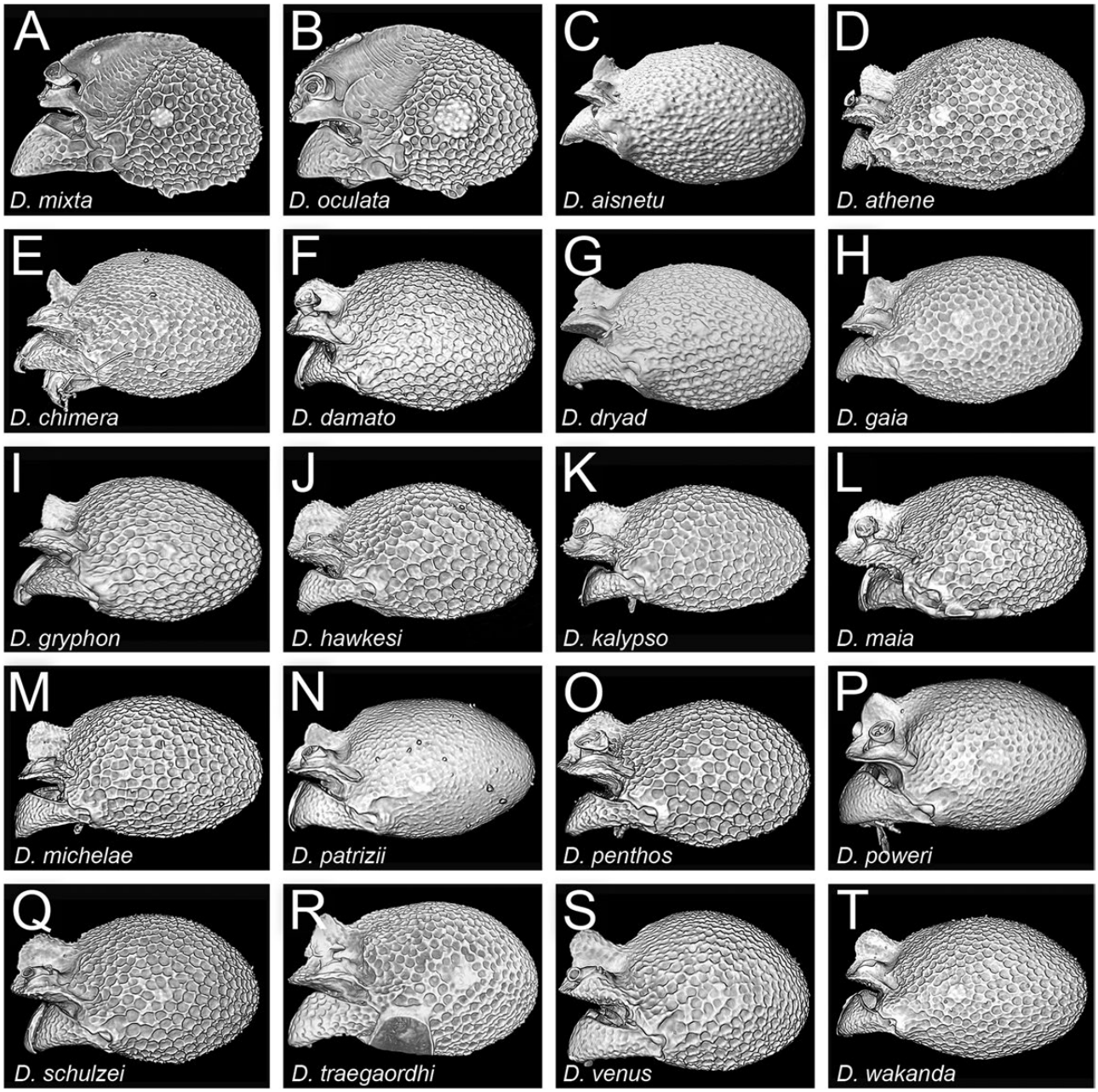

Fig. 7. Diagnostic plate showing still images from surface volume renderings of the head in profile (the remainder of the body virtually removed). All Afrotropical species are shown, species names are embedded in each particular image for better comparison and orientation. Specimen codes are given in Table 1.

anterior tentorial pits. The anterior tentorial pits themselves are located in the usually clearly defined epistomal sulcus corresponding to the internal epistomal ridge connecting the anterior tentorial arms; in *Discothyrea* this sulcus is completely absent. In contrast to the challenges of interpreting frontoclypeal morphology based on external characters, virtual dissection enabled clarification of the structure's composition through comparison of the preoral and pharyngeal skeletomusculature. Despite the high degree of fusion, migration, and modification of the frons and clypeus, the endoskeletal and muscular elements are quite consistent and can be easily identified in the context of the Hymenopteran groundplan.

The frons is intimately fused to the clypeus and anteriorly prolonged over the clypeo-labral articulation. In most species, the clypeus itself is reduced to a thin, sinuate strip that externally contains the anterior tentorial pits and constitutes the anteriormost portion of the shelf overhanging the mandibles. Internally the anteromedial disc of the clypeus is located by the elongated dorsal cibarial dilators, which arise solely from this disc and insert on the distal wall of the cibarium (Fig. 17). The frontal region is located by the antennal insertions and by the origin of several muscle groups, described in detail below. The prominent, posteromedial portion of the frontoclypeal structure, variously produced as a lamella in the *traegaordhi* complex, as a broad rhomboid platform in the *oculata*-complex, and as a triangular to rhomboid swelling in most Asian species, belongs to the frons; because the structure is not derived from the toruli, it is interpreted to comprise the modified, anteromedially fused frontal carinae. The medial portion of the shelf, which usually projects anteriorly past the fusion of the frontal carinae, is also

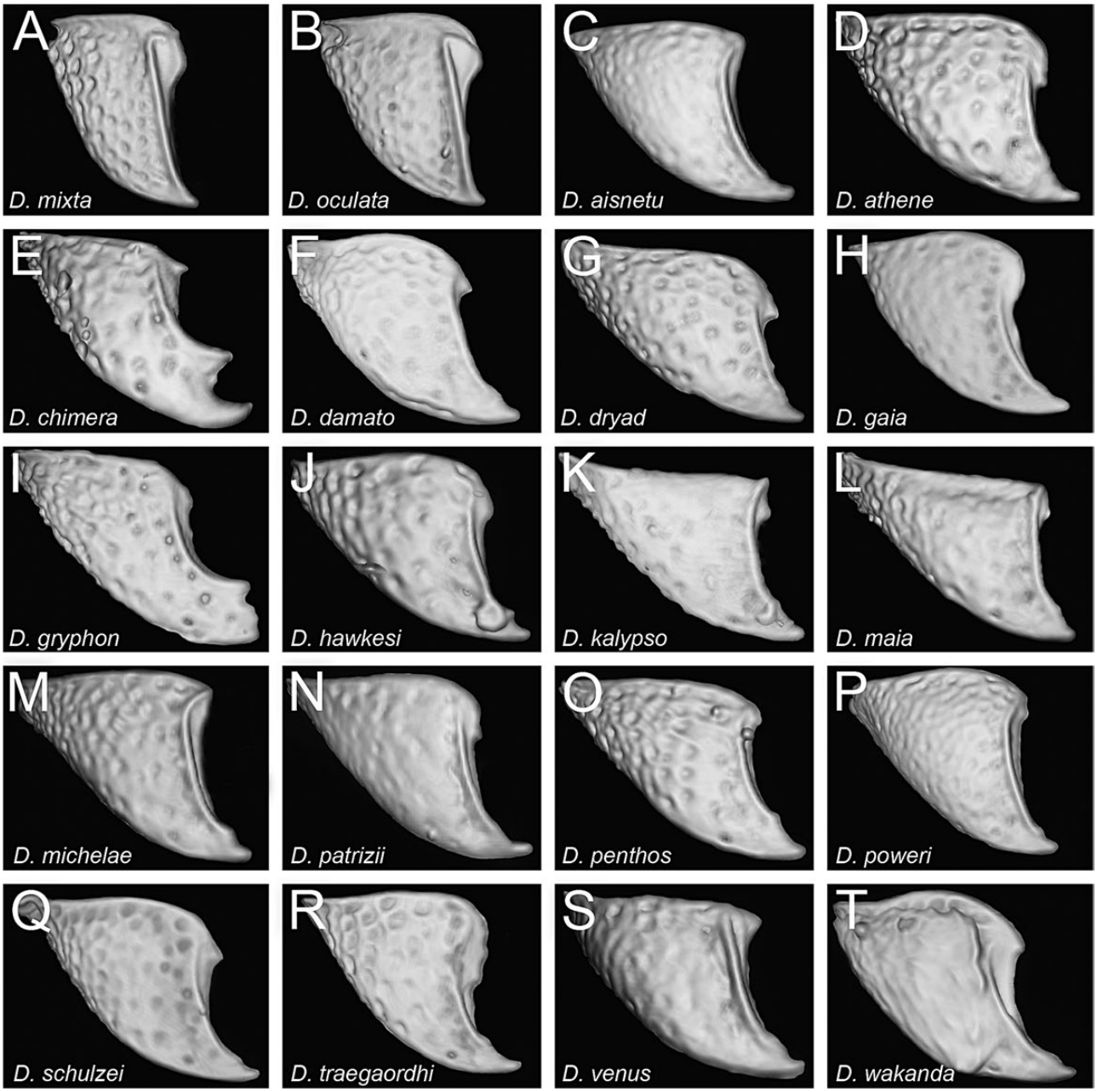

Fig. 8. Diagnostic plate showing still images from surface volume renderings of the right mandible in dorsal view (the remainder of the body virtually removed). All Afrotropical species are shown, species names are embedded in each particular image for better comparison and orientation. Specimen codes are given in Table 1.

formed by the frons, which is delimited anteriorly and laterally by the antennal sockets. An anterior section of the head shows both the narrow space left between the ventral face of the frons and the dorsal face of the clypeus and the anterior fusion and posterior expansion of the frontal carinae (Fig. 17G and H).

Three nonclypeal muscle groups are identified which locate the frons. The dorsal pharyngeal dilators originate just anterad the retractors of the mouth angle which arise from the cephalic dorsum (Fig. 17B, C, and F). The posterior labral retractors, located distal to the dorsolateral arms of the sitophore, originate around the midpoint of the elevated frontal carinae in the *oculata*-complex (Fig. 17D), and posterior to the carinae in the *traegaordhi*-complex (Fig. 17E). The frontal lamella apparently lacks musculature (Fig. 17E and F).

Identification Key to Afrotropical *Discothyrea* Species (Workers)

1. Frontal carinae produced as a broad, elevated rhomboid plate, roof-like in profile (Fig. 5A and B); antennal scrobes present, deep, extending from antennal insertions to just anterad the eye (Fig. 5E and F); eye present, well-developed with multiple silvery globose ommatidia protruding from head (even when eye small) (Fig. 6A and B); AT3 much longer than AT4, around 1.9 to 2.2 times (ASI < 60) (Fig. 2A). [*D. oculata*-complex].....2
- Frontal carinae reduced to thin medial lamella, broadly lobate to acutely triangular in profile (Fig. 5E and F); antennal scrobes absent (Fig. 5E and F); eye variable: either absent, a simple pigmented spot, or if with multiple ommatidia, if the latter then

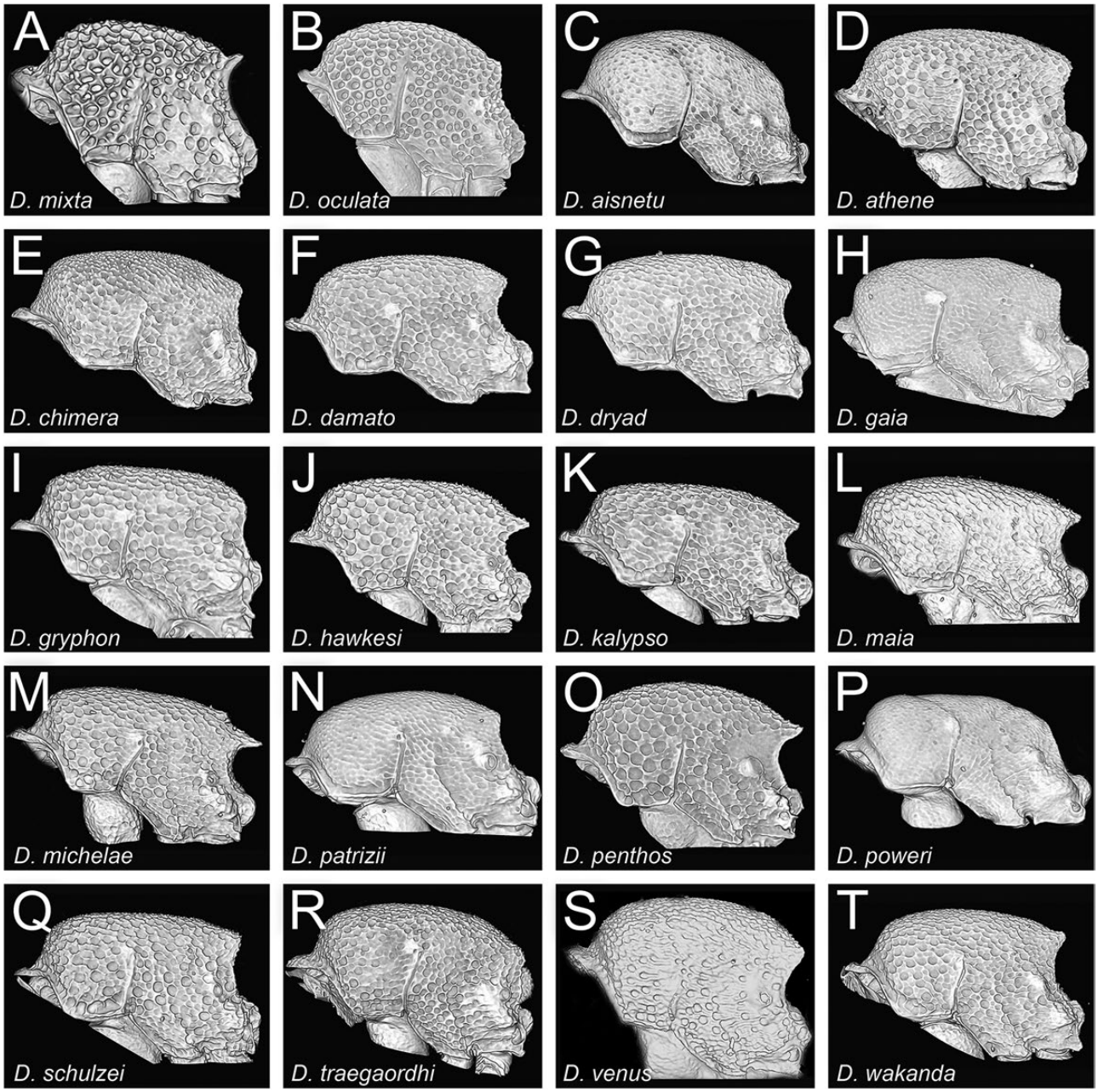

Fig. 9. Diagnostic plate showing still images from surface volume renderings of the mesosoma in profile (the remainder of the body virtually removed). All Afrotropical species are shown, species names are embedded in each particular image for better comparison and orientation. Specimen codes are given in Table 1.

eye small and ommatidia flattened, not protruding from head (Fig. 6C–T); AT3 never as long as above, usually AT3 equal in length or shorter than AT4, sometimes AT3 up to 1.2 times longer than AT4 (ASI 85–168) (Fig. 2B and C). [*D. traegaordhi*-complex].....3

2. Eyes small (OI 5–9), situated laterally on gena (Figs. 6A and 7A); propodeum angulate to dentate, angles subtended and medially joined by narrow carinulae such that propodeum laterally and dorsally marginate (Fig9A); propodeal declivity with median carina but without costae or rugae (Fig. 11A). [Angola, Cameroon, Central African Republic, Democratic Republic of Congo, Ghana, Ivory Coast, Kenya, Liberia, Mozambique, Tanzania, South Africa, Uganda].....*D. mixta*
- Eyes large (OI 14–16), situated anterolaterally on gena (Figs. 6B and 7B); propodeum not angulate or dentate (though declivity concave), lacking carinulae and not marginate (Fig. 9B); propodeal declivity deeply costate to rugose. (Fig. 11B). [Cameroon, Democratic Republic of Congo, Ghana, Guinea, Ivory Coast, Kenya, Mozambique, Nigeria, Tanzania, Zimbabwe].....*D. oculata*
3. Mesotibia with conspicuous apicoventral spur (Fig. 13A–C).....4
- Mesotibia without a conspicuous apicoventral spur; either apically unarmed or with small, distinct seta inserted in apicoventral pit (Fig. 13D–F).....6
4. Dense layer of appressed pubescence with numerous short, but conspicuously standing setae present on abdominal terga (Figs. 14H and 33A); mandible without prebasal angle or denticle (Fig. 8H). [Zimbabwe].....*D. gaia*
- Abdominal terga without any standing setae, only with appressed pubescence (Fig. 14P and R); mandible with small

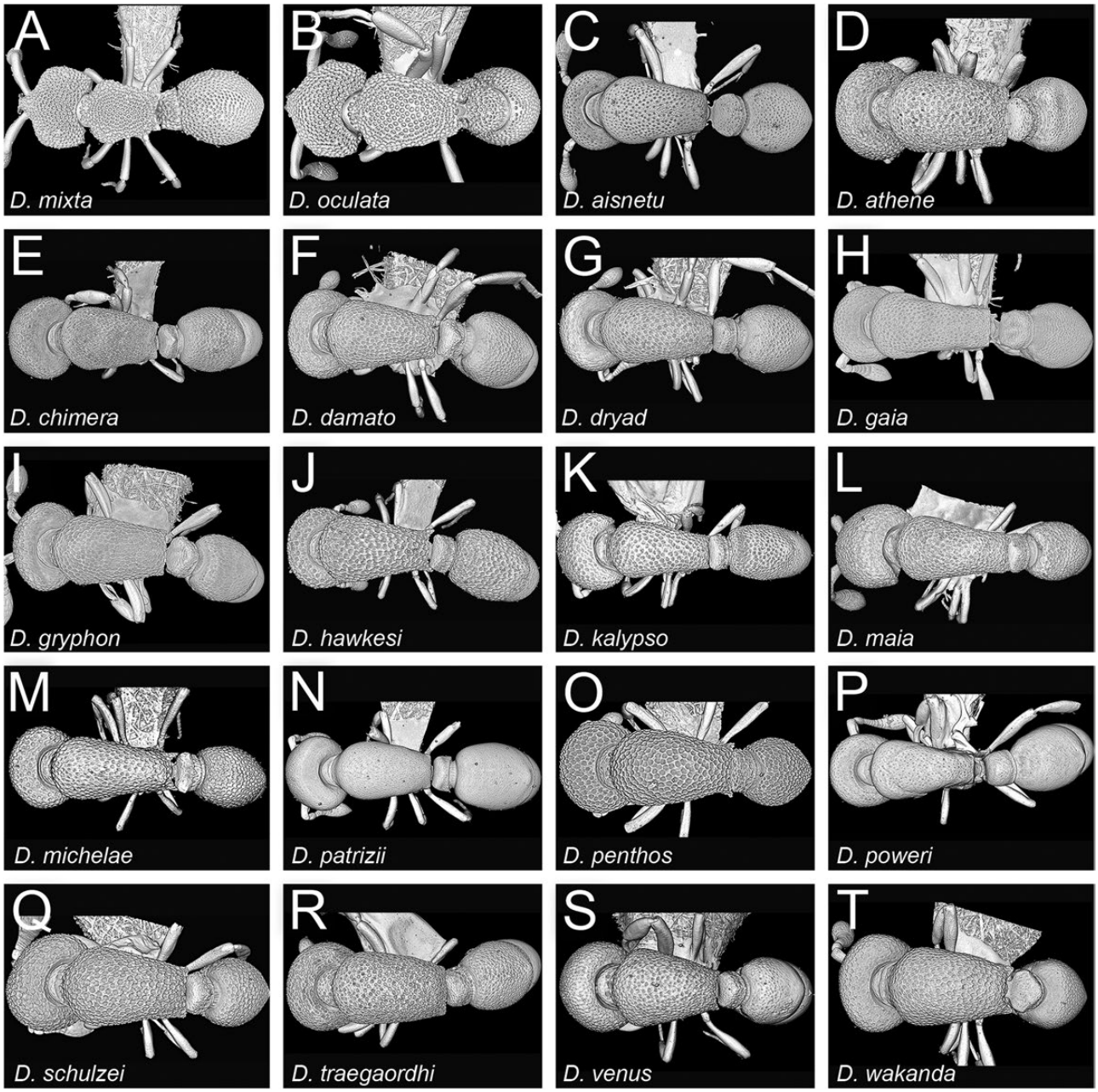

Fig. 10. Diagnostic plate showing still images from surface volume renderings of the body in dorsal view with focus on mesosoma. All Afrotropical species are shown, species names are embedded in each particular image for better comparison and orientation. Specimen codes are given in Table 1.

prebasal denticle (Fig. 8P) or prebasal irregularly shaped median carina (Fig. 8R).....5

5. Generally larger species (WL 0.67–0.84); antennal scapes longer (SI 61–68); legs longer (HFI 61–69); petiole exceptionally thick (DPeI 135–173; LPeI 152–194) (Figs. 50A, B, and 51L); mandible with small, sharp prebasal denticle (8P); sculpture shallow overall, especially smooth on clypeus, propodeal declivity, petiole, and AT3 (Figs. 6P, 9P, 10P, and 12P). [South Africa].....*D. poweri*
- Generally smaller species (WL 0.51–0.57); antennal scapes shorter (SI 50–55); legs shorter (HFI 54–58); petiole thinner (DPeI 235–289; LPeI 236–313) (Figs. 54A, B, and 55L); mandible with broad prebasal irregularly shaped median carina (Fig. 8R); sculpture coarser overall, especially on clypeus, propodeal declivity, petiole, and AT3 (Figs. 6R, 9R, 10R, 12R). [South Africa] .....*D. traegaordhi*
6. Larger species (HW 0.57–0.61; WL 0.80–0.90); mesosoma high-rounded, profile extremely convex (Fig. 9C); propodeum rounded to weakly angulate; first mesotarsomere very elongated, about as long as remaining tarsomeres taken together (Fig. 24R). [Tanzania].....*D. aisnetu*
- Smaller species (HW 0.30–0.49; WL 0.38–0.59); mesosomal profile usually ranging from almost flat to weakly moderately convex (Fig. 9D, F, G, J–M, Q, and T); if mesosoma well rounded, then propodeum conspicuously dentate (Fig. 9O and S); first tarsomere variable in length but never as long as above, usually subequal to tarsomeres II–IV taken together (Figs. 26R, 28R, 32R, 36R, 38R, 40R, and 57R).....7

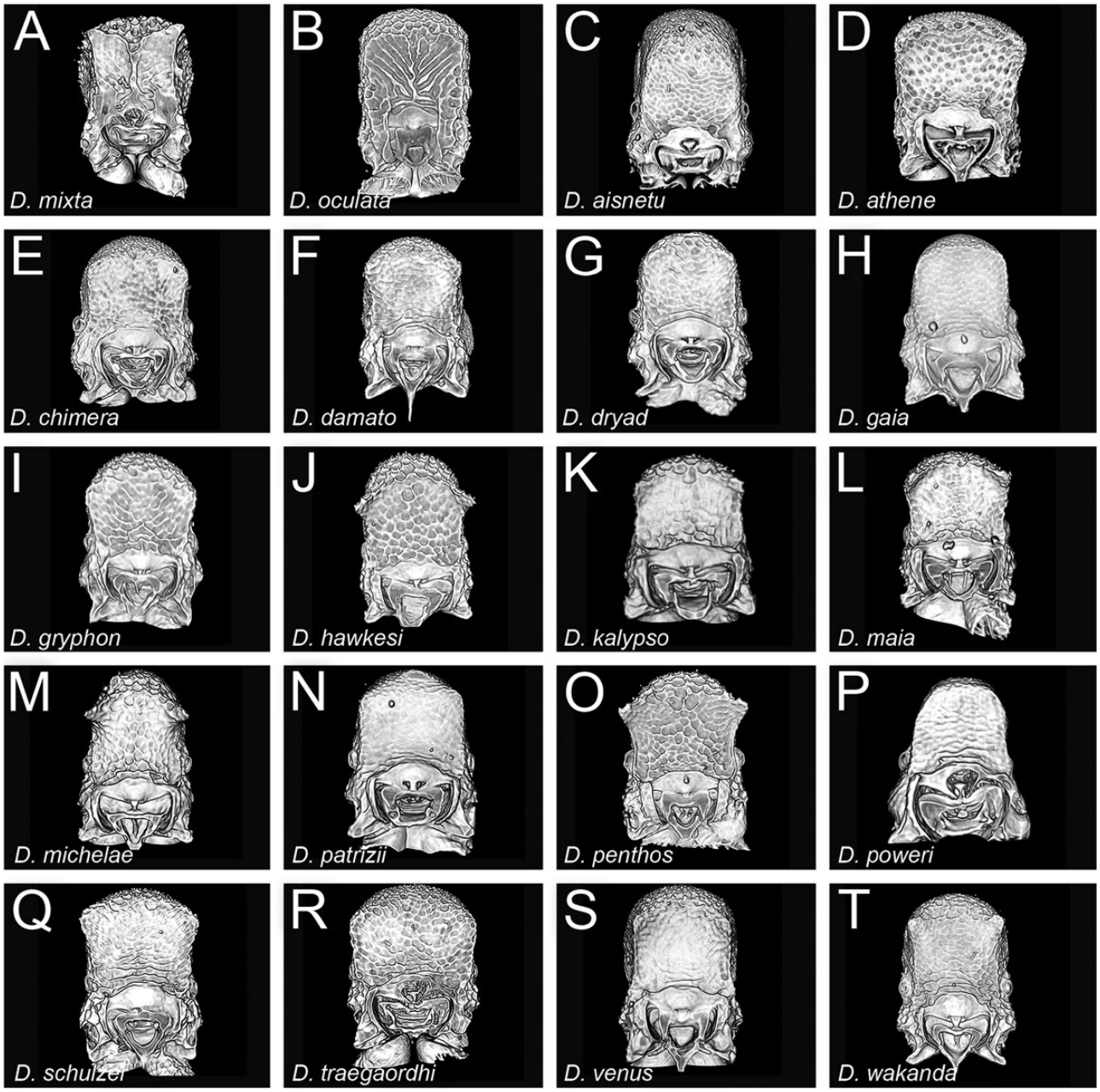

Fig. 11. Diagnostic plate showing still images from surface volume renderings of the posterior propodeum in posterior view (the remainder of the body virtually removed). All Afrotropical species are shown, species names are embedded in each particular image for better comparison and orientation. Specimen codes are given in Table 1.

7. Masticatory margin of mandible with a prominent, well-developed preapical tooth, clearly larger than prebasal denticle or acute basal angle (8E, I); head very broad, subquadrate (CI 87–92), anterolateral corners of gena angulate to denticulate (Fig. 6E and I).....8
- Masticatory margin of mandible without preapical tooth, or if small preapical denticle or angle present, then not well-developed and not clearly larger than prebasal denticle or acute basal angle (Fig. 8D, F, G, J–M, O, Q, S, T); head not as above: usually not as broad (CI 77–89), and anterolateral corner of gena not angulate (Fig. 6D, F, G, J, L, M, O, Q, S, T); if gena somewhat angulate, then head especially elongate (CI 78) (Fig. 6K).....9
8. Dorsal surfaces and antennal scape without standing pilosity, with appressed or decumbent pubescence only (Figs. 14E and 27A); medial clypeus transverse in frontal view (Fig. 6E); eye larger (OI 6); preapical mandibular tooth exceptionally large, strongly curved; apical angle of mandible acute (Fig. 8E). [Tanzania].....*D. chimera*
- Standing pilosity present and abundant on all dorsal surfaces and antennal scape (Figs. 14I and 35A); medial clypeus emarginate in frontal view (Fig. 6I); eye absent or tiny (OI 0–4); preapical mandibular tooth smaller and not strongly curved; apical angle of mandible squared to notched (Fig. 8I). [Rwanda, Tanzania].....*D. gryphon*
9. AT4 conspicuously enlarged, bulbous, much larger and longer than AT3 (ASI 158–183) (Fig. 12S); posterior propodeum laterally and dorsally strongly concave; declivitous face of propodeum mostly smooth, ventral portion transversely substrigulate, clearly

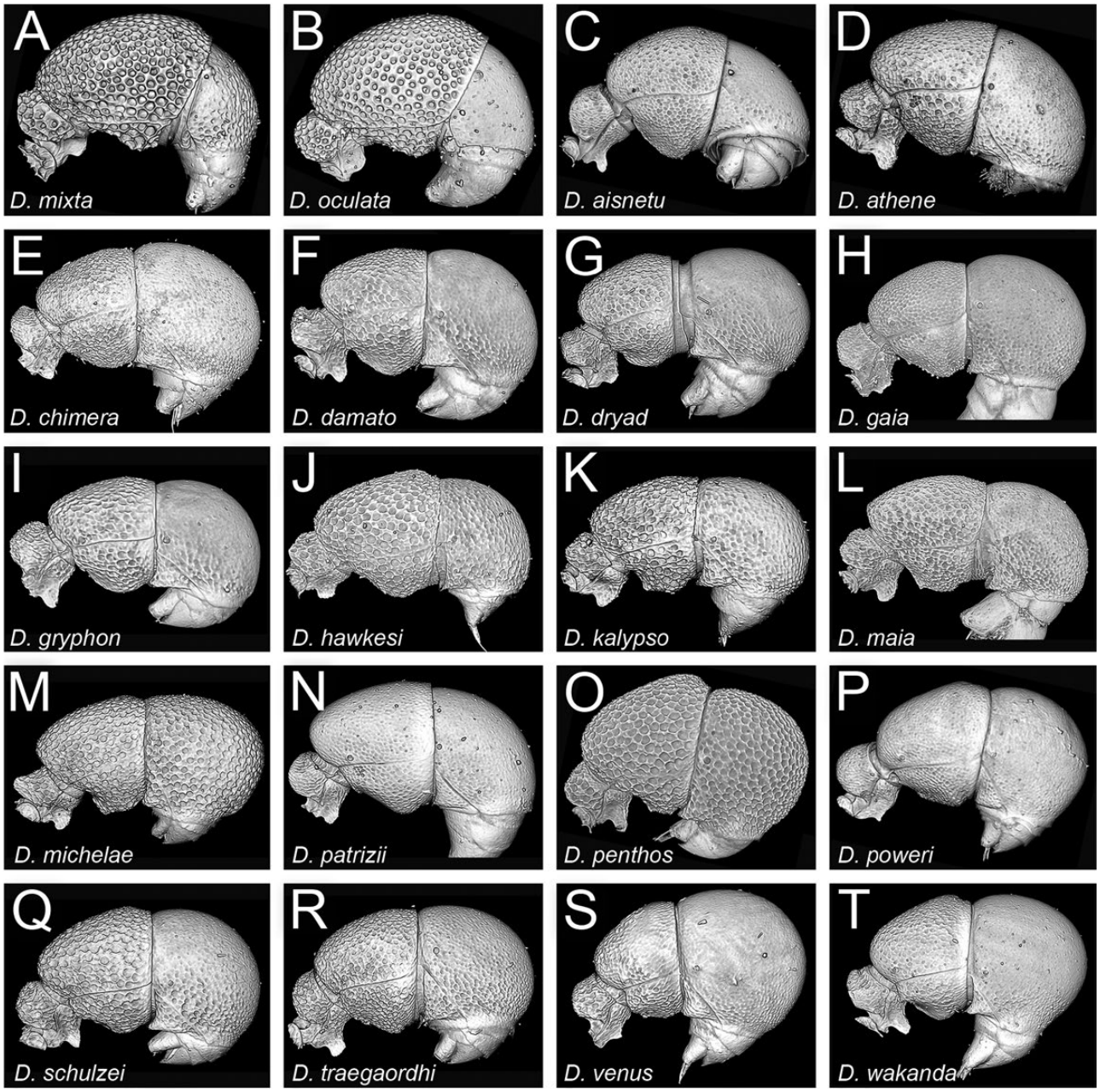

Fig. 12. Diagnostic plate showing still images from surface volume renderings of the petiole and gaster in profile (the remainder of the body virtually removed). All Afrotropical species are shown, species names are embedded in each particular image for better comparison and orientation. Specimen codes are given in Table 1.

differently sculptured than remainder of mesosoma. [Angola, Cameroon, Ghana, Ivory Coast, Uganda] .....*D. venus*

- Character combination never as above; AT4 equal in length to AT3, or if longer then ratio smaller (ASI 100–142) (Fig. 12D, F, G, J–M, O, Q, and T); posterior propodeum variably shaped; declivitous face of propodeum variable, but usually entire surface well-sculptured or entire surface smooth 10

10. Mesosomal and abdominal dorsa with standing pilosity (sometimes best seen in silhouette or on AT4 in dorsal view, but visible at low magnification) (Fig. 14G, M, Q, T, 31A, 43A, 52A, and 58A).....11

- Usually mesosomal and abdominal dorsa without standing pilosity, sometimes abdominal dorsa with short, standing pilosity, but then no standing pilosity on dorsum of mesosoma (Figs. 14D, F, J–L, N, O, 25A, 29A, 37A, 39A, 46A, and 48A).....14

11. Propodeum strongly dentate with deeply concave declivity (Fig. 9M); abdominal sternite 3 with strong median ridge anteriorly surpassing prora, appearing distinctly rectangular in profile (Fig. 12M); petiolar outline rectangular with pointed dorsolateral angles, anterior face of petiolar node strongly impressed, appearing bilobed in oblique anterior view (Fig. 44M and N). [Tanzania].....*D. michelae*

- Propodeum denticulate to weakly dentate with only moderately concave declivity (Fig. 9G, Q, and T); abdominal sternite 3 without a median ridge or if ridge present, not anteriorly surpassing prora, sternite not rectangular in pofile (Fig. 12G, Q, and T); petiole pentagonal to hexagonal, never rectangular, anterior face of petiolar node flat to weakly impressed, never appearing bilobed in oblique anterior view (Figs. 32M, N, 53M, N, and 59M, N).....12

Fig. 13. Diagnostic plate showing still images from surface volume renderings of mesotibiae and mesotarsi with mesotibial apicoventral spur, if present, colorized in green. (A) *D. gaia*, (B) *D. poweri*, (C) *D. traegaordhi*, (D) *D. dryad*, (E) *D. maia*, (F) *D. wakanda*.

12. Mesosoma comparatively elongate and slender (DMI2 87–91; LMI 45–49) (Fig. 10G); frontal lamella bladelike, apex angulate in profile. [Kenya].....*D. dryad*
- Mesosoma comparatively robust and stocky (DMI2 93–100; LMI 49–57) (Fig. 10Q and T); frontal lamella disciform to lobate, apex rounded in profile.....13
13. Smaller species (WL 0.47–0.56; HW 0.39–0.44) with eyes smaller or absent (OI 0–3) (Fig. 7Q) and shorter legs (HFI 55–60); sculpture similarly coarse overall, not notably reduced on petiole or abdominal sternite 3 (Figs. 12Q and 59Q). [Rwanda, Uganda].....*D. schulzei*
- Larger species (WL 0.59–0.65; HW 0.50–0.52) with larger eyes (OI 4–7) (Fig. 7T) and longer legs (HFI 63–68); sculpture on petiole and abdominal segment 3 reduced (Fig. 12T), abdominal sternite 3 very smooth medially (Fig. 59T). [Democratic Republic of Congo] .....*D. wakanda*
14. Surface sculpture very reduced, entire body quite smooth with only minute, shallow punctulation (Fig. 9N); propodeum not strongly angulate or denticulate (Fig. 9N) [Kenya, Tanzania]..... .....*D. patrizii*
- Surface sculpture on head, mesosoma, and AT3 well-developed and coarse, predominantly punctate to foveolate-reticulate (Fig. 9D, F, J–L, and O); propodeum angulate to strongly denticulate (Fig. 9D, F, J–L, and O).....15
15. Mesosoma robust and stocky (DMI2 92–102; LMI 47–56) (Fig. 10D, F, and O); head broader (CI 79–89) (Fig. 6D, F, and O).....16
- Mesoma more slender and elongate (DMI2 81–87; LMI 42–53) (Fig. 10J–L); head narrower and more elongate (CI 78–80) (Fig. 6J–L).....18
16. Propodeum dentate, teeth well-developed (Fig. 9O); lateral propodeum with smooth, unsculptured patch dorsad propodeal spiracle (Fig. 9O); abdominal sternite 3 with strongly developed, narrow median ridge, sternite squared in profile (12O); frontal lamella thick and platelike (Fig. 6O), in profile rhomboid with three clearly demarcated faces, lacking basal fenestra (Fig. 7O). [Ivory Coast].....*D. penthos*
- Propodeum angulate but without differentiated teeth (Fig. 9D and F); lateral mesosoma similarly sculptured over entire surface, without distinct smooth patch on propodeum (Fig. 9D and F); abdominal sternite 3 without a median ridge or ridge broad and rounded, sternite sloping to round in profile (12D, F); frontal lamella narrow (Fig. 6D and F), not rhomboid in profile, usually with well-defined basal fenestra (Fig. 7D and F) 17
17. Petiolar outline in anterior view strongly pentagonal with dorsal faces well-defined and very tall triangular peak (Fig. 30M, N); eye absent to small (OI 0–4) (Fig. 7F); AT4 longer than AT3 (ASI 117–128) (Fig. 12F); petiole thicker, less strongly attenuated (DPeI 233–286; LPeI 243–314). [Kenya, Rwanda, Uganda, Democratic Republic of Congo].....*D. damato*
- Petiolar outline in anterior view weakly pentagonal, dorsal faces poorly defined and with low, rounded peak (Fig. 26M, N); eye present, relatively large (OI 5–9) (Fig. 7D); AT4 somewhat shorter than or subequal to AT3 (ASI 85–103) (Fig. 12D); petiole thinner, more strongly attenuated (DPeI 300–500; LPeI 286–500). [Kenya, Mozambique, Rwanda, Tanzania, Uganda].. .....*D. athene*
18. Anterolateral corners of gena rounded, not sharply angulate (Fig. 6J); abdominal sternite 3 without narrow median ridge, sternite sloping in profile with poorly-defined anterior face (Fig. 12J); petiolar outline in anterior view roughly hexagonal, dorsal face flat (Fig. 38M and N). [Tanzania].....*D. hawkesi*
- Anterolateral corners of gena sharply angulate (Fig. 6K and L); abdominal sternite 3 with narrow median ridge, sternite truncate to squared in profile with clearly defined anterior face (Fig. 12K and L); petiolar outline in anterior view roughly pentagonal, dorsally peaked (Figs. 40M, N, and 42M, N).....19
19. Mesosomal profile more robust (LMI 53), dorsum convex, propodeal denticles larger, propodeal declivity more strongly concave (Fig. 9L); legs longer (HFI 65) and very slender, first mesotarsomere elongate, longer than tarsomeres II–IV taken together; antennal scape longer (SI 58). [Zimbabwe].....*D. maia*
- Mesosomal profile more gracile (LMI 42), dorsum sloping posteriorly but not convex, propodeal denticles smaller, propodeal declivity more shallowly concave (Fig. 9K); legs shorter (HFI 51) and not exceptionally slender, first mesotarsomere short, about as long as tarsomeres II–IV taken together; antennal scape shorter (SI 51). [Tanzania].....*D. kalypso*

Revision of the *Discothyrea oculata* Complex

Discothyrea mixta Brown, 1958

(Figs. 2A, 4A, 5A–D, 6A, 7A, 8A, 9A, 10A, 11A, 12A, 14A, 15A, 15F, 15G, 17B, 17D, 17G, 18, 19; Supp Video S1 [online only])

Discothyrea mixta Brown, 1958a: 343.

Type Material

HOLOTYPE, pinned worker, LIBERIA, Bolahun (*L. Bequaert*) (MCZ: MCZ_Holotype_29872) [examined]. **PARATYPES,** three pinned workers with same data as holotype (MCZ: MCZ_Paratype_29872; MHNG: CASENT0911150; USNM) [examined except USNM]

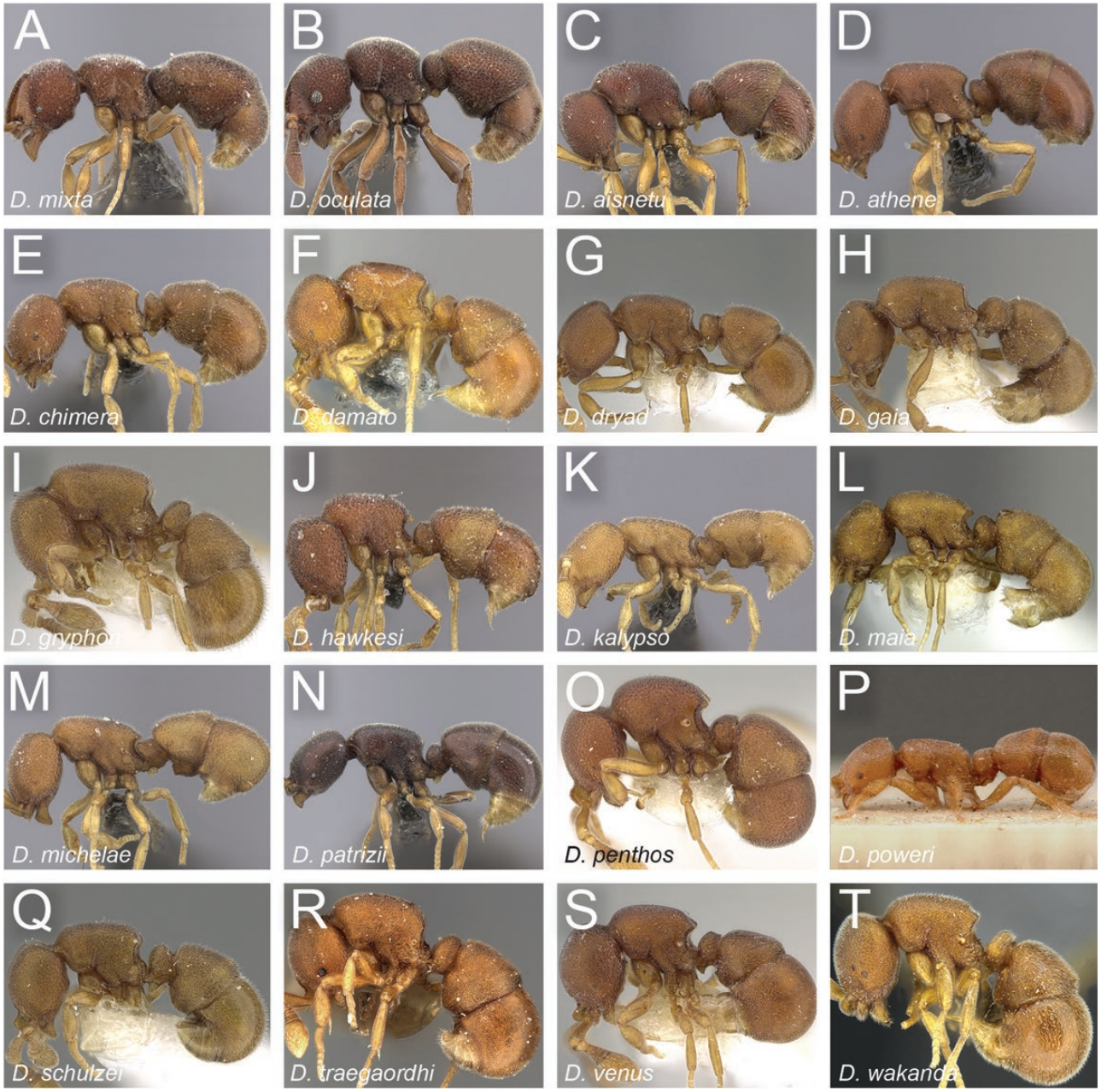

Fig. 14. Diagnostic plate showing differences in body pilosity. (A) *D. mixta* (CASENT0235473), (B) *D. oculata* (CASENT0235467), (C) *D. aisnetu* (CASENT0235475), (D) *D. athene* (CASENT0235476), (E) *D. chimera* (CASENT0235471), (F) *D. damato* (CASENT0247362), (G) *D. dryad* (CASENT0247371), (H) *D. gaia* (CASENT0247040), (I) *D. gryphon* (CASENT0247367), (J) *D. hawkesi* (CASENT0235470), (K) *D. kalypso* (CASENT0235468), (L) *D. maia* (CASENT0790541), (M) *D. michelae* (CASENT0235469), (N) *D. patrizii* (CASENT0235472), (O) *D. penthos* (CASENT0247383), (P) *D. poweri* (SAM-ENT-0011509), (Q) *D. schulzei* (CASENT0247370), (R) *D. traegaordhi* (CASENT0790122), (S) D. venus (CASENT0247017), (T) *D. wakanda* (CASENT0790326). With the exception of F, L, R, T, all other images are from https://www.antweb.org—photographers Michele Esposito and Will Ericson.

Virtual dataset. Volumetric raw data (in DICOM format), 3D rotation video, still images of surface volume rendering, and 3D surface (in PLY format) of a nontype specimen (CASENT0285473) in addition to stacked digital color images illustrating head in full-face view, profile and dorsal views of the body. The data are deposited at Dryad (Hita Garcia et al. 2019, http://doi.org/10.5061/dryad.3qm4183) and can be freely accessed as virtual representation of the species. In addition to the data at Dryad, we also provide a freely accessible 3D surface model at Sketchfab (Model 1).

Nontype Material

ANGOLA: Dundo, R. Mussungue, [–7.3697, 20.813], ca. 630 m, gallery forest, 18.XII.1963 (*Luna-Carvalho*); Dundo, R. Kahingo, [–7.39, 20.51], ca. 650 m, gallery forest, 20.VI.1964 (*Mwaoka*); Route Dundo-Saurimo km 39, 23.XI.1963 (*Luna-Carvalho*); Salazar, [–9.3, 14.916667], ca. 700 m, forest, 9.III.1972 (*P.M. Hammond*); CAMEROON: Abona Mbana, 28.XI.1988 (*A. Dejean*); Ebodjie, [2.63, 9.88], ca. 70 m, 28.X.1991 (*A. Dejean*); Nkoemvon, [2.7517, 11.0814], ca. 630 m, 28.IX.1980 (*D. Jackson*); Mbalmayo, [3.4597, 11.4714], ca. 600 m, XI.1993 (*N. Stork*);

Table 2. Antennomere count given for all Afrotropical species of *Discothyrea*, either based on previous literature (with references in parenthesis), based on visual examination under the light microscope with magnification up to 120× (apparent), or based on virtual dissection (true).

Species	Literature	Apparent	True
D. aisnetu	n.a.	9–11	9
D. athene	n.a.	6–9	9
D. chimera	n.a.	8	7
D. damato	n.a.	8–11	9
D. dryad	n.a.	9–11	9
D. gaia	n.a.	8–9	8
D. gryphon	n.a.	6–8	6
D. hawkesi	n.a.	8–10	9
D. kalypso	n.a.	9	9
D. maia	n.a.	8–9	9
D. michelae	n.a.	10	10
D. mixta	10 (Brown, 1958a)	9–11	11
D. oculata	9 (Emery, 1901)	9–12	9
D. patrizii	8 (Weber, 1949)	7–10	8
D. penthos	n.a.	9–12	11
D. poweri	12 (Arnold 1916)	8–12	11
D. traegaordhi	8–9 (Santschi 1914)	7–8	8
D. venus	n.a.	7–10	9
D. wakanda	n.a.	8–10	9

South, Pan Pan, 1.IV.1990 (*A. Dejean*); Ottotomo, [3.65, 11.3167], ca. 750 m, 12.IX.1988 (*A. Dejean*); DEMOCRATIC REPUBLIC OF CONGO: Epulu, –1.38333, 28.58333, 750 m, 1.XI.1995 (*S.D. Torti*); North Kivu, Kivu, Lubero Territory, Rte. Kimbulu, ruis. Kitagoha, [-0.05311, 29.22183], 1760 m, tamisage de terreau, IV.1954 (*R.P.M.J. Celis*); North Kivu, Massif Ruwenzori, Mt. Ngulingo, prés Nyamgaleke, [0.498, 29.883], 2500 m, ex P.N.A., 13.I.1954 (*H. Synave*); GHANA: Ashanti, Ofinso, [6.93, –1.65], ca. 230 m, cocoa plantation, 2.XI.1992 (*R. Belshaw*); Aiyaola River Forest Reserve, [6.1510, –0.945], ca. 210 m, primary forest, 1.X.1992 (*R. Belshaw*); Atewa Forest Reserve, near Kibi, [6.1747, –0.5861], ca. 400 m, primary forest, 26.II.1992 (*R. Belshaw*); Kibi, 23.III.1970 (*D. Leston*); Sui River Forest Reserve, [6.129, –2.731], ca. 220 m, primary forest, 6.X.1992 (*R. Belshaw*); IVORY COAST: Abidjan, Banco Forest, [5.38694, –4.05275], ca. 20 m, I.1963 (*W.L. Brown*); Abidjan, Banco National Park, [5.38694, –4.05275], ca. 20 m, primary forest, 3.III.1977 (*I. Löbl*); Tai Forest, [5.75, –7.12], ca. 250 m, 14.V.1976 (*T. Diomande*); Anyama, Teke Forest, [5.55194, –4.01111], ca. 80 m, 15.II.1974 (*T. Diomande*); KENYA: Western Province, Kakamega Forest, Buyangu Nature Reserve, Buyangu Hill, 1570 m, 0.343, 34.863, 14.III.2002 (*R.R. Snelling*); Western Province, Kakamega Forest, Buyangu Nature Reserve near Salazar Circuit, secondary rainforest, 0.33, 34.87, 1500 m, 21.IV.2001 (*R.R. Snelling & A. Espira*); Western Province, Kakamega Forest, Mukangu Trail, 0.35328, 34.85886, 1623 m, primary rainforest, VII.2007 (*F. Hita Garcia*); Western Province, Kakamega Forest, Salazar, 0.32667, 34.87083, 1650 m, primary rainforest, 21.VI.2007 (*M. Peters*); MOZAMBIQUE: Sofala, Gorongosa National Park, Camp #1, –18.61865, 34.80866, 216 m, small forest, 18.IV.2013 (*L.E. Alonso*); RWANDA: Kayove, -[1.876, 29.357], 2100 m, 12.VIII.1973 (*P. Werner*); Rangiro, [2.39361, 29.18278], 1800 m, IX.1976 (*P. Werner*); SOUTH AFRICA: KwaZulu-Natal, Ukilinga Research Farm, 10 km SE of Pietermaritzburg, –29.6666, 30.4, 840 m, grassland, 31.XII.1991 (*B. Chambers*); TANZANIA: Iringa, Kilolo, Ndundulu Forest Reserve, –7.78912, 36.48539, 1567 m primary forest, 23.–26.X.2007 (*P. Hawkes, M. Bhoke & U. Richard*); Lindi, Lindi, Ndimba Forest Reserve, –9.62695, 39.62964, 138 m, 25.–28.II.2008 (*P. Hawkes, Y. Mlacha & F. Ninga*); Mkomazi Game Reserve, Kinondo Forest, –3.91667, 37.76667, 1270 m, montane forest, 9.V.1996 (*H.G. Robertson*); Pwani, Mafia, Mlola Forest, Mafia Island, –7.89576, 39.82842, 20 m, primary forest, 9.–13.III.2008 (*P. Hawkes, Y. Mlacha & F. Ninga*); South Pare Forest, –4.13056, 37.88389, 1650 m, montane forest, 29.XI.1995 (*H.G. Robertson*); Tanga, Kilindi, Kilindi Forest Reserve, –5.57934, 37.57971, 1000 m, primary forest, 27.–30.VIII.2005 (*P. Hawkes, J. Makwati & R. Mtana*); UGANDA: Kabarole, Kanyawara, Kibale National Park, 0.56427, 30.35876, 1510 m, montane wet forest, ex sifted leaf litter, collection code JTL7864-s, 8.VIII.2012 (*J. Longino*); Kabarole, Kanyawara, Kibale National Park, 0.55906, 30.35954, 1510 m, montane wet forest, nocturnal foragers, 11.VIII.2012 (*J. Longino*); Kabarole, Kanyawara, Kibale National Park, 0.55878, 30.35998, 1520 m, montane wet forest, nest in dead wood, collection code JTL7912, 13.VIII.2012 (*J. Longino*); Kibale National Park, Kanyawara Biological Station, 0.56437, 0.56437, 1510 m, rainforest, 16.VIII.2012 (*G. Fischer*).

Diagnosis

Discothyrea mixta differs from *D. oculata* by the following combination of characters: smaller species (WL 0.59–0.72); broader head (CI 88–94); smaller eyes (OI 5–9); propodeum strongly angulate to denticulate; declivitious face of propodeum without costae or rugae; propodeum dorsally and laterally finely marginate; shorter legs (HFI 62–68); AT4 roughly sculptured, striate to punctate; scrobal area alveolate to punctate posterolaterally, becoming striulate to strigulate medially.

Worker Measurements and Indices (n = 10)

EL 0.04–0.07; HL 0.63–0.75; HW 0.57–0.68; SL 0.40–0.50; PH 0.31–0.40; PW 0.43–0.53; DML 0.35–0.50; PrH 0.39–0.50; WL 0.59–0.72; HFL 0.38–0.49; PeL 0.10–0.13; PeW 0.30–0.33; PeH 0.28–0.35; LT3 0.54–0.79; LT4 0.27–0.41; OI 5–9; CI 88–94; SI 64–69; LMI 51–56; DMI 68–75; DMI2 107–121; ASI 46–58; HFI 62–68; DPeI 250–313; LPeI 240–313.

Worker Description

Head very broad (CI 88–94), posterior head margin strongly convex, evenly curving into sides, posterodorsal corners of head indistinct; in frontal view sides of head convex, slightly concave between eye and anterolateral corner of gena; eyes small but well developed, setose (OI 5–9), comprising around ten small ommatidia; ommatidia globose, silvery, eyes protruding from head; eyes situated laterally on gena, slightly anterad halfway between anterolateral corner of gena and posterior head margin; frontal carinae produced as broad, elevated plate; rhomboid in frontal view, extending to around posterior third of head, widest point at around anterior eye margin, broad at posterior attachment to head, pointed anteriorly; in profile rooflike, forming broad, deeply depressed scrobal area extending to just anterad eye; anteromedially fused and reduced to thin, translucent septum between antennal sockets; posterolateral portion of torulus flangelike; torulus reduced posteromedially, thus confluent with deep, exposed antennal acetabulum; scrobe mostly strigulate, becoming punctate closer to eyes, merging with alveolate sculpture of head at scrobal margin; medial clypeus rectangular, short, anterior margin transverse, bearing very dense layer of appressed to decumbent white pilosity; sides of medial clypeus subparallel laterad antennal sockets. *Antenna* with moderately long scape (64–69), scape somewhat expanded apically, slightly bent; pedicel a short cylinder, broader than long; true antennomere count eleven; apparent antennomere count

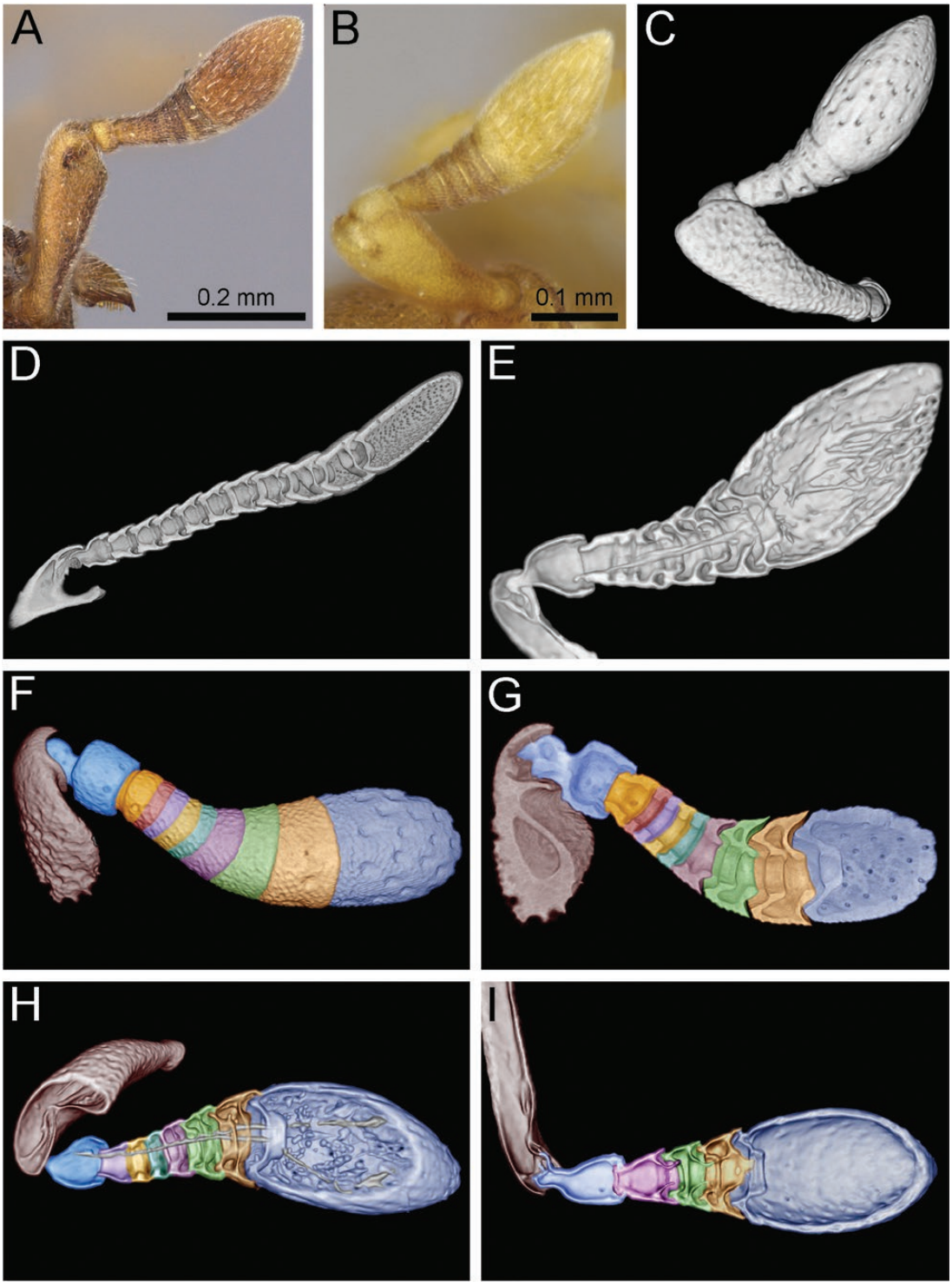

Fig. 15. Antennal anatomy showing flagellar fusion in *Discothyrea*. (A) *D. mixta* (CASENT0285473)—light microscopy, (B) *D. traegaordhi* (CASENT0790122)—light microscopy, (C) *D. traegaordhi* (CASENT0790122)—equivalent view to 15B but performed with surface volume rendering, (D) *Zasphinctus sarowiwai* Hita Garcia, 2017 (CASENT0764654)—sagittal section of surface volume rendering, (E) *D. traegaordhi* (CASENT0790122)—sagittal section of surface volume rendering, (F) *D. mixta* (CASENT0790542)—surface volume rendering showing each antennomere in different color, (G) *D. mixta* (CASENT0790542)—equivalent view to 15F but sagittal section, (H) *D. dryad* (CASENT0247374)—sagittal section of surface volume rendering showing each antennomere in different color, (I) *D. gryphon* (CASENT0790103), sagittal section of surface volume rendering showing each antennomere in different color.

nine to eleven; flagellomeres basad apical club highly compressed, taken together approximately as long as apical club. *Ventral head* surface with two low, somewhat indistinct rounded tumuli situated laterally, slightly posterad midline (in profile); postoccipital ridge with well-developed anteromedial carina, extending about a one-third of the way between occipital foramen and posteromedial extent of hypostoma; medial region of hypostoma semicircular to a low triangle, apex somewhat rounded, hypostomal arms somewhat

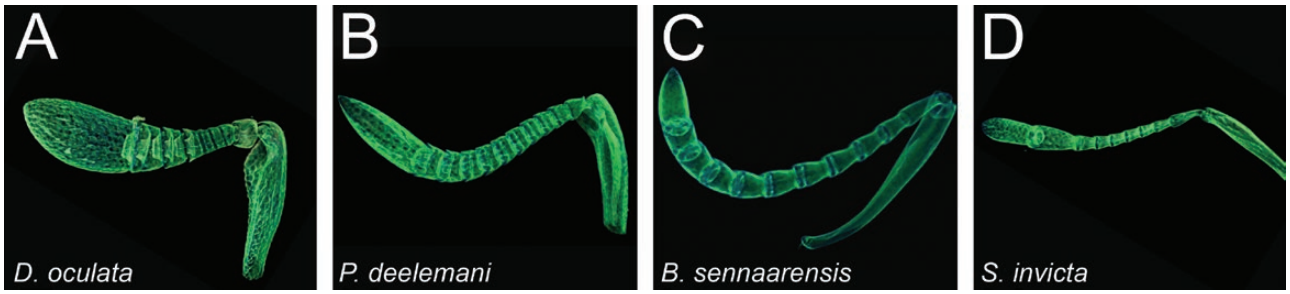

Fig. 16. Shaded surface display of transparent volume renderings showing internal and external flagellar subsegmentation. (A) *Discothyrea oculata* (CASENT0195471), (B) *Proceratium deelemani* Perrault, 1981 (CASENT0790842), (C) *Brachyponera sennaarensis* (Mayr, 1862) (CASENT0790837), (D) *Solenopsis invicta* Buren, 1972 (OKENT0011209).

narrowed, arms expanded slightly apicolaterally; palpal formula not examined. *Mandible* edentate; basal angle rounded; with blunt prebasal angle; ectal face with longitudinal carina extending from prebasal angle to apex, carina becoming confluent with masticatory margin apically, leaving long comma-shaped, depressed, smooth medial region on masticatory margin.

Mesosoma robust, evenly convex, pronotum scarcely higher than propodeum; in dorsal view mesosoma relatively broad and stout (DMI 68–75; DMI2 107–121) and distinctly narrowed posteriorly, pronotum distinctly wider than propodeum; pronotal humeri obliquely rounded; posterior propodeal margin straight; posterodorsal corners of propodeum strongly angulate to denticulate, angles subtended and medially joined by narrow carinulae, thus propodeum laterally and dorsally marginate; in posterior view, carinulae forming two arches, shaped like an inverted lowercase omega, medially joining as unpaired carina traversing declivitous face; declivitous face of propodeum distinctly concave in profile and oblique posterior view; propodeal spiracle small and indistinct, directed posterolaterally; propodeal lobes very short and blunt.

Legs quite long (HFI 62–68) and robust; mesotibia with short but distinct apicoventral spur.

Petiolar node thickly disciform, not attenuated dorsally, about 2.4 to 3.2 times higher than broad (LPeI 240–313); in profile anterior face of node distinctly convex, curving smoothly over dorsum, without distinct apex; posterior face of node vertical; in dorsal view, node roughly a rounded trapezoid, sides strongly diverging posteriorly, anterior margin convex, posterior margin concave, about 2.2 to 3.2 times broader than long (DPeI 215–313); in anterior view, petiolar outline subcircular; in oblique anterodorsal view with weak median concavity; in ventral view, a narrow trapezoid, sides diverging strongly posteriorly; subpetiolar process short, lobate to subquadrate.

Abdominal segment 3 asymmetrically campaniform, tergite evenly convex, widest posteriorly; AS3 somewhat flat to bulging posteriorly, deepest posteriorly, with concave, mostly unsculptured anteromedial region bordered anteriorly by sharply carinate, laterally narrow prora; AT3 approximately 1.9 to 2.2 times longer than AT4 (ASI 46–58); AT4 hemidemispherical to semicylindrical, gently recurved, spiracle sometimes exposed, small but prominent; successive abdominal segments short, telescopic, often concealed.

Sculpture on head, mesosoma, petiole, and abdominal segment 3 alveolate, alveoli giving rise to one or several setae; coarseness of sculpture somewhat variable, equivalently developed on all tagma, or often weakest on lateral mesosoma; ventral head surface posteromedially unsculptured; scape densely punctate; declivitous face of propodeum smooth except for fine medial carina; AT4 densely punctate, punctae usually more distinct posterolaterally; mandibles with numerous piligerous punctae.

Setation fairly consistent on dorsal surfaces of head, mesosoma, and petiole, a dense layer of appressed to erect white setae; gena and lateral mesosoma sometimes with sparser setation; density and length of setae somewhat variable between individuals; scrobal area glabrous and shining; AT3 evenly setose over its dorsal and lateral surfaces, setation shorter and less dense than on mesosoma, not forming distinct dorsal layer; AT4 with long, abundant, fine appressed pubescence and dense dorsal layer of decumbent to erect pilosity; successive abdominal segments with dense, flocculent, erect yellowish setae; ectal face of mandible with fine, curved, appressed to decumbent setae; with row of stout, spatulate setae on mesal face of masticatory margin; legs with fairly dense but relatively fine and entirely appressed white pubescence.

Color testaceous- to luteous-orange; legs and abdominal segments III–VII often bright orange to yellowish, lighter than rest of body.

Distribution and Biology

Discothyrea mixta is better represented in collections than *D. oculata* and most species of the *traegaordhi* complex, which may suggest lifestyle differences, making them more amenable to discovery, or be indicative of truly greater abundance. The species is known from a variety of forest habitats at different elevations throughout most of the Afrotropical region (Fig. 4A).

In foraging experiments, Dejean et al. (1999) found that *D. mixta* only accepted spiderlings and spider eggs as prey items. They rapidly consumed the spiderlings while often storing the eggs as a long-term resource. These findings are supported by unpublished observations made on a nest collection in Kibale Forest, Uganda, which revealed a large number of unidentified, rounded eggs, presumably of spiders.

Comments

The separation of *D. mixta* from *D. oculata* is very easy and both are difficult to mistake for each other. They differ in body size, eye size, and location on the head, as well as the shape of the propodeum and the sculpture on the propodeal declivity.

Something that we cannot rule out, despite considering it not very likely, is that the material here considered as *D. mixta* might represent a complex of cryptic species. The observed variety (see below) is not very pronounced but the highly specialized lifestyle might constrain morphological diversity, which would hinder species recognition purely based on morphology. Future studies including molecular data from most populations of *D. mixta* should revisit this question. However, on the basis of our study there is no evidence for cryptic species.

Variation

Discothyrea mixta varies slightly in overall size (WL 0.59–0.72), number of ommatidia, and coarseness of sculpture. Frequently, the

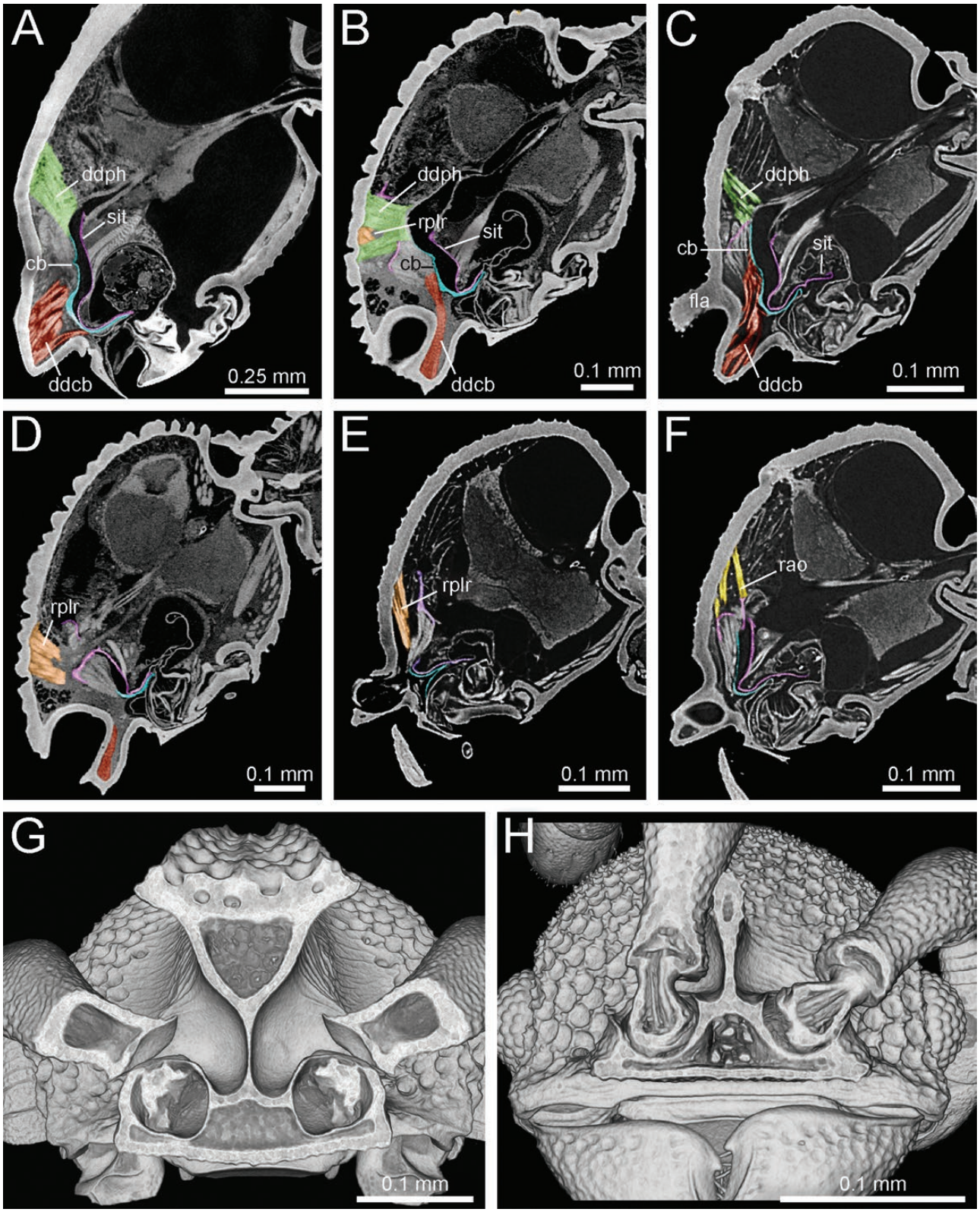

Fig. 17. Microtomographic slides showing sagittal sections of the skeletomusculature within the cephalic capsule. Important endoskeletal and muscular elements have been segmented and labeled as follows: cb = distal wall of cibarium (in blue); ddcb = dorsal cibarial dilators (in red); ddph = dorsal pharyngeal dilators (in green); rao = retractors of the mouth angle (in yellow); rplr = posterior labral retractors (in orange); sit = sitophore (in purple). (A) *Proceratium* sp. (CASENT0790271); (B), (D) *D. mixta* (CASENT0790542), (C), (E), (F) *D.* UG01. Still images generated from shaded surface display volume renderings showing cross sections through the anterior head. (G) *D. mixta*, (H) *Discothyrea* UG01.

sculpture of the lateral mesosoma is somewhat reduced, and the propodeal carinulae can vary slightly in shape and distinctness. The length, abundance, and stature of pilosity are somewhat variable, forming a more or less distinct dorsal layer on the mesosoma and

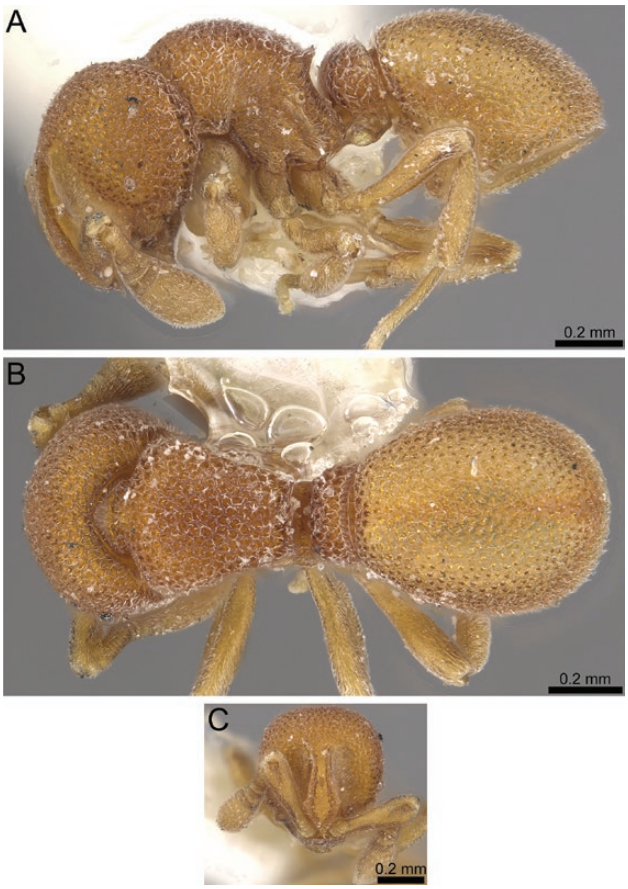

Fig. 18. Stacked digital color images of *D. mixta* Brown, 1958 paratype (CASENT0911150 - from https://www.antweb.org, photographer Will Ericson). (A) body in profile, (B) body in dorsal view, (C) head in full-face view.

abdominal terga. Nevertheless, considering the extremely wide distribution of *D. mixta*, this observed intraspecific variation is not surprising and even lower than one might expect.

Discothyrea oculata Emery, 1901 (Figs. 4B, 6B, 7B, 8B, 9B, 10B, 11B, 12B, 14B, 16A, 20, 21, 22; Supp Video S2 [online only])

Discothyrea oculata Emery, 1901: 52.
Discothyrea oculata var. *sculptior* Santschi, 1913: 302, by monotypy. [Raised to species by Brown, 1958a] **Syn. n.**

Type Material

Of *D. oculata*: LECTOTYPE, by present designation, pinned worker, CAMEROON, 1895 (*L. Conradt*) (MSNG: CASENT0903856) [examined]. **PARALECTOTYPES** [designated here], five pinned workers with same data as lectotype (MHNG: CASENT0247011; CASENT0247012; NHMB: CASENT0915307, CASENT0915307; NHMW: CASENT0915934) [examined].

Of *D. sculptior*: HOLOTYPE, CONGO, Brazzaville (*A. Weiss*) (NHMB: CASENT0915308) [examined].

Virtual dataset. Volumetric raw data (in DICOM format), 3D rotation video, still images of surface volume rendering, and 3D surface (in PLY format) of a nontype specimen (CASENT0195471) in addition to stacked digital color images illustrating head in full-face view, profile and dorsal views of the body. The data are deposited at Dryad (Hita Garcia et al. 2019, http://doi.org/10.5061/dryad.3qm4183) and can be freely accessed as virtual representation of the species. In addition to the data at Dryad, we also provide a freely accessible 3D surface model at Sketchfab (Model 2).

Nontype Material

CAMEROON: 7 km E. Batchenga, [4.289, 11.586], 480 m, 6.X.1966 (*E.S. Ross*); Nkoemvon, [2.7517, 11.0814], ca. 630 m, 1980 (*D. Jackson*); Pan Pan, 28.XII.1990 (*A. Dejean*); Ottotomo, [3.65, 11.3167], ca. 700 m, 2.IV.1989 (*A. Dejean*); DEMOCRATIC REPUBLIC OF CONGO: Kongo Central, Matadi, [–5.83636, 13.43014], 1937 (*Dartevelle*); Leopoldville, [–4.4578, 15.2716], 360 m, 3.IV.1948 (*A.E. Emerson*); 24 mi. S. of Mambasa, [1.13, 29.05], 950 m, 1.X.1957 (*E.S. Ross & R.E. Leech*); GHANA: Eastern, Bunso, near Tafo, [6.28761, –0.46948], ca. 250 m, secondary forest, 17.IV.1992 (*R. Belshaw*); Legon, A.D., [5.65, –0.18333], ca. 100 m, 15.X.1970 (*D. Leston*); Tafo, [6.216, –0.373], ca. 200 m, 6.X.1966 (*D. Leston*); Tafo, [6.216, –0.373], ca. 200 m, 3.X.1970 (*B. Bolton*); GUINEA: Kamsar, [10.655, –14.585], ca. 2 m, 9.X.1972 (*D.H. Kistner*); IVORY COAST: Lamto, [6.217, –5.033], ca. 70 m (*Toumodi*); KENYA: Coastal Province, Arabuko Sokoke Forest, –3.32111, 39.92944, 50 m, coastal dry forest, VI.2009 (*F. Hita Garcia & G. Fischer*); MOZAMBIQUE: Sofala, Gorongosa National Park, Portao 1, 18.99944, 34.20083, 172 m, miombo Forest, 7.VI.2012 (*G.D. Alpert*); NIGERIA: Oyo, Ibadan, IITA, 7.494, 3.887, ca. 220 m, forest, 7.VIII.1981 (*A. Russel-Smith*); TANZANIA: Lindi, Lindi, Ndimba Forest Reserve, –9.62695, 39.62964, 138 m, primary forest, 25.–28.II.2008 (*P. Hawkes, Y. Mlacha & F. Ninga*); Mkomazi Game Reserve, gorge 1 km NW of Ibaya, 3.9667, 37.7833, 791 m, 30.I.1996 (*A. Russel-Smith*); Mkomazi Game Reserve, Umba River camp site, 4.50222, 38.54056, 1317 m, open woodland, 3.XII.1995 (*H.G. Robertson*); ZIMBABWE: Victoria Falls, [-17.93, 25.85], ca. 1003 m, 5.XII.1914 (*G. Arnold*).

Diagnosis

Distinguished from *D. mixta* by the following combination of characters: larger species (WL 0.75–0.90); narrower head (CI 84–87); larger eyes (OI 14–16); propodeum without strong angles, denticles, or margination; declivitous face of propodeum deeply costate to rugose; longer legs (HFI 73–79); AT4 smooth and unsculptured; scrobal area striate to strigulate, without punctate or alveolate sculpture.

Worker Measurements and Indices (*n* = 10)

EL 0.12–0.15; HL 0.83–0.93; HW 0.70–0.78; SL 0.58–0.70; PH 0.44–0.51; PW 0.55–0.65; DML 0.51–0.63; PrH 0.53–0.59; WL 0.75–0.90; HFL 0.58–0.69; PeL 0.15–0.21; PeW 0.36–0.45; PeH 0.37–0.41; LT3 0.71–0.81; LT4 0.38–0.48; OI 14–16; CI 84–87; SI 69–76; LMI 54–58; DMI 66–78; DMI2 102–108; ASI 53–60; HFI 73–79; DPeI 201–275; LPeI 195–258.

Worker Description

Head broader than long (CI 84–87), posterior head margin strongly convex, evenly curving into sides, such that posterodorsal corners of head indistinct; sides of head in frontal view converging anteriorly; eyes large and well developed, setose (OI 14–16), comprising around 30 ommatidia; ommatidia globose, silvery, eyes protruding from head, visible in frontal view; eyes situated anterolaterally on gena, slightly anterad halfway between anterolateral corner of gena and posterior head margin; frontal carinae produced as broad, elevated plate; rhomboid in frontal view, extending to around posterior

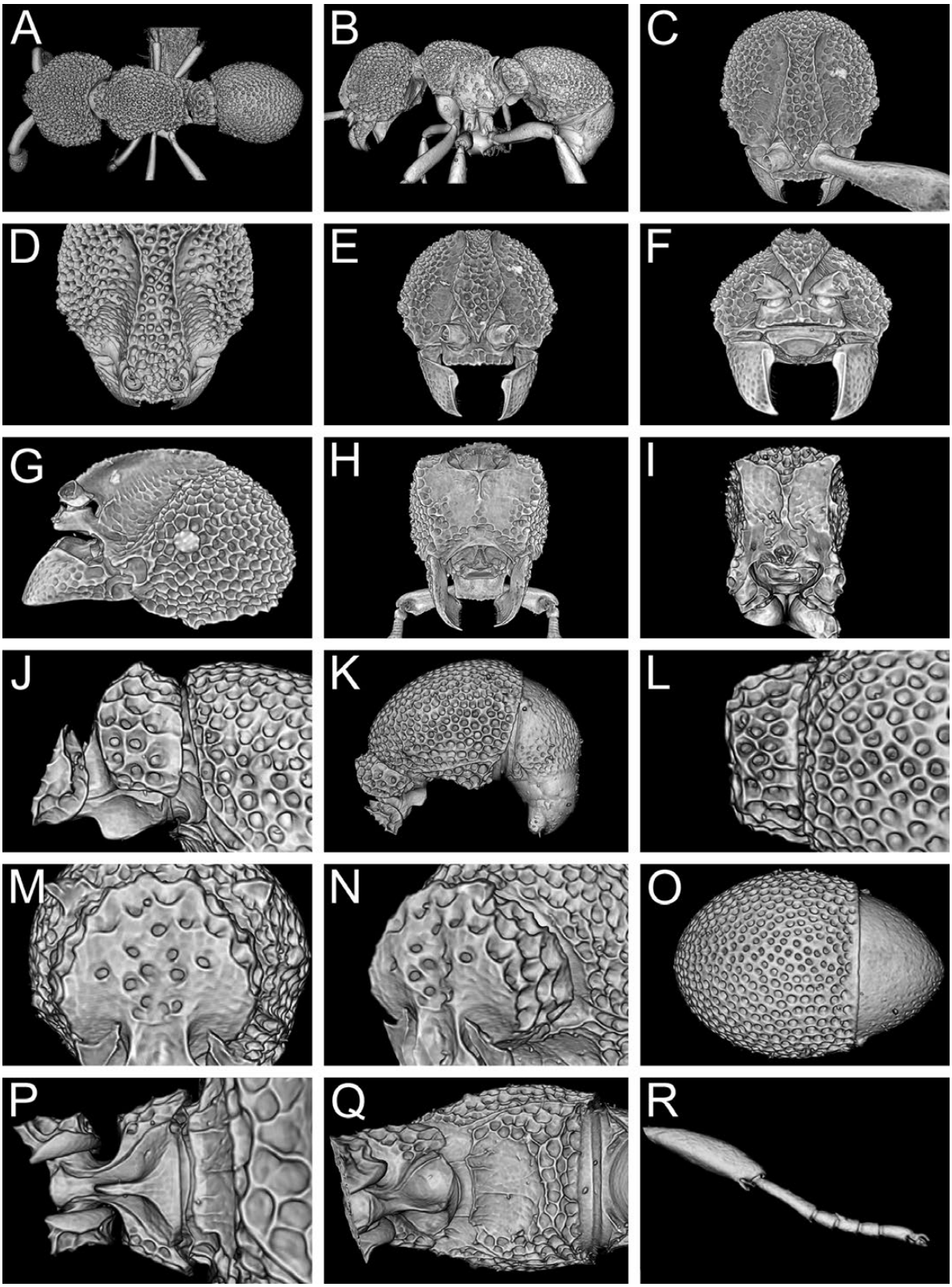

Fig. 19. Still images from shaded surface display volume renderings of *D. mixta* Brown, 1958 (CASENT0285473) showing virtually segmented body parts. (A) Body in dorsal view, (B) body in profile, (C) head in full-face view, (D) head in dorsal view, (E) head in anterodorsal view, (F) head in anterior view, (G) head in profile, (H) head in ventral view, (I) posterior propodeum in posterior view, (J) petiole in profile, (K) petiole and gaster in profile, (L) petiole in dorsal view, (M) petiole in anterior view, (N) petiole oblique anterior view, (O) gaster in dorsal view, (P) petiole in ventral view, (Q) abdominal sternite 3 in ventral view, (R) mesotibia and mesotarsus in anterior view.

Model 1. 3D surface model of *D. mixta* Brown, 1958 (CASENT0285473). An interactive version of this model is available in the HTML version of this article online and at https://sketchfab.com/3d-models/26d1d008e1ac4f1489a87245ef274a76.

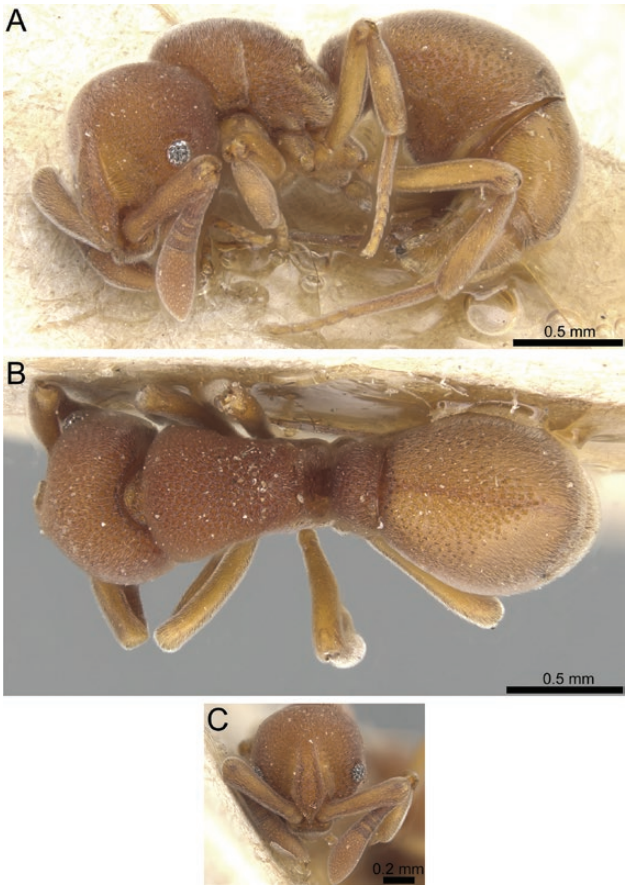

Fig. 20. Stacked digital color images of *D. oculata* Emery, 1901 paralectotype (CASENT0903856 - from https://www.antweb.org, photographer Michele Esposito). (A) body in profile, (B) body in dorsal view, (C) head in full-face view.

third of head, widest point at around anterior eye margin, broad at posterior attachment to head, pointed anteriorly; in profile rooflike, forming broad, deeply depressed scrobal area extending to just anterad eye; anteromedially reduced to thin, translucent septum between antennal sockets; posterolateral portion of torulus flangelike, reduced posteromedially, thus confluent with deep, exposed antennal acetabulum; scrobe strigulate to laterally striate; medial

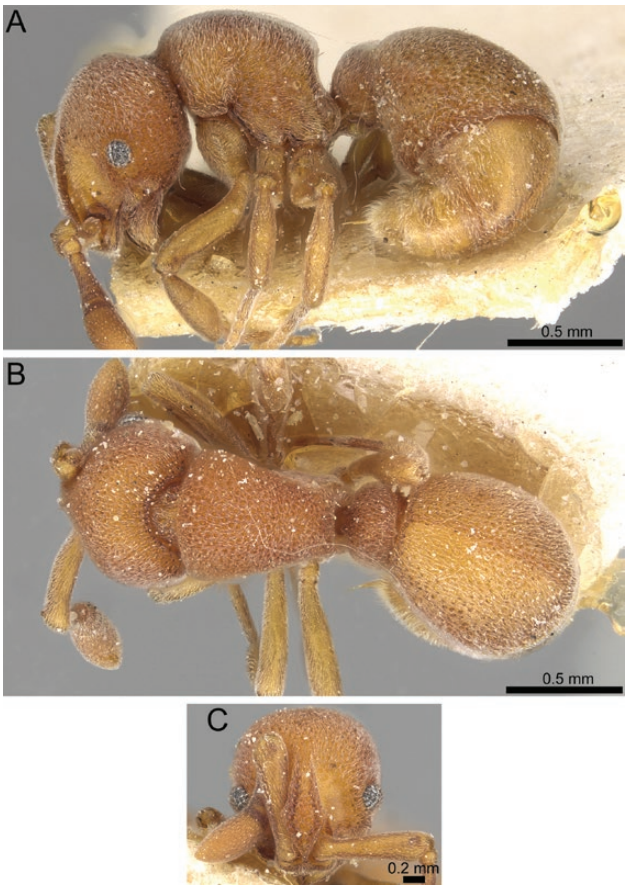

Fig. 21. Stacked digital color images of *D. sculptior* Santschi, 1913 holotype = *D. oculata* (CASENT0915308 - from https://www.antweb.org, photographer Zach Lieberman). (A) body in profile, (B) body in dorsal view, (C) head in full-face view.

clypeus rectangular, strongly projecting, anterior margin transverse, bearing very dense layer of appressed to decumbent white pilosity, sides of medial clypeus subparallel laterad antennal sockets. *Antenna* with long scape (SI 69–76), scape somewhat expanded apically, slightly bent; pedicel a short cylinder, broader than long; true antennomere count nine; apparent antennomere count nine to twelve; flagellomeres basad apical club highly compressed, taken together approximately as long as apical club. *Ventral head* surface with two low but prominent rounded tumuli situated laterally, slightly posterad midline (in profile); postoccipital ridge with small anteromedian carina, extending less than one-fourth of the way between occipital foramen and posteromedial extent of hypostoma; medial region of hypostoma triangular, hypostomal arms slightly narrowed, similar in width throughout their length; palpal formula 6,4 (Keller 2011). *Mandible* edentate; basal angle rounded; with blunt prebasal angle; ectal face with longitudinal carina extending from prebasal angle to apex, carina becoming confluent with masticatory margin slightly less than halfway along masticatory margin, leaving short comma-shaped to triangular, depressed, unsculptured medial region on masticatory margin.

Mesosoma robust, evenly convex, pronotum scarcely higher than propodeum; in dorsal view, mesosoma broad and stout (DMI 66–78; DMI2 102–108) and distinctly narrowed posteriorly, pronotum distinctly wider than propodeum; pronotal humeri obliquely rounded; posterior propodeal margin straight; posterodorsal corners of propodeum rounded, lacking denticles; declivitous face of

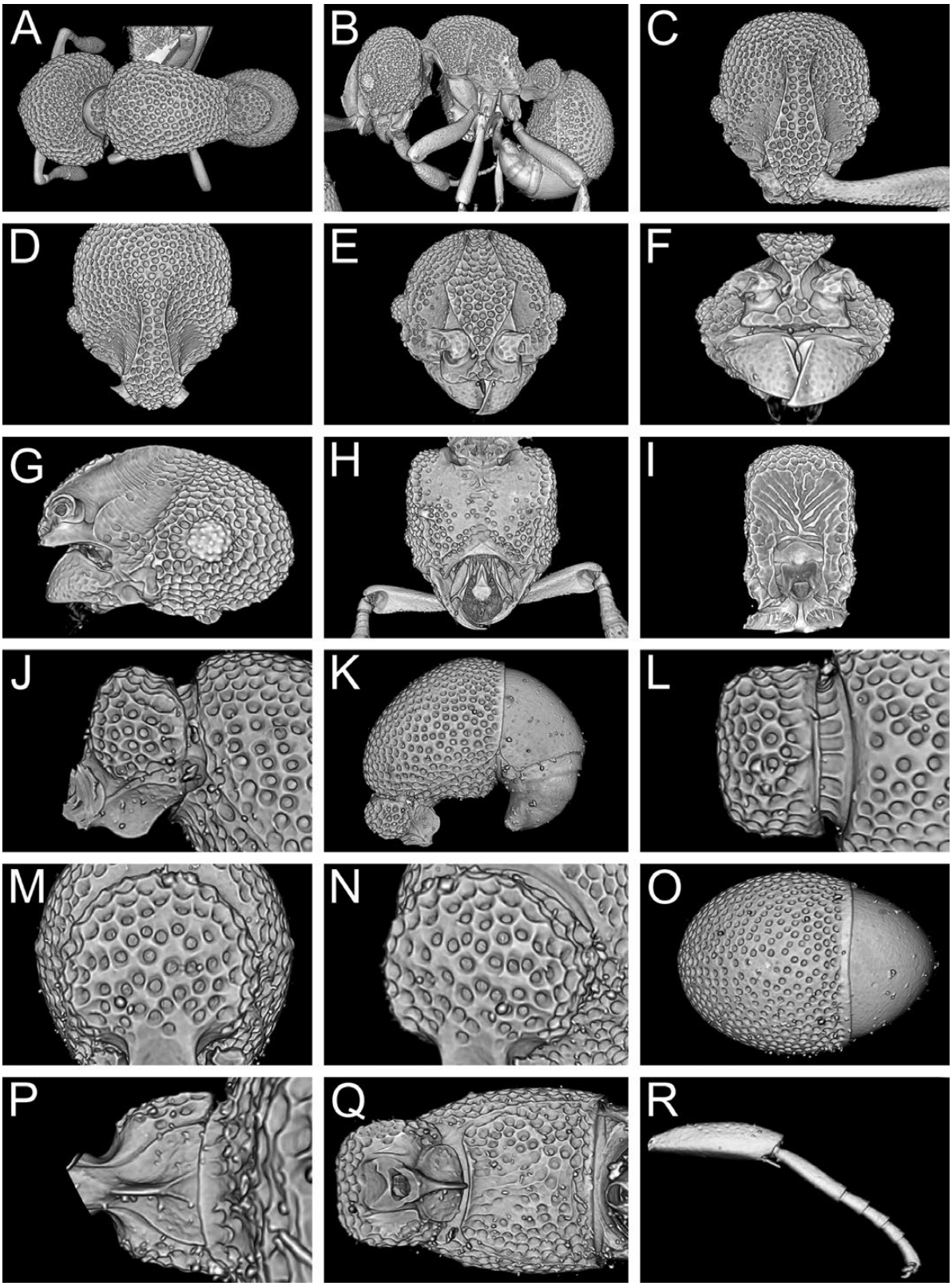

Fig. 22. Still images from shaded surface display volume renderings of *D. oculata* Emery, 1901 (CASENT0195471) showing virtually segmented body parts. (A) Body in dorsal view, (B) body in profile, (C) head in full-face view, (D) head in dorsal view, (E) head in anterodorsal view, (F) head in anterior view, (G) head in profile, (H) head in ventral view, (I) posterior propodeum in posterior view, (J) petiole in profile, (K) petiole and gaster in profile, (L) petiole in dorsal view, (M) petiole in anterior view, (N) petiole oblique anterior view, (O) gaster in dorsal view, (P) petiole in ventral view, (Q) abdominal sternite 3 in ventral view, (R) mesotibia and mesotarsus in anterior view.

Model 2. 3D surface model of *D. oculata* Emery, 1901 (CASENT0285471). An interactive version of this model is available in the HTML version of this article online and at https://sketchfab.com/3d-models/f49c344f0f6a4e88a857f5c6141d38f6.

propodeum slightly concave in profile and oblique posterior view; propodeal spiracle small but distinct, offset by unsculptured annulus around spiracular opening, directed posterolatearally; propodeal lobes rather short and rounded.

Legs quite long (HFI 73–79) and robust; mesotibia with short but distinct apicoventral spur.

Petiolar node thickly disciform, not attenuated dorsally, about 2.0 to 2.6 times higher than broad (LPeI 195–258); in profile anterior face of node distinctly convex, curving smoothly over dorsum, without distinct apex; posterior face of node vertical; in dorsal view, node roughly a rounded trapezoid, sides strongly diverging posteriorly, anterior margin convex, posterior margin concave, about 2.0 to 2.75 times broader than long (DPeI 201–275); in anterior view, petiolar outline subcircular; in oblique anterodorsal view anterior face convex; in ventral view, broad and roughly campaniform, sides weakly curved; subpetiolar process short, lobate to subquadrate.

Abdominal segment 3 asymmetrically campaniform, tergite evenly convex, widest posteriorly; AS3 somewhat flat to bulging posteriorly, deepest posteriorly, with moderatlely concave anteromedial region of reduced sculpture bordered anteriorly by strongly carinate, laterally broad prora; AT3 approximately twice as long as AT4 (ASI 53–60); AT4 hemidemipsherical to semicylindrical, gently recurved, spiracle sometimes exposed, small but prominent; successive abdominal segments short, telescopic, often concealed.

Sculpture on head, mesosoma, petiole, and abdominal segment 3 alveolate, alveoli giving rise to one or several setae; coarseness of sculpture somewhat variable, equivalently developed on all tagma, or often deeper on head and/or weaker on mesosoma; ventral head surface posteromedially with significantly reduced sculpture, only a few scattered foveae present; scape sparsely foveate; declivitous face of propodeum deeply costate to rugose; AT4 and succesive abdominal segments very smooth (unsculptured except for inconspicuous, microscopic piligerous punctulae, appearing polished relative to rest of body); mandible with numerous piligerous punctae.

Setation fairly consistent on dorsal surfaces of head, mesosoma, and petiole, a dense layer of appressed to decumbent white setae; gena and lateral mesosoma sometimes with sparser setation; density of setae somewhat variable between individuals; scrobal area glabrous and shining; AT3 evenly setose over its dorsal and lateral surfaces, setation shorter and less dense than on mesosoma, not forming distinct dorsal layer; AT4 with long, abundant, but fine appressed pubescence; successive abdominal segments with dense, flocculent, erect yellowish setae; ectal face of mandible with fine, curved, appressed to decumbent setae; masticatory margin with row of stout, spatulate setae on mesal face; legs with fairly dense but relatively fine and entirely appressed white pubescence.

Color iron-red, testaceous- to luteous-orange; legs and abdominal segments four through seven orange to yellowish, lighter than remainder of body.

Distribution and Biology

Discothyrea oculata appears to have a broad range throughout most of the Afrotropical region (Fig. 4B), even though it is represented by fairly sparse records. Preferred habitats are drier, more open, and usually at lower elevations than in *D. mixta*, including open patches of forest, dry coastal forest, and even grassland, while it is less often found in dense rainforests. The apparent rarity from museum collections is at odds with the results of Dejean and Dejean (1998) who studied this species extensively in the field and laboratory, suggesting that *D. oculata* may be rather common but difficult to collect with standard sampling methodology. Nearly 200 colonies in southern Cameroon were observed within oothecae of segestriid spiders of the genus *Ariadna,* while laboratory colonies provided with oothecae manipulated the silk to line and operculate their test-tube nests. Successful foundresses did not produce a generation of nanitics, leading the authors to term this highly derived form of colony foundation 'claustral lestobiotic colony founding'. Similar to *D. mixta*, *D. oculata* only accepted spiderlings and eggs in foraging experiments, while ignoring all other potential prey items (Dejean and Dejean 1998).

Comments

On the basis of detailed examination of the type material of both, *D. oculata* (Fig. 20) and *D. sculptior* (Fig. 21), we propose to treat the latter as junior synonym of the first. The original description of *D. sculptior* states details of sculpturation, body color, and proportions of the antennal club and frontal carinae as diagnostic (Santschi 1913), which, on examining the type and various collections of *D. oculata,* fall within reasonable limits of intraspecific variation. Why Brown (1958a) raised the variety to species status is rather puzzling, as he noted he did not examine the types of either *D. oculata* nor *D. sculptior*, and went so far as to say 'Santschi's *sculptior*, described as a variety of *oculata*, may in fact be no more than a variant of that species'. Based on our data, morphological evidence agrees with Brown's sentiment rather than his taxonomic decision.

The differentiation of *D. oculata* from *D. mixta* is straightforward, as can be seen in the identification key. As noted for *D. mixta*, considering the unusually wide distribution and even more specialized lifestyle, we cannot rule out cryptic species within the material of *D. oculata*. However, currently, our data do not permit any conclusions supporting any existence of cryptic species.

Variation

Discothyrea oculata varies slightly in overall size (WL 0.75–0.90), which is neither surprising nor unusual considering its wide distribution range. There is also some moderate diversity in coarseness

of sculpture and number of ommatidia, as well as in the length and abundance of pilosity. Again, as in *D. mixta*, this is considered as regular intraspecific geographical variation over a wide distribution range. The color ranges trivially from luteous-orange to ferrous red.

Revision of the *Discothyrea traegaordhi* Complex

Discothyrea aisnetu Hita Garcia & Lieberman sp. n. (Figs. 4C, 6C, 7C, 8C, 9C, 10C, 11C, 12C, 14C, 23, 24; Supp Video S3 [online only])

Type Material

HOLOTYPE, pinned worker, TANZANIA, Kilimanjaro Region, Mwanga, Kindoroko Forest Reserve, –3.7452, 37.64267, 1739 m, primary forest, leaf litter, Winkler, collection code CEPF-TZ-5.2, 5.–8.IX.2005 (*P. Hawkes, J. Makwati & R. Mtana)* (SAMC: CASENT0235475)**. PARATYPES,** one worker with same data as holotype (BMNH: CASENT0250399); and one worker with same data as holotype except collection code CEPF-TZ-5.4 and hand collected (CASC: CASENT0250394).

Cybertype. Volumetric raw data (in DICOM format), 3D rotation video, still images of surface volume rendering, and 3D surface (in PLY format) of the physical holotype (CASENT0235475) in addition to stacked digital color images illustrating head in full-face view, profile and dorsal views of the body. The data are deposited at Dryad (Hita Garcia et al. 2019, http://doi.org/10.5061/dryad.3qm4183) and can be freely accessed as virtual representation of the type. In addition to the cybertype data at Dryad, we also provide a freely accessible 3D surface model of the holotype at Sketchfab (Model 3).

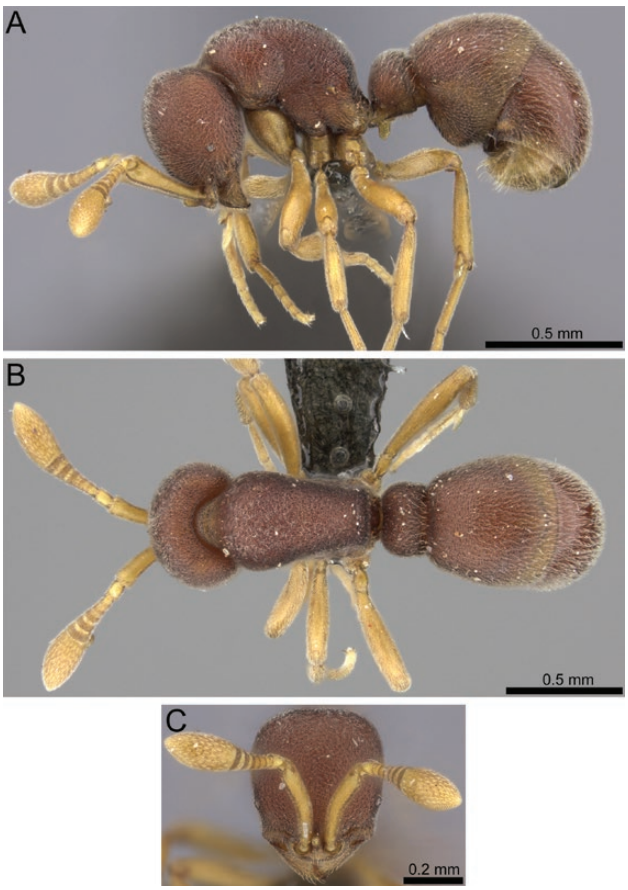

Fig. 23. Stacked digital color images of *D. aisnetu* sp. n. holotype (CASENT0235475 - from https://www.antweb.org, photographer Will Ericson). (A) body in profile, (B) body in dorsal view, (C) head in full-face view.

Diagnosis

The following character combination separates *D. aisnetu* from the other species of the complex: mesosomal profile high-rounded and extremely convex; relatively large species (HW 0.57–0.61; WL 0.80–0.90); in dorsal view mesosoma relatively thin and slender (DMI 53–58; DMI2 85–88); mesotibia without apicoventral spur; AT3 around 1.1 to 1.2 times longer than AT4 (ASI 85–90).

Worker Measurements and Indices (*n* = 3)

EL 0.03; HL 0.68–0.70; HW 0.57–0.61; SL 0.43–0.45; PH 0.40–0.43; PW 0.46–0.48; DML 0.52–0.57; PrH 0.49–0.53; WL 0.80–0.90; HFL 0.55–0.58; PeL 0.15–0.17; PeW 0.33–0.37; PeH 0.30–0.31; LT3 0.50–0.56; LT4 0.45–0.50; OI 4; CI 84–87; SI 63–67; LMI 44–51; DMI 53–58; DMI2 85–88; ASI 85–90; HFI 64–69; DPeI 218–220; LPeI 184–200.

Worker Description

Head slightly longer than broad (CI 84–87), posterior head margin nearly straight; posterodorsal corners of head rounded; sides of head slightly constricted laterally between eyes and anterolateral corner of gena, this region appearing concave in frontal view; eyes present, small (OI 4), round, comprising several ommatidia, situated around one-third of way between corner of gena and posterior head margin; eyes just visible in frontal view; frontal lamella triangular in profile, apex rounded; lamella more or less evenly translucent across its disc, without fenestra; medial clypeus broad, gently convex, lateral clypeus curving gently between antennal sockets and anterolateral corners of head, bearing short, dense, curved setae. *Antenna* with long scape (SI 63–67), scape somewhat expanded apically, gently bent; pedicel campaniform, longer than broad; true antennomere count nine; apparent antennomere count nine to eleven, flagellomeres basad apical club relatively long, taken together longer than apical club; club relatively narrow. *Ventral head* with postoccipital ridge well-defined, with very short anteromedian carina; hypostoma very wide overall, median region bluntly triangular, arms only slightly narrowed, similar in width across their entire length; palpal formula not examined. *Mandible* edentate; basal angle rounded; ectal face with low carina originating near basal angle and becoming confluent with masticatory margin at apical one-fourth, leaving narrow, arcuate, depressed medial region on masticatory margin.

Mesosoma in profile robust, high-rounded and extremely convex; in dorsal view mesosoma relatively thin and slender (DMI 53–58; DMI2 85–88) and distinctly narrowed posteriorly, pronotum significantly wider than propodeum; pronotal humeri broadly rounded; posterior propodeal margin indistinct or appearing straight; in profile, propodeum without distinct juncture between dorsal and declivitous faces, lacking angles or denticles, not marginate; propodeal declivity sloping, at most barely concave in oblique posterior view; propodeal spiracle distinct, aperture round, directed posteriorly; propodeal lobes well-developed, flange-like.

Legs moderately long to long and narrow (HFI 64–69); mesotibia without apicoventral spur, with small but distinct seta inserted in apical pit; mesobasitarsus very elongate, almost as long as remaining tarsomeres taken together.

Petiole node quite thick, about 1.8 to 2.0 times higher than long (LPeI 184–200), rounded-cuneate in profile; in profile anterior

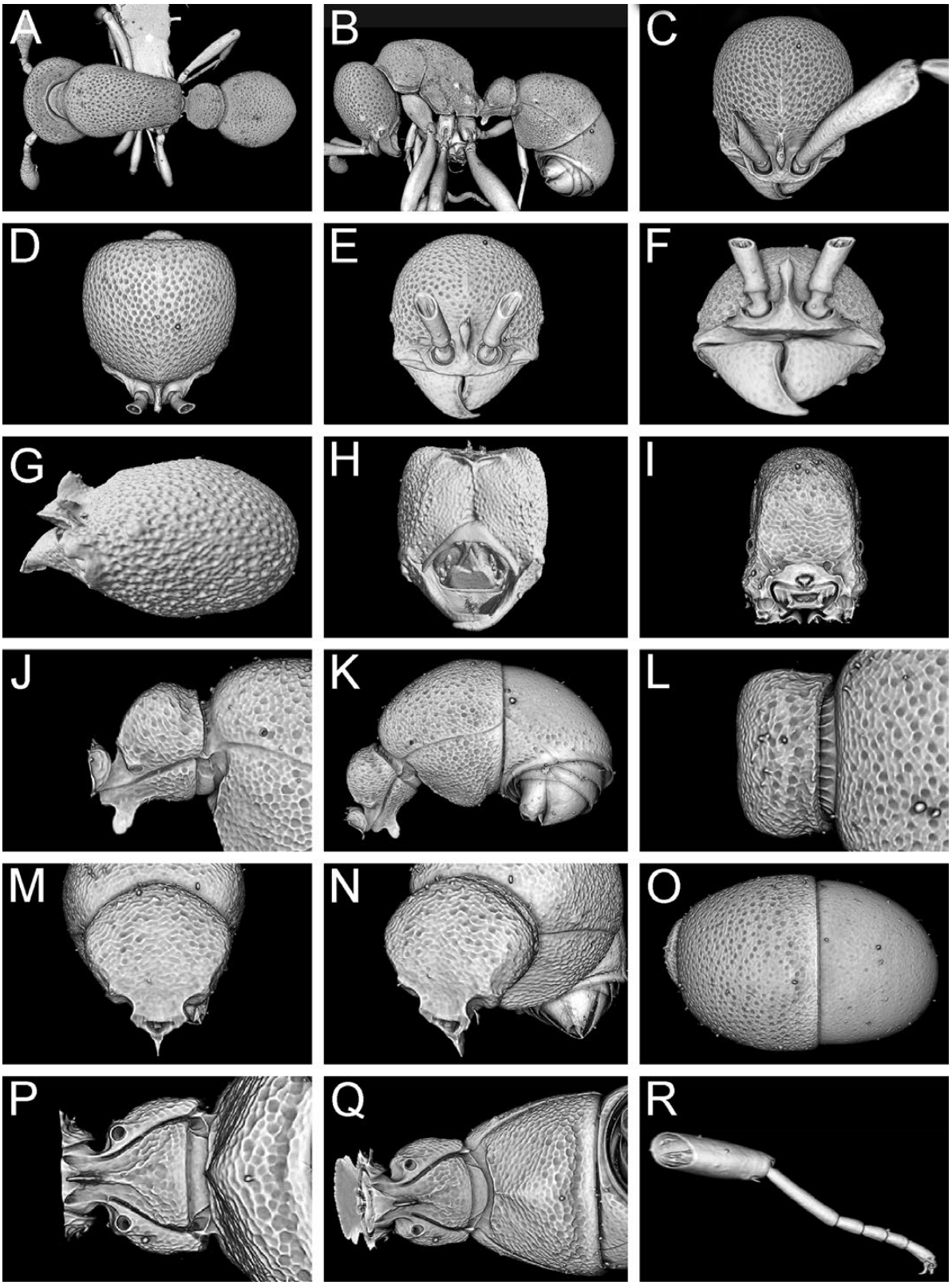

Fig. 24. Still images from shaded surface display volume renderings of *D. aisnetu* sp. n. holotype (CASENT0235475) showing virtually segmented body parts. (A) Body in dorsal view, (B) body in profile, (C) head in full-face view, (D) head in dorsal view, (E) head in anterodorsal view, (F) head in anterior view, (G) head in profile, (H) head in ventral view, (I) posterior propodeum in posterior view, (J) petiole in profile, (K) petiole and gaster in profile, (L) petiole in dorsal view, (M) petiole in anterior view, (N) petiole oblique anterior view, (O) gaster in dorsal view, (P) petiole in ventral view, (Q) abdominal sternite 3 in ventral view, (R) mesotibia and mesotarsus in anterior view.

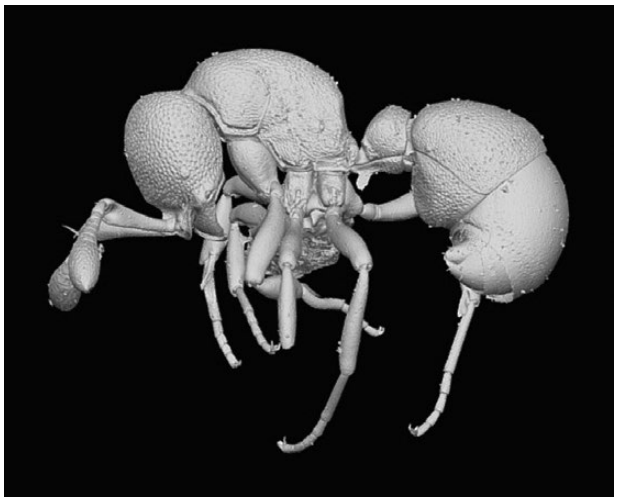

Model 3. 3D surface model of *D. aisnetu* sp. n. holotype (CASENT0235475). An interactive version of this model is available in the HTML version of this article online and at https://sketchfab.com/3d-models/1bf459295c6941d6b1151aa006e3382a.

face of node sloping posterodorsally, gently curved, apex rounded, hence without distinct posterior face; in dorsal view, node rounded-rectangular to nearly elliptical, around 2.2 times broader than long (DPeI 218–220), sides convex; in anterior view, petiolar outline broadly disciform, without distinct angles, dorsally rounded; in ventral view, sides distinctly curved, outline campaniform; subpetiolar process elongate-triangular, weakly spiniform to digitate, anteriorly projecting, apex approximately rounded; petiolar spiracles very large, round in ventral view.

Abdominal segment 3 campaniform, widest posteriorly, sternite rounded and distinctly bulging in profile; AS3 with weak medial carina; prora present as a fine carina, weakly concave in ventral view; AT3 around 1.1 to 1.2 times longer than AT4 (ASI 85–90); AT4 gently recurved hemidemispherical; AS4 with anterior lip short and narrow, scarcely overlapping AS3, anterior margin straight in ventral view; successive abdominal segments short, telescopic, often concealed.

Sculpture on head evenly punctate-reticulate, sculpture equally developed over head except medial clypeus distinctly smoother; mandibles fairly smooth but with fine piligerous punctulae; mesosoma similarly punctate-reticulate on dorsum and sides, punctae sometimes arranged in concentric lines just anterad pronotomesepisternal junction; declivitious face of propodeum finely reticulate to confused-rugulose; petiole and abdominal segment 3 (tergite and sternite) similarly punctate-reticulate, punctures on AT3 piligerous; abdominal tergite 4 distinctively shinier and less coarsely sculptured than AT3 with fine piligerous punctulae and posteriorly with a few scattered, shallow punctae.

Setation on head and scape fairly short, dense, appressed and white pubescence; ectal face of mandible with fairly long, thin, curved, spaced setae; masticatory margin with row of straight, stout setae; mesosoma with well-developed appressed pubescence, more abundant on dorsum and lateral pronotum than remainder of mesosoma, shortest and most diffuse on sides of propodeum; petiole heavily setose, setae appressed to decumbent, quite long and thick, especially on dorsum of node; setae obscuring petiolar sculpture; ventral margin of petiolar sternite with row of straight, erect hairs; abdominal segment 3 with fairly long, mostly appressed setae, similar on tergite and sternite; AT4 more heavily setose; dorsum most strongly pubescent, becoming more diffuse ventrolaterad; successive abdominal segments with long, flexuous, curved pilosity; legs with appressed, fine pubescence, on tibiae and tarsi generally longer than on femora.

Color luteous-orange to deep iron-red, appendages yellow.

Etymology

The specific epithet is the Latin interjection 'Aisne tu?' meaning roughly 'Could it be?' (lit. 'Do you say?'), recalling the authors' reactions upon first viewing this aberrant species.

Distribution and Biology

At present the species is known only from the type locality, the Kindoroko Forest Reserve in Tanzania (Fig. 4C), which is a montane rainforest located at an altitude of 1739 m. *Discothyrea aisnetu* was sampled from leaf litter.

Comments

This highly characteristic species displays a unique mesosomal shape not seen in the remainder of the African *Discothyrea* fauna. Within the *traegaordhi*-complex it is a rather large species with long limbs, comparatively distinct flagellomeres and relatively narrow apical club. This is a character set shared only with *D. poweri*. However, it remains unclear if these two species are closely related since apart from the differently shaped mesosomal outline, *D. aisnetu* also lacks the mesotibial spur present in *D. poweri*, which is an important diagnostic character.

Variation

Discothyrea aisnetu varies slightly in color and in the pattern of punctae on the lateral pronotum just anterad the pronotomesepisternal juncture: they are more or less arranged in concentric broken lines.

Discothyrea athene Hita Garcia & Lieberman sp. n. (Figs. 4D, 6D, 7D, 8D, 9D, 10D, 11D, 12D, 14D, 25, 26; Supp Video S4 [online only])

Type Material

HOLOTYPE, pinned worker, UGANDA, Kibale National Park, Kanyawara Biological Station, 0.56437, 30.3605, 1510 m, rainforest, leaf litter, collection code FHG01060, 6.–16.VIII.2012 (*F. Hita Garcia*) (BMNH: CASENT0764088). **PARATYPES**, four pinned workers with same data as holotype (CASC: CASENT0764102; MHNG: CASENT0764100; SAMC: CASENT0764101; ZMFK: CASENT0764087).

Cybertype. Volumetric raw data (in DICOM format), 3D rotation video, still images of surface volume rendering, and 3D surface (in PLY format) of the physical holotype (CASENT0764088) in addition to stacked digital color images illustrating head in full-face view, profile and dorsal views of the body. The data are deposited at Dryad (Hita Garcia et al. 2019, http://doi.org/10.5061/dryad.3qm4183) and can be freely accessed as virtual representation of the type. In addition to the cybertype data at Dryad, we also provide a freely accessible 3D surface model of the holotype at Sketchfab (Model 4).

Non-type material

KENYA: Coast Province, Arabuko Sokoke Forest, –3.314367, 39.940731, 136 m, mixed forest, pitfall trap, VI.2009 (*G. Fischer,*

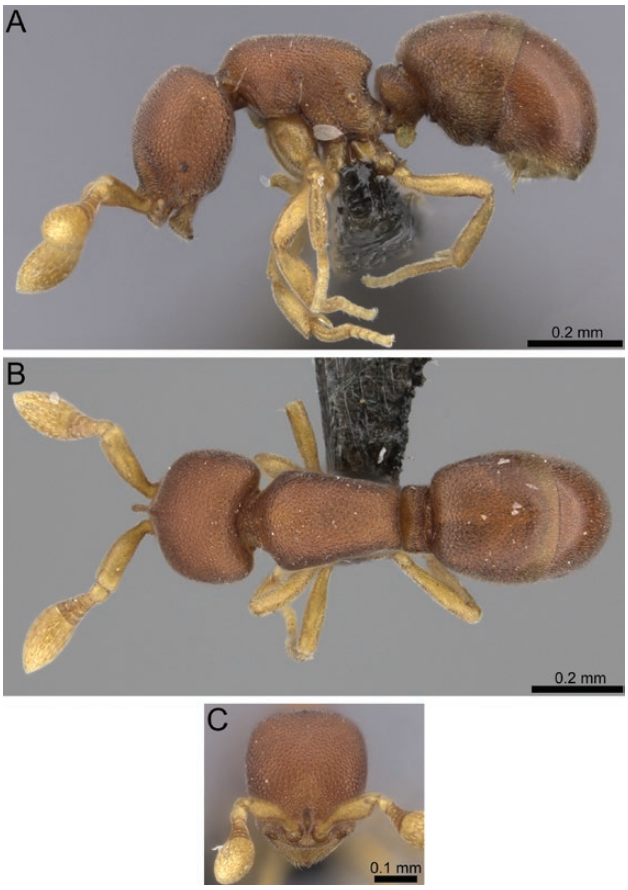

Fig. 25. Stacked digital color images of *D. athene* sp. n. (CASENT0235476 - from https://www.antweb.org, photographer Will Ericson). (A) body in profile, (B) body in dorsal view, (C) head in full-face view.

F. Hita Garcia); Coast Province, Arabuko Sokoke Forest, –3.321139, 39.929194, ca. 50 m, mixed forest, hand collected, VI.2009 (*F. Hita Garcia, G. Fischer*); MOZAMBIQUE: Sofala, Gorongosa, Gorongosa National Park, Camp #3, –19.032989, 34.671758, 115 m, riparian forest along creek, darker and closed, atop creek bed, Winkler, 3.V.2013 (*L. E. Alonso*); RWANDA: Rangiro, [-2.39361, 29.18278], 1800 m, 10.VII.1973 (*P. Werner*); Rangiro, [-2.39361, 29.18278], ca. 1800 m, litter, IX.1976 (*P. Werner*); TANZANIA: Kilimanjaro Region, Gonja Forest Reserve, –4.283333, 38.03333, 550 m, lowland forest, leaf litter, Winkler, 16.V.1996 (*H.G. Robertson*); Kilimanjaro Region, Mkomazi Game Reserve, valley behind Ibaya, –3.966667, 37.80, 900 m, closed woodland next to stream in steep-sided valley, leaf litter, Winkler, 2.XII.1995 (*H.G. Robertson*); Kilimanjaro Region, Mkomazi Game Reserve, at foot of Maji Kununua, –3.883333, 37.816667, 1600 m, *Combretum* thicket at base of valley, leaf litter, Winkler, 12.V.1996 (*H.G. Robertson*); Lindi Region, Rondo Forest Reserve, –10.11569, 39.18858, 870 m, primary forest, leaf litter, Winkler, 20.–23.II.2008 (*P. Hawkes, Y. Mlacha, F. Ninga*); Morogoro Region, Kanga Forest Reserve, –5.94905, 37.68539, 820 m, primary forest, leaf litter, Winkler, 23.–26.VIII.2005 (*P. Hawkes, J. Makwati, R. Mtana*); Morogoro Region, Mkungwe Forest Reserve, –6.89388, 37.90414, 700 m, primary forest, leaf litter, Winkler, 12.–15.X.2007 (*P. Hawkes, M. Bhoke, U. Richard*); Morogoro Region, Sali Forest Reserve, –8.94497, 36.6726, 1150 m, primary forest, leaf litter, Winkler, 17.–20.X.2007 (*P. Hawkes, M. Bhoke, U. Richard*); Tanga Region, Kilindi Forest Reserve, –5.57934, 37.57971, 1015 m, primary forest, leaf litter, Winkler, F21, 27.–30.VIII.2005 (*P. Hawkes, J. Makwati, R. Mtana*); UGANDA: Bundibugyo, Rwankasenyi, Semliki National Park, 0.85617, 30.16583, 690 m, swamp forest, leaf litter, 17.VIII.2012 (*J. Longino*).

Diagnosis

The following character combination distinguishes *Discothyrea athene* from the remainder of the complex: standing pilosity absent from mesosoma and abdominal terga; propodeum denticulate; eyes present, relatively large (OI 5–9); in dorsal view mesosoma relatively broad and robust (DMI 59–67, DMI2 92–100); mesotibia without apicoventral spur; petiole attenuated dorsally (DPeI 300–500, LPeI 286–500); sculpture distinct, declivitous face of propodeum foveolate; generally smaller species (WL 0.30–0.53); color usually orange, variably infuscated.

Worker Measurements and Indices (*n* = 17)

EL 0.03–0.04; HL 0.39–0.49; HW 0.33–0.42; SL 0.19–0.26; PH 0.19–0.27; PW 0.23–0.32; PrH 0.23–0.30; DML 0.23–0.34; WL 0.38–0.53; HFL 0.21–0.30; PeL 0.04–0.07; PeW 0.15–0.21; PeH 0.15–0.20; LT3 0.27–0.39; LT40.25–0.33; OI 5–9; CI 80–89; SI 48–53; LMI 47–51; DMI 59–67; DMI2 92–100; ASI 85–103; HFI 53–60; DPeI 300–500; LPeI 286–500.

Worker Description

Head fairly broad (CI 80–89) and round, posterior head margin gently convex; posterodorsal corners of head broadly rounded; in frontal view, sides of head convex and tapering somewhat anteriorly; eyes present, relatively large (OI 5–9) and round, comprising several ommatidia, placed about a third of the way between anterolateral corner of gena and posterior head margin; eyes visible in frontal view; frontal lamella broadly triangular in profile, apex rounded; lamella with translucent basal region, variably developed, from an indistinct patch to an elliptical and well-defined fenestra; medial clypeus convex, lateral clypeus curving gently between antennal sockets and anterolateral corners of head, bearing short, curved setae. *Antenna* with short scape (SI 48–53), scape strongly incrassate, slightly bent; pedicel subglobose, broader than long; true antennomere count nine; apparent antennomere count seven to nine; flagellomeres basad apical club highly compressed, taken together only about as long as apical club. *Ventral head* with postoccipital ridge weakly developed, without anteromedian carina; hypostoma medially rounded, arms somewhat narrowed, similar in width across their length; palpal formula not examined. *Mandible* edentate except for small, sharp prebasal denticle; basal angle broadly rounded; longitudinal carina on ectal face confluent with masticatory margin for most of its length, leaving small depressed triangular area anterad prebasal denticle.

Mesosoma gently convex, pronotum slightly lower than propodeum. In dorsal view mesosoma broad, robust (DMI 59–67; DMI2 92–100), somewhat narrowed posteriorly, pronotum wider than propodeum; pronotal humeri moderately rounded; posterior propodeal margin concave, distinctly concave between dentae; posterodorsal corners of propodeum angulate to dentate, teeth blunt but distinct; declivitous face of propodeum distinctly concave in profile and oblique posterior view; propodeal spiracle relatively large, subcircular, directed posterolaterally, often conspicuous due to shiny, unsculptured spiracular opening; propodeal lobes short, rounded.

Legs short to moderate in length (HFI 53–60) and slender; mesotibia without apicoventral spur, with small but distinct

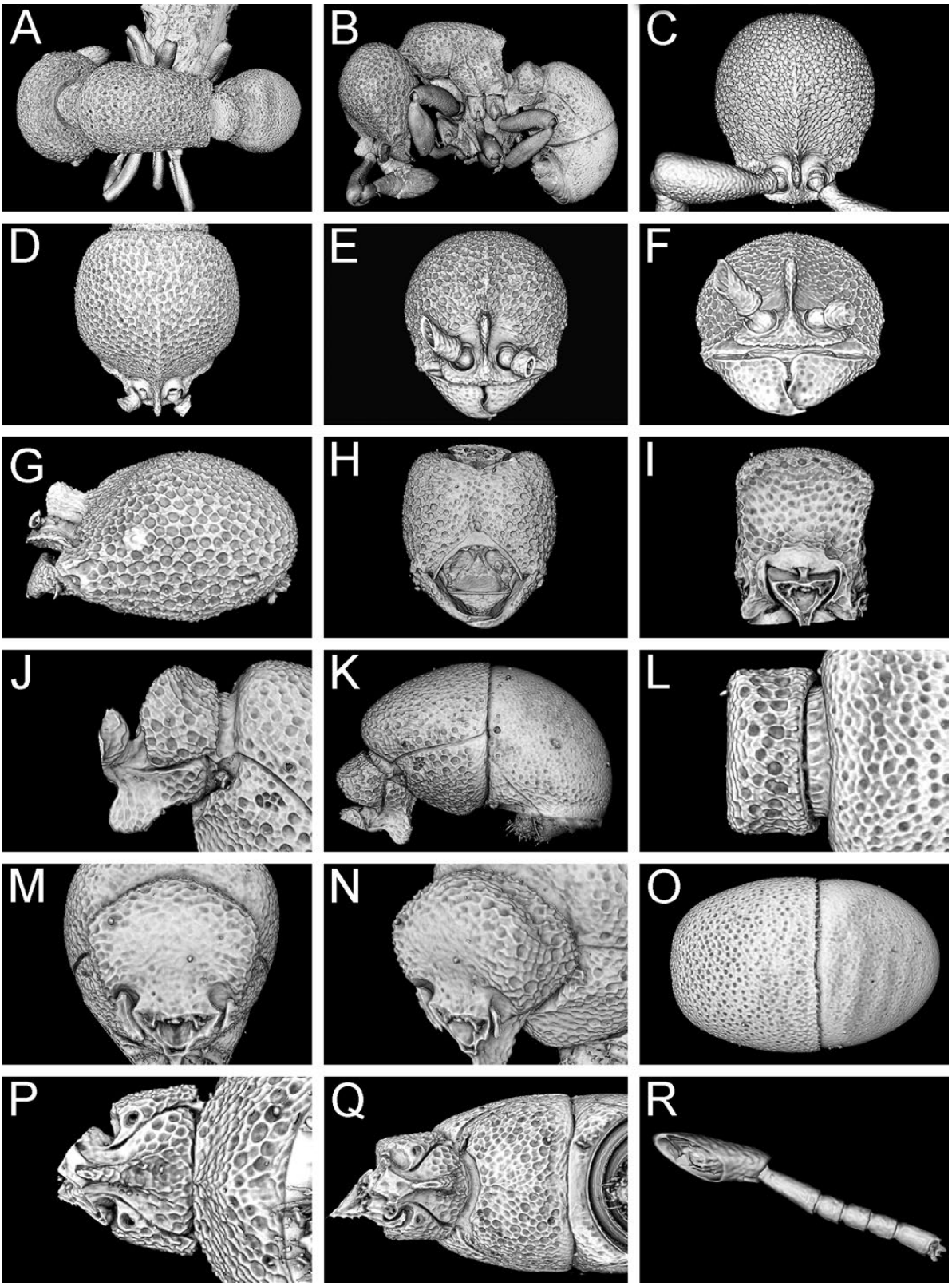

Fig. 26. Still images from shaded surface display volume renderings of *D. athene* sp. n. holotype (CASENT0764088) showing virtually segmented body parts. (A) Body in dorsal view, (B) body in profile, (C) head in full-face view, (D) head in dorsal view, (E) head in anterodorsal view, (F) head in anterior view, (G) head in profile, (H) head in ventral view, (I) posterior propodeum in posterior view, (J) petiole in profile, (K) petiole and gaster in profile, (L) petiole in dorsal view, (M) petiole in anterior view, (N) petiole oblique anterior view, (O) gaster in dorsal view, (P) petiole in ventral view, (Q) abdominal sternite 3 in ventral view, (R) mesotibia and mesotarsus in anterior view.

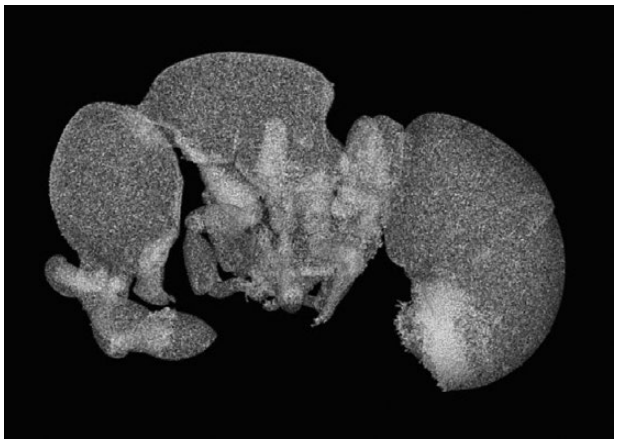

Model 4. 3D surface model of *D. athene* sp. n. holotype (CASENT0764088). An interactive version of this model is available in the HTML version of this article online and at https://sketchfab.com/3d-models/8486543f757b484d8952a7dd01c8d733.

seta inserted in apical pit; mesobasitarsus short, about as long as tarsomeres II-IV taken together.

Petiolar node moderately to strongly attenuated dorsally, about 3.7 times higher than broad (LPeI 286–500). In profile, anterior face of node convex, apex broadly peaked, posterior face sloping posteroventrally. In dorsal view, petiole about 3–5 times wider than long (DPeI 300–500); sides divergent posteriorly, posterior margin slightly concave, anterior margin nearly straight. In anterior view, petiolar outline very wide, pentagonal, edges and apex slightly rounded but distinct; in oblique anterior view, anterior face flat; in ventral view approximately rectangular, sides diverging posteriorly; subpetiolar process large, lobate, apex rounded; petiolar spiracles reniform in ventral view.

Abdominal segment 3 roughly campaniform, tergite prolonged anteriorly pasted anterior sternal margin, tergite widest just anterad end of segment, sternite sloping to convex in profile; AS3 with scarce trace of medial carina; prora present as a very fine carina, shallowly concave in ventral view; AT4 about 0.85 the length of AT3 to slightly longer, usually approximately equal in length (ASI 85–103); AT4 almost perfectly hemidemispherical; AS4 with anterior lip short but fairly broad, covering more than the one-third of the width of AS3, anterior margin straight; successive abdominal segments short, telescopic, often concealed.

Sculpture on head, dorsal mesosoma, and petiole regularly punctate-reticulate or foveolate-reticulate; on ventral head surface and lateral mesosoma becoming foveolate to punctate; lateral mesosoma with interspaces of foveolate forming rugulae, especially on lower surfaces; declivitous face of propodeum shallowly foveolate-reticulate to laterally rugulose; mandibles with fairly coarse piligerous punctae; frontal lamella and medial clypeus roughly granulate; AT3 shallowly punctulate-reticulate; AT4 with minute, dense piligerous punctulae, clearly shinier than AT3.

Setation mostly consisting of very fine, appressed white pubescence, similarly distributed on dorsal surfaces, dilute to absent on lateral surfaces of head and mesosoma; abdominal sternite 3 with longer, curved decumbent white setae; abdominal segments five through seven with longer, flexuous standing setae; appendages with only very fine, appressed white pubescence; ectal face of mandible with curved, appressed to decumbent setae; row of straight, stout setae on masticatory margin.

Color unicolorous luteous-orange to brown, usually brownish orange, upper surfaces often slightly infuscated.

Etymology

The Greek goddess Athene was fabled to have competed against a mortal woman named Arachne, whom the goddess punished for her hubris by transforming her into the first spider. Although the trophic biology of *D. athene* specifically is unknown, the species is named in reference to the known arachnophagic habits of its congeners. Additionally, Athene is archetypically portrayed bearing a helmet and a spear, reflecting the notably thick cuticle and prominent sting of *Discothyrea*.

Distribution and Biology

Discothyrea athene is known from various localities in East Africa including Rwanda, Uganda, Kenya, Tanzania, and Mozambique, where it occurs in forest and woodland, usually but not always below 1000 m (Fig. 4D). It has been collected in riparian forest, swamp forest, and near streams throughout its range, suggesting a possible preference for mesic habitats. The species lives in leaf litter.

Comments

This species is relatively unspecialized in character states but can only be confused with the potentially sympatric species from East Africa possessing a robust and stocky mesosoma (LMI2 92–103), such as *D. damato*, *D. wakanda*, *D. schulzei*, or *D. venus*. However, the latter is unique by having AT4 around 1.6 to 1.8 times longer than AT3 (ASI 158–183), and *D. schulzei* and *D. wakanda* have noticeable standing pilosity on the mesosomal and abdominal dorsa. The closest species is *D. damato*, but both can be differentiated by the eye size, the shape of petiole, and abdominal proportions.

Admittedly, the diversity of habitats and the elevational range of *D. athene* are rather unusual for species of the *D. traegaordhi* complex. Also, considering that there is some pronounced variation in size between series, it possible that the material considered as *D. athene* might represent more than one species. Unfortunately, the number of specimens from each locality is often limited, thus precluding a more in-depth analysis. Additional material from East Africa and molecular data could provide stronger evidence for heterospecificity, but based on the studied specimens we prefer to regard *D. athene* as one species for the present.

Variation

Discothyrea athene varies geographically in size, with specimens from Uganda and Rwanda being generally larger (HW 0.38–0.42; WL 0.45–0.53) than those from Kenya, Tanzania, and Mozambique (HW 0.33–0.39; WL 0.38–0.50). This variation in size is not related to elevation.

There is also some variation in color which may correspond to distribution: most individuals are similarly orange, while those from Rangiro are notably darker. The degree of attenuation of the petiolar node is also quite variable (DPeI 300–500; LPeI 286–500) but does not seem to be correlated to geography since specimens from the same series display pronounced differences.

Discothyrea chimera Hita Garcia & Lieberman sp. n. (Figs. 4E, 6E, 7E, 8E, 9E, 10E, 11E, 12E, 14E, 27, 28; Supp Video S5 [online only])

Type Material

HOLOTYPE, pinned worker, TANZANIA, Morogoro Region, Kilosa, Mamiwa-Kisara Forest Reserve, –6.3753, 36.93711, 1989 m, primary forest, leaf litter, Winkler, collection code CEPF-TZ-1.2,

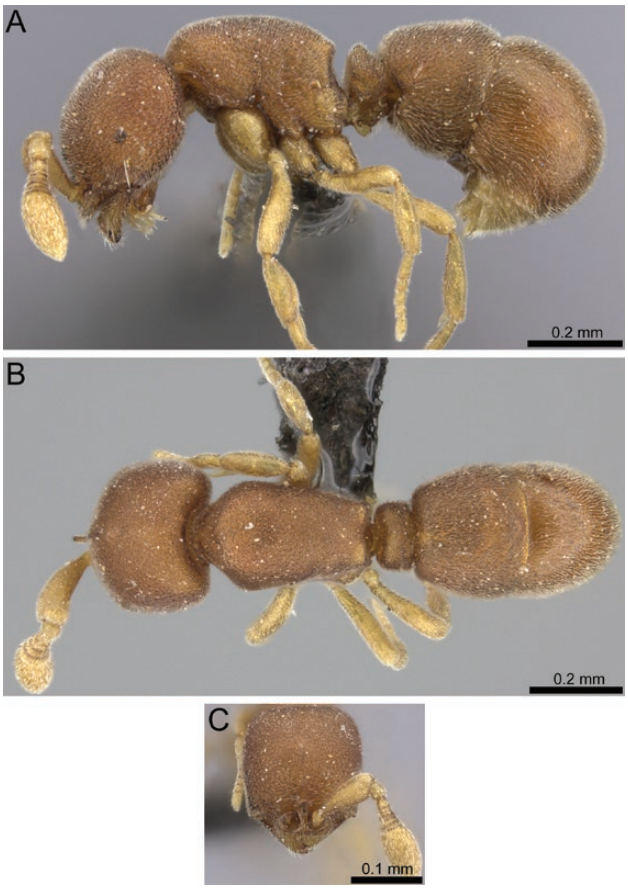

Fig. 27. Stacked digital color images of *D. chimera* sp. n. holotype (CASENT0235471- from https://www.antweb.org, photographer Will Ericson). (A) body in profile, (B) body in dorsal view, (C) head in full-face view.

16.–21.VIII.2005 (*P. Hawkes, J. Makwati & R. Mtana*) (SAMC: CASENT0235471).

Cybertype. Volumetric raw data (in DICOM format), 3D rotation video, still images of surface volume rendering, and 3D surface (in PLY format) of the physical holotype (CASENT0235471) in addition to stacked digital color images illustrating head in full-face view, profile and dorsal views of the body. The data are deposited at Dryad (Hita Garcia et al. 2019, http://doi.org/10.5061/dryad.3qm4183) and can be freely accessed as virtual representation of the type. In addition to the cybertype data at Dryad, we also provide a freely accessible 3D surface model of the holotype at Sketchfab (Model 5).

Diagnosis

The following character combination distinguishes *D. chimera* from the remainder of the complex: masticatory margin of mandible with a conspicuous, curved subapical tooth; subquadrate head with anterolateral genal angles sharply defined; anterior clypeal margin with long erect setae; propodeum not dentate; mesotibia without apicoventral spur; petiolar node strongly attenuated dorsally and squamiform in profile (LPeI 329); AT4 around 1.2 times longer than AT3; erect setae absent on dorsal surfaces.

Worker Measurements and Indices (*n* = 1)

EL 0.03; HL 0.45; HW 0.35; SL 0.23; PH 0.19; PW 0.31; DML 0.33; PrH 0.34; WL 0.54; HFL 0.31; PeL 0.07; PeW 0.20; PeH 0.23; LT3 0.32; LT4 0.39; OI 6; CI 90; SI 60; LMI 52; DMI 57; DMI2 93; ASI 124; HFI 57; DPeI 286; LPeI 329.

Worker Description

Head very broad (CI 90), appearing subquadrate posterad antennal sockets posterior head margin straight; posterodorsal corners of head rounded; in frontal view, sides of head slightly convex; eyes present, relatively long (OI 6), oval, situated slightly less than halfway between anterolateral corner of gena and posterior head margin; eyes just visible in frontal view; anterolateral corner of gena squared, nearly right-angled; frontal lamella bladelike in profile, apex acute, lamella more or less evenly translucent across its disc, without a clearly defined fenestra; medial clypeus broad and sharply transverse, lateral clypeus curving moderately strongly between antennal sockets and anterolateral corners of head, bearing row of long erect setae. *Antenna* with moderately long scape (SI 60), scape very strongly incrassate, gently bent; pedicel subcylindrical, longer than broad; apparent antennomere count eight, flagellomeres basad apical club highly compressed, taken together only about as long as apical club. *Ventral head* with short horizontal postoccipital ridge with very short, triangular anteromedian carina; medial region of hypostooma somewhat truncate, arms narrowed; palpal formula not examined. *Mandible* with prominent, curved subapical tooth and small, sharp prebasal denticle; prebasal denticle located nearly at basal angle; ectal face with longitudinal carina running from preapical tooth to basal angle, leaving short depressed prebasal region on masticatory margin.

Mesosoma gently convex in profile, pronotum distinctly higher than propodeum; in dorsal view mesosoma moderately thick (DMI 57; DMI2 93) and somewhat narrowed posteriorly; pronotal humeri moderately rounded; posterior propodeal margin weakly concave; posterodorsal corners of propodeum subangulate, without teeth; declivitous face of propodeum very shallowly concave in profile and oblique posterior view; propodeal spiracle fairly large and round but inconspicuous, directed posteriorly; propodeal lobes poorly developed, very short and bluntly truncated.

Legs short (HFI 57) and relatively robust; mesotibia without apicoventral spur, with small but distinct seta inserted in apical pit; mesobasitarsus relatively short, about as long as tarsomeres II–IV taken together.

Petiolar node strongly attenuated dorsally and squamiform in profile, about 3.3 times higher than long (LPeI 329); in profile anterior face of node sloping posterodorsally, apex peaked, posterior face sloping posteroventrally; in dorsal view petiole subrectangular, about 2.9 times broader than long (DPeI 286), sides very slightly convex; in anterior view, petiolar outline sharply pentagonal and strongly, sharply peaked, sides and angles well-defined, in oblique anterior view, anterior face flat; in ventral view roughly rectangular, sides weakly diverging posteriorly; subpetiolar process short, lobate, apex rounded, bearing several long, straight, white setae; petiolar spiracles very large and subcircular in ventral view.

Abdominal segment 3 almost thickly cylindrical, only slightly widening posteriorly, tergite weakly peaked just anterad end of segment; sternite evenly and quite shallowly curved in profile; AS3 without carinate prora, but still with anterior face distinctly depressed and anterior margin of ventral face fairly deeply arcuate in ventral view; AT4 1.2 times longer than AT3 (ASI 124); AT4 large, bulbous, hemidemispherical; AS4 with broad, prominent anterior lip, overlapping most of the width of AS3, anterior margin straight in ventral view; successive abdominal segments short, telescopic, often concealed.

Sculpture on gena and ventral head surface foveolate-reticulate, becoming punctate toward front of head, punctae smaller on frontal

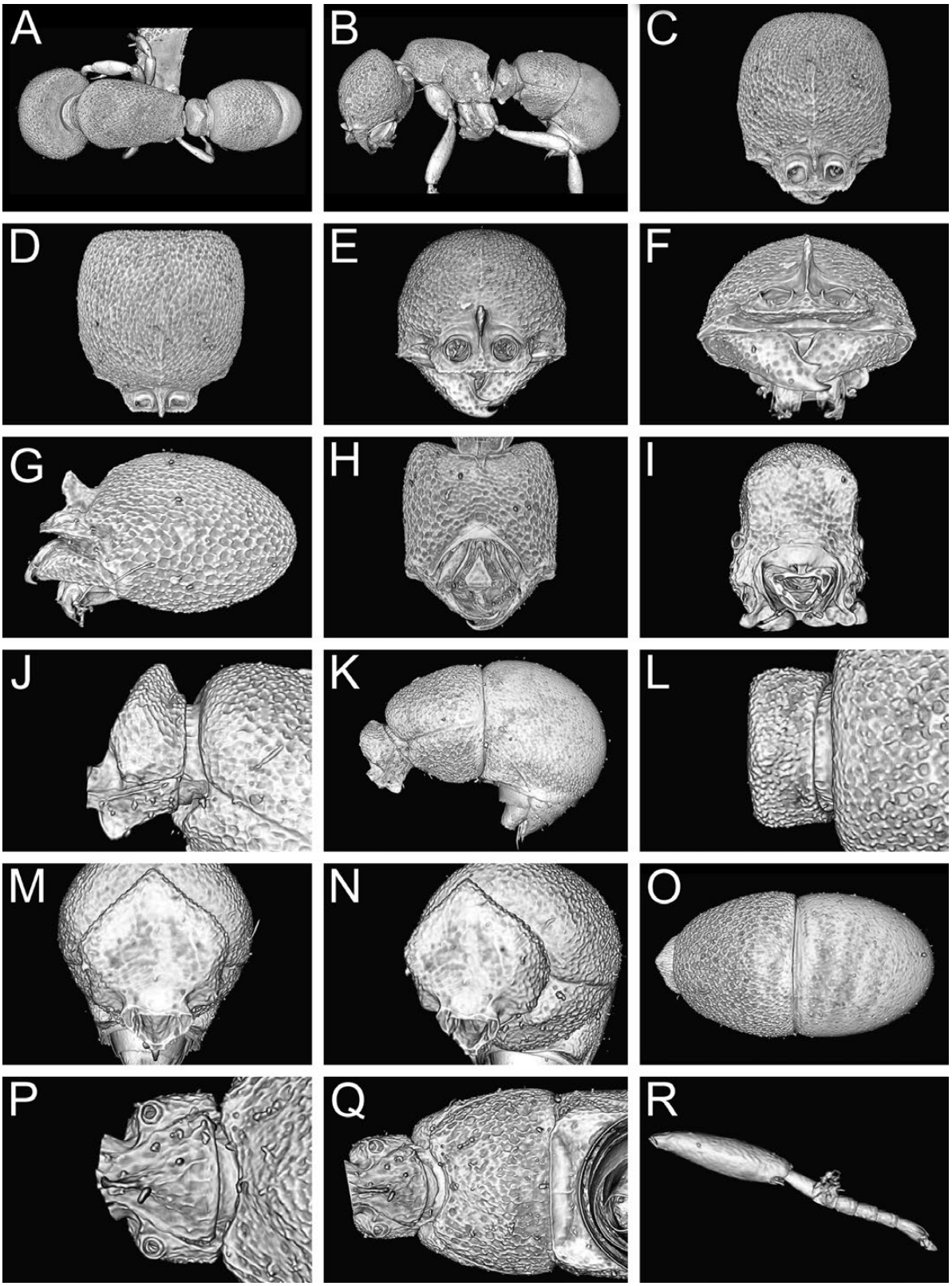

Fig. 28. Still images from shaded surface display volume renderings of *D. chimera* sp. n. holotype (CASENT0235471) showing virtually segmented body parts. (A) Body in dorsal view, (B) body in profile, (C) head in full-face view, (D) head in dorsal view, (E) head in anterodorsal view, (F) head in anterior view, (G) head in profile, (H) head in ventral view, (I) posterior propodeum in posterior view, (J) petiole in profile, (K) petiole and gaster in profile, (L) petiole in dorsal view, (M) petiole in anterior view, (N) petiole oblique anterior view, (O) gaster in dorsal view, (P) petiole in ventral view, (Q) abdominal sternite 3 in ventral view, (R) mesotibia and mesotarsus in anterior view.

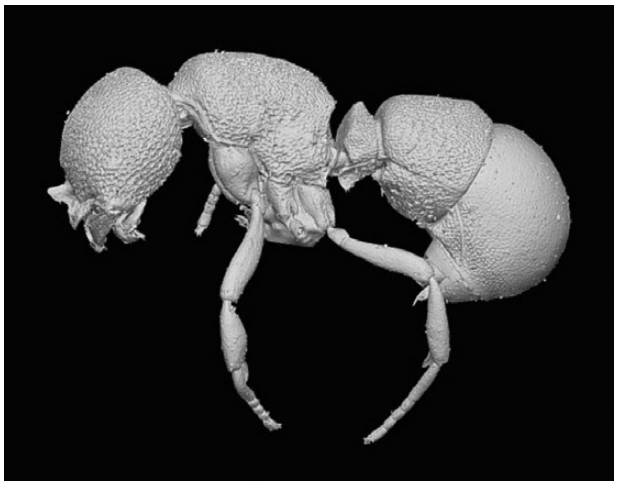

Model 5. 3D surface model of *D. chimera* sp. n. holotype (CASENT0235471). An interactive version of this model is available in the HTML version of this article online and at https://sketchfab.com/3d-models/a9c567dc04c44205a6f5dee0ea080518.

area posterad frontal lamella; mandible rather roughly sculptured with dense piligerous punctae; mesosomal dorsum, petiole, and abdominal segment 3 shallowly, evenly punctate-reticulate; lateral mesosoma irregularly punctate to rugulose on ventrolateral and posteroventral portions of propodeum; AT4 distinctly shinier and smoother than AT3, with fine piligerous punctulae.

Setation on head, antenna, and mesosoma a fairly consistent but short, velvety layer of appressed white pubescence, best developed on mesosomal dorsum; front of head just posterad frontal lamella with longer, more distinct setae directed towards midline; longer hairs, some decumbent, present on gena, best seen in frontal view; ectal face of mandible with numerous long, curved, appressed to suberect setae; masticatory margin without row of straight setae; ventral margin of petiolar sternite with several long suberect hairs; abdominal segment 3 densely clothed with long, appressed pilosity, obscuring sculpture; noticeably longer on sternite than tergite; AT4 with long, appressed pilosity, denser than on mesoma but less so than on AT3; successive abdominal segments with dense, white, standing pilosity; legs densely and more or less evenly pubescent.

Color testaceous, appendages dull yellow.

Etymology

The chimera was a mythological monster whose body was an amalgam of various creatures. The species is named for its singular combination of characters. The specific epithet is given as an appositive noun.

Distribution and Biology

Presently the new species is known only from a single specimen collected from leaf litter in the Mamiwa-Kisara Forest Reserve in Tanzania (Fig. 4E), which is a humid montane forest. *Discothyrea chimera* was collected from leaf litter.

Comments

Not considering the other characters given in the diagnosis above, the presence of a conspicuous subapical mandibular tooth distinguishes *D. chimera* from all other Afrotropical species. While a small and acute subapical denticle is present in *D. gryphon,* it is not comparable to the tooth seen in *D. chimera*. Furthermore, both species

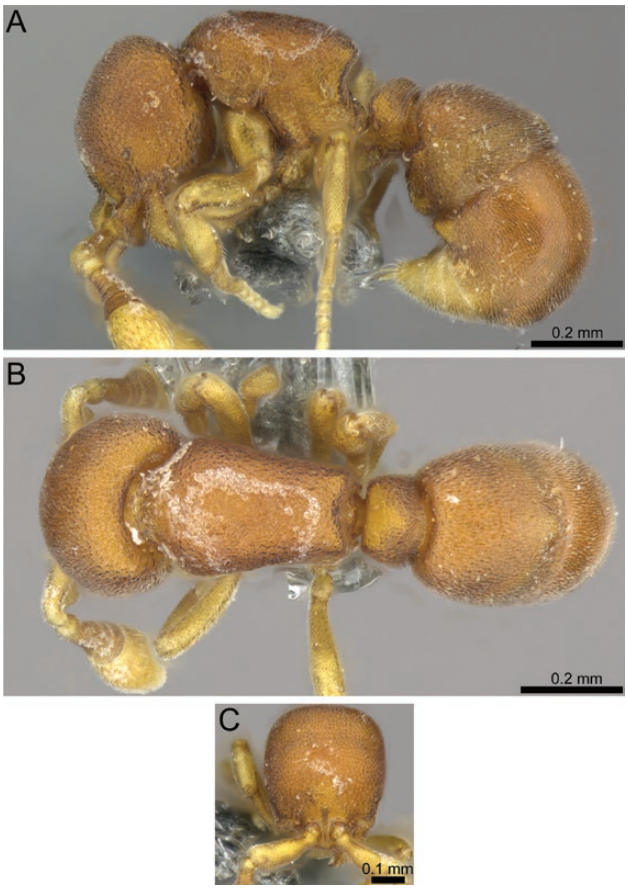

Fig. 29. Stacked digital color images of *D. damato* sp. n. holotype (CASENT0247362). (A) body in profile, (B) body in dorsal view, (C) head in full-face view.

appear morphologically closer to each other than to the remainder of the Afrotropical fauna, but can be well separated by eye size, the shape of the petiole, and pilosity. *Discothyrea chimera* has relatively larger eyes (OI 6), a dorsally much thinner petiole, and lacks erect setae on its dorsal surfaces, whereas *D. gryphon* has either no eyes or smaller eyes (OI 0–4), has a dorsally thicker petiole, and conspicuous standing setae through its body. Nevertheless, the similarity of *D. chimera* and *D. gryphon* regarding the characters of the head, as well as in general habitus, suggest a possible close phylogenetic relationship, but, without molecular phylogenetic data, this is rather speculative.

Variation

There is no information about intraspecific variation since the species is only known from the holotype.

Discothyrea damato Hita Garcia & Lieberman sp. n. (Figs. 4F, 6F, 7F, 8F, 9F, 10F, 11F, 12F, 14F, 29, 30; Supp Video S6 [online only])

Type Material

HOLOTYPE, pinned worker, UGANDA, Western, Kabarole, Kibale National Park, Kanyawara Biological Station, 0.56437, 30.36059, 1510 m, rainforest, ex leaf litter, collection code FHG01047, 6.–16.VIII.2012 (*F. Hita Garcia*) (BMNH: CASENT0247362). Paratypes, seven pinned workers with same data as holotype

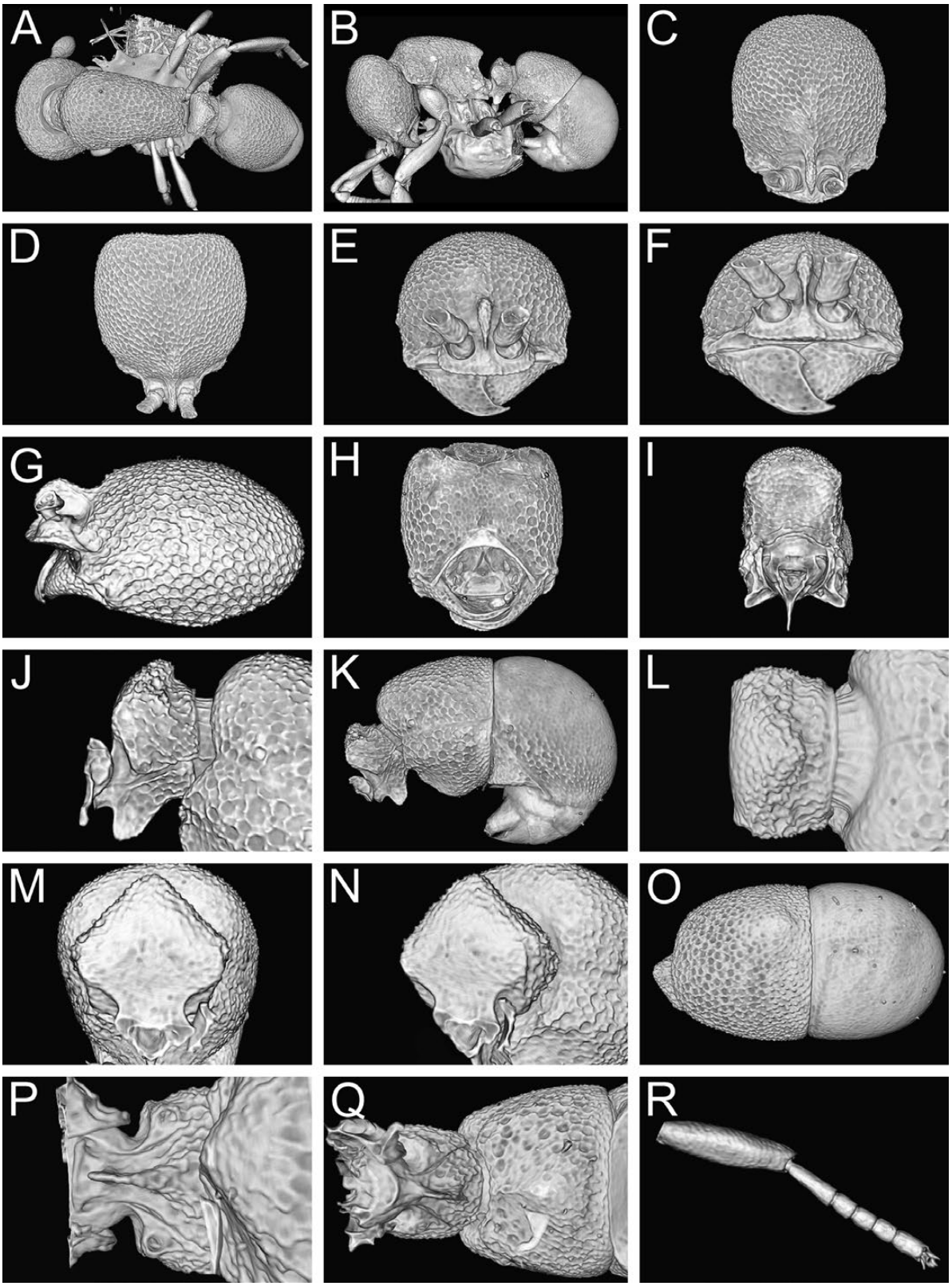

Fig. 30. Still images from shaded surface display volume renderings of *D. damato* sp. n. holotype (CASENT0247362) showing virtually segmented body parts. (A) Body in dorsal view, (B) body in profile, (C) head in full-face view, (D) head in dorsal view, (E) head in anterodorsal view, (F) head in anterior view, (G) head in profile, (H) head in ventral view, (I) posterior propodeum in posterior view, (J) petiole in profile, (K) petiole and gaster in profile, (L) petiole in dorsal view, (M) petiole in anterior view, (N) petiole oblique anterior view, (O) gaster in dorsal view, (P) petiole in ventral view, (Q) abdominal sternite 3 in ventral view, (R) mesotibia and mesotarsus in anterior view.

Model 6. 3D surface model of *D. damato* sp. n. holotype (CASENT0247362). An interactive version of this model is available in the HTML version of this article online and at https://sketchfab.com/3d-models/970757df7eaf41088198af1daccbd09c.

except for collection codes FHG01020, FHG01024, and FHG01039 (CASC: CASENT764586; HLMD: HLMD-Hym-2396; MCZC: MCZ-ENT00593558; KSMA: CASENT0247019; MHNG: CASENT0764587; SAMC: CASENT0764588; ZFMK: CASENT0247363).

Cybertype. Volumetric raw data (in DICOM format), 3D rotation video, still images of surface volume rendering, and 3D surface (in PLY format) of the physical holotype (CASENT0247362) in addition to stacked digital color images illustrating head in full-face view, profile and dorsal views of the body. The data is deposited at Dryad (Hita Garcia et al. 2019, http://doi.org/10.5061/dryad.3qm4183) and can be freely accessed as virtual representation of the type. In addition to the cybertype data at Dryad, we also provide a freely accessible 3D surface model of the holotype at Sketchfab (Model 6).

Nontype Material

DEMOCRATIC REPUBLIC OF CONGO: Kivu, Lubero Territory, Rte. Kimbulu, ruis. Kitagoha, [–0.05311, 29.22183], 1760 m, tamisage de terreau, IV.1954 (*R. P. M. J. Celis*); KENYA: Western Province, Kakamega Forest, Bunyala Forest Fragment, 0.37889, 34.69917, 1448 m, primary forest, 1.VIII.2008 (*G. Fischer*); RWANDA: Gisovu, [–2.25, 29.34], ca. 2200 m, 18.IV.1973 (*P. Werner*); Kamiranzovu, [–2.49, 29.15], 1900 m, I.1976 (*P. Werner*); Kayove, [–1.88, 29.36], 2100 m, 12.VIII.1973 (*P. Werner*).

Diagnosis

The following character combination distinguishes *D. damato* from the remainder of the complex: masticatory margin of mandible edentate; frontal lamella with conspicuous, large, elliptical basal fenestra; anterolateral corner of gena not denticulate/dentate; eyes absent to tiny (OI 0–4); in dorsal view mesosoma conspicuously thick, robust and stocky (DMI 59–66; DMI2 95–102); in profile mesosoma not extremely convex and propodeum angulate to dentate; mesotibia without apicoventral spur; AT4 around 1.2 times longer than AT3 (ASI 117–128); abdominal sternite 3 without any projecting lobe; anterior clypeal margin without conspicuous row of long, straight setae; dorsal surfaces of mesosoma, petiole, and gaster without standing pilosity.

Worker Measurements and Indices (*n* = 15)

EL 0.00–0.02; HL 0.45–0.53; HW 0.37–0.45; SL 0.24–0.29; PH 0.22–0.28; PW 0.28–0.33; DML 0.28–0.35; PrH 0.26–0.37; WL 0.43–0.56; HFL 0.25–0.32; PeL 0.06–0.09; PeW 0.17–0.21; PeH 0.17–0.23; LT3 0.25–0.35; LT4 0.31–0.43; OI 0–4; CI 79–85; SI 51–62; LMI 48–53; DMI 59–66; DMI2 95–102; ASI 117–128; HFI 54–61; DPeI 233–286; LPeI 243–314.

Worker Description

Head subrectangular, longer than broad (CI 79–85), posterior head margin flat to gently convex, with very weak impression medially; posterodorsal corners of head quite broadly rounded; in frontal view, sides of head weakly convex; eyes absent or extremely minute (OI 0–4), if present, tiny, pigmented spot situated about one-third of way between anterolateral corner of gena and posterior head margin, usually not visible in frontal view; frontal lamella rounded-triangular in profile; lamella with very conspicuous, large, elliptical basal fenestra; medial clypeus convex, lateral clypeus strongly curving between antennal sockets and anterolateral corners of head, sides of medial clypeus nearly parallel laterad antennal sockets, bearing very short curved setae. *Antenna* with scape of short to intermediate length (SI 51–62), scape clearly incrassate, gently bent; pedicel subcylindrical, broader than long; true antennomere count nine; apparent antennomere count eight to eleven; flagellomeres basad apical club highly compressed, taken together shorter than apical club. *Ventral* head with narrow, roughly V-shaped postoccipital ridge without anteromedian carina; median region of hypostoma triangular, arms narrowed and slightly spatulate apicolaterally; palpal formula not examined.

Mandible edentate except for small, sharp prebasal denticle; basal angle rounded; ectal face with longitudinal carina nearly confluent with masticatory margin for almost its entire length, leaving very narrow depressed masticatory strip including prebasal denticle.

Mesosoma in profile moderately high and relatively flat, pronotum significantly lower than propodeum, propodeum strongly angulate to dentate, posterolaterally conspicuously concave; in dorsal view mesosoma conspicuously thick, robust and stocky (DMI 59–66; DMI2 95–102), strongly narrowed posteriorly, pronotum much wider than propodeum; pronotal humeri rounded; posterior propodeal margin distinctly concave; propodeal spiracle directed posterolaterally; propodeal lobes well developed, lobate.

Legs short to moderately long (HFI 54–61) and slender; mesotibia without apicoventral spur or seta; mesobasitarsus relatively short, about as long as tarsomeres II–IV taken together.

Petiolar node moderately attenuated dorsally, about 2.4 to 3.1 times higher than long (LPeI 243–314); in profile, anterior face of node convex, apex peaked, posterior face sloping posteroventrally; in dorsal view, petiole subrectangular, sides diverging posteriorly, about 2.3 to 2.9 times as broad as long (DPeI 233–286); in anterior view, petiolar outline clearly pentagonal with somewhat rounded but well-defined angles, strongly peaked; in oblique anterior view, anterior face flat; in ventral view, roughly rectangular sides weakly diverging posteriorly; subpetiolar process comparatively long, lobate, apex rounded, and directed anteroventrally; petiolar spiracles large, elliptical to weakly reniform in ventral view.

Abdominal segment 3 campaniform, widest point just anterad end of segment; sternite more or less evenly convex in profile; AS3 with weak medial carina posteriorly broadening into a swollen lobe at around the sternite's midline; AS3 without carinate prora, but still with anterior face distinctly depressed and anterior margin of ventral face arcuate in ventral view; AT4 hemidemispherical and

around 1.2 to 1.3 times as long as AT3 (ASI 117–128); AS4 well-developed and broad, overlapping most of the width of AS3, anterior margin straight to weakly convex in ventral view; successive abdominal segments short, telescopic, often concealed, projecting strongly anteriorly.

Sculpture of mandible punctulate, moderately shiny; ventral head surface foveolate to punctulate; remainder of head, dorsal mesosoma, lateral petiole, and abdominal segment 3 conspicuously but shallowly foveolate-reticulate to weakly areolate, sculpture on lateral mesosoma less regular, reticulum becoming rugulose, area around propodeal spiracle smoother and shiny; declivitous face of propodeum predominantly finely reticulate-punctate; anterior and dorsal petiole relatively weakly sculptured, rugulose-reticulate to granulate; AT4 finely punctulate.

Setation generally very fine, dense, mostly appressed, very short pubescence; ectal face of mandible with moderately long, curved, subdecumbent to suberect setae; masticatory margin with row of short straight setae; abdominal segments 5 to 7 with moderately short standing setae.

Color usually uniformly orange brown to chestnut brown, with appendages of lighter color.

Etymology

The species name is a patronym dedicated to Anthony D'amato and his family in honor of his contributions to the conservation of life on earth and the discovery of biodiversity. The species epithet is to be treated as an appositive noun.

Distribution and Biology

The new species is only known from Kenya, Rwanda, and Uganda (Fig. 4F) where it occurs in forested areas at comparatively high elevations ranging from 1448 to 2200 m. Based on data from material sampled in Kenya and Uganda, *D. damato* lives in leaf litter.

Comments

Discothyrea damato is in its overall gestalt characterized by the lack of specialized characters compared with most other members of the complex. It is most smilar to *D. dryad*, *D. schulzei*, and *D. wakanda* but lacks the standing pilosity found in these species. Additionally, the sculpture of *D. damato* is notably shallower relative compared with that of *D. schulzei*. Another species close to *D. damato* is *D. athene*, but both differ mostly in eye size (OI 0–4 vs. 5–9) and abdominal proportions (ASI 117–128 vs. 85–103).

Variation

Discothyrea damato displays some apparent intraspecific geographic variation in general body size. The material from Kenya and Uganda is significantly smaller (HW 0.37–0.39; WL 0.43–0.45) than the specimens from Rwanda (HW 0.43–0.45; WL 0.53–0.56). Nevertheless, apart from body size there is no other observable intraspecific variation.

Discothyrea dryad Hita Garcia & Lieberman sp. n. (Figs. 4G, 6G, 7G, 8G, 9G, 10G, 11G, 12G, 13D, 14G, 15H, 31, 32; Supp. Video S7 [online only])

Type Material

HOLOTYPE, pinned worker, KENYA, Rift Valley Province, Mau Forest, between Mau summit and Kedowa, [-0.17, 35.59], ca. 2200 to 2400 m, collection code ANTC37525, litter sample, 7.XI.1974 (*V. Mahnert*) (BMNH: CASENT0247374). Paratypes, two pinned workers with same data as holotype (MCZC: MCZ-ENT00593561; SAMC: CASENT0247373).

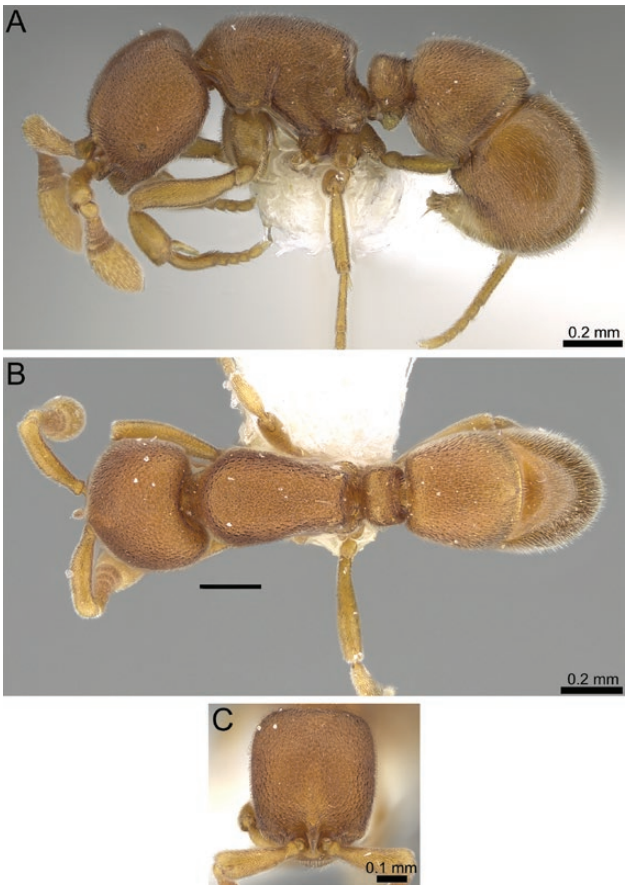

Fig. 31. Stacked digital color images of *D. dryad* sp. n. (CASENT0247371 - from https://www.antweb.org, photographer Michele Esposito). (A) body in profile, (B) body in dorsal view, (C) head in full-face view.

Cybertype. Volumetric raw data (in DICOM format), 3D rotation video, still images of surface volume rendering, and 3D surface (in PLY format) of the physical holotype (CASENT0247374) in addition to stacked digital color images illustrating head in full-face view, profile and dorsal views of the body. The data are deposited at Dryad (Hita Garcia et al. 2019, http://doi.org/10.5061/dryad.3qm4183) and can be freely accessed as virtual representation of the type. In addition to the cybertype data at Dryad, we also provide a freely accessible 3D surface model of the holotype at Sketchfab (Model 7).

Nontype Material

KENYA: Eastern Province, Embu, Irangi Forest Station, –0.3475, 37.485, 2000 m, 11.V.1977 (*V. Mahnert & J.L. Perret*); Eastern Province, Embu, Kirimiri Forest, W. of Runyenje, –0.41861, 37.54278, ca. 1550 m, 3.X.1977 (*V. Mahnert & J.L. Perret*); Rift Valley Province, Nadarua County, Mt. Aberdares National Park, [–0.38, 36.699], 2300 m, sifted leaf litter, 25.XI.1974 (*V. Mahnert*).

Diagnosis

The following character combination distinguishes *Discothyrea dryad* from the remainder of the complex: larger species (WL 0.56–0.60); dense layer of standing pilosity present on dorsal surfaces of body; mesosoma thick but elongate (DMI2 87–91), in dorsal view clearly tapering posteriorly; in profile frontal lamella with anterodorsal corner angulate, with prominent, elongate elliptic basal fenestra; masticatory margin of mandible edentate; anterolateral corner of gena not sharply angled and not denticulate/dentate;

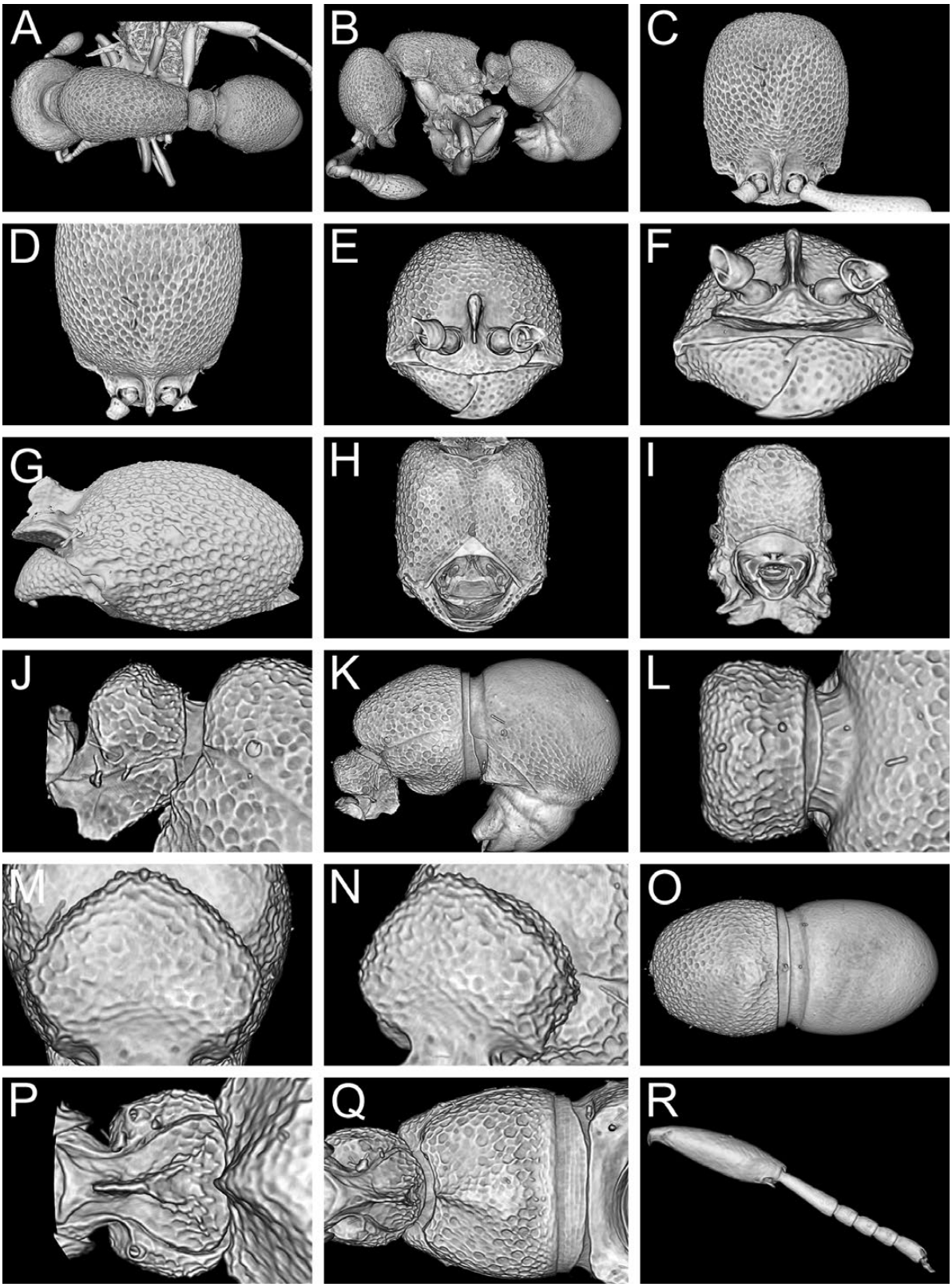

Fig. 32. Still images from shaded surface display volume renderings of *D. dryad* sp. n. holotype (CASENT0247374) showing virtually segmented body parts. (A) Body in dorsal view, (B) body in profile, (C) head in full-face view, (D) head in dorsal view, (E) head in anterodorsal view, (F) head in anterior view, (G) head in profile, (H) head in ventral view, (I) posterior propodeum in posterior view, (J) petiole in profile, (K) petiole and gaster in profile, (L) petiole in dorsal view, (M) petiole in anterior view, (N) petiole oblique anterior view, (O) gaster in dorsal view, (P) petiole in ventral view, (Q) abdominal sternite 3 in ventral view, (R) mesotibia and mesotarsus in anterior view.

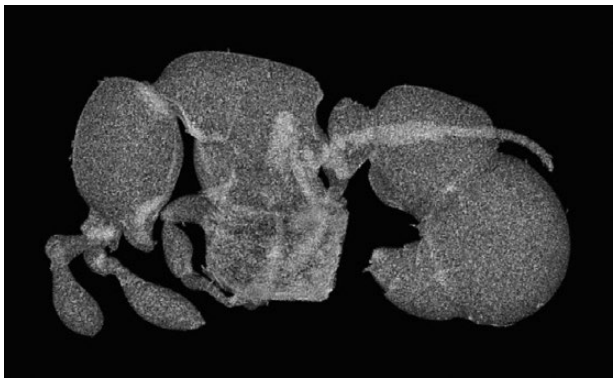

Model 7. 3D surface model of *D. dryad* sp. n. holotype (CASENT0247374). An interactive version of this model is available in the HTML version of this article online and at https://sketchfab.com/3d-models/33779d9ea2884e729cc6bddcb0375f5e.

mesosomal outline weakly to moderately convex; propodeum angulate to weakly dentate; mesotibia without apicoventral spur; AT4 around 1.2 to 1.3 times longer than AT3 (ASI 122–133); subpetiolar process shorter, blunt or rounded, not projecting anteroventrally; abdominal sternite 3 rounded and without any projecting lobe; anterior clypeal margin bearing only short curved setae.

Worker Measurements and Indices (*n* = 5)

EL 0.01–0.02; HL 0.52–0.57; HW 0.42–0.45; SL 0.29–0.32; PH 0.33–0.35; PW 0.33–0.34; DML 0.36–0.39; PrH 0.33–0.35; WL 0.56–0.60; HFL 0.31–0.36; PeL 0.08–0.09; PeW 0.19–0.21; PeH 0.22–0.23; LT3 0.31–0.34; LT4 0.44–0.46; OI 2–4; CI 79–81; SI 55–56; LMI 45–49; DMI 56–58; DMI2 87–91; ASI 122–133; HFI 54–60; DPeI 222–250; LPeI 244–288.

Worker Description

Head subrectangular, clearly longer than broad, (CI 79–81), posterior head margin more or less straight; posterodorsal corners of head rounded; in frontal view, sides of head slightly convex; eyes minute (OI 2–4), a simple pigmented spot or with a few tiny ommatidia, situated slightly anterad one-third of the way between anterolateral corner of gena and posterior head margin, sometimes just visible in frontal view; frontal lamella short, dentiform in profile, apex acute; lamella with well-defined, elliptical translucent basal fenestra; medial clypeus gently convex, lateral clypeus curving gently between antennal sockets and anterolateral corners of head, bearing short curved setae. *Antenna* with moderately long scape (SI 55–56), scape moderately incrassate, gently bent; pedicel campaniform, slightly longer than broad; true antennomere count nine; apparent antennomere count nine to eleven, flagellomeres basad apical club highly compressed, taken together only about as long as apical club. *Ventral head* with weakly developed postoccipital ridge without anteromedial carina; medial region of hypostoma strongly triangular, arms narrowed, slightly spatulate apicolaterally; palpal formula not examined. *Mandible* edentate except for relatively large, curved prebasal denticle; an indistinct preapical swelling sometimes present; ectal face with longtudinal carina confluent with masticatory margin for most of its length, leaving just preapical denticle offset in smooth depressed region.

Mesosoma weakly to moderately convex, pronotum approximately at same level as propodeum; in dorsal view mesosoma moderately thick (DMI 56–58; DMI2 87–91) and narrowed posteriorly, pronotum wider than propodeum; pronotal humeri rounded; posterior propodeal margin concave; posterodorsal corners of propodeum denticulate to weakly dentate; declivitous face of propodeum distinctly concave in profile and oblique posterior view; propodeal spiracle small, inconspicuous, directed posterolaterally; propodeal lobes dorsoventrally broad but anteroposteriorly short, blunt-flangelike.

Legs short to intermediate in length (HFI 54–60); mesotibia without apicoventral spur; with small but distinct seta inserted in apical pit; mesobasitarsus relatively short, slightly longer than tarsomeres II–IV taken together.

Petiolar node not strongly attenuated dorsally, though peaked in profile, about 2.5 to 2.9 times as high as long (LPeI 244–288); in profile anterior face of node posterodorsally sloping, apex peaked, posterior face sloping posteroventrally; in dorsal view, petiole rectangular, sides subparallel to somewhat convex, about 2.2 to 2.5 times as broad as long (DPeI 222–250); in anterior view, petiolar outline roughly pentagonal, angles rounded but faces well defined; in oblique anterior view, anterior face flat; in ventral view, broadly rectangular, sides weakly diverging posteriorly; subpetiolar process relatively short, lobate to triangular with rounded apex; petiolar spiracles very large, elliptical to roughly reniform in ventral view.

Abdominal segment 3 roughly campaniform, tergite prolonged anteriorly past anterior sternal margin; sternite convex in profile; AS3 with thick ridge broadening to lobe at about sternite's midline; AS3 without carinate prora, but still with anterior face distinctly depressed and anterior margin of ventral face concave in ventral view; AT4 around 1.2 to 1.3 times longer than AT3 (ASI 122–133); AT4 almost perfectly hemidemispherical; AS4 with well-developed anterior lip, overlapping most of the width of AS3, anterior margin straight to very weakly sinuate in ventral view; successive abdominal segments short, telescopic, often concealed.

Sculpture on head, mesosoma, petiole, and abdominal segment 3 regularly foveolate-reticulate, usually somewhat coarser on head than mesosoma; ventral head AT3 sometimes more sparsely punctate; sculpture becoming weak or absent posterad antennal sockets; ventral head surface punctate to finely punctulate-reticulate; mandible roughly sculptured with piligerous punctulae; AT4 distinctly smoother and shinier than AT3, with abundant but fine piligerous punctulae, becoming finely rugulose posteriorly.

Setation on head mostly fine, appressed, white pubescence; a few short erect hairs sometimes present on head; mesosomal, petiolar, and abdominal dorsa with fairly abundant standing pilosity, mostly subdecumbent or suberect, with scattered erect setae, in addition to appressed pubescence, longer and more abundant than on head; appressed pubescence on lateral mesosoma, sides of AT3, and abdominal sternite 3 very dilute and inconspicuous, that on AT4 longer and evenly distributed over entire tergite; successive abdominal segments with standing pilosity not significantly longer than that on AT4 though somewhat more conspicuous due to reduced sculpture; scape and legs with evenly distributed appressed pubescence; ectal face of mandible with relatively long, curved, appressed to decumbent setae; masticatory margin with row of straight setae.

Color dull testaceous orange, head and gastral dorsa sometimes lightly infuscated.

Etymology

In Greek mythology, the dryads were forest spirits that personified and protected their habitat. The species is named in recognition of the patchy and threatened status of the forests from which most Afrotropical *Discothyrea* originate. The specific epithet is given as an appositive noun.

Distribution and Biology

The new species is known from three Afromontane forest locations in Kenya (Fig. 4G), at elevations from around 1500 to 2300 m, where it seems to live in leaf litter.

Comments

Discothyrea dryad bears some similarity to *D. athene*, *D. damato*, *D. wakanda*, and *D. schulzei* based on the conspicuous elliptical basal fenestra on the frontal lamella and the absence of a mesotibial spur. Notably it differs from these species in the shape of the frontal lamella and the mesosoma. In *D. dryad*, the lamella has a distinctively angulate profile, while it is rounded in the others. The mesosoma of *D. dryad* is more elongate (LMI 51–57; DMI 56–58; DMI2 87–91 versus LMI 48–57; DMI 58–66; DMI2 102–103) and in dorsal view distinctly narrows posteriorly. The presence of standing pilosity on the mesosomal and abdominal terga separates *D. dryad*, *D. wakanda*, and *D. schulzei* from *D. damato*. Additionally, *D. dryad* is larger than *D. schulzei* (WL 0.56–0.60 vs. 0.47–0.56, respectively) and smaller than *D. wakanda* (WL 0.59–0.65). Nevertheless, based on their character sets and geographical distribution, these three species appear to be closely related.

Variation

Discothyrea dryad varies mostly in the number and arrangement of fully erect setae among the standing pilosity. This character is prone to distortion from the media and conditions of collection and preservation.

Discothyrea gaia Hita Garcia & Lieberman sp. n. (Figs. 4H, 6H, 7H, 8H, 9H, 10H, 11H, 12H, 13A, 14H, 33, 34; Supp Video S8 [online only])

Type Material

HOLOTYPE, pinned worker, ZIMBABWE, Manicaland, Melsetter, Umtali (=Mutare), –19.8, 32.86667, 1700 m, collection code ANTC42123, II.1969 (*R. Mussard*) (BMNH: CASENT0790100). **PARATYPES**, six pinned workers with same data as holotype (BMNH: CASENT0790101; CASC: CASENT0247040; MCZC: MCZ-ENT00593562; MHNG: CASENT0247037, CASENT0247038, CASENT0790099, MHNG-ENTO- 00012649; SAMC: CASENT0790102).

Cybertype Volumetric raw data (in DICOM format), 3D rotation video, still images of surface volume rendering, and 3D surface (in PLY format) of the physical holotype (CASENT0790100) in addition to stacked digital color images illustrating head in full-face view, profile and dorsal views of the body. The data are deposited at Dryad (Hita Garcia et al. 2019, http://doi.org/10.5061/dryad.3qm4183) and can be freely accessed as virtual representation of the type. In addition to the cybertype data at Dryad, we also provide a freely accessible 3D surface model of the holotype at Sketchfab (Model 8).

Nontype Material

ZIMBABWE, Manicaland, Melsetter, Umtali (=Mutare), [–18.94, 32.69], ca. 1700 m, II.1969 (R. Mussard).

Diagnosis

The following character combination distinguishes *D. gaia* from the remainder of the complex: moderately thick petiole (DPeI 192–255; LPeI 194–264); comparatively shorter legs (HFI 54–58); mesotibia with distinct apicoventral spur; abundant, short and fine appressed pubescence more or less evenly distributed over entire body.

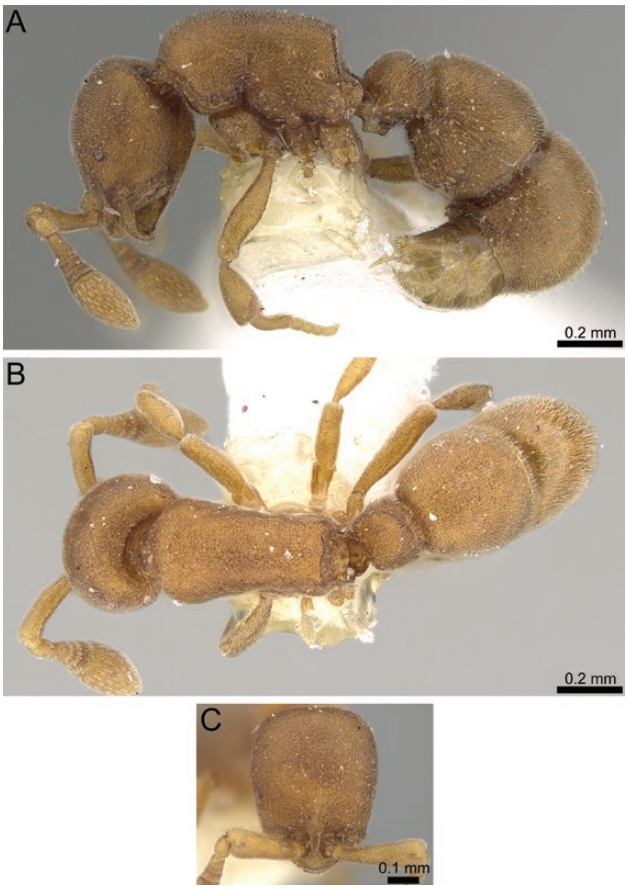

Fig. 33. Stacked digital color images of *D. gaia* sp. n. paratype (CASENT0247040—from https://www.antweb.org, photographer Michele Esposito). (A) body in profile, (B) body in dorsal view, (C) head in full-face view.

Worker Measurements and Indices (*n* = 8)

EL 0.04–0.05; HL 0.53–0.61; HW 0.43–0.51; SL 0.29–0.36; PH 0.29–0.35; PW 0.31–0.38; DML 0.43–0.51; PrH 0.33–0.40; WL 0.60–0.74; HFL 0.35–0.41; PeL 0.09–0.12; PeW 0.21–0.25; PeH 0.20–0.27; LT3 0.30–0.41; LT4 0.36–0.47; OI 7–9; CI 79–84; SI 54–60; LMI 46–49; DMI 50–53; DMI2 67–76; ASI 112–125; HFI 54–58; DPeI 192–255; LPeI 194–264.

Worker Description

Head clearly longer than broad (CI 79–84), subrectangular; posterior head margin straight, posterodorsal corners of head rounded. In frontal view, sides of head subparallel; eyes relatively large (OI 7–9), round, usually with several distinct ommatidia, situated almost halfway between anterolateral corner of gena and posterior head margin; eyes just visible in frontal view; frontal lamella in profile quite low, broadly triangular to lobate, apex convex to subacute; lamella slightly translucent, evenly so across its disc, without basal fenestra; medial clypeus gently to distinctly convex, prolonged anteromedially, lateral clypeus curving broadly between antennal sockets and anterolateral corners of head, bearing short curved setae. *Antenna* with moderately long scape (SI 54–60), scape moderately incrassate, gently bent; pedicel campaniform, longer than broad; true antennomere count eight; apparent antennomere count eight to eleven, flagellomeres basad apical club highly compressed, taken together only slightly longer than apical club. *Ventral head* with moderately developed postoccipital ridge, without or with very

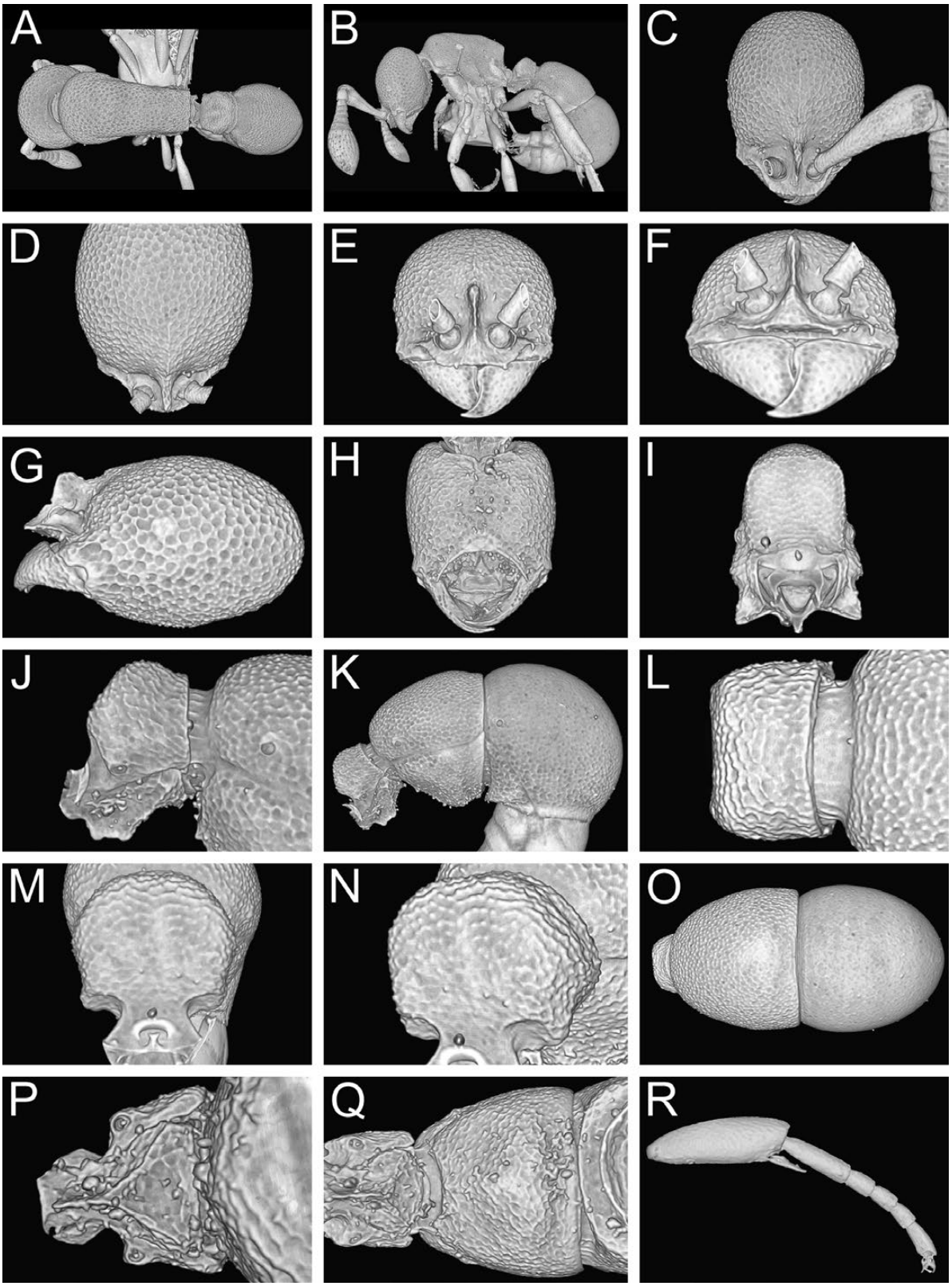

Fig. 34. Still images from shaded surface display volume renderings of *D. gaia* sp. n. holotype (CASENT0790100) showing virtually segmented body parts. (A) Body in dorsal view, (B) body in profile, (C) head in full-face view, (D) head in dorsal view, (E) head in anterodorsal view, (F) head in anterior view, (G) head in profile, (H) head in ventral view, (I) posterior propodeum in posterior view, (J) petiole in profile, (K) petiole and gaster in profile, (L) petiole in dorsal view, (M) petiole in anterior view, (N) petiole oblique anterior view, (O) gaster in dorsal view, (P) petiole in ventral view, (Q) abdominal sternite 3 in ventral view, (R) mesotibia and mesotarsus in anterior view.

Model 8. 3D surface model of *D. gaia* sp. n. holotype (CASENT0790100). An interactive version of this model is available in the HTML version of this article online and at https://sketchfab.com/3d-models/9956253ce2a04153b463d0efe493b464.

short anteromedian carina; medial region of hypostoma rounded-triangular, arms strongly narrowed, similar in width across their length; palpal formula not examined. *Mandible* edentate; basal angle round to somewhat truncate confluent with prebasal median irregularly shaped carina running halfway of masticatory margin; ectal face with longitudinal carina confluent with masticatory margin for most of its length, leaving a narrow comma-shaped depressed region including basal angle.

Mesosoma gently sloping posteroventrally, pronotum slightly higher than propodeum; in dorsal view mesosoma conspicuously slender and elongate (DMI 50–53; DMI2 67–76) with concave sides, pronotum wider than propodeum and narrowest point of mesosoma around midpoint; pronotal humeri rounded; posterior propodeal margin straight; posterodorsal corners of propodeum rounded; declivitous face of propodeum very weakly concave in profile and oblique posterior view; propodeal spiracle inconspicuous, directed posterolaterally; propodeal lobes well-developed, lobate.

Legs short (HFI 55–56); mesotibia with apicoventral spur; mesobasitarsus relatively short, about as long as tarsomeres II–IV taken together.

Petiolar node thick, scarcely attenuated dorsally, about 1.9 to 2.6 times higher than broad (LPeI 194–264); in profile anterior face of node subvertical to shallowly sloping posterodorsally, apex thickly rounded to truncate, posterior face shallowly sloping posteroventrally; in dorsal view, petiole rectangular, sides divergent posteriorly, about 1.9 to 2.5 times broader than long (DPeI 192–255); in anterior view, petiolar outline roughly disciform, dorsum broadly rounded, angles not distinct; in oblique anterior view, anterior face flat; in ventral view, roughly trapezoidal, sides divering posteriorly; subpetiolar process variable in shape, lobate to subrectangular, in general fairly short, apex broadly rounded to flat; petiolar spiracles elliptical to reniform in ventral view.

Abdominal segment 3 campaniform, widest point of tergite just anterad end of segment; AS3 deepest around its midpoint in profile, lacking distinct medial ridge or lobe; AS3 without carinate prora, but still with anterior face distinctly depressed, anterior margin of ventral face weakly concave in ventral view; AT4 between 1.1 and 1.3 times longer than AT3 (ASI 112–125); AT4 hemidemispherical; AS4 with moderately well-developed anterior lip, overlapping around the median one-third of AS3, anterior margin convex in ventral view; successive abdominal segments short, telescopic, often concealed.

Sculpture generally reduced; head, petiole, mesosomal dorsum, abdominal segment 3 shallowly punctulate-reticulate, gena somewhat more coarsely punctate; lateral mesosoma and declivitous face of propodeum becoming weakly rugulose to substrigulate, particularly on lower surfaces; mandible rather roughly sculptured with piligerous punctulae; AT4 somewhat shinier than AT3, mostly smooth but with numerous minute piligerous punctulae.

Setation consisting of abundant but short and fine appressed pubescence more or less evenly distributed over entire body; petiolar node, AT3 and AT4 with variably developed layer of standing pilosity, sometimes predominantly decumbent with a few scattered erect setae, at other times numerous short erect setae present; successive abdominal segments with dense, distinctly longer, standing pilosity; ectal face of mandible with abundant, curved, appressed to decumbent setae; masticatory margin with row of straight setae inserted on mesal face.

Color uniformly dull testaceous orange to matte sandy brown, head sometimes slightly darker.

Etymology

In Greek mythology, Gaia was the primordial goddess of the Earth. The species is named for the habit of *Discothyrea* nesting cryptically in humus and leaf litter. The specific epithet is given as an appositive noun.

Distribution and Biology

Discothyrea gaia is known only from the type locality in eastern Zimbabwe (Fig. 4H). Based on the location of the collecting site, it appears that it was collected in savannah or woodland.

Comments

Discothyrea gaia is an easily recognizable species within the Afrotropical fauna. The presence of a conspicuous apicoventral spur on the mesotibia separates it from most other group members, except *D. poweri* and *D. traegaordhi*. The latter two lack any standing pilosity on the dorsal surfaces of the body, which is present in *D. gaia*. Not considering setation, *D. gaia* possesses shorter legs (HFI 54–58) and a thinner petiole (DPeI 192–255; LPeI 194–264) compared with *D. poweri* (DPeI 135–173; LPeI 152–194). The petiole of *D. gaia* is also generally thinner compared with the one of *D. traegaordhi* (DPeI 235–289; LPeI 236–313). However, there is some overlap in the morphometric ranges of these species. Furthermore, on the basis of the presence of a distinct mesotibial spur, relatively larger eyes (OI 7–10), and a Southern African distribution, it seems intuitive that *D. gaia* belongs to a putative clade that also contains *D. poweri* and *D. traegaordhi*.

Variation

Varies mainly in the shape of the subpetiolar process, which may be lobate or nearly rectangular. The color is inconsequentially variable from testaceous orange to matte brownish, with variable infuscation of the head.

Discothyrea gryphon Hita Garcia & Lieberman sp. n. (Figs. 4I, 6I, 7I, 8I, 9I, 10I, 11I, 12I, 14I, 15I, 35, 36; Supp Video S9 [online only])

Type Material

HOLOTYPE, pinned worker, RWANDA, Kayove, [-1.876, 29.357], 2100 m, collection code ANTC37492, 12.VIII.1973 (*P. Werner*)

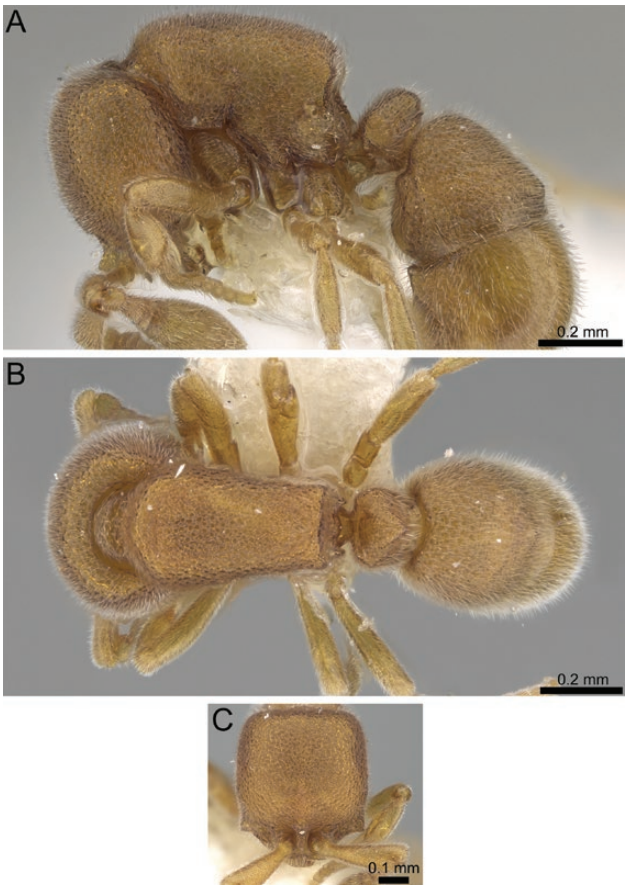

Fig. 35. Stacked digital color images of *D. gryphon* sp. n. paratype (CASENT0247367—from https://www.antweb.org, photographer Will Ericson). (A) body in profile, (B) body in dorsal view, (C) head in full-face view.

(BMNH: CASENT0790103). **PARATYPES**, two pinned workers with same data as holotype (BMNH: CASENT0790104; SAMC: CASENT0247366); and two workers from RWANDA, Kayove, [-1.876, 29.357], 2100 m, collection code ANTC42122, 23.IV.1973 (*P. Werner*) (CASC: CASENT0247367; MHNG: CASENT0247368).

Cybertype. Volumetric raw data (in DICOM format), 3D rotation video, still images of surface volume rendering, and 3D surface (in PLY format) of the physical holotype (CASENT0790103) in addition to stacked digital color images illustrating head in full-face view, profile and dorsal views of the body. The data are deposited at Dryad (Hita Garcia et al. 2019, http://doi.org/10.5061/dryad.3qm4183) and can be freely accessed as virtual representation of the type. In addition to the cybertype data at Dryad, we also provide a freely accessible 3D surface model of the holotype at Sketchfab (Model 9).

Nontype Material

TANZANIA: Mkomazi Game Reserve, Maji Kununua, –3.8833, 37.81667, 1600 m, montane forest, 7.XII.1995 (*H.G. Robertson*).

Diagnosis

The following character combination distinguishes *D. gryphon* from the remainder of the complex: mandible with square apical tooth and subapical denticle; subquadrate head with anterolateral corner of gena sharply defined, nearly denticulate; anterior clypeal margin with long erect setae; mesosomal outline weakly convex; propodeum without strong angles or denticles; mesotibia without apicoventral spur; AT4 about 1.1 times longer than AT3 (ASI 108–113); erect pilosity abundant on mesosoma and abdominal terga.

Worker Measurements and Indices (*n* = 6)

EL 0.00–0.02; HL 0.51–0.53; HW 0.44–0.48; SL 0.30–0.32; PH 0.27–0.29; PW 0.30–0.33; DML 0.36–0.39; PrH 0.31–0.35; WL 0.56–0.58; HFL 0.29–0.31; PeL 0.08–0.11; PeW 0.20–0.22; PeH 0.20–0.23; LT3 0.30–0.33; LT4 0.33–0.36; OI 0–4; CI 87–92; SI 59–62; LMI 47–51; DMI 54–57; DMI2 82–86; ASI 108–113; HFI 52–54; DPeI 192–250; LPeI 200–275.

Worker Description

Head very broad (CI 87–92); posterior head margin straight, posterodorsal corners of head rounded; in frontal view sides of head slightly convex; head appearing subquadrate posterad antennal sockets; eyes absent or minute (OI 0–4), an asymmetrical pigmented spot, situated about one-third of the way between anterolateral corner of gena and posterior head margin; when present, eyes not visible in frontal view; anterolateral corner of gena sharply squared, appearing denticulate/dentate, somewhat projecting laterally; frontal lamella short and dentate in profile, apex acute; lamella translucent across entire disc, slightly more so basally but without distinct fenestra; medial clypeus broad, emarginate medially between antennae, lateral clypeus conspicuously narrowed, curving broadly between antennal sockets and anterolateral corners of head, entire clypeal margin bearing row of long erect setae. *Antenna* with moderately long scape (SI 59–62), scape moderately incrassate, gently bent; pedicel subcylindrical, longer than broad; true antennomere count six; apparent antennomere count six to eight, flagellomeres basad apical club highly compressed, taken together only about as long as apical club. *Ventral head* with poorly developed postoccipital ridge with very short but broad anteromedian carina; median region of hypostoma triangular, arms strongly narrowed and very weakly spatulate; palpal formula not examined. *Mandible* with squared apical tooth subtended by pointed preapical denticle; small prebasal angle present; basal angle rounded to somewhat truncate; ectal face with longitudinal carina confluent with masticatory margin for much of its length, leaving narrow strip of depressed region including prebasal denticle.

Mesosoma in profile robust, dorsally feebly convex, sloping posteroventrally, pronotum distinctly higher than propodeum; in dorsal view mesosoma moderately thick (DMI 54–57; DMI2 82–86) and narrowed posteriorly, pronotum wider than propodeum; posterior propodeal margin very weakly concave; posterodorsal corners of propodeum rounded, without teeth or angles; declivitous face of propodeum shallowly but clearly concave in profile and oblique posterior view; propodeal spiracle small and inconspicuous, directed posterolaterally; propodeal lobes short, truncate.

Legs short (HFI 52–54) and rather slender; mesotibia without apicoventral spur.

Petiolar node not strongly attenuated dorsally, rather robust in profile, about 2.0 to 2.8 times higher than broad (LPeI 200–275); in profile anterior face of node convex, apex blunt to rounded, posterior face convex; in dorsal view petiole rectangular, sides subparallel, about 1.9 to 2.5 times broader than long (DPeI 192–250); in anterior view, petiolar outline clearly pentagonal, edges well-defined, angles slightly rounded, apex somewhat broadly peaked; in oblique anterior view anterior face flat; in ventral view subrectangular to weakly campaniform, sides slightly divergent posteriorly to weakly convex; subpetiolar process large, lobate-triangular, apex rounded,

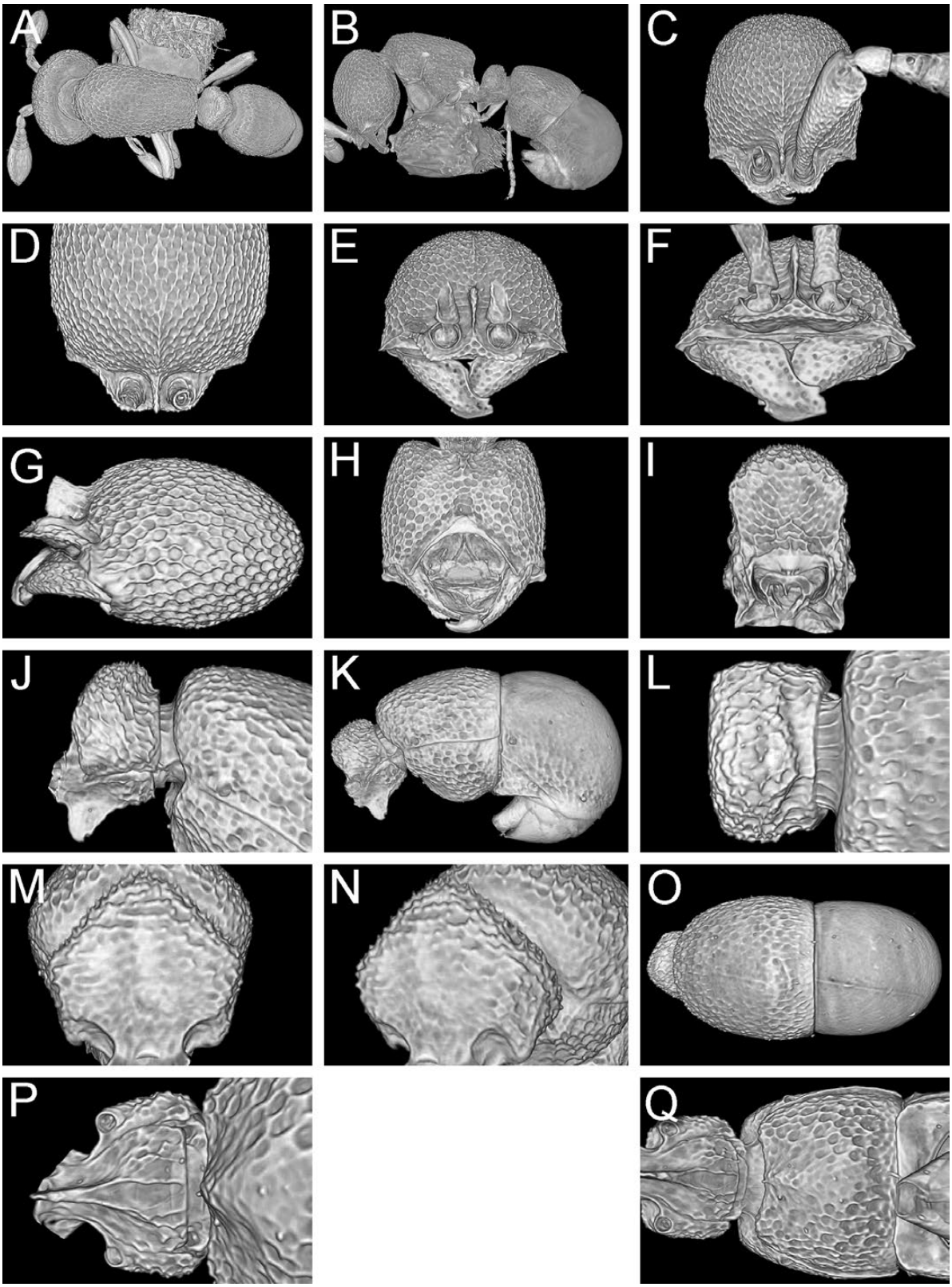

Fig. 36. Still images from shaded surface display volume renderings of *D. gryphon* sp. n. holotype (CASENT0790103) showing virtually segmented body parts. (A) Body in dorsal view, (B) body in profile, (C) head in full-face view, (D) head in dorsal view, (E) head in anterodorsal view, (F) head in anterior view, (G) head in profile, (H) head in ventral view, (I) posterior propodeum in posterior view, (J) petiole in profile, (K) petiole and gaster in profile, (L) petiole in dorsal view, (M) petiole in anterior view, (N) petiole oblique anterior view, (O) gaster in dorsal view, (P) petiole in ventral view, (Q) abdominal sternite 3 in ventral view, (R) mesotibia and mesotarsus in anterior view.

Model 9. 3D surface model of *D. gryphon* sp. n. holotype (CASENT0790103). An interactive version of this model is available in the HTML version of this article online and at https://sketchfab.com/3d-models/b89fada99bce4f169c7b7d55f977326a.

bearing numerous long, straight, white setae; petiolar spiracles large, round to slightly elliptical in ventral view.

Abdominal segment 3 asymmetrically campaniform, tergite prolonged anteriorly beyond anterior margin of sternite and widest point just anterad end of segment; AS3 evenly rounded in profile, deepest point at about the longitudinal midline in profile, with thick median ridge; AS3 without carinate prora, but still with anterior face distinctly depressed and anterior margin of ventral face weakly concave in ventral view; AT4 about 1.1 times longer than AT3 (ASI 108–113); AT4 evenly rounded hemidemispherical; AS4 with very well-developed anterior lip, overlapping nearly the entire width of AS3, anterior margin very weakly concave in ventral view; successive abdominal segments short, telescopic, often concealed.

Sculpture on head foveolate-reticulate to areolate, foveolae smaller on front of head; mandible rather roughly sculptured with dense piligerous punctae; frontal lamella and medial clypeus distinctly punctate; mesosoma, petiole, and abdominal segment 3 foveolate-reticulate, foveolae smaller and more regular on dorsal than lateral mesosoma, with rugulae present between foveolae on lateral mesosoma, especially posteriorly; declivitous face of propodeum with narrow transverse rugulae and sometimes punctae; AT4 quite smooth and shiny despite numerous minute piligerous punctulae.

Setation consisting of distinct, erect, white pilosity on front of head, mesosomal, petiolar and abdominal dorsa, generally becoming longer and denser with each succesive tagma in the posterior direction; lateral mesosoma with mostly appressed pubescence; sides of abdominal segments 3 and 4, petiolar sternite, and abdominal sternite 3 also bearing long erect setae in addition to underlayer of appressed pubescence; abdominal segments five through seven with similar pilosity to AT4, setae not noticeably longer or more curved; scape and legs with long, dense pubescence, mostly appressed to decumbent, with scattered erect setae; ectal face of mandible with abundant, long, curved, erect to suberect setae; setation of masticatory margin undetermined.

Color uniformly dull testaceous-yellow to light brown.

Etymology

The gryphon of mythology was a legendary creature with a body composed of different animals. *Discothyrea gryphon* is named like for its strange combination of characters, which are approximated only by the aberrant *D. chimera*. The archaic spelling *gryphon* is used in preference to the Latinate *griffin* as wordplay on the Greek root *grypos*, meaning hooked, in reference to the recurved abdomen of *Discothyrea*. The specific epithet is given as an appositive noun.

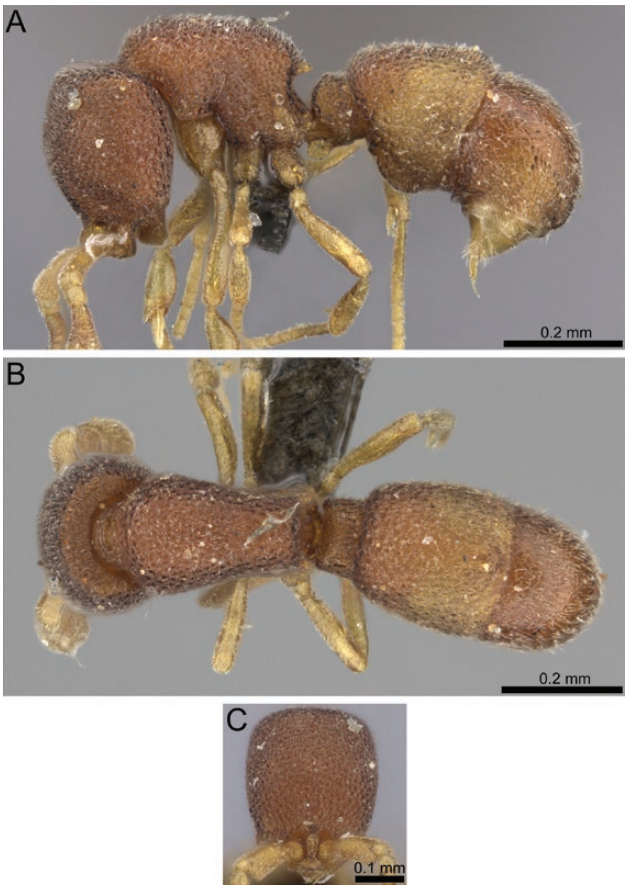

Fig. 37. Stacked digital color images of *D. hawkesi* sp. n. holotype (CASENT0235470—from https://www.antweb.org, photographer Will Ericson). (A) body in profile, (B) body in dorsal view, (C) head in full-face view.

Distribution and Biology

At present, known only from the type locality in Kayove in Rwanda and Mkomazi in Tanzania (Fig. 4I). Both localities are montane forest at elevations from 1600 to 2100 m. *Discothyrea gryphon* lives in leaf litter.

Comments

Discothyrea gryphon is easily recognizable on the basis of a combination of highly species-specific character states. The presence of a subapical tooth, dense standing pilosity, subquadrate head shape with sharply defined genal corners, and the row of long, straight setae on the anterior clypeal margin rapidly discriminate it from the remainder of the complex. As noted above, the similarity of *D. gryphon* and *D. chimera*, in the characters of the head and general habitus, suggest that they may constitute a natural group.

Variation

All examined specimens are consistent in virtually all characters. However, the development of the subapical mandibular denticle ranges from an indistinct angle to a relatively distinct, small denticle. This variation may be due to the denticle being worn down with age.

Discothyrea hawkesi Hita Garcia & Lieberman sp. n.

(Figs. 4J, 6J, 7J, 8J, 9J, 10J, 11J, 12J, 14J, 37, 38; Supp Video S10 [online only])

Type Material

HOLOTYPE, pinned worker, TANZANIA, Morogoro, Morogoro, Mkungwe Forest Reserve, –6.89388, 37.90414, 700 m, primary

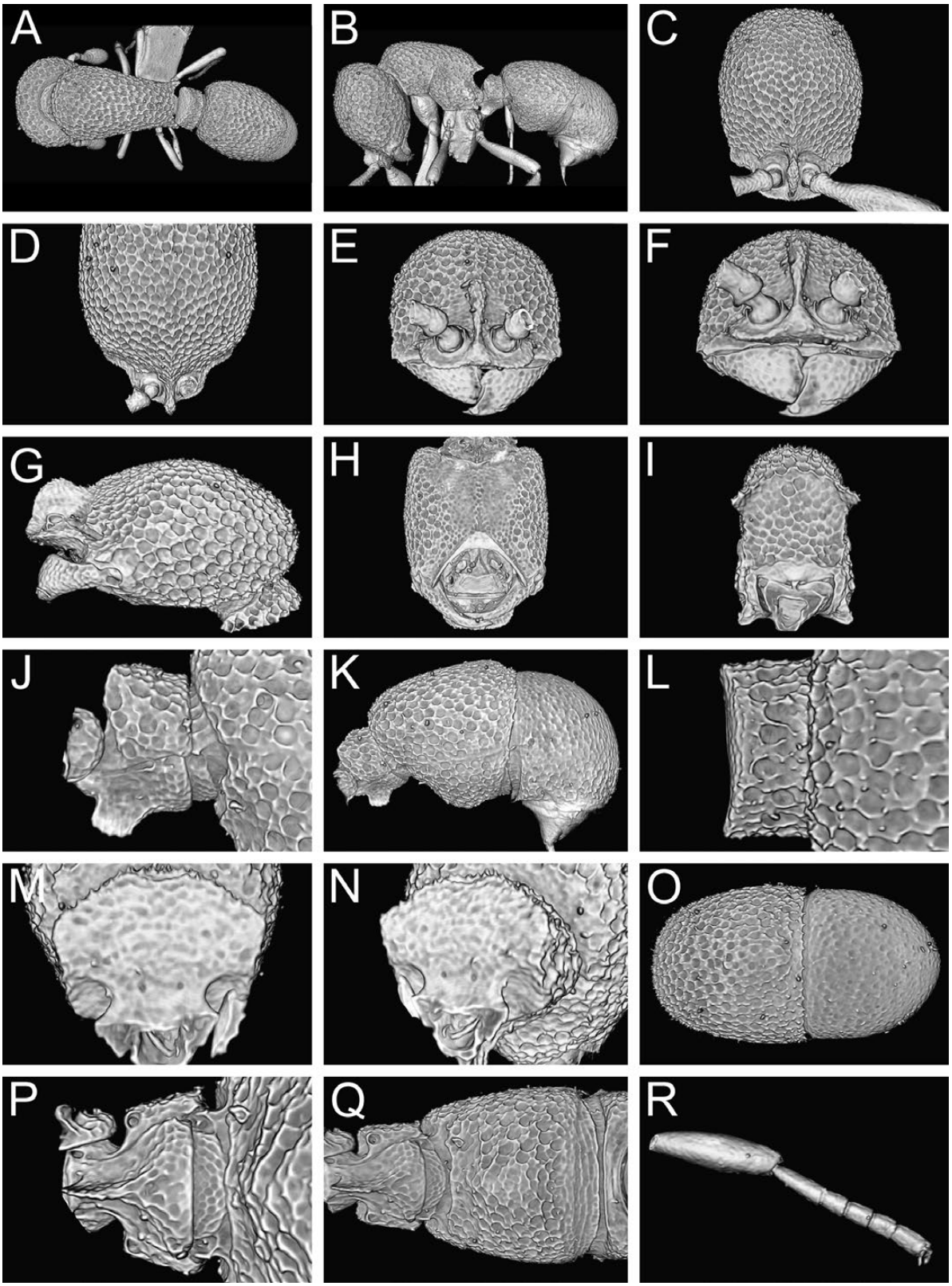

Fig. 38. Still images from shaded surface display volume renderings of *D. hawkesi* sp. n. holotype (CASENT0235470) showing virtually segmented body parts. (A) Body in dorsal view, (B) body in profile, (C) head in full-face view, (D) head in dorsal view, (E) head in anterodorsal view, (F) head in anterior view, (G) head in profile, (H) head in ventral view, (I) posterior propodeum in posterior view, (J) petiole in profile, (K) petiole and gaster in profile, (L) petiole in dorsal view, (M) petiole in anterior view, (N) petiole oblique anterior view, (O) gaster in dorsal view, (P) petiole in ventral view, (Q) abdominal sternite 3 in ventral view, (R) mesotibia and mesotarsus in anterior view.

Model 10. 3D surface model of *D. hawkesi* sp. n. holotype (CASENT0235470). An interactive version of this model is available in the HTML version of this article online and at https://sketchfab.com/3d-models/fb11baa775634f20a8af4c4533b41ab1.

forest, leaf litter, collection code CEPF-TZ-6.2, 12.–15.X.2007 (*P. Hawkes, M. Bhoke & U. Richard*) (SAMC: CASENT0235470). **PARATYPE**, one pinned worker with same data as holotype (BMNH: CASENT0250385).

Cybertype. Volumetric raw data (in DICOM format), 3D rotation video, still images of surface volume rendering, and 3D surface (in PLY format) of the physical holotype (CASENT0235470) in addition to stacked digital color images illustrating head in full-face view, profile and dorsal views of the body. The data are deposited at Dryad (Hita Garcia et al. 2019, http://doi.org/10.5061/dryad.3qm4183) and can be freely accessed as virtual representation of the type. In addition to the cybertype data at Dryad, we also provide a freely accessible 3D surface model of the holotype at Sketchfab (Model 10).

Diagnosis

The following character combination distinguishes *D. hawkesi* from the remainder of the complex: masticatory margin of mandible edentate; anterior clypeal margin bearing only few tiny, recurved setae; anterolateral corner of gena not sharply angled and not denticulate/dentate; eye absent, or reduced to a tiny pigmented spot; head distinctly longer than broad; mesosoma evenly and gently convex in profile; propodeum conspicuously dentate, declivitous face strongly concave; mesotibia without apicoventral spur; AT3 around 1.1 times longer than AT4 (ASI 89–92); abdominal sternite 3 not squared in profile; medial clypeus broad, not clearly projecting; erect pilosity absent on mesosoma and abdominal terga.

Worker Measurements and Indices (*n* = 2)

EL 0.00; HL 0.46; HW 0.45–0.46; HW 0.36; SL 0.22–0.25; PH 0.22–0.23; PW 0.27–0.28; DML 0.31–0.32; PrH 0.25–0.27; WL 0.55–0.58; HFL 0.25; PeL 0.06–0.07; PeW 0.17; PeH 0.17; LT3 0.31–0.32; LT4 0.28; OI 0; CI 78–80; SI 49–54; LMI 49–50; DMI 58–61; DMI2 86–87; ASI 89–92; HFI 54–56; DPeI 283–320; LPeI 243–283.

Worker Description

Head clearly longer than broad, subrectangular (CI 78–80); posterior head margin straight; posterodorsal corners of head rounded; sides of head in frontal view subparallel; eye absent, or reduced to a tiny pigmented spot; frontal lamella rather low in profile, apex gently rounded; with distinct translucent basal fenestra, offset from remainder of disc which is more or less opaque; medial clypeus transverse to gently convex, lateral clypeus curving moderately strongly between antennal sockets and anterolateral corners of head, sides of medial clypeus subparallel laterad antennal sockets, bearing a few tiny, recurved setae. *Antennae* with relatively shorter scape (49–54), scape strongly incrassate, gently bent; pedicel subglobose, slightly longer than broad; true antennomere count nine; apparent antennomere count eight to ten, flagellomeres basad apical club highly compressed, taken together only about as long as apical club. *Ventral head* with narrow, weakly sinuate postoccipital ridge without anteromedian carina; medial region of hypostoma rounded-triangular, arms somewhat narrowed, similar in width across their length; palpal formula not examined. *Mandible* edentate; basal angle broadly rounded, with blunt prebasal angle; ectal face with longitudinal carina running from prebasal angle to apex, confluent with masticatory margin in its distal half, creating a long, comma-shaped depressed region.

Mesosoma evenly and gently convex in profile, pronotum very slightly higher than propodeum; in dorsal view mesosoma moderately thick (DMI 58–61; DMI2 86–87) and narrowed posteriorly, pronotum wider than propodeum; pronotal humeri broadly rounded; posterior propodeal margin very concave between denticles; posterodorsal corners of propodeum denticulate; denticles small but distinct, triangular, laterally flattened and slightly translucent; declivitous face of propodeum clearly concave in profile and oblique posterior view; propodeal spiracle fairly inconspicuous, directed posterolaterally; propodeal lobes well-developed, rounded.

Legs rather short and thin (HFI 54–56); mesotibia without apicoventral spur or seta; mesobasitarsus short, subequal to or shorter than tarsomeres II–IV taken together.

Petiolar node somewhat thick in profile, about 2.4 to 2.8 times higher than long (LPeI 243–283); in profile anterior face of node convex, apex rounded to sloping posteroventrally, posterior face straight; in dorsal view, node roughly subrectangular, about 2.8 to 3.2 times broader than long (DPeI 283–320), sides slightly divergent posteriorly; in anterior view, petiolar outline very broad, roughly hexagonal, dorsal angles more poorly defined than lateral angles; in oblique anterior view, anterior face weakly concave; in ventral view, roughly trapezoidal, sides diverging posteriorly; subpetiolar process broad, lobate to rectangular, apex rounded to truncate; petiolar spiracles relatively small, reniform in ventral view.

Abdominal segment 3 roughly campaniform, widest just anterad end of segment; tergite slightly anteriorly prolonged past anterior margin of AS3; AS3 bulging unevenly, deepest point posterad longitudinal midline in profile, with thick median lobe; prora sinuate; AT3 around 1.1 times longer than AT4 (ASI 89–92); AT4 gently recurved, hemidemispherical; AS4 with quite short but broad anterior lip, overlapping most of the width of AS3, anterior margin straight to weakly convex in ventral view; successive abdominal segments short, telescopic, often concealed.

Sculpture on head densely foveolate, foveolae becoming smaller and denser towards midline of head; mandibles with sparse but distinct piligerous punctae; mesosoma and petiole similarly sculptured to head, becoming punctate-reticulate, mesosoma equally sculptured on dorsum and sides; abdominal segment 3 somewhat sparsely but coarsely punctate, sculpture similar on tergite and sternite; AT4 coriarious-punctate and notably shinier than AT3, sometimes appearing finely granulate or scabriculous due to distribution of punctae.

Setation on head consisting of very fine, inconspicuous appressed pubescence; scape with longer, denser, but still quite fine white

appressed pubescence; ectal face of mandible with fairly long, curved, mostly appressed setae; masticatory margin with row of straight setae; mesosomal dorsum, petiolar node, and gastral dorsum with distinct, well-spaced pilosity, appressed to suberect; more standing hairs present on AT3 than other segments; sides of mesosoma and petiole glabrous; sides of gastral terga with some diffuse, fine appressed pubescence; petiolar sternite and abdominal sternite 3 with a few short, erect hairs; abdominal segments five through seven with relatively long, flexuous hairs; legs mostly hairless, with scattered appressed pubescence.

Color testaceous orange, sometimes becoming yellowish in places on gaster; appendages dull yellow.

Etymology

The species name is a patronym in honor of our great colleague Peter Hawkes from Pretoria, South Africa, who is likely the most important contemporary collector of Afrotropical ants. He was so kind as to provide invaluable material, without which this revision would not have been possible. The specific epithet is given as a genitive noun.

Distribution and Biology

Currently, *D. hawkesi* is known only from the Mkungwe Forest Reserve in Tanzania (Fig. 4J), where it was collected in primary forest at an elevation of 700 m and apparently lives in leaf litter.

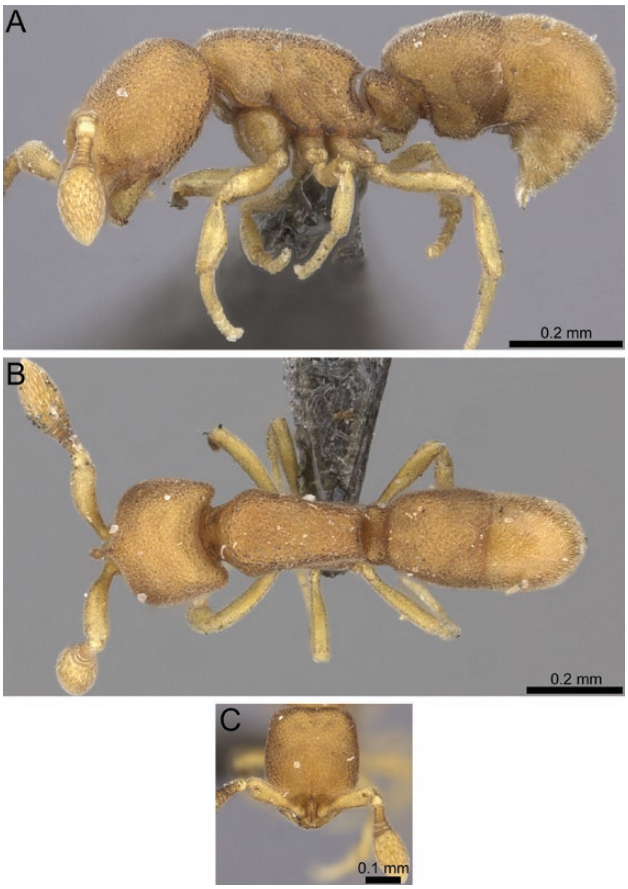

Fig. 39. Stacked digital color images of *D. kalypso* sp. n. holotype (CASENT0235468—from https://www.antweb.org, photographer Will Ericson). (A) body in profile, (B) body in dorsal view, (C) head in full-face view.

Comments

Discothyrea hawkesi is a member of a possible natural group within the *traegaordhi*-complex that also includes the species *D. kalypso*, *D. maia*, *D. michelae*, and *D. penthos*. These species are united by the presence of differentiated denticles on the propodeum. However, within this assemblage, *D. hawkesi* lacks the structure of the third abdominal sternite found in these species.

Variation

The two known specimens do not display any significant variation.

Discothyrea kalypso Hita Garcia & Lieberman sp. n. (Figs. 2B, 4K, 6K, 7K, 8K, 9K, 10K, 11K, 12K, 14K, 39, 40; Supp Video S11 [online only])

Type Material

HOLOTYPE, pinned worker, TANZANIA, Pwani, Mafia, Mafia Island, Mlola Forest, –7.89576, 39.82842, 20 m, primary forest, leaf litter, 9.–13.III.2008 (*P. Hawkes, Y. Mlacha & F. Ninga*) (SAMC: CASENT0235468).

Cybertype. Volumetric raw data (in DICOM format), 3D rotation video, still images of surface volume rendering, and 3D surface (in PLY format) of the physical holotype (CASENT0235468) in addition to stacked digital color images illustrating head in full-face view, profile and dorsal views of the body. The data are deposited at Dryad (Hita Garcia et al. 2019, http://doi.org/10.5061/dryad.3qm4183) and can be freely accessed as virtual representation of the type. In addition to the cybertype data at Dryad, we also provide a freely accessible 3D surface model of the holotype at Sketchfab (Model 11).

Diagnosis

The following character combination distinguishes *D. kalypso* from the remainder of the complex: eyes absent; frontal lamella disciform in profile, without conspicuous, round basal fenestra; mesosoma low, gracile (LMI 42; DMI2 81), not dorsally convex in profile; propodeum denticulate, denticles short and somewhat blunt; mesotibia without distinct ventral spur; abdominal sternite 3 rectangular in profile, ventral margin straight; erect pilosity absent from mesosoma and abdominal terga.

Worker Measurements and Indices (*n* = 1)

EL 0.00; HL 0.45; HW 0.35; SL 0.23; PH 0.19; PW 0.28; DML 0.30; PrH 0.22; WL 0.45; HFL 0.24; PeL 0.05; PeW 0.16; PeH 0.15; LT3 0.28; LT4 0.26; OI 0; CI 78; SI 51; LMI 42; DMI 62; DMI2 81; ASI 86; HFI 53; DPeI 320; LPeI 300.

Worker Description

Head somewhat elongate (CI 78), posterior head margin straight to weakly concave; posterodorsal corners of head rounded; in frontal view, sides of head gently convex; anterolateral corners of gena relatively well-defined; eyes absent; frontal lamella low and disciform in profile, without distinct apex, with conspicuous, elliptical basal fenestra; medial clypeus very narrow, anteromedially projecting, slightly emarginate apically, lateral clypeus broadly curving between antennal sockets and anterolateral corners of head, bearing very short curved setae. *Antenna* with relatively shorter scape (SI 54), scape moderately incrassate, gently bent; pedicel campaniform, slightly longer than broad; true antennomere count nine; apparent antennomere count

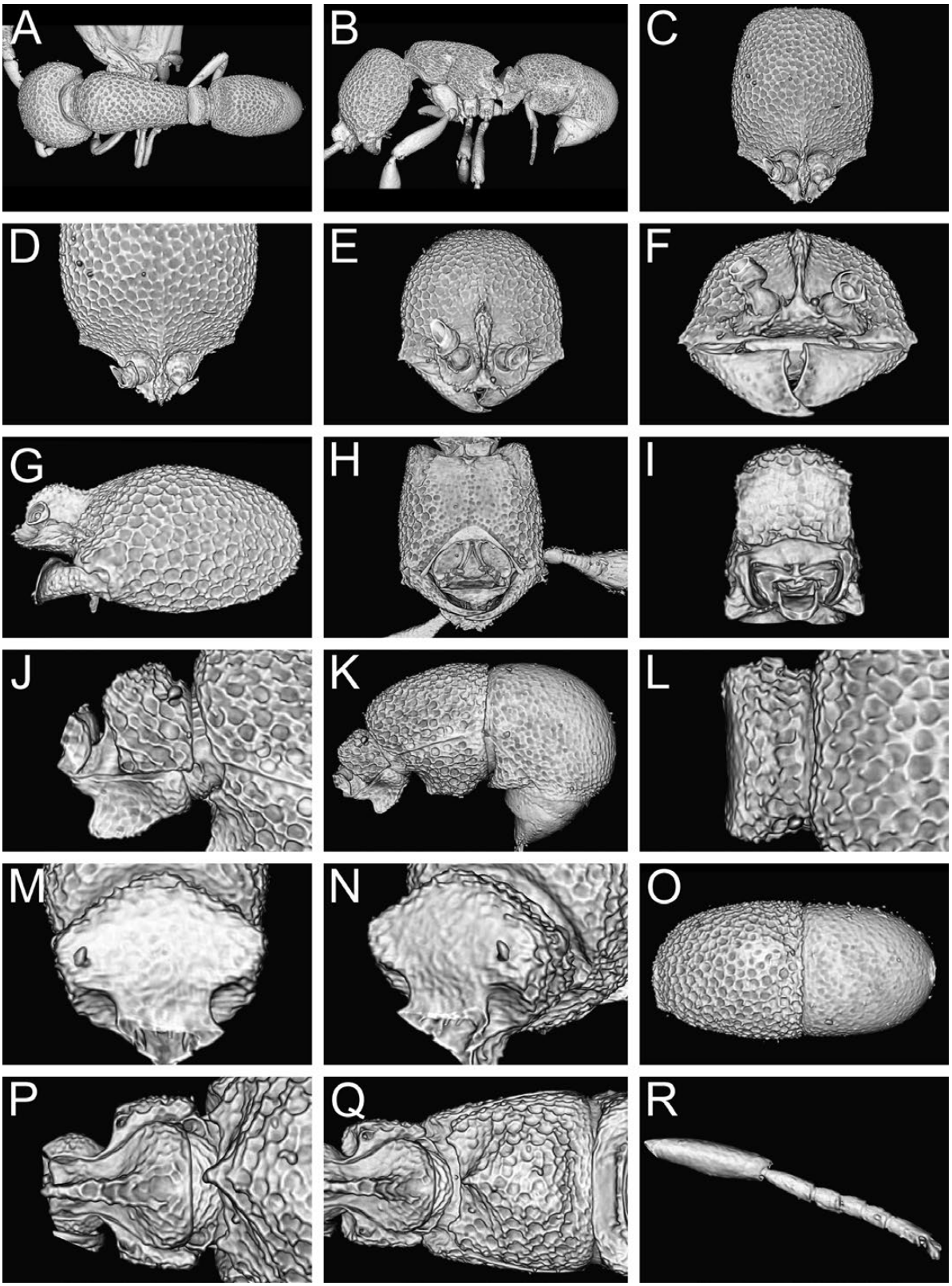

Fig. 40. Still images from shaded surface display volume renderings of *D. kalypso* sp. n. holotype (CASENT0235468) showing virtually segmented body parts. (A) Body in dorsal view, (B) body in profile, (C) head in full-face view, (D) head in dorsal view, (E) head in anterodorsal view, (F) head in anterior view, (G) head in profile, (H) head in ventral view, (I) posterior propodeum in posterior view, (J) petiole in profile, (K) petiole and gaster in profile, (L) petiole in dorsal view, (M) petiole in anterior view, (N) petiole oblique anterior view, (O) gaster in dorsal view, (P) petiole in ventral view, (Q) abdominal sternite 3 in ventral view, (R) mesotibia and mesotarsus in anterior view.

nine; flagellomeres basad apical club highly compressed, taken together only about as long as apical club. *Ventral head* with narrow, horizontal postoccipital ridge with very short, roughly triangular anteromedian prolongation; median region of hypostoma rounded, arms narrowed, somewhat spatulate apicolaterally; palpal formula not examined. *Mandible* edentate except for well-defined, triangular prebasal denticle; basal angle squared; ectal face of mandible with carina running from baswal angle to apex, confluent with margin distal to prebasal denticle.

Mesosoma gracile, sloping posteroventrally, pronotum slightly higher than propodeum; in dorsal view mesosoma conspicuously slender and elongate (DMI 54; DMI2 81), pronotum not significantly wider than propodeum; pronotal humeri slightly rounded; posterior propodeal margin concave; posterodorsal corners of propodeum denticulate, denticles distinct but very short, laterally flattened, slightly diverging posterolaterally; declivitous face of propodeum distinctly concave in profile and oblique posterior view; propodeal spiracle small and very inconspicuous, directed posterodorsally; propodeal lobes well-developed, lobate.

Legs short (HFI 53) and rather slender; mesotibia without distinct ventral spur.

Petiolar node strongly attenuated dorsally, about 3.0 times higher than long (LPeI 300); in profile anterior face of node sloping posterodorsally, apex peaked, posterior face sloping posteroventrally; in dorsal view, petiole rectangular, about 3.2 times wider than long (DPeI 320), sides slightly convex; in anterior view, petiolar outline pentagonal, edges well-defined, angles somewhat rounded; in oblique anterior view, anterior face flat; subpetiolar process broad, lobate, apex rounded.

Abdominal segment 3 with tergite elongate-campaniform, anteriorly prolonged slightly over petiole, widest posteriorly; sternite subquadrate, in profile anterior and ventral faces flat, posterior face sloping slightly posterodorsally; prora well-defined, laterally with two triangular projections, medially straight; AS3 with large median ridge extending anteriorly to prora; AT3 weakly longer than AT4 (ASI 86); AT4 slightly prolate hemidemispherical; AS4 with anterior overlapping about median one-third of AS3, anterior margin straight in ventral view; successive abdominal segments short, telescopic, often concealed.

Sculpture on head, mesosoma, and abdominal segment 3 foveolate-reticulate, foveolae becoming smaller on front of head and more dilute on lateral mesosoma; mandible with fine piligerous punctulae with fairly shiny interspaces; AT4 coriarious-punctulate, somewhat shinier than AT3.

Setation on head very dilute, short appressed pubescence, appearing glabrous at lower magnification; scape with velvety appressed pubescence; mesosoma and AT3 with short, dilute appressed pubescence almost entirely restricted to dorsal surfaces; AT4 with slightly longer but still inconspicuous appressed pubescence; successive abdominal segments with relatively short, mostly decumbent or subdecumbent setae, a few longer and more erect setae present on posterior segmental margins; legs with velvety appressed pubescence, similar to that on scape; ectal face of mandible with relatively long but fine appressed to decumbent setae; masticatory margin with row of straight, stout setae.

Color uniformly dull but clear yellowish.

Etymology

Kalypso was a nymph in Greek mythology who lived on a secluded island, best known from Homer's epos 'The Odyssey'. The species is named in reference to the isolated type locality on Mafia Island, Tanzania. The specific epithet is given as an appositive noun.

Distribution and Biology

At present known only from the type locality, the Mlola Forest on Mafia Island, Tanzania (Fig. 4K). It was collected from leaf litter in a primary coastal forest habitat at an elevation of 20 m.

Model 11. 3D surface model of *D. kalypso* sp. n. holotype (CASENT0235468). An interactive version of this model is available in the HTML version of this article online and at https://sketchfab.com/3d-models/2ae729d691ae4faa96be3ce6e27b19c3.

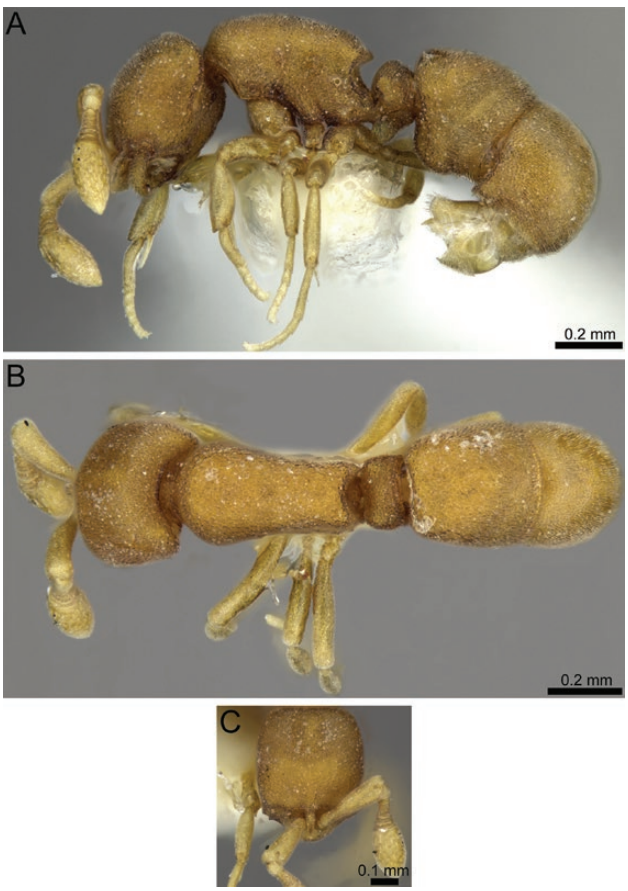

Fig. 41. Stacked digital color images of *D. maia* sp. n. holotype (CASENT0790541). (A) Body in profile, (B) body in dorsal view, (C) head in full-face view.

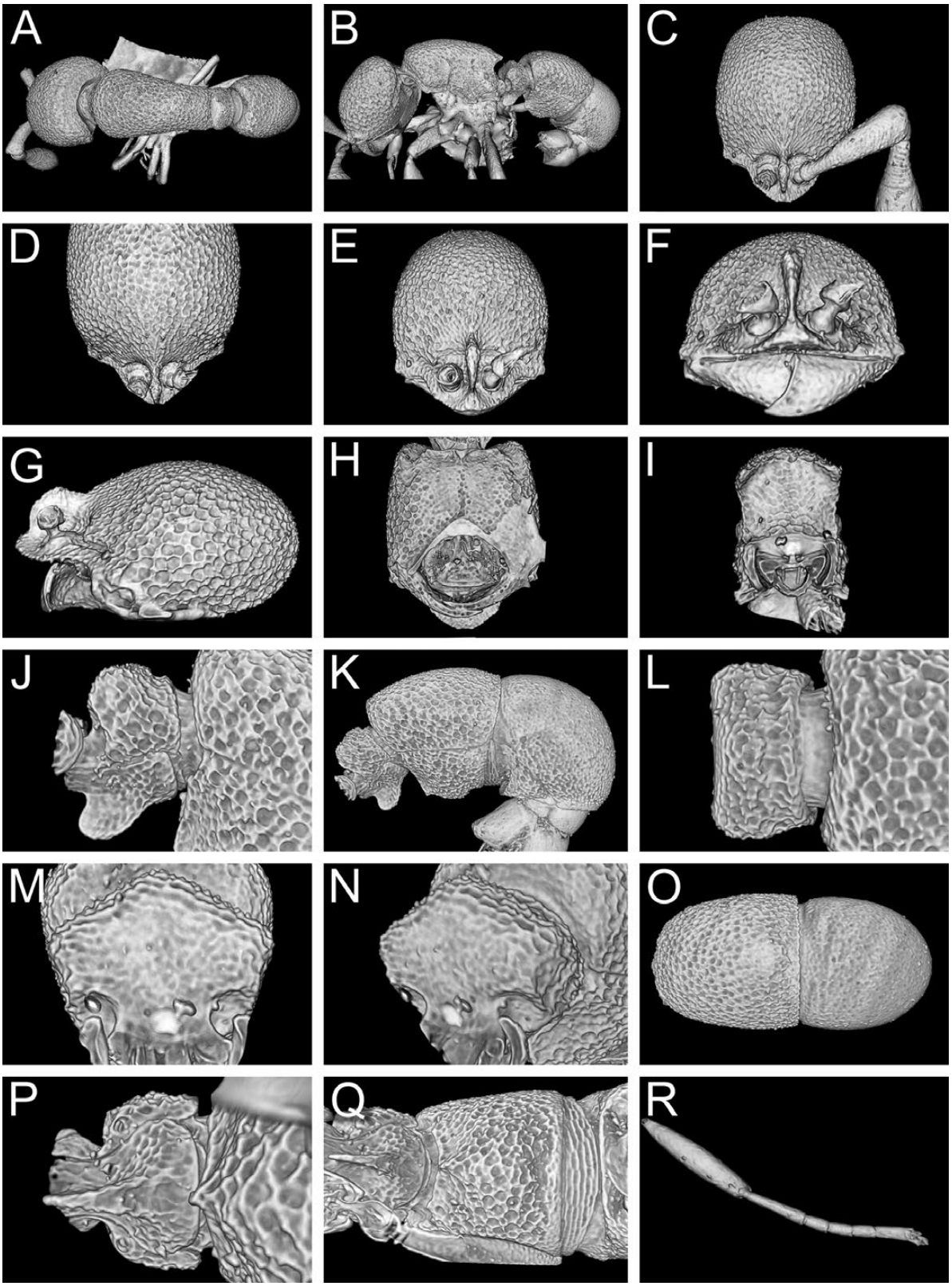

Fig. 42. Still images from shaded surface display volume renderings of *D. maia* sp. n. holotype (CASENT0790541) showing virtually segmented body parts. (A) Body in dorsal view, (B) body in profile, (C) head in full-face view, (D) head in dorsal view, (E) head in anterodorsal view, (F) head in anterior view, (G) head in profile, (H) head in ventral view, (I) posterior propodeum in posterior view, (J) petiole in profile, (K) petiole and gaster in profile, (L) petiole in dorsal view, (M) petiole in anterior view, (N) petiole oblique anterior view, (O) gaster in dorsal view, (P) petiole in ventral view, (Q) abdominal sternite 3 in ventral view, (R) mesotibia and mesotarsus in anterior view.

Comments

The only other species known from Mafia Island is *D. mixta* but both belong to different species complexes and cannot be confused with each other. Furthermore, *D. kalypso* is moderately similar to *D. maia,* from which it can be distinguished most readily by the proportions of the mesosoma and development of the propodeal denticles and declivity, and the characters of the third abdominal sternite, which has a more strongly developed median ridge and a characteristically shaped prora. Additional differences are shorter appendages and overall smaller size, and the evenly rounded profile of the frontal lamella which has (indistinct) faces in the *D. maia*. Although both species are known only from the holotype, the ranges are entirely disjunct and widely separated. *Discothyrea kalypso* is also quite similar in general habitus to *D. michelae*, being rather slender and gracile, but lacks the characteristic petiolar shape and standing pilosity of the latter.

Variation

Since *D. kalypso* is only known from the holotype, there is no information about intraspecific variation.

Discothyrea maia Hita Garcia & Lieberman sp. n. (Figs. 4L, 6L, 7L, 8L, 9L, 10L, 11L, 12L, 13E, 14L, 41, 42; Supp Video S12 [online only])

Type Material

Holotype, pinned worker, ZIMBABWE, Chishawasha, [–17.883, 31.227], 1535 m, I.1981 (*A. Watsham*) (BMNH: CASENT0790541).

Cybertype. Volumetric raw data (in DICOM format), 3D rotation video, still images of surface volume rendering, and 3D surface (in PLY format) of the physical holotype (CASENT0790541) in addition to stacked digital color images illustrating head in full-face view, profile and dorsal views of the body. The data are deposited at Dryad (Hita Garcia et al. 2019, http://doi.org/10.5061/dryad.3qm4183) and can be freely accessed as virtual representation of the type. In addition to the cybertype data at Dryad, we also provide a freely accessible 3D surface model of the holotype at Sketchfab (Model 12).

Diagnosis

The following character combination distinguishes *D. maia* from the remainder of the complex: abdominal sternite 3 not rectangular in profile, ventral margin rounded; mesosoma somewhat slender but not especially gracile (LMI 53; DMI2 81), dorsally convex in profile; propodeum denticulate denticles well-developed, propodeal declivity strongly concave; erect pilosity absent from mesosoma and abdominal terga; eyes absent; frontal lamella with elliptical basal fenestra.

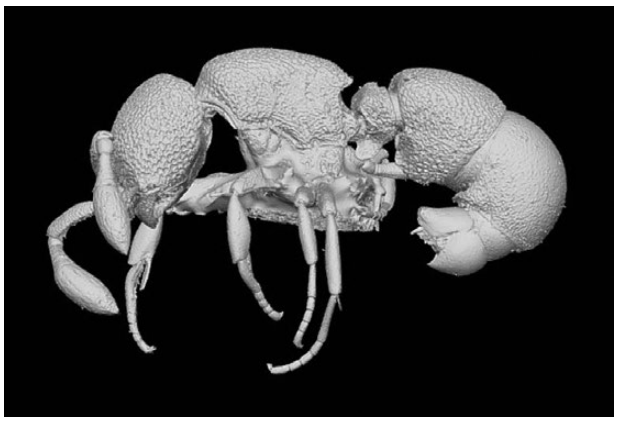

Model 12. 3D surface model of *D. maia* sp. n. holotype (CASENT0790541). An interactive version of this model is available in the HTML version of this article online and at https://sketchfab.com/3d-models/a26ae6a2819a4473a6b83152e2e82dff.

Worker Measurements and Indices (*n* = 1)

EL 0.00; HL 0.50; SL 0.29; PH 0.26; PW 0.29; PrH 0.29; DML 0.36; WL 0.49; HFL 0.32; PeL 0.07; PeW 0.20; PeH 0.25; LT3 0.28; LT4 0.27; OI 0; CI 78; SI 58; LMI 53; DMI 59; DMI2 81; ASI 98; HFI 65; DPeI 286; LPeI 357.

Worker Description

Head somewhat elongate (CI 78); posterior head margin straight to weakly concave; posterodorsal corners of head rounded; in frontal view, sides of head weakly conexl anterolateral corners of gena well-defined; eyes absent; frontal lamella low and lobate in profile, with elliptical basal fenestra; medial clypeus narrow, anteriomedially projecting, lateral clypeus very weakly convex apically, lateral clypeus broadly curving between antennal sockets and anterolateral corners of head, entire clypeal margin bearing very short curved setae. *Antenna* with moderately long scape (SI 58), scape moderately incrassate, gently bent; pedicel subcylindrical, scarcely longer than broad; true antennomere count nine; apparent antennomere count 8–9, flagellomeres basad apical club highly compressed, taken together slightly shorter than apical club. *Ventral head* with well-developed, sinuate preoccipital ridge, with very short, triangular anteromedial carina; medial region of hypostoma rounded-triangular, arms slightly narrowed, somewhat spatulate apicolaterally; palpal formula not examined. *Mandible* edentate except for small prebasal angle; basal angle squared; ectal face with carina running from prebasal angle to apex, confluent with masticatory margin for entire length except laterad prebasal angle.

Mesosoma slender, gently convex in profile, pronotum somewhat higher than than propodeum; in dorsal view mesosoma elongate (DMI 59; DMI2 81), pronotum slightly wider than propodeum; pronotal humeri rounded; posterior propodeal margin strongly concave; posterodorsal corners of propodeum denticulate, denticles well-developed, dorsoventrally flattened, weakly diverging posterolaterally; declivitous face of propodeum distinctly concave in profile and oblique posterior view; propodeal spiracle relatively large, circular, directed posterodorsally; propodeal lobes well-developed, lobate.

Legs moderately long (HFI 65) and very slender; mesotibia without apicoventral spur or seta; mesobasitarsus fairly long, slightly longer than tarsomeres II–IV taken together.

Petiolar node strongly attenuated dorsally, about 3.6 times higher than long (LPeI 357); in profile anterior face of node sloping posteroventrally; in dorsal view, petiole subrectangular, about 2.9 times wider than long (DPeI 286), sides slightly convex; in anterior view, petiolar outline pentagonal, edges well-defined, dorsolateral angles rounded; in oblique anterodorsal view, anterior face flat; subpetiolar process fairly long, lobate, apex rounded.

Abdominal segment 3 elongate-campaniform, anteriorly prolonged slightly over anterior sternal margin, widest posteriorly; sternite in profile somewhat truncate; AS3 with well-defined median ridge broadening to indistinct lobe posteriorly, reaching prora anteriorly; prora carinulate, concave; AT3 approximately

as long as AT4; successive abdominal segments short, telescopic, concealed.

Sculpture on head, petiolar node, and abdominal segment 3 foveolate-reticulate, foveolae larger on lateral head surfaces, replaced by very fine rugulae anteromedially around frontal lamella; ventral head surface punctate to punctulate, mostly smooth medially except for small punctures arond subgenal sulcus; frontal lamella and clypeus rough, granulose to weakly rugulose; mandible with very small punctulae; dorsal mesosoma densely punctate-reticulate; punctae on lateral mesosoma sparser, sculpture more predominantly rugulose to reticulate; declivitous face of propodeum finely reticulate, reticulum most prominent ventrally; petiolar sternite densely punctate; abdominal tergite 4 conspicuously smoother than AT3, with very, shallow punctulae, becoming more strongly punctate posteriorly.

Setation on head dilute, short appressed pubescence; scape with slightly longer but tightly appressed pubescence; mesosoma and AT3 with very short, dilute, fine appressed pubesence, mostly restricted to dorsal surfaces of mesosoma; AT4 with longer, more conspicuous pubescence; successive abdominal segments with relatively short decumbent to erect setae, longer on terminal segments; legs with relatively long but tightly appressed pubescence, similar to scape; ectal face of mandible with fairly long, distinctly spaced, curved subdecubent setae; masticatory margin of mandible with row of straight, stout setae.

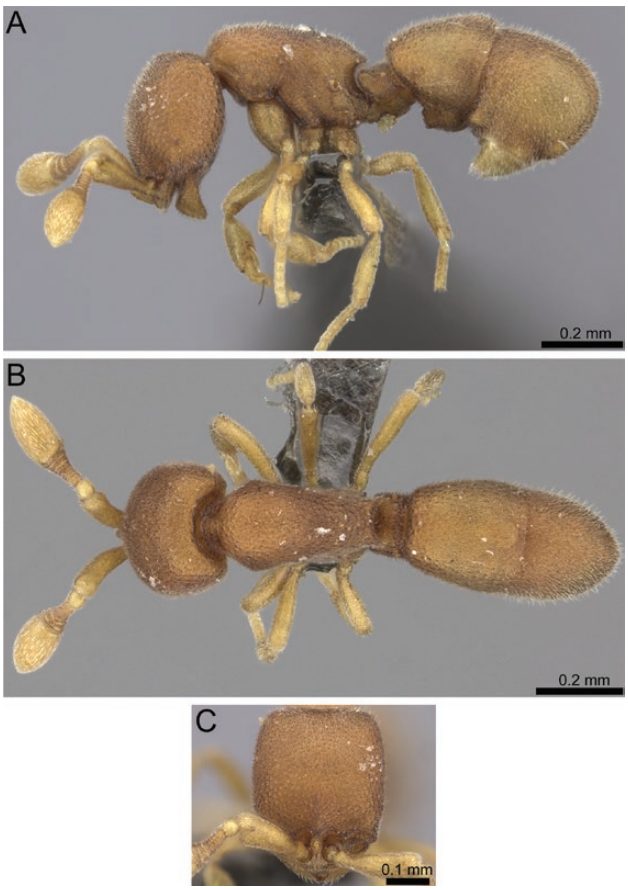

Fig. 43. Stacked digital color images of *D. michelae* sp. n. holotype (CASENT0235469—from https://www.antweb.org, photographer Will Ericson). (A) body in profile, (B) body in dorsal view, (C) head in full-face view.

Color uniformly dull yellowish, appendages slightly lighter and more clear.

Etymology

In Greek mythology, Maia was a nymph of the seven Pleiades, mainland-dwelling sisters to the insular Kalypso; the new species is named for its morphological affinity to *D. kalypso*. In addition, *maia* in Greek means 'midwife', which is considered appropriate for an eusocial insect with an all-female working caste. The species epithet is to be treated as an appositive noun.

Distribution and Biology

At present, known only from the type locality in Zimbabwe (Fig. 4L). Unfortunately, no ecological information is provided on the collection label, but it may originate from savanna woodland.

Comments

Discothyrea maia is morphologically distinct from all mainland species of the *traegaordhi* complex except *D. michelae*, but the latter species is easily distinguished based on its standing pilosity, squared third abdominal tergite, and bilobed petiolar node, as well as by the form of the medial clypeus which is broad and transverse in *D. michelae* and anteriorly prolonged in *D. maia*. Presently, the only other member of the complex known from Zimbabwe is *D. gaia*, but both are unlikely to be confused due to noticeable differences in body size, overall shape, and pilosity.

Discothyrea michelae Hita Garcia & Lieberman sp. n. (Figs. 4M, 6M, 7M, 8M, 9M, 10M, 11M, 12M, 14M, 43, 44; Supp. Video S13 [online only])

Type Material

HOLOTYPE, pinned worker, TANZANIA, Kilimanjaro, Mwanga, Kindoroko Forest Reserve, –3.7452, 37.64267, 1739 m, primary forest, leaf litter, collection code CEPF-TZ-5.2, 5.–8.IX.2005 (*P. Hawkes, J. Makwati & R. Mtana*) (SAMC: CASENT0235469). Paratype, pinned worker with same data as holotype (BMNH: CASENT0250384).

Cybertype. Volumetric raw data (in DICOM format), 3D rotation video, still images of surface volume rendering, and 3D surface (in PLY format) of the physical holotype (CASENT0235469) in addition to stacked digital color images illustrating head in full-face view, profile and dorsal views of the body. The data are deposited at Dryad (Hita Garcia et al. 2019, http://doi.org/10.5061/dryad.3qm4183) and can be freely accessed as virtual representation of the type. In addition to the cybertype data at Dryad, we also provide a freely accessible 3D surface model of the holotype at Sketchfab (Model 13).

Diagnosis

The structure of the petiole is unique among the Afrotropical fauna: no other species approximates the rectangular outline of the petiolar node, with sharp dorsolateral peaks and a deeply impressed anterior face, the node therefore appearing bilobed. The following character combination further distinguishes *D. michelae* from the remainder of the complex: abdominal sternite 3 with strongly developed median ridge anteriorly surpassing prora, appearing rectangular in profile; standing pilosity present on mesosoma and abdominal terga; propodeum denticulate, declivity deeply concave.

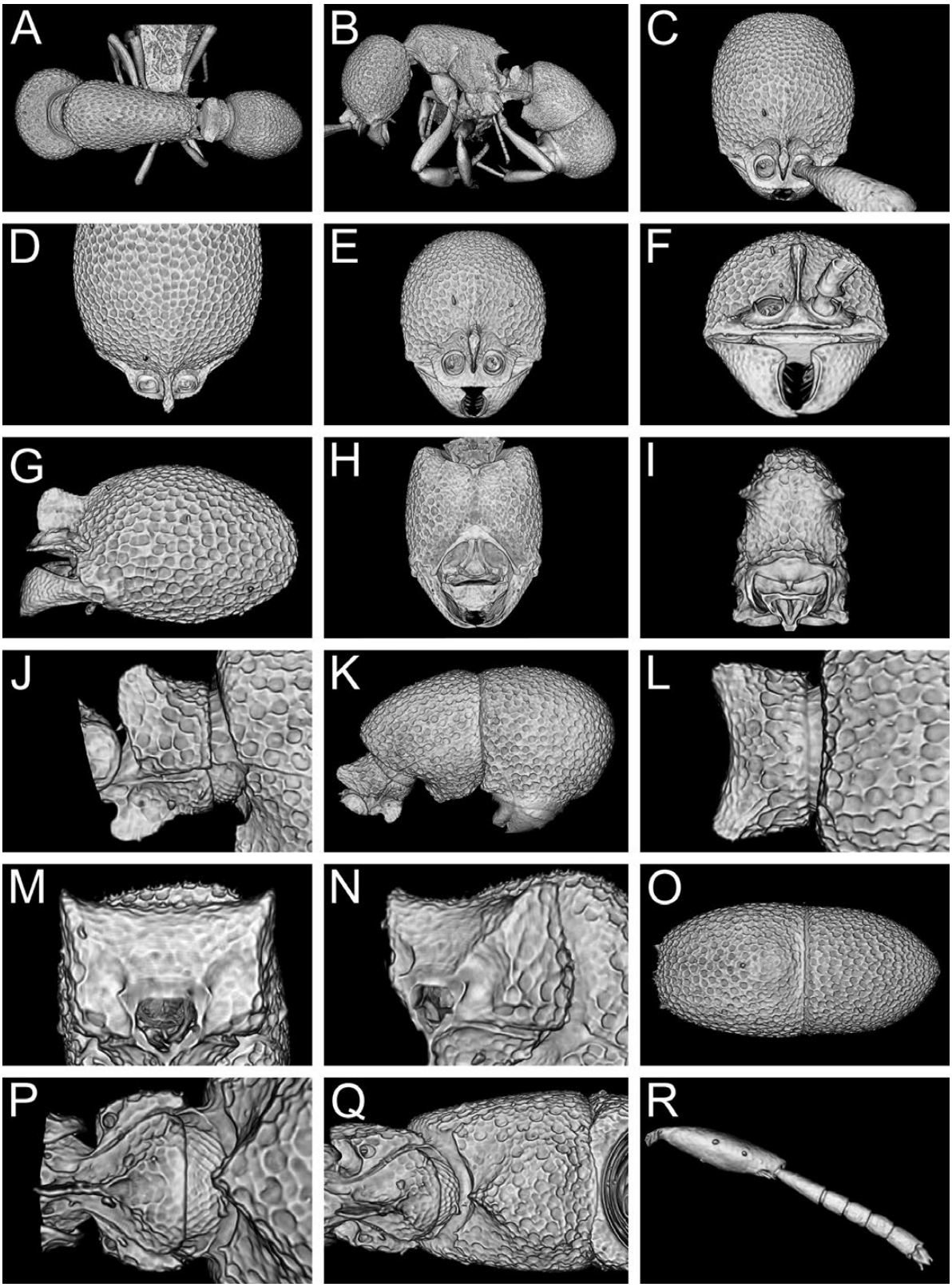

Fig. 44. Still images from shaded surface display volume renderings of *D. michelae* sp. n. holotype (CASENT0235469) showing virtually segmented body parts. (A) Body in dorsal view, (B) body in profile, (C) head in full-face view, (D) head in dorsal view, (E) head in anterodorsal view, (F) head in anterior view, (G) head in profile, (H) head in ventral view, (I) posterior propodeum in posterior view, (J) petiole in profile, (K) petiole and gaster in profile, (L) petiole in dorsal view, (M) petiole in anterior view, (N) petiole oblique anterior view, (O) gaster in dorsal view, (P) petiole in ventral view, (Q) abdominal sternite 3 in ventral view, (R) mesotibia and mesotarsus in anterior view.

Model 13. 3D surface model of *D. michelae* sp. n. holotype (CASENT0235469). An interactive version of this model is available in the HTML version of this article online and at https://sketchfab.com/3d-models/9d4a4201b8ee408c9c70fb0043c596d4.

Worker Measurements and Indices (*n* = 2)

EL 0.01–0.02; HL 0.50–0.52; HW 0.41–0.43; SL 0.26; PH 0.26–0.28; PW 0.28–0.30; DML 0.38; PrH 0.28–0.33; WL 0.55–0.58; HFL 0.30; PeL 0.05–0.06; PeW 0.19–0.20; PeH 0.20–0.21; LT3 0.35–0.38; LT4 0.38–0.40; OI 2–4; CI 82–83; SI 50–52; LMI 47–48; DMI 51–52; DMI2 73–78; ASI 107; HFI 52–55; DPeI 333–380; LPeI 333–420.

Worker Description

Head longer than broad (CI 82–83), posterior head margin straight, posterodorsal corners of head rounded; sides of head in frontal view slightly convex; eyes minute, a simple pigmented spot, situated slightly less than one-third of the way between anterolateral corner of gena and posterior head margin, not visible in frontal view; frontal lamella broadly rounded-triangular in profile, apex rounded; lamella more translucent basally, but without clearly defined fenestra; medial clypeus transverse to weakly convex, lateral clypeus curving gently between antennal sockets and anterolateral corners of head, bearing numerous short, curved setae, densest medially. *Antenna* with fairly short scape (SI 50–52), scape strongly incrassate, gently bent; pedicel campaniform, longer than broad; true antennomere count ten; apparent antennomere count ten; flagellomeres basad apical club highly compressed, taken together only about as long as apical club. *Ventral* head with moderately well-developed, weakly sinuate preoccipital ridge, with short, triangular anteromedial carina; medial region of hypostoma broadly triangular, arms somewhat narrowed and spatulate apicolaterally; palpal formula not examined. *Mandible* with slight subapical angle; subbasal angle and basal angle squared; ectal face with bracket-shaped carina running from just distad basal angle to subapical angle, leaving long, narrow depressed region.

Mesosoma gracile, sloping posteroventrally, pronotum slightly higher than propodeum; in dorsal view mesosoma conspicuously slender and elongate (DMI 51–52; DMI2 73–78), slightly narrowed posteriorly, pronotum much wider than propodeum; pronotal humeri rounded to almost angulate; posterior propodeal margin strongly convex between denticles; posterodorsal corners of propodeum dentate, teeth acutely triangular, laterally flattened, diverging posterolaterally; declivitous face of propodeum strongly concave in profile and oblique posterior view; propodeal spiracle inconspicuous, directed posteroventrally; propodeal lobes well-developed, rounded-flangelike.

Legs short (HFI 52–55); mesotibia without apicoventral spur, with small but distinct apicoventral seta inserted in pit; mesobasitarsus short, shorter than tarsomeres II–IV taken together.

Petiolar node strongly attenuated dorsomedially, about 3.3 to 4.2 times higher than long (LPeI 333–420); in profile attenuation not as apparent (since node shortest medially); anterior face of node subvertical to anteriorly sloping, apex truncate to peaked, posterior face sloping posteroventrally; in dorsal view, petiole about 3.3 to 3.8 times wider than long (DPeI 333–380); sides divergent posteriorly, posterior margin slightly concave, anterior margin strongly concave; in anterior view, petiolar outline basically rectangular, dorsolateral corners sharply peaked, dorsal maring therefore concave; in oblique anterodorsal view, anterior face strongly impressed medially, node appearing bilobed; subpetiolar process short, lobate to rectangular, apex flat to truncate.

Abdominal segment 3 with tergite elongate-campaniform, anteriorly prolonged slightly over helcium, widest posteriorly; sternite distinctly squared in profile; AS3 with very strongly developed median ridge with defined anteroventral and posterior faces, ridge broadening to a lobe posteriorly, anteriorly surpassing prora; prora well-defined, concave in ventral view; AT4 weakly longer than AT3 (ASI 107); AT4 shaped as quarter-section of prolate ellipsoid; AS4 with well-developed, fairly broad anterior lip, overlapping about two-third the width of AS3, anterior margin concave with rounded anterolateral edges in ventral view; successive abdominal segments short, telescopic, often concealed.

Sculpture on head foveolate laterally, foveolae becoming denser and smaller on front of head; ventral surface of head foveolate to punctulate, smoothest medially; small foveolae extending to frontal lamella and clypeus; mandible with numerous, fine piligerous punctulae; mesosoma and petiole more or less regularly, shallowly punctate-reticulate, some foveolae coarser on lateral pronotum; declivitous face of propodeum foveolate-reticulate; abdominal segment 3 and AT4 similarly sculptured, foveolae slightly smaller than those on mesosoma, shallower on AT4; AT4 slightly shinier than AT3.

Setation on head mostly appressed fine pubescence, some suberect hairs present particularly on front of head and posterior head margin; scape with long pubescence, a few decumbent hairs present apically; ectal face of mandible with moderately long, fine, appressed to decumbent setae; masticatory margin with row of straight, stout setae; lateral mesosoma and abdominal terga with very dilute pubescence; numerous short decumbent to erect setae present on mesosomal and abdominal dorsa; petiolar sternite and abdominal sternite 3 without standing hairs; abdominal segments 5 to 7 with relatively short, abundant standing hairs, not much longer than those on AT4; legs with appressed pubescence and a few scattered decumbent to erect setae.

Etymology

Discothyrea michelae is named in appreciation of Michele Esposito from San Francisco, USA, the incomparable data manager for AntWeb. For years, she has worked tirelessly as part of the AntWeb team to organize and make available huge quantities of data used by countless myrmecologists. Like the new species, Michele is unique among her peers. The specific epithet is given as a genitive noun.

Distribution and Biology

The species is known only from the type locality in the Kindoroko Forest, Tanzania, where it was collected from leaf litter in a primary montane forest at an elevation of 1739 m (Fig. 4M).

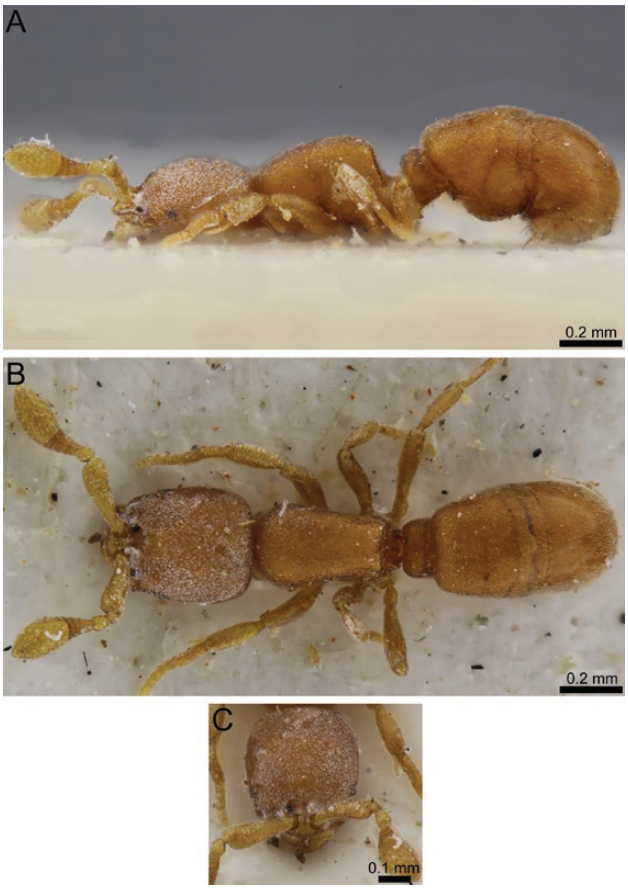

Fig. 45. Stacked digital color images of *D. patrizii* Weber, 1949 holotype (MCZ_Type_32184). (A) Body in profile, (B) body in dorsal view, (C) head in full-face view.

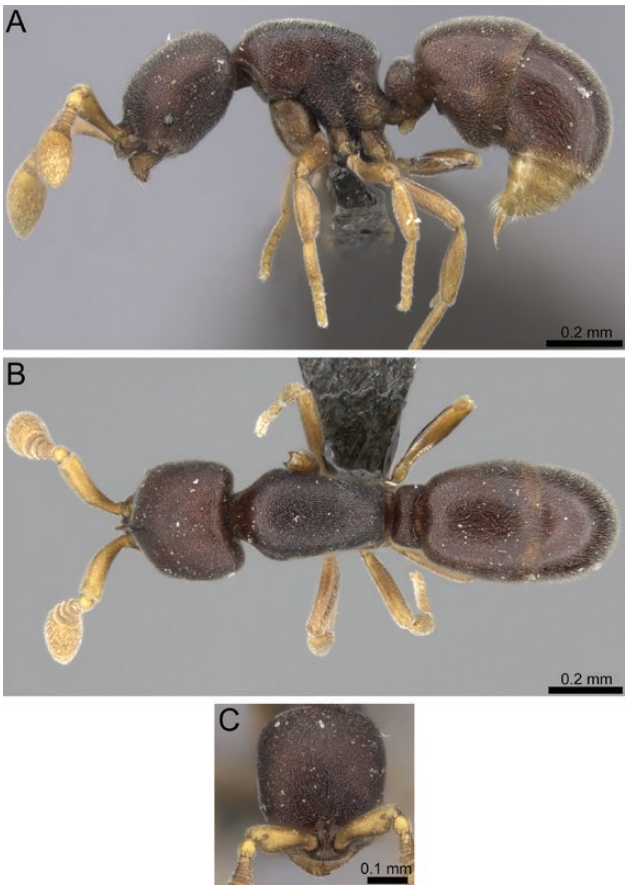

Fig. 46. Stacked digital color images of *D. patrizii* Weber, 1949 (CASENT0235472—from https://www.antweb.org, photographer Will Ericson). (A) body in profile, (B) body in dorsal view, (C) head in full-face view.

Comments

The shape of the petiolar node is unique among the Afrotropical fauna and is unusual for *Discothyrea* in general. This species is otherwise quite similar in general habitus to *D. kalypso*, and is allied with *D. hawkesi*, *D. maia*, and *D. penthos* by the denticulate propodeum and a modified abdominal sternite 3.

Variation

Since the material available is limited, it is not possible to assess variation. Based on the small type series, *D. michelae* varies somewhat in the structure of the subpetiolar process, which may be more slightly more lobate or more rectangular.

Discothyrea patrizii Weber, 1949

(Figs. 4N, 6N, 7N, 8N, 9N, 10N, 11N, 12N, 14N, 45, 46, 47; Supp Video S14 [online only])

Discothyrea patrizzii Weber, 1949: 2. [Justified emendation of spelling to *Discothyrea patrizii* by Brown, 1958a].

Type Material

HOLOTYPE, pinned queen, KENYA, high East African plains, densely wooded donga or ravine, floor cover of leaves and humus, 1670 to 1770 m, 5.II.1948 [holotype presumably lost, not at MCZC]. **PARATYPE**, pinned worker, KENYA, Nairobi, [–1.317, 36.763], ca. 1750 m, 1945 (*Patrizi*) (MCZC: MCZ_Type_32184) [examined].

Virtual dataset. Volumetric raw data (in DICOM format), 3D rotation video, still images of surface volume rendering, and 3D surface (in PLY format) of a nontype specimen (CASENT0235472) in addition to stacked digital color images illustrating head in full-face view, profile and dorsal views of the body. The data are deposited at Dryad (Hita Garcia et al. 2019, http://doi.org/10.5061/dryad.3qm4183) and can be freely accessed as virtual representation of the species. In addition to the data at Dryad, we also provide a freely accessible 3D surface model at Sketchfab (Model 14).

Nontype Material

KENYA: Nairobi, –1.317, 36.763, ca. 1750 m, soil sample, 4.XI.1974 (*V. Mahnert*); TANZANIA: Kilimanjaro Region, Kindoroko Forest Reserve, –3.74520, 37.64267, 1739 m, primary forest, leaf litter, Winkler, 5.–8.IX.2005 (*P. Hawkes, J. Makwati, R. Mtana*); Kilimanjaro, Mt. Kilimanjaro, –3.16699, 37.23584, 1920 m, montane forest, 20.X.–10.XI.2011 (*M. Peters*); Kilimanjaro, Mt. Kilimajaro, –3.186, 37.2546, 1640 m, farmland near montane forest, 1.XI.2011 (*A. Mayr*); Kilimanjaro, Mt. Kilimanjaro, –3.2604, 37.4180, 1620 m, montane forest, 12.XII.2011 (*M. Peters*); Iringa Region, Ndudulu Forest Reserve, –7.78912, 36.48539, 1567 m, primary forest, hand collected, 23.–26.X.2007 (*P. Hawkes, M. Bhoke, U. Richard*); Mkomazi Game Reserve, forest above Ibaya, –3.96667, 37.78333, montane forest, Winkler bag extraction from sifted leaf litter from fern-covered rock, 27.XI.1995 (*H.G. Robertson*); Mkomazi Game Reserve, Kinondo forest, –3.91667, 37.76667,

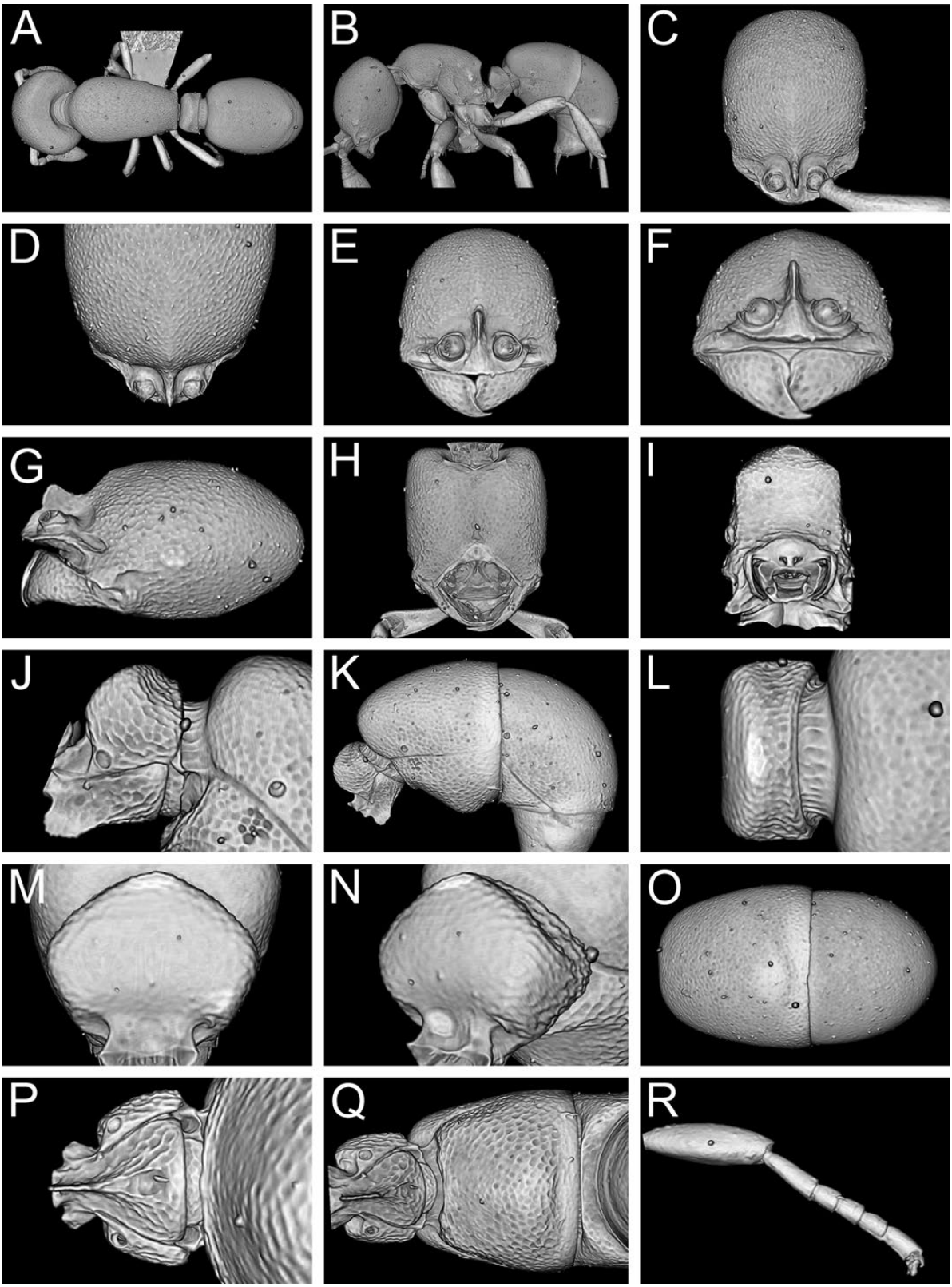

Fig. 47. Still images from shaded surface display volume renderings of *D. patrizii* Weber, 1949 (CASENT0235472) showing virtually segmented body parts. (A) Body in dorsal view, (B) body in profile, (C) head in full-face view, (D) head in dorsal view, (E) head in anterodorsal view, (F) head in anterior view, (G) head in profile, (H) head in ventral view, (I) posterior propodeum in posterior view, (J) petiole in profile, (K) petiole and gaster in profile, (L) petiole in dorsal view, (M) petiole in anterior view, (N) petiole oblique anterior view, (O) gaster in dorsal view, (P) petiole in ventral view, (Q) abdominal sternite 3 in ventral view, (R) mesotibia and mesotarsus in anterior view.

Model 14. 3D surface model of *D. patrizii* Weber, 1949 (CASENT0235472). An interactive version of this model is available in the HTML version of this article online and at https://sketchfab.com/3d-models/9fe9753fa49a435db5838fb0d6486dbf.

montane forest, Winkler bag extraction ex leaf litter, 9.V.1996 (*H.G. Robertson*); Mkomazi Game Reserve, Maji Kununua, –3.88333, 37.81667, 1600 m, montane forest, Winkler bag leaf litter extraction, 7.XII.1995 (*H.G. Robertson*); Morogoro Region, Mamiwa-Kisara Forest Reserve, –6.37530, 36.93711, 1989 m, primary forest, leaf litter, Winkler, 16.–21.VIII.2005 (*P. Hawkes, J. Makwati, R. Mtana*); Morogoro Region, Mamiwa-Kisara Forest Reserve, –6.37530, 36.93711, 1989 m, primary forest, pitfall trap, 16.–21.VIII.2005 (*P. Hawkes, J. Makwati, R. Mtana*); South Pare Forest, –4.130556, 37.88389, montane forest, Winkler bag leaf litter extraction, 29.XI.1995 (*H.G. Robertson*); South Pare Mountains, –4.13333, 37.88333, 1598 m, montane forest, Winkler bag extraction ex leaf litter, 18.IV.1996 (*S. van Noort*); Tanga Region, Nilo Forest Reserve, –4.91456, 38.67712, 1006 m, primary forest, hand collected, 1.–4.IX.2005 (*P. Hawkes, J. Makwati, R. Mtana*); West Usambara Mountains, Shume Gologolo, –4.70, 38.23, disturbed montane forest, Winkler bag extraction ex leaf litter, 13.V.1996 (*H.G. Robertson*); West Usambara Mountains, Site 2, –4.733, 38.25, 2001 m, montane forest, Winkler bag extraction ex leaf litter, 1.V.1996 (*M. Stander, S. van Noort*).

Diagnosis

The following character combination distinguishes *D. patrizii* from the remainder of the complex: standing pilosity absent from mesosoma and abdominal terga; propodeum without strong angles or denticles; eyes present, relatively large, and round (OI 5–8); in dorsal view mesosoma relatively slender (DMI 52–58; DMI2 78–87) and moderately narrowed posteriorly; in profile mesosomal outline comparatively flat; mesotibia without apicoventral spur; petiolar node strongly attenuated dorsally (DPeI 314–489; LPeI 314–467); sculpture generally reduced, declivitous face of propodeum without foveolae; color highly variable: unicolorous matte orange to very deep brown with yellowish appendages.

Worker Measurements and Indices (*n* = 15)

EL 0.03–0.04; HL 0.38–0.54; HW 0.30–0.47; SL 0.19–0.30; PH 0.19–0.28; DML 0.26–0.39; PW 0.23–0.33; PrH 0.23–0.34; WL 0.40–0.57; HFL 0.22–0.35; PeL 0.04–0.07; PeW 0.16–0.22; PeH 0.16–0.22; LT3 0.28–0.40; LT4 0.24–0.38; OI 5–8; CI 78–87; SI 50–58; LMI 44–50; DMI 52–58; DMI2 78–87; ASI 85–98; HFI 54–63; DPeI 314–489; LPeI 314–467.

Worker Description

Head conspicuously longer than broad (CI 78–87), posterior head margin straight to convex, posterodorsal corners of head broadly rounded; sides of head in frontal view gently subparallel to convex posterad eyes, very slightly concave between eyes and anterolateral corner of gena; eyes present, relatively large (OI 5–8), round, comprising several ommatidia, placed about a third of the way between anterolateral corner of gena and posterior head margin; eyes visible in frontal view; frontal lamella fairly short and triangular in profile, apex rounded to acute; lamella more or less evenly translucent across its disc, sometimes with a thinner basal spot, but lacking a distinct fenestra; medial clypeus convex, lateral clypeus curving broadly between antennal sockets and anterolateral corners of head, bearing short, curved setae. *Antenna* with shorter to moderately long scape (SI 50–58), scape slightly expanded apically, very gently bent; pedicel campaniform, slightly longer than broad; true antennomere count eight; apparent antennomere count seven to ten, flagellomeres basad apical club highly compressed, taken together only about as long as apical club. *Ventral head* with narrowly carinulate, V-shaped preoccipital ridge without anteromedian carina; medial area of hypostoma triangular, arms slightly narrowed, similar in width across their length; palpal formula not examined. *Mandible* edentate except for small, curved prebasal denticle; occasionally a slight preapical swelling present; basal angle rounded; ectal face with weak carina running from about midway between basal angle and prebasal denticle or mandibular apex, becoming confluent with masticatory margin around halfway along its length, leaving a short, comma-shaped depressed area.

Mesosoma sloping posteroventrally, pronotum clearly higher than propodeum; in dorsal view mesosoma relatively slender (DMI 52–58; DMI2 78–87) and moderately narrowed posteriorly, pronotum somewhat wider than propodeum; pronotal humeri rounded; posterior propodeal margin straight; posterodorsal corners of propodeum rounded angulate but not denticulate; declivitous face of propodeum slightly to moderately concave in profile and oblique posterior view; propodeal spiracle small but sometimes distinct (more so in darker morphs), directed posterolaterally; propodeal lobes well-developed, flangelike.

Legs short to intermediate in length (HFI 54–63) and somewhat narrow; mesotibia without apicoventral spur; mesobasitarsus fairly short, subequal in length to tarsomeres II–IV taken together.

Petiolar node attenuated dorsally, somewhat variable in shape, about 2.9 to 3.8 times higher than long (LPeI 286–383); in profile anterior face of node convex, apex peaked, somewhat rounded to subacute, posterior face posteroventrally sloping to subvertical; in dorsal view, node rectangular, about 3.0 to 3.8 times broader than long (DPeI 300–383), sides subparallel to slightly divergent posteriorly; in anterior view, petiolar outline pentagonal, angles well-rounded; in oblique anterodorsal view, anterior face flat; subpetiolar process variable in shape, dentate to broadly lobate, apex acute to rounded.

Abdominal segment 3 campaniform, widest just anterad end of segment; tergite slightly anteriorly prolonged over petiole; sternite evenly curved to posteriorly bulging in profile (deepest point at around or slightly posterad longitudinal midline); AS3 without median ridge, without carinate prora, but anterior face still depressed, anterior margin of ventral face flat to weakly concave in ventral view; AT3 and AT4 approximately equal in length, or AT4 only slightly (about 1.2 times) longer than AT3 (ASI 100–115); AT4 gently recurved, hemidemispherical; AS4 with poorly developed anterior lip, overlapping slightly more than half the width of AS3, anterior margin straight in ventral view; successive abdominal segments short, telescopic, often concealed.

Sculpture on head, mesosoma, and petiole very finely, shallowly punctulate, often appearing colliculate or even scabriculous in darker morphs; punctulae on lateral mesosoma becoming reticulate to substrigulate; declivitous face of propodeum predominantly smooth; mandibles similarly sculptured to head, somewhat shining between piligerous punctulae; abdominal segment 3 with coarser, more distinct punctae, similarly distributed on tergite and sternite; AT4 with minute but distinct, very densely arranged piligerous punctae, clearly shinier than AT3.

Setation mostly consisting of appressed white pubescence, of similar density on head and mesosomal dorsum, generally longer and denser on gastral terga, more dilute on lateral mesosoma and lateral portions of abdominal terga; setae on head often inclined towards the longitudinal midline; ectal face of mandible with moderately long, fine, appressed to decumbent setae; masticatory margin with row of straight, stout setae; occasionally a few short decumbent to erect hairs present on dorsal surfaces, particularly of AT3; appearance of setation highly variable between color morphs: in light individuals pubescence inconspicuous, while very distinct on dark individuals; abdominal segments 5 through 7 with long, flexuous standing setae. Appendages with well-developed, evenly distributed appressed pubescence.

Color highly variable: unicolorous matte orange to very deep brown with yellowish appendages.

Distribution and Biology

Discothyrea patrizii is known from montane forests in Kenya and Tanzania (Fig. 4N) where it usually occurs at high elevations between around 1600 m and 1800 m, though a few specimens have been collected both lower and higher than this range. Based on collection techniques it likely inhabits leaf litter.

Comments

Despite an intensive search in the MCZC collection in collaboration with the curatorial staff, the holotype was not to be found and is presumably lost. Fortunately, however, the paratype was available for examination (Fig. 45). In this case, we refrain from designating a neotype since the identity of *D. patrizii* is clear and stable. The original description does not provide any significant details that could distinguish *D. patrizii* from other *traegaordhi*-complex species, and Weber (1949) listed antennomere count (an unstable character; see Materials and Methods) and the shape of the frontal lamella as diagnostic features delineating the species from *D. traegaordhi* and *D. hewitti*. The paratype specimen however, while in less than ideal condition, is well enough preserved to associate it with recently collected material, from which a thorough description and diagnosis are possible. Despite the apparent rarity prior to this study, after association of most of the unidentified material to the type, *D. patrizii* turns out to be widespread in East Africa.

Variation

Varies most noticeably in color, which ranges from uniformly matte orange (as in the paratype, see Fig. 45) to dark earthy brown with yellowish appendages, as in many Tanzanian individuals (Fig. 46). Pubescence is not highly variable in development, but is much less conspicuous on lighter morphs, while contrasting in darker forms. The subpetiolar process is quite variable, too, ranging from dentate with apex acute to broadly lobate, with apex rounded.

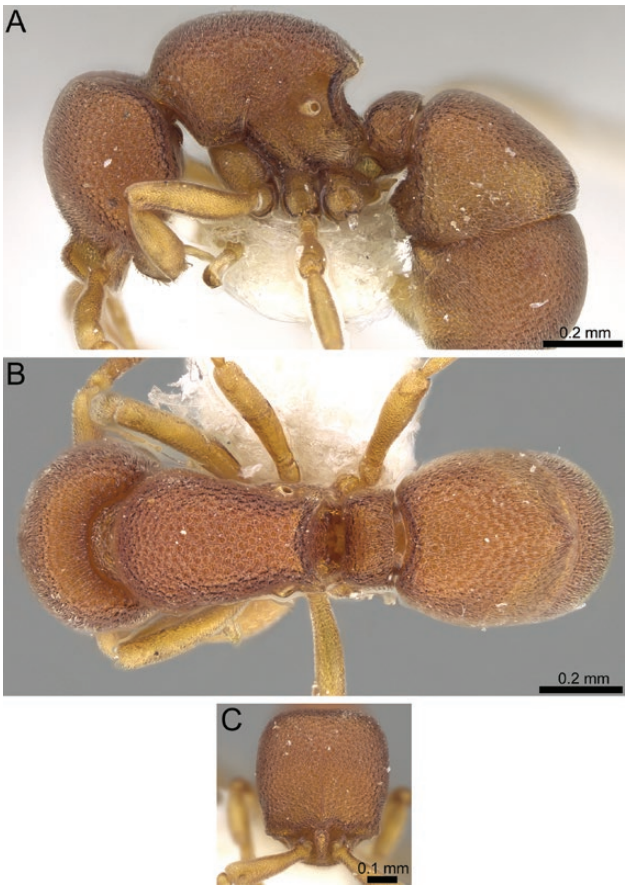

Fig. 48. Stacked digital color images of *D. penthos* sp. n. paratype (CASENT0247383—from https://www.antweb.org, photographer Will Ericson). (A) body in profile, (B) body in dorsal view, (C) head in full-face view.

Discothyrea penthos Hita Garcia & Lieberman sp. n. (Figs. 4O, 6O, 7O, 8O, 9O, 10O, 11O, 12O, 14O, 48, 49; Supp. Video S15 [online only])

Type Material

HOLOTYPE, pinned worker, IVORY COAST, Monogaga, [4.81833, –6.49028], ca. 20 m, collection code ANTC42121, 24.X.1980 (*V. Mahnert & J.L. Perret*) (BMNH: CASENT0790105). **PARATYPES**, seven pinned workers with same data as holotype (BMNH: CASENT0790107; CASC: CASENT0247383; MCZC: MCZENT00593560; MHNG: CASENT0247381, CASENT0247382, CASENT0790106; SAMC: CASENT0247379).

Cybertype. Volumetric raw data (in DICOM format), 3D rotation video, still images of surface volume rendering, and 3D surface (in PLY format) of the physical holotype (CASENT0790105) in addition to stacked digital color images illustrating head in full-face view, profile and dorsal views of the body. The data are deposited at Dryad (Hita Garcia et al. 2019, http://doi.org/10.5061/dryad.3qm4183) and can be freely accessed as virtual representation of the type. In addition to the cybertype data at Dryad, we also provide a freely accessible 3D surface model of the holotype at Sketchfab (Model 15).

Nontype Material

IVORY COAST: Abidjan, Adiopodoume Forest Biological Reserve, [5.335, –4.131], ca. 30 m, 4.III.1977 (*I. Löbl*); Abidjan, Banco Forest,

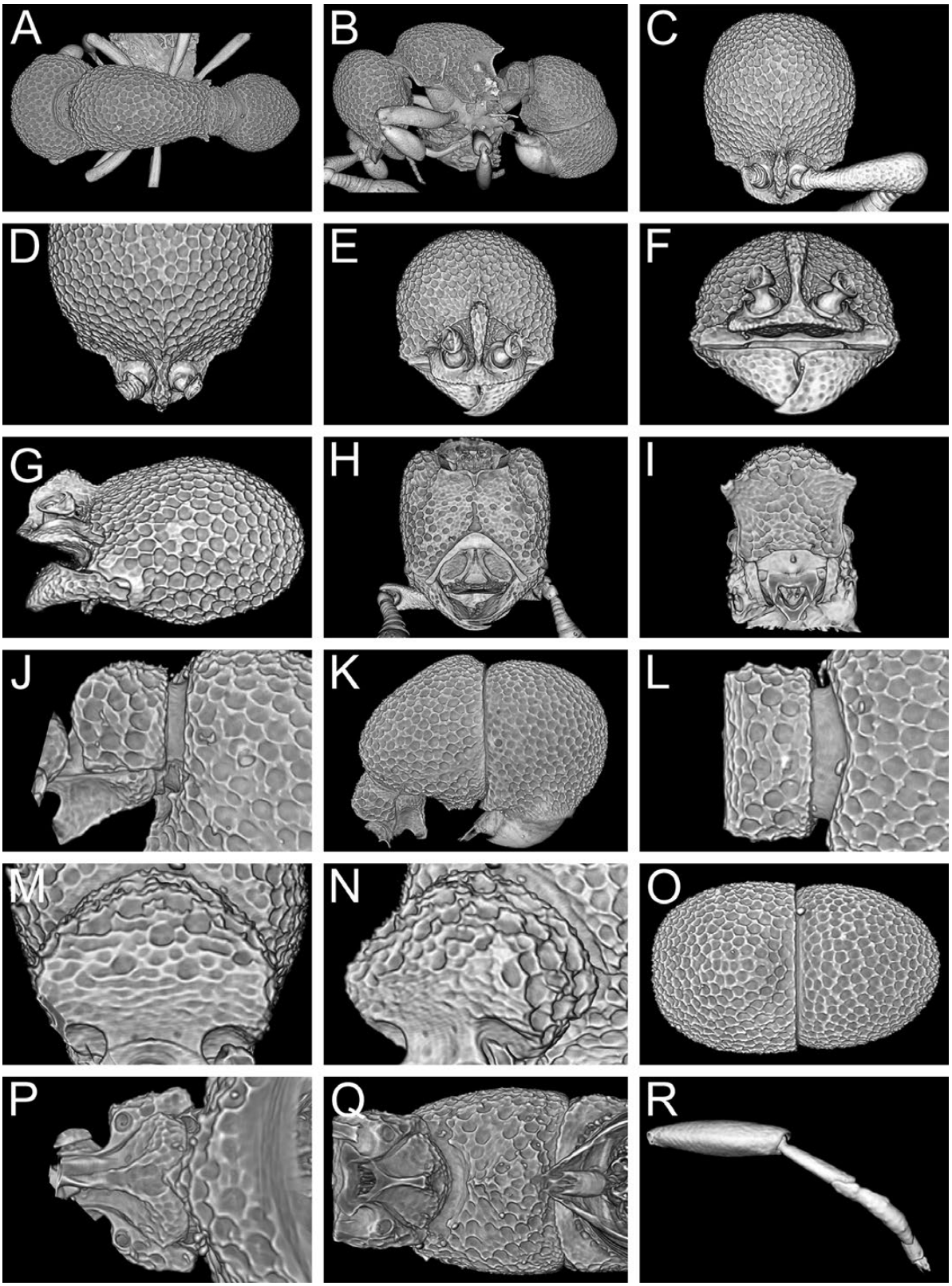

Fig. 49. Still images from shaded surface display volume renderings of *D. penthos* sp. n. holotype (CASENT0790105) showing virtually segmented body parts. (A) Body in dorsal view, (B) body in profile, (C) head in full-face view, (D) head in dorsal view, (E) head in anterodorsal view, (F) head in anterior view, (G) head in profile, (H) head in ventral view, (I) posterior propodeum in posterior view, (J) petiole in profile, (K) petiole and gaster in profile, (L) petiole in dorsal view, (M) petiole in anterior view, (N) petiole oblique anterior view, (O) gaster in dorsal view, (P) petiole in ventral view, (Q) abdominal sternite 3 in ventral view, (R) mesotibia and mesotarsus in anterior view.

Model 15. 3D surface model of *D. penthos* sp. n. holotype (CASENT0790105). An interactive version of this model is available in the HTML version of this article online and at https://sketchfab.com/3d-models/77dcda4c218d4a7fbbea30c6bb2832c5.

[5.38694, –4.05275], ca. 20 m, I.1963 (*W.L. Brown*); Tai Forest, [5.75, –7.12], ca. 250 m, 12.VIII.1975 (*T. Diomande*); Tai Forest, [5.75, –7.12], ca. 250 m, 17.X.1980 (*V. Mahnert & J.L. Perret*).

Diagnosis

The following character combination distinguishes *D. penthos* from the remainder of the complex: masticatory margin of mandible edentate; anterior clypeal margin usually asetose or with only short, inconspicuous setae; anterolateral corner of gena sharply demarcated but not dentate; in dorsal view mesosoma conspicuously thick, robust and stocky (DMI 62–65; DMI2 94–95); mesotibiae without apicoventral spur; propodeum dentate, teeth relatively large and subtended by narrow lamellulae; abdominal sternite 3 produced as squared to trapezoidal lobe, with distinct anterior, ventral, and posterior surfaces in profile; AT4 only weakly longer than AT3 (ASI 105–112); erect pilosity absent on all dorsal surfaces.

Worker Measurements and Indices (*n* = 10)

EL 0.01–0.02; HL 0.53–058; HW 0.46–0.49; SL 0.30–0.31; PH 0.29–0.33; DML 0.34–0.39; PW 0.33–0.37; PrH 0.34–0.38; WL 0.52–0.59; HFL 0.32–0.38; PeL 0.06–0.08; PeW 0.20–0.26; PeH 0.21–0.23; LT3 0.33–0.38; LT4 0.36–0.40; OI 2–4; CI 84–87; SI 52–57; LMI 53–56; DMI 62–65; DMI2 94–99; ASI 105–112; HFI 61–68; DPeI 329–429; LPeI 300–386.

Worker Description

Head broad (CI 84–87); posterior head margin straight, posterodorsal corners of head broadly rounded. In frontal view sides of head subparallel to slightly convex; head appearing subquadrate posterad antennal sockets; eyes very small (OI 2–4) but distinct and round, situated about a third of the way between anterolateral corner of gena and posterior head margin; eyes just visible in frontal view; anterolateral corner of gena sharply demarcated, approximately right-angled, sometimes slightly projecting laterally; frontal lamella roughly rhomboid in profile, with three distinct edges: anterior edge shortest, sloping posterodorsally; dorsal edge longest, sloping dorsally; lamella thinner and more translucent basally but without distinct fenestra; medial clypeus convex, lateral clypeus curving fairly strongly between antennal sockets and anterolateral corners of head, bearing numerous short curved setae. *Antenna* with moderately long scape (SI 52–57), scape moderately incrassate, gently bent; pedicel subglobose, broader than long; true antennomere count eleven; apparent antennomere count nine to twelve; flagellomeres basad apical club highly compressed, taken together only about as long as apical club. *Ventral head* with well-developed, sinuate preoccipital ridge with short, triangular anteromedian carina; medial region of hypostoma rounded, arms wide, spatulate apicolaterally; palpal formula not examined. *Mandible* with a small subapical angle; basal angle rounded to angulate; ectal face with weak carina extending from subapical angle to basal angle, leaving narrow, curved, depressed region.

Mesosoma in dorsal view conspicuously thick, robust and stocky (DMI 62–65; DMI2 94–95); evenly convex, pronotum only slightly higher than propodeum; in dorsal view, mesosoma narrowed posteriorly, pronotum distinctly wider than propodeum, inclusive of laterally divergent propodeal dentae; pronotal humeri somewhat narrowly rounded; posterior propodeal margin strongly concave; posterodorsal corners of propodeum dentate, dentae large, triangular, laterally flattened, mostly opaque, subtended by narrow but darkly pigmented lamellulae outlining propodeal concavity, hence propodeum laterally marginate; declivitous face of propodeum strongly concave in profile and oblique posterior view; propodeal spiracle large, directed posterodorsally; spiracle conspicuous due to polished, unsculptured area posterodorsad spiracle, extending to base of propodeal tooth, strongly contrasting with surrounding foveolate sculpture; propodeal lobes well-developed, flangelike.

Legs moderately long (HFI 61–68) and slender; mesotibia without apicoventral spur or seta; mesobasitarsus relatively short, about as long as tarsomeres II–IV taken together.

Petiolar node strongly attenuated dorsally, but appearing thick in profile since attenuation strongest medially; node about 3.0 to 3.8 times higher than long (LPeI 300–383); in profile, anterior face of node convex, apex blunt to rounded, curving evenly into convex posterior face, hence posterior face indistinct; in dorsal view, petiole roughly trapezoidal, sides divergent posteriorly, anterior face concave, about 3.3 to 4.3 times broader than long (DPeI 329–429); in anterior view, petiolar outline roughly pentagonal, edges poorly defined, angles strongly rounded; in oblique anterodorsal view, anterior face concave; subpetiolar process broadly falcate, curved, apex rounded.

Abdominal segment 3 with tergite broadly campaniform, widest just anterad end of segment; sternite somewhat squared in profile; AS3 with wide median ridge extending anteriorly to prora, broadening to lobe posteriorly; prora well-defined, concave in ventral view; constriction between abdominal segments 3 and 4 distinct; AT4 weakly longer than AT3, about 1.1 times longer (ASI 105–112); AT4 bulbous, hemidemispherical; AS4 with well-developed, wide anterior lip, overlapping most of the width of AS3, anterior border weakly convex in ventral view; successive abdominal segments short, telescopic, often concealed.

Sculpture similarly foveolate on head, dorsal mesosoma, declivitous face of propodeum, petiole, abdominal segment 3 and AT4; foveolae becoming smaller on front of head; becoming foveolate-reticulate on lateral mesosoma; area posterodorsad propodeal spiracle smooth and unsculptured; mandible with numerous, fine piligerous punctulae.

Setation very dilute and inconspicuous, consisting entirely of appressed pubescence, slightly longer on abdominal terga; body appearing glabrous at lower magnification; metapleural gland bulla with distinctly longer but fine, yellowish guard setae; scape and legs with short, somewhat sparse velvety appressed pubescence; ectal face of mandible with relatively long, curved, appressed setae; masticatory margin with row of short, straight seate.

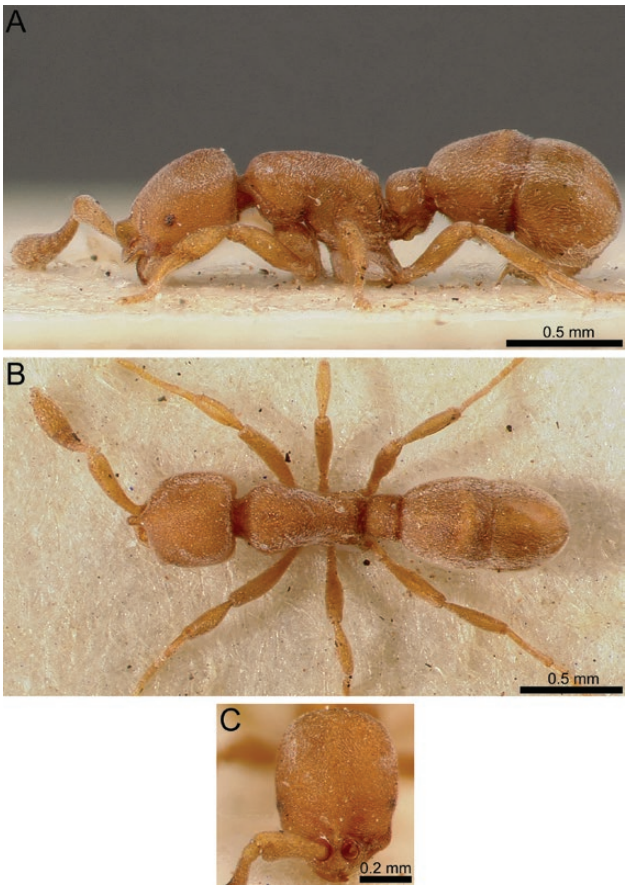

Fig. 50. Stacked digital color images of *D. poweri* (Arnold, 1916) holotype (SAM-ENT-0011509—from https://www.antweb.org, photographer unknown). (A) body in profile, (B) body in dorsal view, (C) head in full-face view.

Color more or less uniformly bright luteous-orange to yellowish.

Etymology

In Greek mythology, 'Penthos' was the spirit of grief, lamentation, and mourning. The specific epithet recognizes the highly threatened and rapidly diminishing rainforest habitat from which this species and most other Afrotropical *Discothyrea* originate. The specific epithet is given as an appositive noun.

Distribution and Biology

Discothyrea penthos is only known from four rainforest localities in Ivory Coast where it seems to live in leaf litter (Fig. 4O). This is the only species apparently endemic to the Guinean rainforests of West Africa.

Comments

This is another distinctive species distinguishable on the basis of the almost subquadrate head, conspicuous propodeal teeth, and the distinctive shape of abdominal sternite 3. The latter character is only found in two other species: *D. hawkesi* and *D. kalypso*. These two are easily separated since they are generally smaller, have shorter limbs, and are also more elongated and less robust than *D. penthos*. Furthermore, *D. penthos* is strongly sculptured throughout most of the body but displays a distinctly smooth and shiny area around the propodeal spiracle. The only species of the complex found in sympatry with *D. penthos* is *D. venus*, but both cannot be confused. Among a series of other differences, *D. venus* possesses a much larger AT4 in relation to AT3 (ASI 158–183), has much more reduced sculpture, and lacks the conspicuous shape of abdominal sternite 3.

Variation

Despite being known from several localities in Ivory Coast, intraspecific variation appears to be negligible in this species.

Discothyrea poweri (Arnold, 1916) (Figs. 4P, 6P, 7P, 8P, 9P, 10P, 11P, 12P, 13B, 14P, 50, 51; Supp. Video S16)

Pseudosysphincta poweri Arnold, 1916: 162, by monotypy. [Combination in *Discothyrea* by Brown, 1958a].

Type Material

HOLOTYPE, pinned worker, SOUTH AFRICA, Northern Cape, Kimberley, [-28.73, 24.77], 1225 m, 1912 (*B. Power*) (SAMC: SAM-ENT-0011509) [examined].

Virtual dataset. Volumetric raw data (in DICOM format), 3D rotation video, still images of surface volume rendering, and 3D surface (in PLY format) of the nontype specimen (CASENT0764095) in addition to stacked digital color images illustrating head in full-face view, profile and dorsal views of the body. The data are deposited at Dryad (Hita Garcia et al. 2019, http://doi.org/10.5061/dryad.3qm4183) and can be freely accessed as virtual representation of the species. In addition to the data at Dryad, we also provide a freely accessible 3D surface model at Sketchfab (Model 16).

Nontype Material

SOUTH AFRICA: Eastern Cape, Fern Kloof, vic. Grahamstown, 20.II.1969 (*W.L. Brown*); Eastern Cape, Hogsback, [–32.551, 26.949], ca. 1700 m, wet native forest, 26.II.1969 (*W.L. Brown*); Eastern Cape, Hogsback, [–32.551, 26.949], ca. 1700 m, indigenous evergreen forest, 26.III.1986 (*H.G. Robertson*); Eastern Cape, Signal Hill, vic. Grahamstown, [–33.3335, 26.549], ca. 750 m, pine native scrub, 18.II.1969 (*W.L. Brown*); Free State Province, Bloemfontein Botanical Garden, –29.05167, 26.21333, 1400 m, bushveld and riparian vegetation, 24.X.2011 (*L. Almeida*); KwaZulu-Natal, 75 km WSW Estcourt, Cathedral Peak Forest Station, –28.994, 29.282, 1500 m, podocarp forest, rotted stump of *Cussonia spicata*, 18.XII.1979 (*S. & J. Peck*); Western Cape, Cape of Good Hope N.R., Olifantsbos, nr. Skaife Centre, –34.2626667, 18.3855, 20 m, strandveld and mountain fynbos, 8.X.1998 (*H.G. Robertson*); Western Cape, Cape of Good Hope Nature Reserve, –34.2563, 18.3866, 19 m, X.2008 (*G. Fischer & F. Hita Garcia*); Western Cape, Cape Town, Kirstenbosch Botanical Garden, –33.988, 18.431, ca. 150 m, X.2008 (*F. Hita Garcia & G. Fischer*); Western Cape, Koeberg, –33.71667, 18.55, ca. 210 m, renosterbos vegetation, 4.XI.1994 (*H.G. Robertson*); Western Cape, Groeneweide Nature Walk, –33.95667, 22.53833, 197 m, indigenous forest, 20.X.2011 (*L. Almeida*); Western Cape, junction of Newlands Ravine Path and Contour Path, –33.9666, 18.4333, ca. 540 m, indigenous evergreen forest, 2.I.1997 (*H.G. Robertson*); Western Cape, Swellendam district, Grootvadersbosch, [-33.98471, 20.8084], 394 m, VII.1958 (*J. Smith*).

Diagnosis

The following character combination distinguishes *D. poweri* from the remainder of the complex: generally larger species (WL

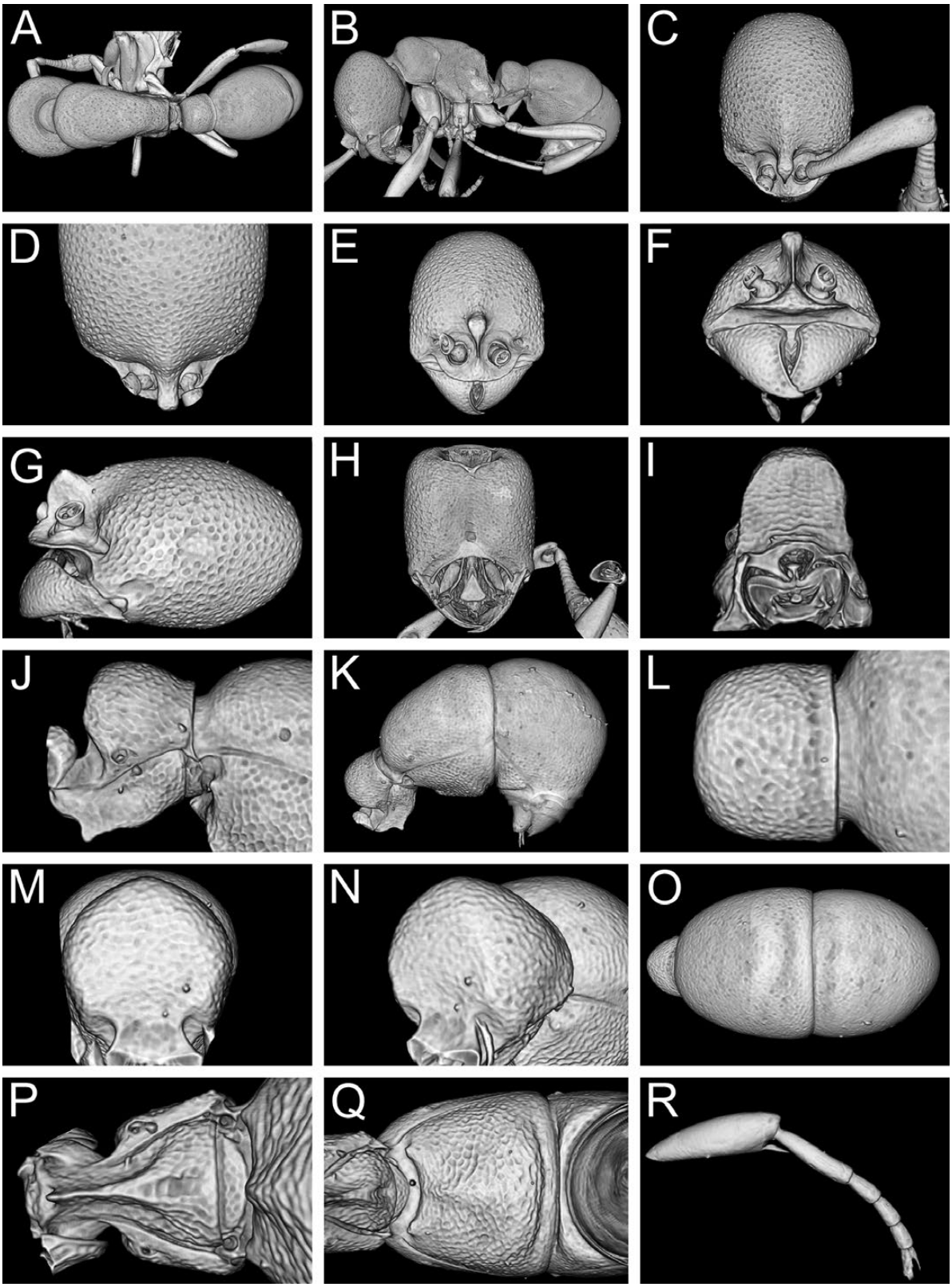

Fig. 51. Still images from shaded surface display volume renderings of *D. poweri* (Arnold, 1916) (CASENT0764095) showing virtually segmented body parts. (A) Body in dorsal view, (B) body in profile, (C) head in full-face view, (D) head in dorsal view, (E) head in anterodorsal view, (F) head in anterior view, (G) head in profile, (H) head in ventral view, (I) posterior propodeum in posterior view, (J) petiole in profile, (K) petiole and gaster in profile, (L) petiole in dorsal view, (M) petiole in anterior view, (N) petiole oblique anterior view, (O) gaster in dorsal view, (P) petiole in ventral view, (Q) abdominal sternite 3 in ventral view, (R) mesotibia and mesotarsus in anterior view.

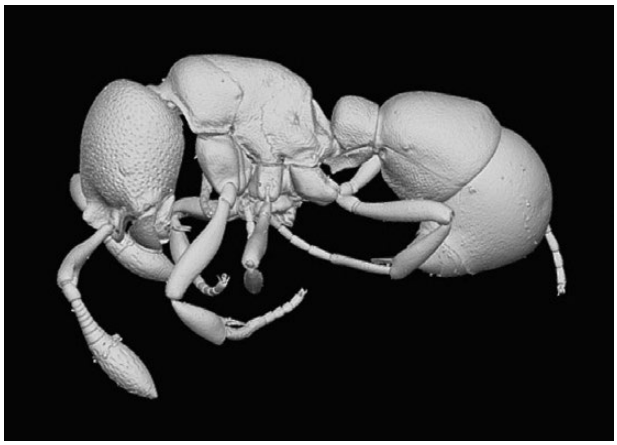

Model 16. 3D surface model of *D. poweri* (Arnold, 1916) (CASENT0764095). An interactive version of this model is available in the HTML version of this article online and at https://sketchfab.com/3d-models/7fe9a5060b004ebe8f475424d89d770b.

0.67–0.84); comparatively long antennal scapes (SI 61–68); in dorsal view mesosoma very thin and elongate (DMI 45–52; DMI2 72–81) and distinctly narrowing posteriorly with pronotum much wider than propodeum; comparatively longer legs (HFI 61–69); mesotibia with conspicuous apicoventral spur; petiole relatively thick (DPeI 135–173; LPeI 152–194); abdominal terga without any standing pilosity, only with appressed pubescence.

Worker Measurements and Indices (*n* = 10)

EL 0.04–0.07; HL 0.59–0.70; HW 0.46–0.57; SL 0.37–0.47; PH 0.31–0.39; DML 0.43–0.55; PW 0.33–0.43; PrH 0.33–0.45; WL 0.67–0.84; HFL 0.42–0.55; PeL 0.13–0.18; PeW 0.23–0.29; PeH 0.26–0.30; LT3 0.38–0.47; LT4 0.41–0.50; OI 7–10; CI 77–84; SI 61–68; LMI 45–46; DMI 45–52; DMI2 72–81; ASI 105–110; HFI 61–69; DPeI 135–173; LPeI 152–194.

Worker Description

Head somewhat longer than broad (CI 77–84), posterior head margin convex, posterodorsal corners of head round, indistinct; in frontal view, sides of head slightly converging anteriorly; eyes relatively large (OI 7–10), round, setose, with several distinct ommatidia, situated almost halfway between anterolateral corner of gena and posterior head margin; eyes visible in frontal view; frontal lamella low, broadly triangular in profile, apex rounded; lamella quite thick apically, weakly translucent, thinner basally but without distinct fenestra; medial clypeus weakly to distinctly convex, slightly prolonged, lateral clypeus curving gently between antennal sockets and anterolateral corners of head; bearing short curved setae. *Antenna* with moderately long to longer scape (SI 61–68), scape only slightly expanded apically, gently bent; pedicel subcylindrical, longer than broad; apparent antennomere count nine to twelve, flagellomeres basad apical club compressed, taken together only slightly longer than apical club; apical club relatively narrow. *Ventral head* with low but clearly defined preoccipital ridge without anteromedian carina or with very slight anteromedial prolongation; medial region of hypostoma triangular, arms distinctively narrowed, spatulate apicolaterally; palpal formula not examined. *Mandible* with a slight preapical swelling and small prebasal denticle; basal angle rounded to squared; ectal face with carina originating at basal angle, becoming confluent with masticatory margin preapically, leaving narrow, curved depressed region.

Mesosoma elongate, gently sloping posteriorly to weakly convex, pronotum slightly higher than propodeum; occasionally metanotal area slightly bulging but not clearly demarcated; in dorsal view mesosoma very thin and elongate (DMI 45–52; DMI2 72–81) and distinctly narrowing posteriorly with pronotum much wider than propodeum; pronotal humeri narrowly rounded; posterior propodeal margin straight; posterodorsal corners of propodeum rounded; declivitious face of propodeum sloping, not concave in profile or oblique posterior view; propodeal spiracle relatively large, directed dorsolaterally; propodeal lobes well-developed, flangelike.

Legs moderately long and robust (HFI 61–69); mesotibia with distinct apicoventral spur; mesobasitarsus relatively short, about equal in length to tarsomeres II–IV taken together.

Petiolar node very thick, rounded-cuneate, not attenuated dorsally, about 1.5 to 1.9 times higher than broad (LPeI 152–194); in profile, anterior face of node sloping posterodorsally, apex thickly rounded, hence posterior face indistinct; in dorsal view, petiole campaniform to trapezoidal, sides divering posteriorly, about 1.4–1.7 times broader than long (DPeI 135–173); in anterior view, petiolar outline rounded, without clear faces; in oblique anterio view, anterior face flat or scarcely impressed medially. Subpetiolar process short, somewhat variable in shape but often rhomboid, sometimes with small digitate projection, with numerous decumbent to erect setae.

Abdominal segment 3 broadly campaniform, widest point just anterad end of segment; tergite more or less evenly convex, sternite poorly rounded to nearly flat in profile; AS3 with low, broad median ridge, somewhat broader posteriorly in ventral view; prora without carina but strongly raised, concave in ventral view, anterolateral corners projecting more strongly; AT4 slightly longer than AT3 (ASI 105–110); AT4 hemidemispherical; AS4 with poorly-developed anterior lip, overlapping median third of AS3, anterior margin straight in ventral view; successive abdominal segments short, telescopic, often concealed.

Sculpture generally reduced; head, petiole, and abdominal segment 3 very shallowly punctulate-reticulate, somewhat more coarsely punctate on gena; mesosoma with sparse, very shallow punctulae; declivitous face of propodeum weakly rugulose to strigulate, particularly on lower half; mandible rather roughly sculptured with piligerous punctae; AT4 somewhat shinier than AT3, punctulae minute and very dense, tergite appearing shagreened.

Setation consisting of abundant but short and fine appressed pubescence more or less evenly distributed over entire body, slightly longer on abdominal terga; standing hairs entirely absent from dorsal surfaces; petiolar sternite and abdominal sternite 3 with fairly long, thick decumbent to suberect hairs; successive abdominal segments with dense, distinctly longer, standing pilosity; ectal face of mandible with abundant, curved, appressed to decumbent setae; masticatory margin with row of straight setae inserted on mesal face.

Color uniformly dull testaceous orange to matte brownish, sometimes with patchy infuscation on head, mesosomal, and abdominal dorsa.

Distribution and Biology

Discothyrea poweri appears to be relatively widespread in South Africa, ranging from the Western and Northern Cape to KwaZulu-Natal (Fig. 4P). It was found in a variety of habitats at elevations ranging from just above sea level to about 1700 m, which were predominantly forests, but also bushland, coastal shrub or botanical gardens. It has been collected from leaf litter, rotten wood, and under stones.

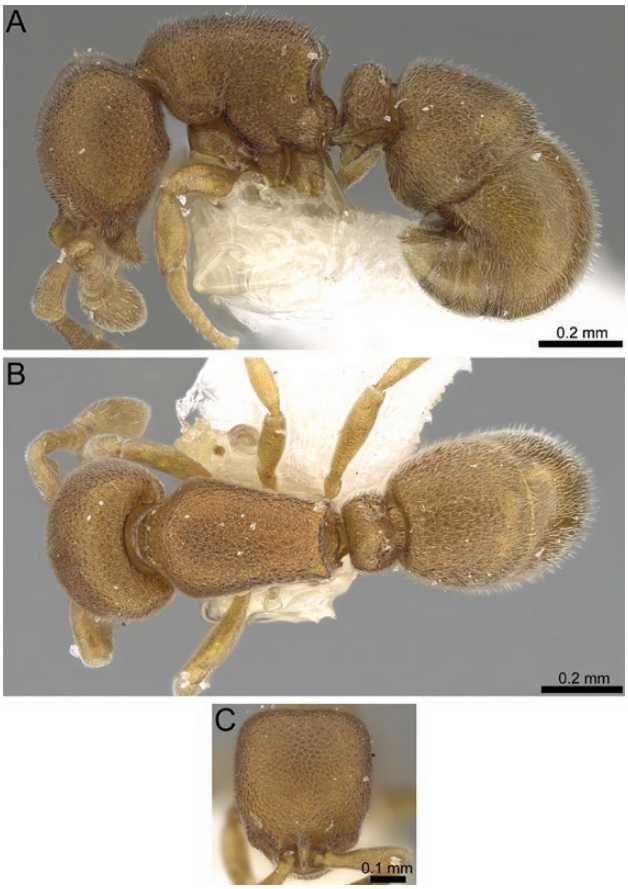

Fig. 52. Stacked digital color images of *D. schulzei* sp. n. paratype (CASENT0247370—from https://www.antweb.org, photographer Michele Esposito). (A) body in profile, (B) body in dorsal view, (C) head in full-face view.

Comments

Discothyrea poweri is one of the more conspicuous species within the Afrotropical *traegaordhi* complex. Generally, it is a relatively large species with long legs, long antennae, and an exceptionally thick petiole. It is one of the largest species of the complex together with *D. aisnetu* and *D. gaia*. Compared to most other Afrotropical *Discothyrea*, the antennae of *D. poweri* appear especially elongate due to the relatively distinct flagellomeres and narrow apical club. The presence of a distinct mesotibial spur distinguishes it from most species of the complex, except for *D. gaia* and *D. traegaordhi*. The latter species is the only other member of the complex also occurring in South Africa, but it is easily distinguished from *D. poweri* on the basis of smaller body size (WL 0.51–0.57 vs. WL 0.67–0.84), a thinner petiole (DPeI 235–289 vs. DPeI 135–173; LPeI 236–313 vs. LPeI 152–194), and shorter antennal scapes (SI 50–55 vs. SI 61–68). *Discothyrea gaia* appears to be morphologically close to *D. poweri* but can be separated by the presence of standing pilosity on the abdominal terga. In addition, *D. gaia* also has shorter legs (HFI 54–58 vs. HFI 61–69) and a thinner petiole (DPeI 192–255 vs. DPeI 135–173; LPeI 194–264 vs. LPeI 152–194). Nevertheless, it seems as if *D. poweri* belongs to a natural clade with *D. gaia* and *D. traegaordhi*, which is restricted in its distribution to Southern Africa.

Give the substantial variation in size, the wide range of habitats inhabited, and the limited material available for examination it is possible that *D. poweri* might actually be a complex of more or less cryptic species. However, due to very little other intraspecific variation we consider all the material listed here as one species with an unusual body size variation.

Variation

There is some noticeable size variation within this species (WL 0.67–0.84) not seen in most other congeners. This size variation is also visible when comparing eyes. In larger specimens there are considerably more ommatidia than in smaller specimens, in which the eyes superficially appear smaller. However, after measuring it becomes clear that eye size is constant and not correlated with body size (OI 7–10). The shape of the subpetiolar process is also somewhat variable.

Discothyrea schulzei Hita Garcia & Lieberman sp. n. (Figs. 4Q, 6Q, 7Q, 8Q, 9Q, 10Q, 11Q, 12Q, 14Q, 52, 53; Supp. Video S17 [online only])

Type Material

HOLOTYPE, pinned worker, RWANDA, Western, Rangiro, [2.39361, 29.18278], 1800 m, collection code ANTC37497, from litter, 6.VIII.1973 (*P. Werner*) (BMNH: CASENT0790121). **PARATYPES**, two pinned workers with same data as holotype (MHNG: CASENT0247365, CASENT0790120); and one pinned worker with same data as holotype except collection code ANTC42124 and collected 10.VII.1973 (*P. Werner*) (CASC: CASENT0247370).

Cybertype. Volumetric raw data (in DICOM format), 3D rotation video, still images of surface volume rendering, and 3D surface (in PLY format) of the physical holotype (CASENT0790121) in addition to stacked digital color images illustrating head in full-face view, profile and dorsal views of the body. The data are deposited at Dryad (Hita Garcia et al. 2019, http://doi.org/10.5061/dryad.3qm4183) and can be freely accessed as virtual representation of the type. In addition to the cybertype data at Dryad, we also provide a freely accessible 3D surface model of the holotype at Sketchfab (Model 17).

Nontype Material

UGANDA: Bundibugyo, Semliki National Park, Kirumia River trail, 0.80909, 30.09510, 720 m, 20.VIII.2012 (*J. Longino*); Kabarole, Kibale National Park, Kanyawara Bioligcal Station, rainforest, 0.56437, 30.36059, 1510 m, 6.–16.VIII.2012 (*F. Hita Garcia*).

Diagnosis

The following character combination distinguishes *D. schulzei* from the remainder of the complex: smaller species (WL 0.47–0.56); in profile frontal lamella with anterodorsal corner rounded, with conspicuous, large, basal fenestra; moderately long, distinct, well-spaced and almost entirely erect pilosity present on mesosoma and abdominal tergites; in dorsal view mesosoma conspicuously thick, robust and stocky (DMI 58–66; DMI2 95–100); anterolateral corner of gena weakly angled and not denticulate/dentate; mesosoma not extremely convex and propodeum denticulate/dentate; masticatory margin of mandible edentate; mesotibia without apicoventral spur; subpetiolar process long, dentate to spinose with rounded apex; AT4 around 1.1 to 1.2 times longer than AT3 (ASI 114–124); abdominal sternite 3 rounded, without any projecting lobe; anterior clypeal margin without conspicuous row of long, straight setae.

Worker Measurements and Indices (*n* = 6)

EL 0.00–0.02; HL 0.46–0.54; HW 0.39–0.44; SL 0.25–0.29; PH 0.23–0.29; PW 0.29–0.35; DML 0.29–0.36; PrH 0.29–0.35; WL 0.47–0.56; HFL 0.26–0.33; PeL 0.07–0.08; PeW 0.18–0.21; PeH

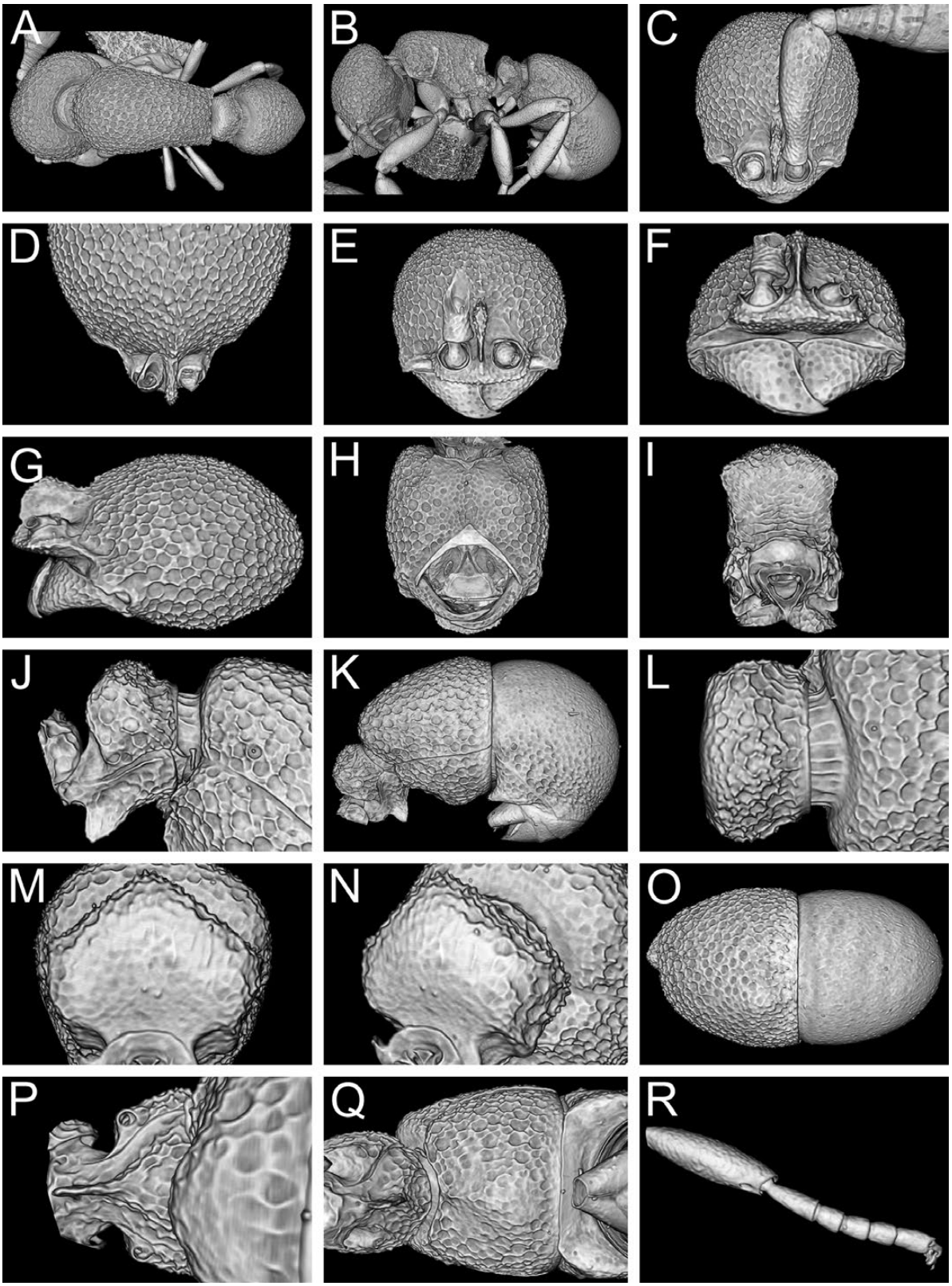

Fig. 53. Still images from shaded surface display volume renderings of *D. schulzei* sp. n. holotype (CASENT0790121) showing virtually segmented body parts. (A) Body in dorsal view, (B) body in profile, (C) head in full-face view, (D) head in dorsal view, (E) head in anterodorsal view, (F) head in anterior view, (G) head in profile, (H) head in ventral view, (I) posterior propodeum in posterior view, (J) petiole in profile, (K) petiole and gaster in profile, (L) petiole in dorsal view, (M) petiole in anterior view, (N) petiole oblique anterior view, (O) gaster in dorsal view, (P) petiole in ventral view, (Q) abdominal sternite 3 in ventral view, (R) mesotibia and mesotarsus in anterior view.

0.18–0.24; LT3 0.28–0.33; LT4 0.33–0.39; OI 0–3; CI 81–86; SI 50–56; LMI 49–55; DMI 58–66; DMI2 95–100; ASI 114–124; HFI 55–60; DPeI 234–270; LPeI 263–300.

Worker Description

Head longer than broad (CI 81–86), posterior head margin straight; posterodorsal corners of head rounded; in frontal view, sides of head converging gently anteriorly; eyes absent or very small (OI 0–3), an indistinct pigmented spot, situated slightly anterad one-third of the way between anterolateral corner of gena and posterior head margin, not visible in frontal view; frontal lamella lobate in profile, with anterodorsal corner rounded; lamella with conspicuous, large, basal fenestra; medial clypeus convex, lateral clypeus curving fairly strongly between antennal sockets and anterolateral corners of head, bearing short curved to erect setae. *Antenna* with moderately long scape (SI 50–56), scape moderately incrassate, gently bent; pedicel campaniform, slightly longer than broad; apparent antennomere count nine to eleven, flagellomeres basad apical club highly compressed, taken together only about as long as apical club. *Ventral head* with fairly low, sinuate preoccipital ridge with short, triangular anteromedial projection; median region of hypostoma triangular, arms only very slightly narrowed, squared apicolaterally; palpal formula not examined. *Mandible* edentate except for curved prebasal denticle; basal angle rounded; ectal face with carina confluent with masticatory margin for most of its length, leaving only a small depressed region containing prebasal denticle.

Mesosoma weakly convex, pronotum only scarcely higher than propodeum; in dorsal view, mesosoma conspicuously thick, robust and stocky (DMI 58–66; DMI2 95–100), slightly narrowed posteriorly, pronotum not much wider than propodeum; pronotal humeri rounded; posterior propodeal margin concave; posterodorsal corners of propodeum rounded; declivitous face of propodeum distinctly concave in profile and oblique posterior view; propodeal spiracle inconspicuous, directed posterodorsally; propodeal lobes moderately well-developed, lobate.

Legs short to moderately long (HFI 55–60); mesotibia without apicoventral spur; with small but distinct seta inserted in apicoventral pit; mesobasitarsus quite short, shorter than tarsomeres II–IV taken together.

Petiolar node not strongly attenuated dorsally, somewhat blunt in profile, about 2.6 to 3.0 times higher than long (LPeI 263–300); in profile anterior face of node sloping posterodorsally, apex rounded, posterior face sloping posteroventrally; in dorsal view, petiole rounded-rectangular, anterior margin and sides convex, posterior margin concave; about 2.3 to 2.7 times broader than long (DPeI 234–270); in anterior view, petiolar outline, edges and angles well-defined; in oblique anterior view, anterior face flat; subpetiolar process long, dentate to spinose with rounded or truncate apex.

Abdominal segment 3 campaniform, tergite somewhat prolonged anteriorly past anterior sternal margin; sternite convex in profile; AS3 with short, low anterior median ridge, with broad posterior lobe; prora carinulate, concave in ventral view; AT4 around 1.1 to 1.2 times longer than AT3 (ASI 114–124); AT4 hemidemispherical; AS4 with broad, well-developed anterior lip, overlapping most of the width of AS3, anterior margn straight in ventral view; successive abdominal segments short, telescopic, often concealed.

Sculpture on head, mesosomal dorsum, petiole, and dorsal surface of AT3 coarsely foveolate-reticulate to alveolate, more sparsely so on lateral mesoma and abdominal segment 3; gena becoming somewhat more punctate to foveolate on ventral head surface; mandible roughly sculptured with piligerous punctulae; coarse sculpture persistent on frontal lamella and clypeus; rugulae present on lower portions of lateral mesosoma; declivitous face of propodeum longitudinally rugulose to costulate; AT4 distinctly smoother and shinier than AT3, with abundant but fine piligerous punctulae.

Model 17. 3D surface model of *D. schulzei* sp. n. holotype (CASENT0790121). An interactive version of this model is available in the HTML version of this article online and at https://sketchfab.com/3d-models/c87c2fed1b87462a8068867e5cf5e68d.

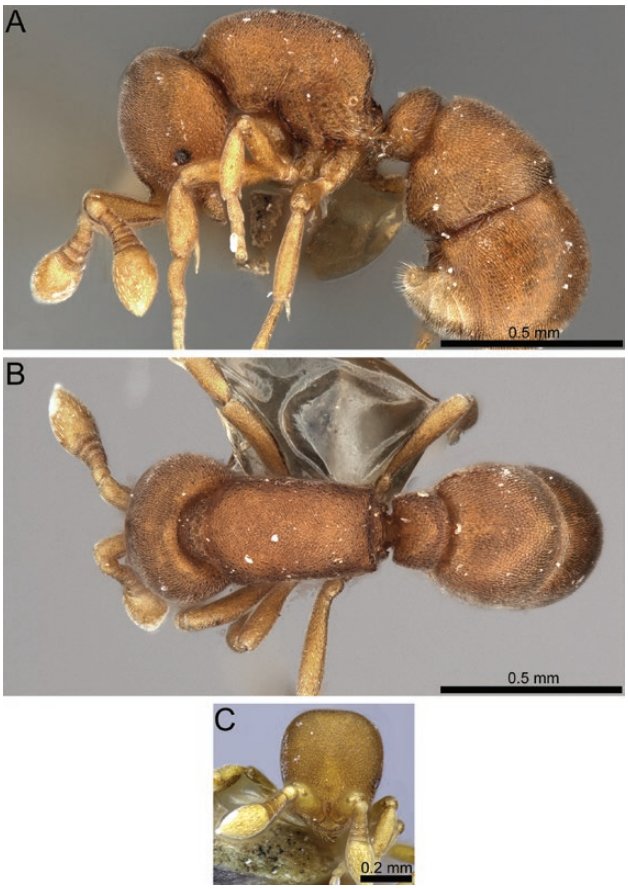

Fig. 54. Stacked digital color images of *D. traegaordhi* Santschi, 1914 neotype (CASENT0790122). (A) body in profile, (B) body in dorsal view, (C) head in full-face view.

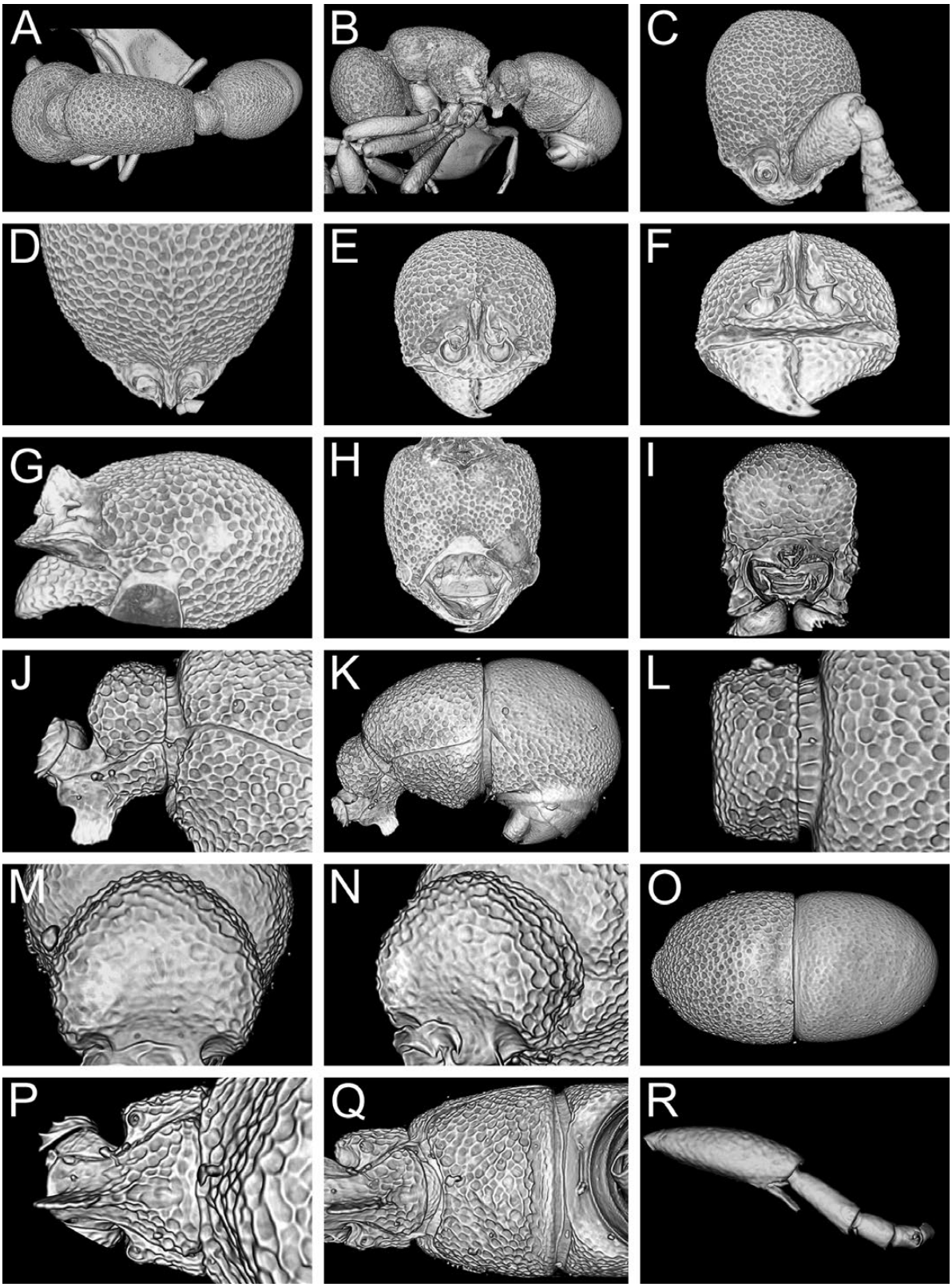

Fig. 55. Still images from shaded surface display volume renderings of *D. traegaordhi* Santschi, 1914 neotype (CASENT0790122) showing virtually segmented body parts. (A) Body in dorsal view, (B) body in profile, (C) head in full-face view, (D) head in dorsal view, (E) head in anterodorsal view, (F) head in anterior view, (G) head in profile, (H) head in ventral view, (I) posterior propodeum in posterior view, (J) petiole in profile, (K) petiole and gaster in profile, (L) petiole in dorsal view, (M) petiole in anterior view, (N) petiole oblique anterior view, (O) gaster in dorsal view, (P) petiole in ventral view, (Q) abdominal sternite 3 in ventral view, (R) mesotibia and mesotarsus in anterior view.

Setation on head, mesosoma, petiole, and AT3 consisting of fine, dilute appressed pubescence on lateral surfaces, dorsal surfaces with distinct, abundant, erect white pilosity; abdominal sternite 3 and AT4 similarly setose, but pubescence longer and more distinct on lateral surfaces, and erect pilosity somewhat longer on AT4; successive abdominal segments with similar pattern, pubescence and pilosity equivalent to or slightly longer and more abundant than on AT4; scape and legs with evenly distributed, dense, appressed pubescence; ectal face of mandible with relatively short, curved, appressed to decumbent setae; masticatory margin with row of straight setae.

Color rather dull testaceous-yellow to reddish, chestnut brown, appendages usually lighter.

Etymology

The name of the new species is a patronym dedicated to Arne Schulze from Frankfurt, Germany. The first author wants to thank him for his support and friendship during the time of this study. The specific epithet is given as a genitive noun.

Distribution and Biology

At present, *D. schulzei* is only known from Rangiro in Rwanda and Kibale Forest and Semliki National Park in Uganda (Fig. 4Q). The former two localities are rainforest sites at elevations ranging from 1510 to 1800 m while the latter is moist semideciduous forest with patches of swamp forest between 670 and 760 m. Based on the collection data from the Kibale specimens, the species lives in leaf litter. We strongly suspect that the species will be found in more rainforests along the Albertine Rift in Burundi, Rwanda, and Uganda.

Comments

Discothyrea schulzei can be recognized based on its lack of mesotibial spurs, the presence of an extremely well-developed basal fenestra on the frontal lamella, its standing pilosity, size, and mesosomal shape. As mentioned above, *D. schulzei* is morphologically very close to *D. damato*. Indeed, they are only separable on the basis of setation. It is possible that they are conspecific and the differences in setation are just intraspecific variation. However, we prefer to propose them both as heterospecific for the following reasons. First, major pilosity phenotypes appear to be very stable at species level throughout the Afrotropical *Discothyrea* fauna. Second, and more importantly, *D. damato* and *D. schulzei* are found in sympatry and retain their different pilosity patterns in a very consistent way without any intermediate forms. Other species close to *D. schulzei* are *D. dryad* and *D. wakanda* since they agree in most characters. Nevertheless, they differ in body size (despite some overlap), profile of the frontal lamella, and the shape of the subpetiolar process; the mesosoma is similarly stocky in *D. schulzei* and *D. wakanda* but more elongate and posteriorly attenuate in *D. dryad*. The sculpture of *D. schulzei* is notably deeper than that of either *D. dryad* or *D. damato*.

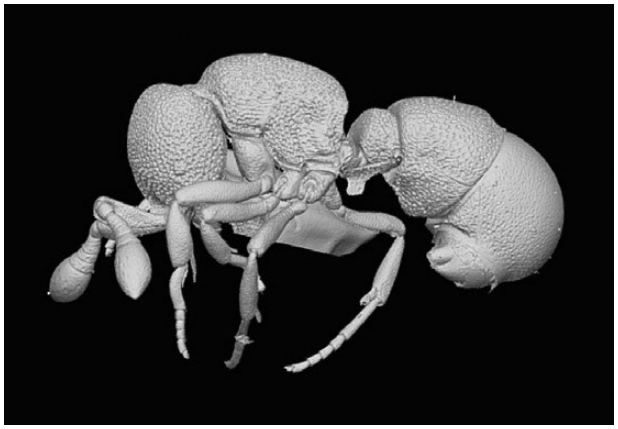

Model 18. 3D surface model of *D. traegaordhi* Santschi, 1914 neotype (CASENT0790122). An interactive version of this model is available in the HTML version of this article online and at https://sketchfab.com/3d-models/fd0e0ae7fb63416c808feb43ce2a7235.

Variation

Specimens from Rangiro have slightly longer pilosity than those from Kibale. Otherwise, there is no other noticeable intraspecific variation.

Discothyrea traegaordhi Santschi, 1914

(Figs. 4R, 6R, 7R, 8R, 9R, 10R, 11R, 12R, 13C, 14R, 15B, 15E, 54, 55; Supp Video S18 [online only])

Discothyrea traegaordhi Santschi, 1914: 3, by monotypy
Discothyrea hewitti Arnold, 1916: 160. **Syn. n.**

Type Material

Of *D. traegaordhi*: HOLOTYPE, pinned worker, SOUTH AFRICA Natal, Pietermaritzburg, 21.III.1905 (*I. Trägårdh*) (not in NHMB, apparently lost; see below).

NEOTYPE, by present designation, pinned worker, SOUTH AFRICA, KwaZulu-Natal, Town Bush, near Pietermaritzburg [–29.5616, 30.323], 900 m, native forest, 20.I.1977 (*W.L. & D.E. Brown*) (BMNH: CASENT0790122)

Of *D. hewitti*: SYNTYPES, two pinned queens, SOUTH AFRICA, Grahamstown [–33.3, 26.53333], ca. 533 m, IV.1915 (*Hewitt*) (AMGS; SAMC: SAM-ENT-11508) [SAMC type examined].

Virtual dataset. Volumetric raw data (in DICOM format), 3D rotation video, still images of surface volume rendering, and 3D surface (in PLY format) of the neotype (CASENT0790122) in addition to stacked digital color images illustrating head in full-face view, profile and dorsal views of the body. The data are deposited at Dryad (Hita Garcia et al. 2019, http://doi.org/10.5061/dryad.3qm4183) and can be freely accessed as virtual representation of the species. In addition to the data at Dryad, we also provide a freely accessible 3D surface model at Sketchfab (Model 18).

Nontype Material

SOUTH AFRICA: Eastern Cape, Mountain Zebra National Park, –32.23333, 25.46667, 1200 m, 27.X.1985 (*H.G. Robertson*); Eastern Cape, Riet River near Port Alfred, –33.566, 27.0166, ca. 4 m, 5.IV.1986 (*H.G. Robertson*); Eastern Cape, Silaka, near Port St Johns, –31.65, 29.5, ca. 80 m, indigenous wet forest along stream, 24.XI.1987 (*S. Endrody-Younga*); KwaZulu-Natal, Dukuduku Forest Reserve, 12–15 km E. Mtubatuba, [-28.365, 32.336], ca. 30 m, coast vine forest on sand, 26.I.1977 (*W.L. & D.E. Brown*); KwaZulu-Natal, St. Lucia Estuary, [-28.382, 32.41], ca. 25 m, 23.IX.1977 (*D.J. Brothers*).

Diagnosis

The following character combination distinguishes *D. traegaordhi* from the remainder of the species complex: smaller species (WL 0.51–0.57); shorter antennal scapes (SI 50–55); apicoventral

mesotibial spur present; relatively shorter legs (HFI 54–58); petiole relatively thinner (DPeI 235–289; LPeI 236–313); gastral terga without erect setae, only with appressed pubescence.

Worker Measurements and Indices (*n* = 10)

EL 0.03–0.05; HL 0.47–0.52; HW 0.39–0.43; SL 0.24–0.28; PH 0.25–0.28; PW 0.24–0.31; DML 0.33–0.39; PrH 0.29–0.33; WL 0.51–0.57; HFL 0.28–0.32; PeL 0.07–0.09; PeW 0.19–0.23; LT3 0.28–0.35; LT4 0.34–0.43; OI 7–10; CI 82–84; SI 50–55; LMI 47–52; DMI 48–55; DMI2 67–76; ASI 113–124; HFI 54–58; DPeI 235–289; LPeI 236–313.

Worker Description

Head somewhat longer than broad (CI 82–84), posterior head margin straight to weakly convex, posterodorsal corners of head broadly rounded; sides of head in frontal view convex; eyes present, relatively large (OI 7–10), round, usually comprising five to eight ommatidia, placed about a third of the way between anterolateral corner of gena and posterior head margin; eyes visible in frontal view; frontal lamella fairly short and roughly triangular in profile, apex rounded to acute; lamella not translucent across its disc, lacking a distinct fenestra; medial clypeus convex, lateral clypeus curving shallowly between antennal sockets and anterolateral corners of head, bearing short, curved setae. *Antenna* with short to moderately long scape (SI 50–55), scape slightly expanded apically, gently bent; pedicel subglobose, approximately as long as broad to slightly broader than long; apparent antennomere count seven to nine, but eight in most cases, flagellomeres basad apical club highly compressed, taken together shorter than apical club. *Ventral* head with low, V-shaped preoccipital ridge with short, triangular anteromedial projection; median area of hypostoma broadly triangular, arms narrowed, similar in width across their length; palpal formula not examined. *Mandible* edentate except for long, square to crenulate prebasal angle; basal angle rounded to squared; ectal face with carina originating at basal angle, becoming confluent with masticatory margin at around apical one-third, leaving narrow depressed region including prebasal angle.

Mesosoma weakly convex, pronotum either slightly higher than propodeum or at about same height; in dorsal view, mesosoma conspicuously slender and elongate (DMI 48–55; DMI2 73–83), moderately narrowed posteriorly, pronotum somewhat wider than propodeum; pronotal humeri rounded; posterior propodeal margin straight to very slightly concave; posterodorsal corners of propodeum rounded, without denticles or strong angles; declivitous face of propodeum slightly concave in profile and oblique posterior view; propodeal spiracle distinct, directed posterolaterally; propodeal lobes short, rounded.

Legs short (HFI 54–58); mesotibia with distinct apicoventral spur; mesobasitarsus relatively short, subequal in length to tarsomeres II–IV taken together.

Petiolar node weakly attenuated dorsally, about 2.4 to 3.1 times higher than long (LPeI 236–313) in profile anterior face of node straight to weakly convex, apex peaked, petiolar dorsum straight or sloping down anteriorly, posterior face subvertical; in dorsal view, node approximately rectangular, about 2.3 to 2.9 times broader than long (DPeI 235–289), sides divergent posteriorly; in anterior view, petiolar outline broadly pentagonal to round, angles rounded; in oblique anterior view; anterior face flat; subpetiolar process variable in shape, moderately long, broadly lobate, subrectangular to rectangular.

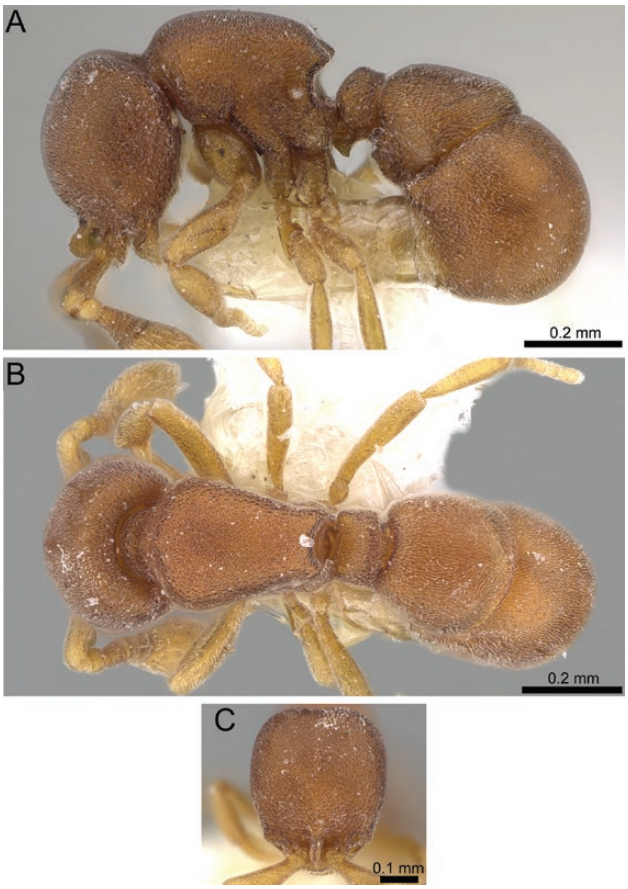

Fig. 56. Stacked digital color images of *D. venus* sp. n. paratype (CASENT0247017—from https://www.antweb.org, photographer Michele Esposito). (A) body in profile, (B) body in dorsal view, (C) head in full-face view.

Abdominal segment 3 campaniform, widest just anterad end of segment; tergite slightly anteriorly prolonged over petiole; sternite evenly curved to posteriorly bulging in profile; AS3 without median ridge, posterior lobe broad and indistinct; prora carinate, concave in ventral view; AT4 around 1.1 to 1.2 times longer than AT3 (ASI 105–124); AT4 evenly rounded hemidemispherical; AS4 with anterior lip overlapping about median two-third the width of AS3, anterior face convex in ventral view; successive abdominal segments short, telescopic, often concealed.

Sculpture of head, mesosoma, petiole, and abdominal segment 3 shallowly punctate-reticulate; mandibles moderately shining with piligerous punctulae; punctae on lateral mesosoma somewhat larger but sparser; absent or nearly so on declivitous face of propodeum, the disc of which more strongly shining than remainder of mesosoma; fine rugulae present on ventrolateral and declivitous surfaces of propodeum; AT4 with minute but distinct, very densely arranged piligerous punctae, clearly shinier than AT3.

Setation mostly consisting of appressed white pubescence, more or less evenly distributed over entire body, sometimes more diluted on head; abdominal segments five through seven with long, flexuous standing setae; appendages with well-developed, evenly distributed appressed pubescence; ectal face of mandible with abundant, curved, appressed to decumbent setae; with row of straight, stout setae on masticatory margin.

Color unicolorous luteous to matte orange brown to darker chestnut brown with lighter appendages.

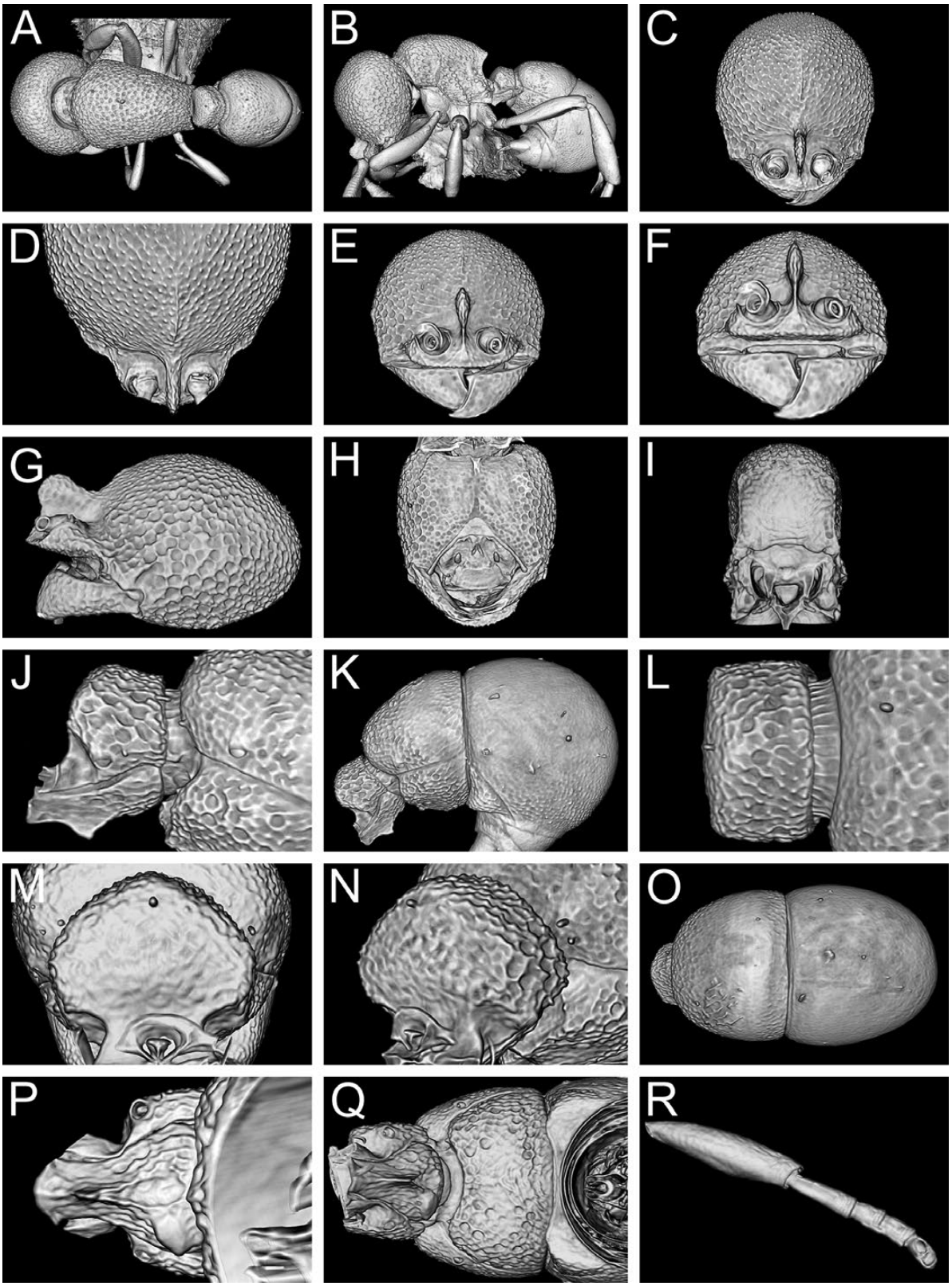

Fig. 57. Still images from shaded surface display volume renderings of *D. venus* sp. n. holotype (CASENT0790116) showing virtually segmented body parts. (A) Body in dorsal view, (B) body in profile, (C) head in full-face view, (D) head in dorsal view, (E) head in anterodorsal view, (F) head in anterior view, (G) head in profile, (H) head in ventral view, (I) posterior propodeum in posterior view, (J) petiole in profile, (K) petiole and gaster in profile, (L) petiole in dorsal view, (M) petiole in anterior view, (N) petiole oblique anterior view, (O) gaster in dorsal view, (P) petiole in ventral view, (Q) abdominal sternite 3 in ventral view, (R) mesotibia and mesotarsus in anterior view.

Model 19. 3D surface model of *D. venus* Santschi, 1914 holotype (CASENT0790116). An interactive version of this model is available in the HTML version of this article online and at https://sketchfab.com/3d-models/e0479eb664da4ecdb93ad9091e120281.

Distribution and Biology

At present, *D. traegaordhi* is only known from South Africa (Fig. 4R). It seems to be moderately distributed from the Eastern Cape to Kwa-Zulu Natal. Based on the limited data available, *D. traegaordhi* prefers forested habitats at low to medium elevations.

Comments

The original holotype with the data SOUTH AFRICA, Natal, Pietermaritzburg, 21.III.1905 (*Tragaordh*) (NHMB: CASENT0915310) is presumably lost. The pin with the original label located in the collection of NHMB lacks a specimen. This was confirmed by us, as well as by the curatorial staff of NHMB. Since the original description does not provide sufficient diagnostic information to properly delineate this species and no type material exists, we consider it necessary to designate a neotype in order to clarify and stabilize the taxonomic and nomenclatorial status of *D. traegaordhi*. The chosen neotype is from the same area around Pietermaritzburg in Kwa-Zulu Natal as the original holotype representing a very close geographical approximation to the type location from the original publication.

In the original description of *D. hewitti* Arnold (1916) already suggested that both taxa could represent the same species, but due to the lack of workers of *D. hewitti* and queens of *D. traegaordhi* he hesitated to unite them under one name. Later, Brown (1958a) opined that the only dissimilarities between the two taxa are typical caste-specific differences. Based on the comparison of one syntype queen of *D. hewitti* with two queens associated with *D. traegaordhi*, we are able to solve this problem. Since the material of both does not show any significant morphological differences, it is apparent that both species are conspecific. Consequently, we propose *D. hewitti* as junior synonym of *D. traegaordhi*.

As noted above, *D. traegaordhi* can be grouped with *D. gaia* and *D. poweri* since they all possess a conspicuously large apicoventral spur on the mesotibia and relatively large eyes (OI 7–10). Nevertheless, the separation of these three species is straightforward. *Discothyrea traegaordhi* has a considerably thinner petiole (DPeI 235–289; LPeI 236–313) and shorter antennal scapes (SI 50–55) than *D. poweri* (DPeI 135–173; LPeI 152–194; SI 61–68). In addition, the latter species is also much larger (WL 0.67–0.84 vs. WL 0.51–0.57) and has longer legs (HFI 61–69 vs. HFI 54–58). *Discothyrea gaia* possesses numerous erect setae, especially on AT3, and a generally thicker petiole (DPeI 192–255; LPeI 194–264), both distinguishing it clearly from *D. traegaordhi*. Otherwise, these two species are morphologically very close and could be sister species.

Variation

There is some slight variation in the thickness of the petiole and the coarseness of the sculpture, but all well within species-specific boundaries.

Discothyrea venus Hita Garcia & Lieberman sp. n. (Figs. 2C, 4S, 6S, 7S, 8S, 9S, 10S, 11S, 12S, 14S, 56, 57; Supp. Video S19 [online only])

Type Material

HOLOTYPES, pinned worker, IVORY COAST, Abidjan, Banco National Park, [5.38694, –4.05275], ca. 20 m, primary forest, dead trunk, collection code ANTC42125, 3.II.1977 (*I. Löbl*) (BMNH: CASENT0790116). **PARATYPES**, six workers with same data as holotype (BMNH: CASENT0790115; CASC: CASENT0247017; HLMD: HLMD-Hym-2397; MCZC: MCZ-ENT00593559; MHNG: CASENT0247013; SAMC: CASENT0247016).

Cybertype. Volumetric raw data (in DICOM format), 3D rotation video, still images of surface volume rendering, and 3D surface (in PLY format) of the physical holotype (CASENT0790116) in addition to stacked digital color images illustrating head in full-face view, profile and dorsal views of the body. The data are deposited at Dryad (Hita Garcia et al. 2019, http://doi.org/10.5061/dryad.3qm4183) and can be freely accessed as virtual representation of the type. In addition to the cybertype data at Dryad, we also provide a freely accessible 3D surface model of the holotype at Sketchfab (Model 19).

Nontype Material

ANGOLA: R. Kahingo, [–7.39, 20.51], ca. 650 m, gallery forest, 20.VI.1964 (*Mwaoke*); R. Mussungue, mouth, Route Turisme, [–7.3697, 20.813], ca. 630 m, gallery forest, 8.XI.1963 (*L. Carvalho*); CAMEROON: Ebolowa, [2.92, 11.13], 640 m, 22.VIII.1940 (*A.I. Good*); Nkoemvon, [2.7517, 11.0814], ca. 630 m, 5.I.1980 (*D. Jackson*); GHANA: Aiyaola Forest Reserve, Kade, [6.1510, –0.945], ca. 210 m, primary forest, 6.X.1992 (*R. Belshaw*); Ashanti, Ofinso, [6.93, –1.65], ca. 230 m, cocoa plantation, 2.XI.1992 (*R. Belshaw*); Atewa Forest Reserve, nr. Kibi, [6.1747, –0.5861], ca. 400 m, 26.II.1992 (*R. Belshaw*); Eastern, Bunso, nr. Tafo, [6.28761, –0.46948], ca. 240 m, primary forest, 6.XI.1992 (*R. Belshaw*); IVORY COAST: Abidjan, Banco National Park, [5.38694, –4.05275], ca. 20 m, primary forest, 3.II.1977 (*I. Löbl*); Adiopodoume, [5.335, –4.131], ca. 30 m, 31.X.1980 (*V. Mahnert & J.L. Perret*); Abidjan, Banco Forest, collection code A50, [5.39, –4.05], 79 m, 11.I.1963 (*W.L. Brown*); Agboville, Yapo Forest, near Yapo-Gare, [5.77105, –4.12376], ca. 80 m, 21.–23.III.1977 (*I. Löbl*); Man, ravine at foot of Mt. Tonkoui, [7.4014, –7.5791], ca. 640 m, 9.III.1977 (*I. Löbl*); Nzi Noua, N. of Ndouci, [6.03283, –4.84893], ca. 60 m, degraded forest, 13.I.1977 (*W.L. & D.E. Brown*); UGANDA: Kibale National Park, Kanyawara Biological Station, 0.56437, 30.36059, 1510 m, rainforest, 6.–16.VIII.2012 (*G. Fischer*).

Diagnosis

The following character combination distinguishes *D. venus* from the remainder of the complex: masticatory margin of mandible edentate; anterolateral corner of gena not denticulate/dentate; propodeum laterally and dorsally strongly concave posteriorly; metatibae without apicoventral spur; lower portion of declivitous face of propodeum

transversely substrigulate; AT4 extremely enlarged, bulbous, and much longer than AT3 (ASI 158–183).

Worker Measurements and Indices (*n* = 12)

EL 0.00–0.01; HL 0.41–0.48; HW 0.33–0.40; SL 0.20–0.26; PH 0.20–0.25; PW 0.26–0.32; DML 0.24–0.30; PrH 0.25–0.29; WL 0.39–0.47; HFL 0.25–0.33; PeL 0.05–0.07; PeW 0.15–0.19; PeH 0.14–0.18; LT3 0.19–0.24; LT4 0.33–0.39; OI 0–3; CI 80–84; SI 48–55; LMI 51–55; DMI 62–69; DMI2 95–107; ASI 158–183; HFI 63–74; DPeI 250–321; LPeI 233–300.

Worker Description

Head longer than broad (CI 80–84), posterior head margin slightly convex overall, with very weak impression medially; posterodorsal corners of head quite broadly rounded; in frontal view, sides of head convex; eyes absent or extremely minute (OI 0–3), a tiny pigmented spot situated about a third of the way between anterolateral corner of gena and posterior head margin, not visible in frontal view; frontal lamella lobate in profile, apex blunt to rounded; lamella with well-defined translucent basal fenestra; medial clypeus broad, convex, sides of medial clypeus subparallel laterad antennal sockets, lateral clypeus curving fairly strongly between antennal sockets and anteroalteral corners of head, entire clypeal margin bearing very short curved setae. *Antenna* with usually shorter scape (SI 48–55), scape moderately incrassate, gently bent; pedicel subglobose, width and length subequal or slightly broader than long; apparent antennomere count seven to eleven (usually seven to eight) but often not discernable and extremely difficult to count, flagellomeres basad apical club highly compressed, taken together only about as long as apical club. *Ventral* head with weakly sinuate preoccipital ridge with short but distinct anteromedial carina; median region of hypostoma rounded-triangular, arms distinctly narrowed, slightly spatulate apicolaterally; palpal formula not examined. *Mandible* edentate or with slight preapical swelling, without prebasal denticle; basal angle denticulate; ectal face with carina extending from base of basal denticle, becoming confluent with masticatory margin preapically, leaving narrow, comma-shaped depressed region.

Mesosoma gently convex in profile, pronotum slightly higher than propodeum; in dorsal view, mesosoma conspicuously thick, robust and stocky (DMI 59–66; DMI2 95–102), strongly narrowed posteriorly, pronotum much wider than propodeum; pronotal humeri rounded; posterior propodeal margin distinctly concave; posterodorsal corners of propodeum strongly angulate but lacking differentiated denticles; declivitous face of propodeum strongly concave in profile and oblique posterior view; propodeal spiracle directed posterolaterally, often relatively conspicuous due to small patch of shiny, polished sculpture offsetting spiracular opening from remainder of propodeum; propodeal lobes short, truncate.

Legs relatively long (HFI 63–74) and slender; mesotibia without apicoventral spur; mesobasitarsus relatively short, subequal in length to tarsomeres II–IV taken together.

Petiolar node moderately attenauted dorsally, about 2.3 to 3.0 times as high as long (LPeI 233–300); in profile, anterior face of node convex, apex peaked, posterior face sloping posteroventrally; in dorsal view, petiole subrectangular, sides diverging posteriorly, about 2.5 to 3.2 times as broad as long (DPeI 250–321); in anterior view, petiolar outline roughly pentagonal, edges poorly defined and angles rounded; in oblique anterior view, anterior face flat; subpetiolar process short, dentate, apex acute.

Fig. 58. Stacked digital color images of *D. wakanda* sp. n. holotype (CASENT0790326). (A) body in profile, (B) body in dorsal view, (C) head in full-face view.

Abdominal segment 3 short, broadly campaniform, widest point just anterad end of segment; sternite more or less evenly convex in profile; AS3 without median ridge or lobe; prora finely carinulate, concave in ventral view; AT4 around 1.6 to 1.8 times as long as AT3 (ASI 158–183), AT4 bulbous, swollen hemidemispherical, or more elongate, shaped as quarter of prolate ellipsoid; AS4 with broad, well-developed anterior lip, overlapping most of the width of AS3, anterior margin concave in ventral view; successive abdominal segments short, telescopic, often concealed, projecting strongly anteriorly due to size and shape of AT4.

Sculpture in general shallow and somewhat indistinct; head, dorsal mesosoma, and petiole similarly and evenly punctate-reticulate, punctae often more pronounced on head than mesosoma; mandible fairly smooth except for small piligerous punctae; lateral mesosoma with punctae particularly indistinct, interspaces of punctae variably coalescent, forming weak rugulae; declivitous face of propodeum transversely substrigulate over around the ventral half; abdominal segment 3 weakly punctulate; AT4 with even finer piligerous punctulae.

Setation generally very fine and dilute, similar over all tagma and consisting entirely of short, appressed white pubescence; pubescence slightly longer on abdominal segment 3 and AT4, slightly reduced on lateral mesosoma; ectal face of mandible with moderately long, curved, appressed to decumbent setae; masticatory margin with row of short straight setae; scape and legs with similarly short, velvety pubescence; abdominal segments 5 to 7 with standing setae, quite

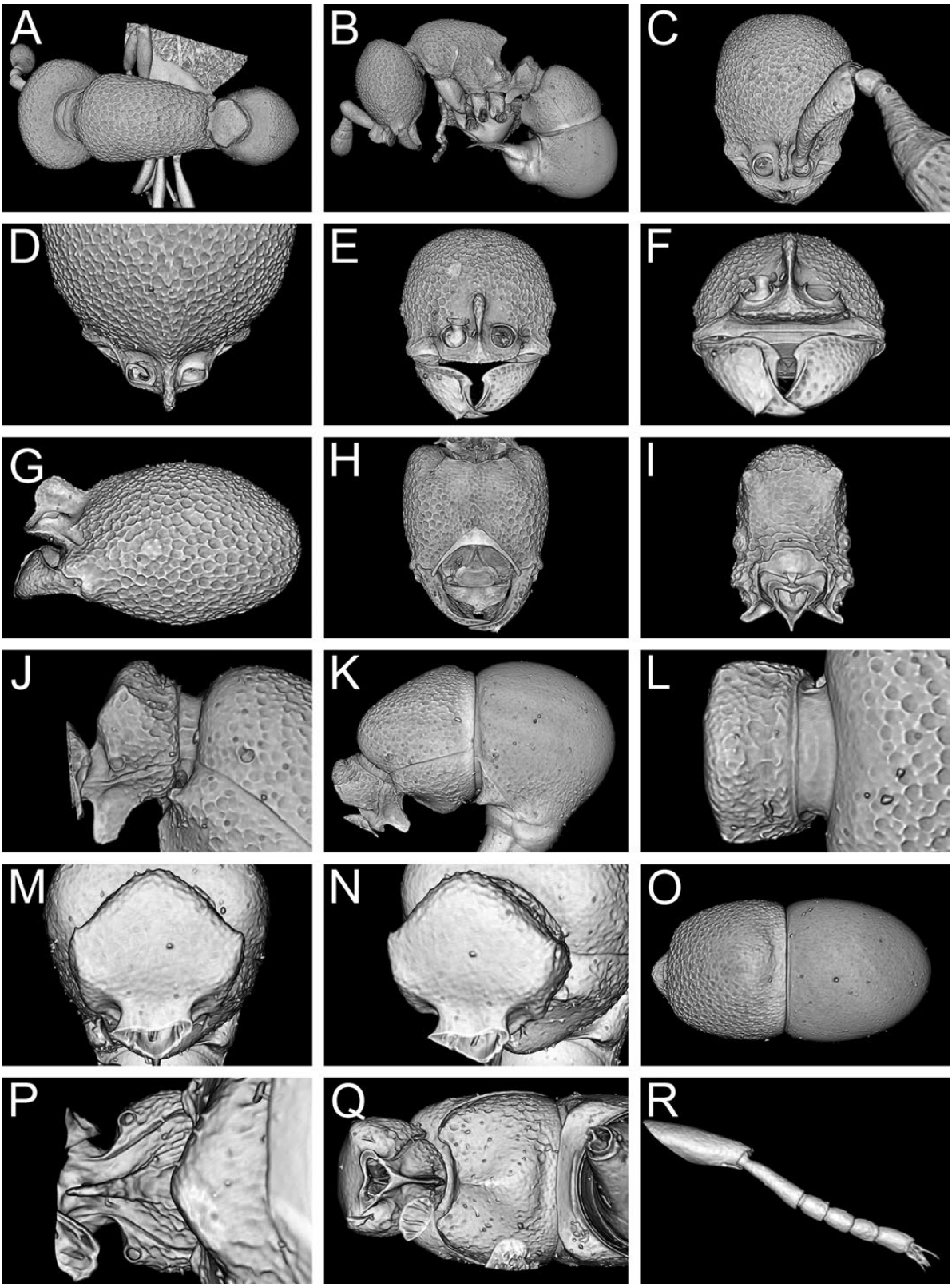

Fig. 59. Still images from shaded surface display volume renderings of *D. wakanda* sp. n. holotype (CASENT0790326) showing virtually segmented body parts. (A) Body in dorsal view, (B) body in profile, (C) head in full-face view, (D) head in dorsal view, (E) head in anterodorsal view, (F) head in anterior view, (G) head in profile, (H) head in ventral view, (I) posterior propodeum in posterior view, (J) petiole in profile, (K) petiole and gaster in profile, (L) petiole in dorsal view, (M) petiole in anterior view, (N) petiole oblique anterior view, (O) gaster in dorsal view, (P) petiole in ventral view, (Q) abdominal sternite 3 in ventral view, (R) mesotibia and mesotarsus in anterior view.

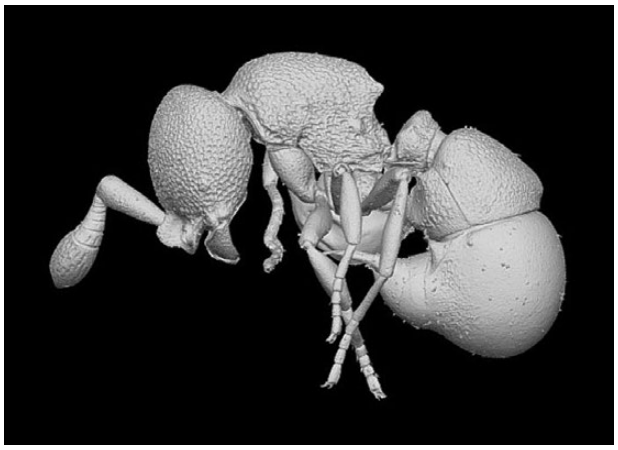

Model 20. 3D surface model of *D. wakanda* sp. n. holotype (CASENT0790326). An interactive version of this model is available in the HTML version of this article online and at https://sketchfab.com/3d-models/862743aa29d24113957b4c3ca277d82a.

long relative to setation on remainder of body (but rather short relative to that of segments 5 to 7 on most other Afrotropical species).

Color testaceous-orange, sometimes lightly infuscated on dorsal surfaces.

Etymology

Venus was the Roman goddess of love, beauty, and prosperity. Among her local epithets was Venus Kallipygos, 'she of the beautiful buttocks'; the species is named in reference to the hypertrophied fourth abdominal tergite. The specific epithet is given as an appositive noun.

Distribution and Biology

This species is patchily but widely distributed throughout Equatorial Africa (Fig. 4S). Currently, it is known from many localities in Ivory Coast and Ghana, some in Cameroon and Angola, and one in Western Uganda. With the exception of Kibale Forest in Uganda, which is situated at an elevation of around 1500 m, all other known localities are lowland rainforests ranging from 30 m to 650 m elevation. The highly disjunct distribution is likely due to a sampling bias, and we think it is highly probable that *D. venus* will also be found in more or even all countries of the Congo Basin.

Comments

Discothyrea venus is a highly conspicuous species within the Afrotropical fauna. The character combination given in the diagnosis above discriminates it clearly from the remainder of the genus. To the best of our knowledge, the dramatically enlarged fourth abdominal tergite in particular (ASI 156–194) is not approximated by any other congener.

Variation

Considering the relatively broad distribution in West and Central Africa, it is surprising to see only very little variation. The eyes are entirely absent in some individuals, while in others they are present but minute, more like an indistinct pigmented spot. The length of the abdominal terga is somewhat variable but the fourth tergite is always significantly larger than the third. The development of sculpturation, particularly on the lateral mesosoma, is somewhat variable between individuals, with some possessing more pronounced punctae, but overall is similarly shallow and indistinct.

Discothyrea wakanda Hita Garcia & Lieberman sp. n. (Figs. 4T, 5E–F, 6T, 7T, 8T, 9T, 10T, 11T, 12T, 13F, 14T, 58, 59; Supp. Video S20 [online only])

Type Material

HOLOTYPE, pinned worker, DEMOCRATIC REPUBLIC OF CONGO, North Kivu, Virunga National Park, Massif Ruwenzori, Lamya-Ruanoli, Muhira, [0.498, 29.884], 2600 m, bamboo, 9.I.1963 (*R.P.M.J. Celis*) (MRAC: CASENT0790326). **PARATYPES**, four pinned workers with same data as holotype (MRAC: MRACFOR000117, MRACFOR000118, MRACFOR000119, MRACFOR000120).

Cybertype. Volumetric raw data (in DICOM format), 3D rotation video, still images of surface volume rendering, and 3D surface (in PLY format) of the physical holotype (CASENT0790326) in addition to stacked digital color images illustrating head in full-face view, profile and dorsal views of the body. The data are deposited at Dryad (Hita Garcia et al. 2019, http://doi.org/10.5061/dryad.3qm4183) and can be freely accessed as virtual representation of the type. In addition to the cybertype data at Dryad, we also provide a freely accessible 3D surface model of the holotype at Sketchfab (Model 20).

Nontype Material

DEMOCRATIC REPUBLIC OF CONGO: North Kivu, Virunga National Park, Massif Ruwenzori, Lamya-Ruanoli, [0.498, 29.883], 2500 m, bamboo, 9.I.1963 (*R.P.M.J. Celis*); North Kivu, Virunga National Park, Massif Ruwenzori, Lamya-Ruanoli, [0.497, 29.887], 2700 m, bamboo, 9.I.1963 (*R.P.M.J. Celis*); North Kivu, Virunga National Park, Massif Ruwenzori, Lamya-Ruanoli, Kaleberwa, [0.499, 29.88], 2300 m, montane forest, bamboo, 9.I.1963 (*R.P.M.J. Celis*); North Kivu, Virunga National Park, Massif Ruwenzori, Kalonge, Katsambu River, affl. dr. Butahu, [0.43936, 29.17389], 2200 m, 26.I.–19.II.1953 (*P. Vanschuytbroeck; J. Kekenbosch*).

Diagnosis

The following character combination distinguishes *D. wakanda* from the remainder of the complex: large species (WL 0.59–0.65); in profile frontal lamella with prominent, elongate elliptical basal fenestra; propodeum denticulate, in dorsal view posterior propodeal margin strongly concave; standing pilosity present on mesosomal and abdominal terga; medial and lateral clypeus abruptly differentiated from posterolaterad antennal sockets, lateral clypeus very narrow and strongly concave between anterolateral corner of gena and antennal socket; sides of head slightly constricted laterally between eyes and anterolateral corner of gena, appearing concave in frontal view.

Worker Measurements and Indices (*n*= 15)

EL 0.03–0.04; HL 0.60–0.64; HW 0.50–0.52; SL 0.34–0.36; PH 0.33–0.36; PW 0.36–0.40; PrH 0.39–0.41; DML 0.37–0.41; WL 0.59–0.65; HFL 0.39–0.41; PeL 0.09–0.10; PeW 0.22–0.25; PeH 0.23–0.25; LT3 0.37–0.40; LT4 0.42–0.51; OI 4–7; CI 81–85; SI 55–58; LMI 51–57; DMI 59–62; DMI2 92–103; ASI 115–125; HFI 63–68; DPeI 240–267; LPeI 230–278.

Worker Description

Head longer than broad (CI 81–85), posterior head margin weakly emarginate medially; posterodorsal corners of head broadly rounded, sides of head subparallel from posterodorssal corner to eye,

constricted laterally between eyes and anterolateral corner of gena, this region appearing concave in frontal view; eyes present, relatively large (OI 4–7), round, situated slightly more than one-third of way between corner of gena and posterior head margin; eyes just visible in frontal view; frontal lamella lobate in profile, with anterodorsal corner rounded; lamella with conspicuous, large, basal fenestra; medial clypeus weakly sinuate, with differentiated anteromedial lobe; posterolaterad antennal sockets, lateral clypeus strongly excavated, concave between antennal socket and anterolateral corner of head; entire anterior border of clypeus bearing relatively distinct, curved, suberect to erect white setae. *Antenna* with moderately long scape (SI 55–58); scape moderately incrassate, gently bent; pedicel subcylindrical, slightly broader than long; true antennomere count nine; apparent antennomere count 8–10, flagellomeres basad apical club highly compressed, taken together only about as long as apical club. *Ventral head* with very fine, sinuate postoccipital ridge without anteromedian carina; medial region of hypostoma broadly triangular, arms somewhat narrowed, similar in width across their length; palpal formula not examined. *Mandible* edentate except for small, curved prebasal denticle not strongly differentiated from rounded basal angle; ectal face with carina originating around distal point of prebasal denticle and becoming confluent with masticatory margin at around distal half of mandible length.

Mesosoma weakly to moderately convex, pronotum scarecly higher than propodeum; in dorsal view, mesoma robust and stocky (DMI 59–62; DMI2 92–103), somewhat narrowed posteriorly, pronotum wider than propodeum; pronotal humeri rounded; posterodorsal corners of propodeum dentate, teeth thick, opaque; declivitous face of propodeum concave in profile and oblique posterior view; propodeal spiracle relatively large, round, directed posterolaterally; propodeal lobes moderately well-developed, lobate.

Legs moderately long (HFI 63–68) and slender. Mesotibia without apicoventral spur.

Petiolar node not strongly attenuated dorsally, about 2.3–2.8 times higher than long (LPeI 230–278); in profile anterior face of node sloping posterodorsally, apex peaked, posterior face sloping posteroventrally; in dorsal view, petiole subrectangular, sides subparallel to weakly convex, about 2.4–2.7 times as broad as long (DPeI 240–267); in anterior view, petiolar outline pentagonal, edges fairly well-defined, dorsally rounded; in oblique anterior view, anterior face flat; subpetiolar process relatively long, lobate to rounded-triangular.

Abdominal segment 3 roughly campaniform, tergite slightly prolonged anteriorly past anterior sternal margin; sternite convex in profile; AS3 with well-defined median ridge broadening posteriorly to a broad lobe; prora sharply carinulate, lunate with strongly defined anterolateral corners; AT4 around 1.2 times longer than AT3 (ASI 115–125); AT4 almost perfectly hemidemispherical; AS4 with well-developed, broad anterior lip overlapping most of the width of AS3, anterior margin straight to slightly curved in ventral view; successive abdominal segments short, telescopic, often concealed.

Sculpture on head densely foveolate to foveolate-reticulate, often becoming weakly sculptured just anterad occiput; mandibles, frontal lamella, clypeus, and ventral head surface roughly punctate to punctulate, postgenal bridge smoothest posteromedially; mesosoma dorsally and alterally foveolate-reticulate, fine rugulae present on lower areas of lateral mesosoma; declivitous face of propodeum horizontally rugulose, rugulae strongest ventrally; AT3 and AS3 shallowly punctate to weakly foveolate, AS4 becoming smooth for most of its ventromedial surface; AT4 very smooth with shallow scattered punctulae, a few more prominent punctae present posteriorly.

Setation on head fine, appressed, white pubescence, sometimes longer in posterior third of head; mesosomal, petiolar, and abdominal dorsa with fairly abundant standing pilosity, subdecumbent to erect, in addition to decumbent and appressed pubescence, usually longer on petiolar node than mesosoma and abdominal terga; appressed pubescence on lateral mesosoma fairly long but inconspicuous; on AT4 long and evenly disributed over entire tergite; AT4 usually with more fully erect setae than remainder of dorsal surfaces; scape and legs evenly distributed appressed to decumbent pubescence, scape usually with subdecumbent setae apically; ectal face of mandible with long, distinct, appressed to erect setae, curved to straight.

Color dull orange to testaceous orange, dorsal surfaces sometimes lightly infuscated.

Etymology

The specific epithet refers to the fictional nation of Wakanda from the Marvel comic universe. The new species is endemic to the Rwenzori Mountains in the Albertine Rift, the location of Wakanda in the Black Panther comics. Wakanda is a peaceful, prosperous country which was never colonized, where ancient cultural traditions coexist with conservation of natural resources and high-technology modernity. *Discothyrea wakanda* is named in honor of these ideals for Africa and the world. The species epithet is to be treated as an appositive noun.

Distribution and Biology

At present *D. wakanda* is known only from a few nearby high-elevation localities in the Rwenzori Mountains of eastern Democratic Republic of Congo (Fig. 4T), mostly from montane forest in the bamboo zone above 2500 m. Considering the lack of ant collections in the Albertine Rift in general, it is likely that it might be more common and wider distributed. Nothing is known of its biology.

Comments

Discothyrea wakanda is similar to *D. damato*, *D. dryad*, and *D. schulzei*, with which it shares the conspicuous elliptical basal fenestra on the frontal lamella. Like the latter two species but unlike *D. damato*, there is standing pilosity present on the mesosomal and abdominal terga. The profile of the frontal lamella, having a rounded rather than acute apex is similar to *D. schulzei*, as is the stocky shape of the mesosoma, which is more elongate and, in dorsal view, posteriorly tapered in *D. dryad*. These three species notably differ in size, with *D. wakanda* representing the largest (WL 0.59–65). *Discothyrea wakanda* is unique among this group of possibly related species in several cephalic characters: the slight medial emargination of the posterior head margin, the compression of the sides of the head between the eye and the anterolateral corners of the head, the weakly sinuate anterior border of the clypeus, and the excavation of the lateral clypeus laterad the antennal sockets.

Variation

There is some variation in size (WL 0.59–0.65) and in the degree of attenuation of the petiolar node (DPeI 240–267; LPeI 230–278). Also, there is some notable variability in the development of the propodeal denticles, which are always present and prominent but may be larger and more laterally divergent in some individuals. The density of the cephalic pilosity also varies somewhat, being rather thicker in some individuals, but the general distribution and stature of setae is consistent.

Discussion

Species Richness and Biogeography

While previously only seven species of *Discothyrea* were known from the Afrotropical region (Brown 1958a), this study has revealed a much higher diversity in the region. We recognize 20 species for the region, of which we confirm the previous status of five species while proposing two taxa as junior synonyms, and describe 15 new species. Our results increase the total count of global species from 35 to 48, which means that a large proportion of the known diversity seems centered in the Afrotropics. However, this is a preliminary assessment, since based on our own superficial examinations of natural history collections, it is very likely that there are at least five undescribed species from the Neotropics, perhaps five from the Malagasy region, and at least 10 more from the Indomalayan region.

The species richness revealed in this study is actually around twice higher than previous estimates based on extrapolations of taxonomic progress for the Afrotropical region (Robertson 2000), and also much higher than we expected at the beginning of the project. While some species, notably both *D. oculata* complex members and a few species from the *D. traegaordhi* complex, have broad distribution ranges, the majority of species from the latter complex are either restricted to a single locality or a narrow distribution range (Fig. 4). Many species also well overlap within their ranges and based on the available data, it seems that in most well-sampled localities in Equatorial and eastern Africa there are at least two or three sympatric *Discothyrea* species.

Nevertheless, the distribution patterns are not random, and despite having a limited dataset compared with the vastness of sub-Saharan Africa, we can draw some conclusions. One surprising result is, as mentioned above, the very broad distribution ranges of *D. mixta* and *D. oculata*, which are found in most of the region where forested areas occur and ant sampling data are available (Fig. 4A and B). Both species have large winged queens with a well-developed thorax, and we suspect they can fly well and far, which at least partly explains the broad distribution and obviously successful dispersal ability. In addition, it seems that if there are forested habitats with certain spider prey available, then one can expect either *D. mixta* or *D. oculata*, or rarely both together.

From a biogeographical perspective, the distribution ranges of the 18 species of the *D. traegaordhi* complex seem more interesting since they are significantly smaller and seem to indicate lower dispersal abilities. Remarkably, species distributions of the *D. traegaordhi* complex fit very well within modern partitioning of the Afrotropical region into well-defined subregions (Burgess et al. 2004, Linder et al. 2012). *Discothyrea penthos* is the only species apparently endemic to the Eastern Guinean Forests (Fig. 4O). While *D. venus* is also found in these western rainforests its distribution extends to most of the Guineo-Congolian Forests reaching western Uganda and northern Angola (Fig. 4S). Surprisingly though, the species richness within the Congo Basin is relatively low, which could however also be due to a sampling bias. Southern Africa is another larger subregion remarkably species-poor with just two species, *D. poweri* and *D. traegaordhi*, that are widespread in South Africa but not known from surrounding countries yet (Fig. 4P and R). Further north, two species are known from Zimbabwe but we suspect they represent faunal elements of two different subregions. Based on morphological similarities with *D. poweri* and *D. traegaordhi*, we consider *D. gaia* to be another Southern African species (Fig. 4H), whereas *D. maia* appears closer related to eastern African species (Fig. 4L).

The vast majority of species of the *D. traegaordhi* complex, however, are distributed in the Afromontane subregions of Eastern Africa at high to very high elevations. Some species, such as *D. damato*, *D. schulzei*, and *D. wakanda*, are only found in the Albertine Rift area in the Democratic Republic of the Congo, Burundi, Rwanda, and Uganda (Fig. 4F, Q, T). Other species seem to be endemic to either the East African Montane Forests in Kenya (*D. dryad*, Fig. 4G) or the Eastern Arc Mountains in Tanzania (*D. aisnetu* Fig. 4C, *D. chimera* Fig. 4E and *D. michelae* Fig. 4M), with *D. gryphon* being found in the Albertine Rift and the Eastern Arcs (Fig. 4I). However, other species, such as *D. hawkesi* and *D. kalypso*, appear to be endemic to low elevation forests in Tanzania (Fig. 4J, K) while *D. patrizii* and *D. athene* are widely distributed throughout most of eastern Africa, predominantly at lower elevations (Fig. 4D, N).

This observed high endemism and species richness of *Discothyrea* is not that surprising though, especially if one considers the diversity of terrestrial ecoregions in eastern Africa (Burgess et al. 2004). Previous authors have noted the comparatively high endemism, diversity, and extreme importance for conservation of this region (Burgess et al. 1998, 2006; Balmford et al. 2001; Fisher 2010). The whole area can be considered as a biological laboratory with ideal conditions for biological diversification through allopatric and/or parapatric speciation. It encompasses a distinct 'arid corridor' from Ethiopia and Somalia south to Namibia that separates the East African coastal and montane forests from the rainforest zone in Central and West Africa (Lovett and Wasser 1993, Burgess et al. 1998, Bobe 2006). Furthermore, both, the Great Rift Valley in the east and the Albertine Rift in the west of eastern Africa, provide mosaics of arid and humid habitats at different elevations, often sharply separated from each other. Despite the lack of more sampling and natural history data, we believe that the above biogeographical background can explain the patterns of high endemism and species richness of *Discothyrea*, as well as the pronounced morphological diversity, observed in eastern Africa.

Mandible diversity

Mandibles are essential for a variety of tasks performed by insects in general but are of crucial importance for ants since they are used as tools for manipulating a multitude of objects in applications ranging from hunting, transport of food, food processing, nest building, and brood care to defense. Ants have evolved a wide diversity of mandible shapes compared to other insects reflecting their many different lifestyles (Hölldobler and Wilson 1990). Within the subfamily Proceratiinae most species are considered to be specialized predators of arthropod eggs, although evidence exists only for few species (Brown 1958b, Baroni Urbani and De Andrade 2003, Fisher 2005). Considering such specialization of proceratiines in general, one would suspect that the shape of the mandible should be relatively constrained in order to be able to gather, transport and manipulate prey eggs. Surprisingly though, our examinations of all Afrotropical *Discothyrea* through virtual dissections of micro-CT data have revealed a previously unknown and remarkable diversity in mandible shape (Fig. 8).

Despite this wide diversity found within the genus in the Afrotropical region, it is rather difficult to associate the varying mandible shapes to diet or lifestyle due to the complete lack of knowledge of any of the species from the *D. traegaordhi* complex. The observed variety in shape within this complex could mean that while some species are at least in parts oophagous, others could have different food sources. However, is also possible that all species are predominantly oophagous but the prey eggs are not necessarily from spiders, and

the differing mandible shapes correspond with differently sized and shaped eggs from different prey taxa. The dentate mandible of *D. chimera* (Fig. 8E) could serve a more predatory purpose targeting living prey, or the described tooth could serve to reduce the contact area for the transport of smaller eggs compared to other species. However, admittedly, at this point all these considerations are rather speculative.

In contrast, and as mentioned above, it is known that the two species of the *D. oculata* complex are either completely or mostly egg predators (Brown 1958b, Dejean and Dejean 1998, Dejean et al. 1999), and while *D. oculata* clearly displays claustral lestobiotic colony foundation this is not known for *D. mixta*. However, considering the great similarities in morphology of both species, it is possible. Therefore, we believe it very likely that the more constrained mandible shape in the *D. oculata* complex is well explained by the oophagous lifestyle (Fig. 8A, B).

Antennomere Count

As noted earlier, a majority of authors have used the antennomere count as an important or sole character for species diagnostics prior to this study (Arnold 1916, Weber 1949, Kubota and Terayama 1999, Zacharias and Rajan 2004, Sosa-Calvo and Longino 2008, Terayama 2009, Xu et al. 2014, Bharti et al. 2015). However, the flagellomeres of *Discothyrea,* excluding the apical club, are generally highly reduced, compressed, and often fused (Fig. 15), a problem already acknowledged by Santschi in Bruch (1919) and discussed in detail by Brown (1958a).

In members of the *oculata*-complex, and in larger species of the *traegaordhi*-complex, such as *D. aisnetu* and larger individuals of *D. poweri*, the flagellomeres are often relatively discrete. By contrast, in most species in the Afrotropics and worldwide, which are usually distinctly smaller, the annuli are typically minute and variably consolidated. This renders antennomere count practically impossible to definitively ascertain by light microscopy, even at high magnifications. As noted by Brown (1958a) and observed in this study, the apparent antenomere count varies intraspecifically and sometimes even between the left and right antennae of the same individual, and different values may be obtained by changing the lighting or counting on the ectal and mesal faces of the flagellum. Our observations clearly show that it is not possible to standardize either an observational regime, or to identify any specific characters, such as pigmentation or the origin of small setae, which could yield a consistent antennomere count. Examinations of surface volume rendering of micro-CT data alone similarly provided unreliable visualizations, in which one could subjectively assign several counts to a given antenna. Examination of other species from other subfamilies and genera through virtual dissections of micro-CT data also showed that this problem of antennomere count and fusion is rather specific to *Discothyrea* (Fig. 16).

Although the internal anatomy of the antenna preserves the true subsegmentation, we consider antennomere count to be an uninformative character for species recognition because it is not discernable externally, and dissection of the flagellum is rarely feasible. Furthermore, based on the data presented in Table 2, it might appear as if the antennomere count is species-specific, but due to the low sample sizes dissected per species we are cautious to take this conclusion. This would require more virtual dissections with numerous specimens per species, which was not feasible in and out of focus of this study. Given the availability of many more visible, stable species-level characters, we decline to use antennomere count in the identification key or diagnoses. We further recommend that authors fully refrain from using antennomere count for taxonomy of any *Discothyrea* species from any regions, although the true count may be included in species descriptions when dissections are possible.

Frontoclypeal Structure

The frons and clypeus are uniquely fused and modified in *Discothyrea*, forming a mosaic structure of previously unclear homology termed the 'frontoclypeal shelflike projection' by Keller (2011) in reference to this uncertainty. Other authors have referred to the structure in various ways: the anteromedial disc overhanging the mandibles is sometimes acknowledged to be a fusion of the clypeus and frons (Ogata 1987) but is more often referred to as only a projecting portion of the clypeus (Santschi 1914, Arnold 1916, Weber 1949, Lattke 1994, Xu et al. 2014, Bharti et al. 2015). Interpretations of the posterior, lamellate, triangular, or elevated portion of the structure include a fusion of the frontal lobes (Xu et al. 2014, Bharti et al. 2015), a fusion of the frontal carinae (Ogata 1987, Fisher 2005), a dilation of the frontal carinae (Zacharias and Rajan 2004), or as an unspecified frontoclypeal fusion (Brown 1958a, Fisher 2005).

Clarifying the homology of the structure has been obstructed by both morphological and ontological barriers. Nomenclaturally, the terms 'frontal lobes' and 'frontal carinae' have been interchangeably employed to refer to nonhomologous structures: either to a modification of the median torular arch or to a lateral expansion of the frontal carinae (Keller 2011). No prior taxonomic treatment of *Discothyrea* employing these terms defines them precisely, nor have prior authors offered a rationale for their interpretation of the frontoclypeal apparatus. Morphologically, the extreme and unique modification of the structure, including the loss of important landmarks, has rendered it intractable to even high-resolution external visualization such as SEM.

In this work, we clarify the morphological terminology for the frontoclypeal area for the first time. We identify the clypeus as comprising the anteriormost portion of the mosaic structure, including the narrow, often impressed lateral region between the projecting shelf and the anterolateral corners of the gena, and the medial disc (Fig. 3). The anterior tentorial pits are situated on the clypeal sclerite (Fig. 3). The frontal carinae, which are not derived from the medial torular arch (and therefore should not be referred to as frontal lobes), are fused anteromedially and are produced posteriorly in various shapes among species complexes. Because there is no internal or external evidence for the median delimitation of the frontal carinae and the remainder of the frons, we propose that the entire swollen triangular to rhomboid structure be referred to as the *frontal carinae*. This is the phenotype observed in the *oculata* complex. In the case of the *traegaordhi* complex, we propose the term *frontal lamella* due to its distinctive form. Nevertheless, the lamellate fusion of the frontal carinae appears to be homologous to the rooflike platform present in the *oculata* complex. Based on gross anatomy, it is possible that the frontal lamella of the *traegaordhi*-complex is the result of a reduction of an *oculata*-like ancestral state, potentially through an intermediate trait like that of the Asian and Oceanian species. However, in the absence of any phylogenetic data, we refrain from drawing any conclusions about the transformation series leading to the phenotypes present in *Discothyrea*.

Microtomography

As in Hita Garcia et al. (2017a), diagnostic character assessment and discovery, as well as species delimitation, were performed by a combined approach of specimen examinations with optical microscopy and computer-generated reconstructions of 3D models based on micro-CT. The latter provides several notable advantages over light

and scanning electron microscopy (SEM), including improved resolution, nondestructive specimen preparation protocols, and a particular strength in reconstructing morphological traits which tend to be obscure under the optical microscope (Faulwetter et al. 2013, Fernández et al. 2014, Hita Garcia et al. 2017b). In this study, we demonstrate that the large-scale application of micro-CT for virtual study of morphology in 3D works well for taxonomic revisionary studies including numerous species, as is commonly the case in ants and insects.

Micro-CT was especially powerful in revealing surface sculpturation, which in *Discothyrea* is often structurally complex but shallow and prone to being obfuscated by the presence of dense pilosity, reflectivity of the cuticle, and the overall small size of specimens. As in a recent revision of Chinese *Proceratium* (Staab et al. 2018), we turned the weakness of poor recovery of body pilosity when scanning full bodies of small specimens encountered by Hita Garcia et al. (2017b) into an advantage. *Discothyrea* is very similar to *Proceratium* in that all species are moderately to extremely hairy and possess a dense, furry pelt that covers most surface sculpturation, as well as other morphological characters, and is often very dirty due to numerous soil particles caught in between the hairs. However, compared to *Proceratium* species *Discothyrea* are significantly smaller in body size, thus even more difficult to examine under the light microscope, even at higher magnifications. The digital removal of body hairs from the 3D models of the species treated herein allowed an enhanced evaluation of how to characterize the surface sculpture in the species descriptions. It was also instrumental in characterizing sculptural details of certain body surfaces that were concealed due to preservation and orientation. These were notably the ventral surfaces of the head, the petiole, and the first two abdominal sterna, as well as the declivitous face of the propodeum, which is frequently tightly covered by the petiole and third abdominal tergite, but informatively varies interspecifically. Consequently, we believe that the use of "virtually shaved" 3D models has greatly improved the description of surface sculpture compared to other treatments of proceratiines, which characterize surface sculpture rather sketchily. This application might be of considerable potential for other hairy ant genera or other insects.

Nevertheless, compared with Hita Garcia et al. (Hita Garcia et al. 2017a) the virtual reconstructions in this study are of lower resolution. In contrast to the latter study, we only performed full-body scans and refrained from also doing standardized scans of head, mesosoma, and metasoma. Full-body scans yield great results for medium-sized ants, such as *Pheidole* Westwood (Fischer et al. 2016, Sarnat et al. 2016), *Terataner* Emery (Hita Garcia et al. 2017b) or *Tetramorium* Mayr (Agavekar et al. 2017). However, most *Discothyrea* species in this study are significantly smaller, thus the results are of lower quality. Even though our results are still appropriate for an overall detailed morphological examination, admittedly, there are some obvious disadvantages. As noted above, by uncovering the microsculpture through removal of body pilosity, for the first time it is possible to characterize some sculpture. However, due to the lower resolution of our scan data, SEM images would have yielded much better results and permitted an even superior description of microsculpture. The same is true for eyes and the propodeal spiracle, both of which are often difficult to discern in our 3D models. However, these characters are clearly visible in the stacked digital color images provided in this study.

Higher resolution and higher richness in details could only have been achieved by CT scanning individual body parts separately, but the relatively high number of 20 African species treated in this study plus four species from other regions would have meant to generate at least 92 scans. This is a considerable amount of scanning, data storage, and postprocessing time and after due consideration and assessment of the sufficiently high quality of the fully body scans, we decided to refrain from that. This is definitely a downside for the use of micro-CT for larger taxonomic revisions of smaller ants. However, new technological innovations in the development of scanning machinery and software will likely improve this situation by reducing scanning and postprocessing time of 3D data in the future, thus permitting higher resolution 3D models for larger number of species with a shorter processing time.

The nondestructive nature of micro-CT and computer-based virtual reconstructions was of crucial importance for this revision. As in previous studies (Agavekar et al. 2017, Hita Garcia et al. 2017a, Staab et al. 2018), the material for many *Discothyrea* species is limited and for several species only one or two specimens exist. Due to the rarity of these species and the overall scarce sampling in the Afrotropics, it is not to be expected to acquire additional specimens in the near future. The generation of virtual 3D models permitted an in-depth morphological examination of the whole body without any harm to the valuable specimens by reducing handling time and avoiding any destructive dissections or specimen manipulations. Furthermore, as in previous studies (Agavekar et al. 2017; Hita Garcia et al. 2017a,b; Staab et al. 2018), we provide freely available cybertype datasets of all holotypes from all new species described herein, as well as virtual datasets from previously described ones (Hita Garcia et al. 2019, http://doi.org/10.5061/dryad.3qm4183). Considering that the holotypes will be deposited in numerous natural history museums, of which some have restricted loan policies, it will be a rather challenging task to examine and/or acquire loans from all type material designated in this study. However, the high quality of the 3D models and the open availability of the virtual datasets allow any future taxonomists detailed and comprehensive examinations of Afrotropical *Discothyrea*, thus alleviating the need to gather multiple loans or traveling through several countries on three continents to visit natural history collections.

Conclusions

Our investigation revealed that the Afrotropical region harbors a higher diversity of *Discothyrea* than previously thought, with 15 new out of a total of 20 species recognized here. This remarkable species richness is also accompanied by a notable morphological diversity. Through virtual 'shaving' of these hairy ants, as well as virtual sectioning and dissections in 3D, we found a wealth of morphological characters of great usefulness for species-level diagnostics, thus permitting the generation of a taxonomic system with multiple valuable character states for each species of Afrotropical *Discothyrea*. Against the background of a complete lack of any molecular phylogeny for the genus, the taxonomic data in this study represent a great foundation for any reconstruction of the evolutionary history of *Discothyrea*, either for the Afrotropics or globally.

Furthermore, the in-depth examination of the antennae and cephalic capsule through virtual dissections of 3D data provided the foundation to clarify morphological terminology about the frontoclypeal structure for the first time, as well as resolving taxonomic problems related to the fusion of antennal flagellomeres. It is likely that the morphological diversity observed within an otherwise constrained bodyplan represents interesting variants on their remarkable feeding habits, but detailed behavioral studies of more species are necessary to fully understand the evolutionary significance of this variation. *Discothyrea* are one of the rarest and most interesting

ant clades in the world, and this study represents a further step toward a full accounting of its diversity and better understanding of its remarkable morphology.

Supplementary Data

Supplementary data are available at *Insect Systematics and Diversity* online.

Acknowledgments

First of all, we would like to express our great gratitude to our grand colleagues from South Africa: Peter Hawkes from Pretoria and Mbanyana Nokuthula from Cape Town (SAMC). Without their material from South and East Africa, this revision would not have been possible. We are thankful to Suzanne Ryder from BMNH, Isabell Zürcher-Pfänder from NHMB, Giulio Cuccodoro from MHNG, Jignasha Rana and Stefan Cover from MCZC, and Maria Tavano from MSNG for providing loans of types and/or welcoming FHG to their collections. Kiko Gomez was so kind to send material from additional European museum, which we greatly appreciate. Roberto Keller provided indispensable insight on morphological details and a homology-based approach to taxonomy. We thank Kenneth Dudley for the generation of the maps used in this study. We also want to thank Brian L. Fisher for the tremendous job of making images of type material from most species from many museums around the world available to the myrmecological community through AntWeb. Furthermore, we thank Istvan Miko and Brendon E. Boudinot for editing this special edition on morphology in Insect Systematics and Diversity, and Phil S. Ward and Sebastian Salata for critically reviewing and greatly improving a previous version of this manuscript. We thank the Okinawa Institute of Science and Technology Graduate University Imaging Section for providing access to the Zeiss Xradia micro-CT scanner and Shinya Komoto for support. FHG and ZEL authors benefited from Ernst Mayr Travel Grants from the MCZ (two to FHG to visit BMNH and MCZC, and one to ZEL to visit HLMD). This work was also supported by Japan Society for the Promotion of Science grants-in-aid [No. 17K15180 to EPE.; No. 18K14768 to FHG]. All authors were also supported by subsidy funding to Okinawa Institute of Science and Technology Graduate University.

References Cited

Agavekar, G., F. Hita Garcia, and E. P. Economo. 2017. Taxonomic overview of the hyperdiverse ant genus *Tetramorium* Mayr (Hymenoptera, Formicidae) in India with descriptions and X-ray microtomography of two new species from the Andaman Islands. PeerJ. 5: e3800.

Akkari, N., H. Enghoff, and B. D. Metscher. 2015. A new dimension in documenting new species: high-detail imaging for myriapod taxonomy and first 3D cybertype of a new millipede species (Diplopoda, Julida, Julidae). PLoS One. 10(8): e0135243.

Arnold, G. 1916. A monograph of the Formicidae of South Africa. Part II. Ponerinae, Dorylinae. Ann. South African Mus. 14: 159–270.

Balmford, A., J. L. Moore, T. Brooks, N. Burgess, L. A. Hansen, P. Williams, and C. Rahbeck. 2001. Conservation conflicts across Africa. Science. 291: 2616–2619.

Baroni Urbani, C., and M. L. De Andrade. 2003. The ant genus *Proceratium* in the extant and fossil record (Hymenoptera: Formicidae). Museo. Reg. Sci. Nat. Boll. Monogr. 36: 1–480.

Bharti, H., S. A. Akbar, and J. Singh. 2015. *Discothyrea periyarensis* sp. n., a new proceratiine ant species (Hymenoptera: Formicidae: Proceratiinae) from India. Caucasian Entomol. Bull. 11: 121–124.

Bobe, R. 2006. The evolution of arid ecosystems in eastern Africa. J. Arid Environ. 66: 564–584.

Bolton, B. 2003. Synopsis and classification of Formicidae. Mem. Am. Entomol. Inst. 71: 1–370.

Bolton, B. 2019. An online catalog of the ants of the world. Available from http://antcat.org/. (accessed 20 January 2019).

Brown, W. L. 1958a. Contributions toward a reclassification of the Formicidae. II. Tribe Ectatommini (Hymenoptera). Bull. Mus. Comp. Zool. 118: 173–362.

Brown, W. L. 1958b. Predation of arthropod eggs by the ant genera *Proceratium* and *Discothyrea*. Psyche. 64: 115.

Bruch, C. 1919. Descripción de una curiosa ponerina de Córdoba *Discothyrea neotropica* n. sp. Physis (Buenos Aires). 4: 400–402.

Burgess, N. D., G. P. Clarke, and W. A. Rodgers. 1998. Coastal forests of eastern Africa: status, endemism patterns and their potential causes. Biol J. Linn. Soc. 64: 337–367.

Burgess, N. D., J. D'Amico Hales, E. Underwood, E. Dinerstein, D. Olson, I. Itoua, J. Schipper, and T. Ricketts. 2004. Terrestrial ecoregions of Africa and Madagascar: a continental assessment. Island Press, Washington, DC.

Burgess, N. D., J. D'Amico Hales, T. H. Ricketts, and E. Dinerstein. 2006. Factoring species, non-species values and threats into biodiversity prioritisation across the ecoregions of Africa and its islands. Biol. Conserv. 127: 383–401.

Carbayo, F., T. M. Francoy, and G. Giribet. 2016. Non-destructive imaging to describe a new species of *Obama* land planarian (Platyhelminthes, Tricladida). Zool. Scripta. 45: 566–578.

Csösz, S. 2012. Nematode infection as significant source of unjustified taxonomic descriptions in ants (Hymenoptera: Formicidae). Myrmecol. News. 17: 27–31.

De Queiroz, K. 2007. Species concepts and species delimitation. Syst. Biol. 56: 879–886.

Dejean, A., and A. Dejean. 1998. How a ponerine ant acquired the most evolved mode of colony foundation. Insect. Soc. 45: 343–346.

Dejean, A., B. Schatz, J. Orivel, G. Beugnon, J. P. Lachaud, and B. Corbara. 1999. Feeding preferences in African ponerine ants: a cafeteria experiment (Hymenoptera: Formicidae). Sociobiology. 34: 555–568.

Emery, C. 1901. Notes sur les sous-familles des Dorylines et Ponérines (Famille des Formicides). Ann. Soc. Entomol. Belg. 45: 32–54.

Evenhuis, N. 2018. The insect and spider collections of the world website. http://hbs.bishopmuseum.org/codens/.

Faulwetter, S., A. Vasileiadou, M. Kouratoras, T. Dailianias, and C. Arvanitidis. 2013. Micro-computed tomography: introducing new dimensions to taxonomy. ZooKeys 263: 1–45.

Faulwetter, S., T. Dailianis, K. Vasileiadou, M. Kouratoras, and C. Arvanitidis. 2014. Can micro-CT become an essential tool for the 21st century taxonomist? An evaluation using marine polychaetes. Microsc. Anal. 28: s9–s11.

Fernández, R., S. Kvist, J. Lenihan, G. Giribet, and A. Ziegler. 2014. Sine systemate chaos? A versatile tool for earthworm taxonomy: non-destructive imaging of freshly fixed and museum specimens using micro-computed tomography. PLoS One. 9: e96617.

Fisher, B. L. 2005. A new species of *Discothyrea* Roger from Mauritius and a new species of *Proceratium* Roger from Madagascar (Hymenoptera: Formicidae). Proc. Calif. Acad. Sci. 56: 657–667.

Fisher, B. L. 2010. Biogeography, pp. 18–37. In L. Lach, C. L. Parr and K. L. Abbott (eds.), Ant ecology. Oxford University Press, Oxford.

Fischer, G., E. Sarnat, and E. P. Economo. 2016. Revision and microtomography of the *Pheidole knowlesi* group, an endemic ant radiation in Fiji (Hymenoptera, Formicidae, Myrmicinae). PLoS One. 11: e0158544.

Friedrich, F., and R. G. Beutel. 2008. Micro-computer tomography and a renaissance of insect morphology. Proc. SPIE 2008 7078: 70781U.

Friedrich, F., Y. Matsumura, H. Pohl, M. Bai, T. Hörnschemeyer, and R. G. Beutel. 2014. Insect morphology in the age of phylogenomics: innovative techniques and its future role in systematics. Entomol. Sci. 17: 1–24.

Gotwald Jr, W. H. 1969. Comparative morphological studies of the ants, with particular reference to the mouthparts (Hymenoptera: Formicidae). Mem. Cornell Univ. Agric. Exp. Stn. 408: 1–150.

Guénard, B., M. Weiser, K. Gomez, N. Narula, and E. P. Economo. 2017. The Global Ant Biodiversity Informatics (GABI) database: a synthesis of ant species geographic distributions. Myrmecol. News. 24: 83–89.

Harris, R. A. 1979. A glossary of surface sculpturing. Calif. Depart. Food Agric. Bureau Entomol. 28: 1–31.

Hita Garcia, F., and B. L. Fisher. 2014. Taxonomic revision of the cryptic ant genus *Probolomyrmex* Mayr (Hymenoptera, Formicidae, Proceratiinae) in Madagascar. Deut. Entomol. Z. 61: 65–76.

Hita Garcia, F., P. G. Hawkes, and G. D. Alpert. 2014. Taxonomy of the ant genus *Proceratium* Roger (Hymenoptera, Formicidae) in the Afrotropical region with a revision of the *P. arnoldi* clade and description of four new species. Zookeys. 447: 47–86.

Hita Garcia, F., E. M. Sarnat, and E. P. Economo. 2015. Revision of the ant genus *Proceratium* Roger (Hymenoptera, Proceratiinae) in Fiji. ZooKeys. 475: 97–112.

Hita Garcia, F., G. Fischer, C. Liu, T. L. Audisio, and E. P. Economo. 2017a. Next-generation morphological character discovery and evaluation: an X-ray micro-CT enhanced revision of the ant genus *Zasphinctus* Wheeler (Hymenoptera, Formicidae, Dorylinae) in the Afrotropics. Zookeys. 693: 33–93.

Hita Garcia, F., G. Fischer, C. Liu, T. L. Audisio, G. D. Alpert, B. L. Fisher, and E. P. Economo. 2017b. X-Ray microtomography for ant taxonomy: an exploration and case study with two new *Terataner* (Hymenoptera, Formicidae, Myrmicinae) species from Madagascar. PLoS One. 12: e0172641.

Hölldobler, B., and E. O. Wilson. 1990. The ants. Harvard University Press, Cambridge, MA.

Janicki, J., N. Narula, M. Ziegler, B. Guénard, and E. P. Economo. 2016. Visualizing and interacting with large-volume biodiversity data using client-server web-mapping applications: the design and implementation of antmaps.org. Ecol. Inform. 32: 185–193.

van de Kamp, T., T. dos Santos Rolo, P. Vagovič, T. Baumbach, and A. Riedel. 2014. Three-dimensional reconstructions come to life – interactive 3D PDF animations in functional morphology. PLoS One. 9: e102355.

Katayama, M. 2013. Predatory behaviours of *Discothyrea kamiteta* (Proceratiinae) on spider eggs. Asian Myrmecol. 5: 121–124.

Keller, R. A. 2011. A phylogenetic analysis of ant morphology (Hymenoptera, Formicidae) with special reference to the poneromorph subfamilies. Bull. Am. Mus. Nat. Hist. 355: 1–90.

Kubota, M., and M. Terayama. 1999. A description of a new species of the genus *Discothyrea* Roger from the Ryukyus, Japan (Hymenoptera: Formicidae). Mem. Myrmecol. Soc. Japan. 1: 1–5.

Landschoff, J., and R. Lemaitre. 2017. Differentiation of three common deep-water hermit crabs (Crustacea, Decapoda, Anomura, Parapaguridae) from the South African demersal abundance surveys, including the description of a new species of *Paragiopagurus* Lemaitre. Zookeys. 676: 21–45.

Lattke, J. E. 1994. Phylogenetic relationships and classification of ectatommine ants (Hymenoptera: Formicidae). Entomol. Scand. 25: 105–119.

Linder, H. P., H. M. de Klerk, J. Born, N. D. Burgess, J. Fjeldsa, and C. Rahbek. 2012. The partitioning of Africa: statistically defined biogeographical regions in sub-Saharan Africa. J. Biogeogr. 39: 1189–1205.

Lovett, J. C., and S. K. Wasser. 1993. Biogeography and ecology of the rain forests of eastern Africa. Cambridge University Press, Cambridge.

Morisita, M., M. Kubota, K. Onoyama, K. Ogata, M. Terayama, M. Kondoh, and H. T. Imai. 1989. A guide for the identification of Japanese ants. I. Ponerinae, Cerapachyinae, Pseudomyrmecinae, Dorylinae, and Leptanillinae (Hymenoptera: Formicidae), Myrmecological Society of Japan, Tokyo.

Ogata, K. 1987. A generic synopsis of the poneroid complex of the family Formicidae in Japan (Hymenoptera). Part 1. Subfamilies Ponerinae and Cerapachyinae. Esakia. 25: 97–132.

Robertson, H. G. 2000. Afrotropical ants (Hymenoptera: Formicidae): taxonomic progress and estimation of species richness. J. Hymenoptera Res. 9: 71–84.

Roger, J. 1863. Die neu aufgeführten Gattungen und Arten meines Formiciden-Verzeichnisses nebst Ergänzung einiger frühergegebenen Beschreibungen. Berliner Entomol. Z. 7: 131–214.

Santschi, F. 1913. Glanures de fourmis africaines. Ann. Soc. Entomol. Belg. 53: 302–314.

Santschi, F. 1914. Meddelanden från Göteborgs Musei Zoologiska Afdelning. 3. Fourmis du Natal et du Zoulouland récoltées par le Dr. I. Trägårdh. Göteborgs Kungliga Vetenskaps och Vitterhets Samhälles Handlingar 15: 1–44.

Sarnat, E. M., and E. P. Economo. 2012. The ants of Fiji. Univ. Calif. Publ. Entomol. 132: 1–398.

Sarnat, E., G. Fischer, and E. Economo. 2016. Inordinate spinescence: taxonomic revision and microtomography of the *Pheidole cervicornis* species group (Hymenoptera, Formicidae). PLoS One. 11: e0156709.

Sartori, M., M. Kubiak, and P. Michalik. 2016. Deciphering genital anatomy of rare, delicate and precious specimens: first study of two type specimens of mayflies using micro-computed X-ray tomography (Ephemeroptera; Heptageniidae). Zoosymposia. 11: 028–032.

Simonsen, T. J., and I. J. Kitching. 2014. Virtual dissections through micro-CT scanning: a method for non-destructive genitalia 'dissections' of valuable Lepidoptera material. Syst. Entomol. 39: 606–618.

Sosa-Calvo, J., and J. T. Longino. 2008. Subfamilia Proceratiinae, pp. 219–237. In E. Jiménez, F. Fernández, T. M. Arias, and F. H. Lozano-Zambrano (eds.), Sistemática, biogeografía y conservación de las hormigas cazadoras de Colombia. Instituto de Investigación de Recursos Biológicos Alexander von Humboldt, Bogotá.

Staab, M., F. Hita Garcia, C. Liu, Z.-H. Xu, and E. P. Economo. 2018. Systematics of the ant genus *Proceratium* Roger (Hymenoptera, Formicidae, Proceratiinae) in China – with descriptions of three new species based on micro-CT enhanced next-generation-morphology. Zookeys. 770: 137–192.

Stoev, P., A. Komerički, N. Akkari, S. Liu, X. Zhou, A. M. Weigand, J. Hostens, C. I. Hunter, S. C. Edmunds, D. Porco, et al. 2013. *Eupolybothrus cavernicolus* Komerički & Stoev sp. n. (Chilopoda: Lithobiomorpha: Lithobiidae): the first eukaryotic species description combining transcriptomic, DNA barcoding and micro-CT imaging data. Biodivers. Data J. 1: e1013.

Terayama, M. 2009. A synopsis of the family Formicidae of Taiwan (Insecta: Hymenoptera). Research Bulletin of Kanto Gakuen University. Liberal Arts. 17: 81–266.

Vilhelmsen, L. 1996. The preoral cavity of lower Hymenoptera (Insecta): comparative morphology and phylogenetic significance. Zool. Scripta. 25: 143–170.

Ward, P. S. 1988. Mesic elements in the Western Nearctic ant fauna: taxonomic and biological notes on *Amblyopone*, *Proceratium*, and *Smithistruma* (Hymenoptera: Formicidae). J. Kansas Entomol. Soc. 61: 102–124.

Weber, N. A. 1949. New ponerine ants from equatorial Africa. Am. Mus. Novit. 1398: 1–9.

Wheeler, W. M. 1916. *Prodiscothyrea*, a new genus of ponerine ants from Queensland. Trans. R. Soc. South Austr. 40: 33–37.

Wheeler, W. M. 1922. Ants collected by the American Museum Congo Expedition. A contribution to the myrmecology of Africa. Bull. Am. Mus. Nat. Hist. 45: 1-1055.

Wilson, E. O. 1955. A monographic revision of the ant genus *Lasius*. Bull. Mus. Comp. Zool. 113: 1–201.

Wipfler, B., H. Pohl, M. I. Yavorskaya, and R. G. Beutel. 2016. A review of methods for analysing insect structures — the role of morphology in the age of phylogenomics. Curr. Opin. Insect Sci. 18: 60–68.

Xu, Z., C. J. Burwell, and A. Nakamura. 2014. Two new species of the proceratiine ant genus *Discothyrea* Roger from Yunnan, China, with a key to the known Oriental species. Asian Myrmecol. 6: 33–41.

Zacharias, M., and P. D. Rajan. 2004. *Discothyrea sringerensis* (Hymenoptera: Formicidae) a new ant species from India. Zootaxa. 484: 1–4.